

2



United States Army
Research Office Workshop

DTIC
SELECTE
MAR 07 1990
S D & D

DTIC FILE COPY

AD-A218 884

High Intensity Electro-Magnetic and Ultrasonic Effects on Inorganic Materials Behavior and Processing

July 17-18, 1989

North Carolina State University
Raleigh, NC 27695

DISTRIBUTION STATEMENT A
Approved for public release
Distribution Unlimited

Department of Materials Science & Engineering
Division for Lifelong Education



90 03 06 054

SECURITY CLASSIFICATION OF THIS PAGE

REPORT DOCUMENTATION PAGE

1a. REPORT SECURITY CLASSIFICATION Unclassified		1b. RESTRICTIVE MARKINGS	
2a. SECURITY CLASSIFICATION AUTHORITY		3. DISTRIBUTION/AVAILABILITY OF REPORT Approved for public release; distribution unlimited.	
2b. DECLASSIFICATION/DOWNGRADING SCHEDULE		4. PERFORMING ORGANIZATION REPORT NUMBER(S)	
4. PERFORMING ORGANIZATION REPORT NUMBER(S)		5. MONITORING ORGANIZATION REPORT NUMBER(S) ARO 26690.1-MS-CF	
6a. NAME OF PERFORMING ORGANIZATION North Carolina State Univ.	6b. OFFICE SYMBOL (If applicable)	7a. NAME OF MONITORING ORGANIZATION U. S. Army Research Office	
6c. ADDRESS (City, State, and ZIP Code) Raleigh, NC 27695		7b. ADDRESS (City, State, and ZIP Code) P. O. Box 12211 Research Triangle Park, NC 27709-2211	
8a. NAME OF FUNDING/SPONSORING ORGANIZATION U. S. Army Research Office	8b. OFFICE SYMBOL (If applicable)	9. PROCUREMENT INSTRUMENT IDENTIFICATION NUMBER DAAL03-89-G-0032	
8c. ADDRESS (City, State, and ZIP Code) P. O. Box 12211 Research Triangle Park, NC 27709-2211		10. SOURCE OF FUNDING NUMBERS	
		PROGRAM ELEMENT NO.	PROJECT NO.
		TASK NO.	WORK UNIT ACCESSION NO.
11. TITLE (Include Security Classification) High Intensity Electro-Magnetic and Ultrasonic Effects on Inorganic Materials Behavior and Processing			
12. PERSONAL AUTHOR(S) Hans Conrad			
13a. TYPE OF REPORT Final	13b. TIME COVERED FROM 4/1/89 TO 3/31/90	14. DATE OF REPORT (Year, Month, Day) February 1990	15. PAGE COUNT
16. SUPPLEMENTARY NOTATION The view, opinions and/or findings contained in this report are those of the author(s) and should not be construed as an official Department of the Army position, policy, or decision, unless so designated by other documentation.			
17. COSATI CODES		18. SUBJECT TERMS (Continue on reverse if necessary and identify by block number)	
FIELD	GROUP	Workshop, Inorganic Materials, Electro-Magnetic Effects, Ultrasonic Effects, Materials Behavior, Materials Processing, Solid State Theory, Material Processing Technology, J-2	
19. ABSTRACT (Continue on reverse if necessary and identify by block number)			
<p>The objectives of this workshop were to review the ongoing work on the effects of the various forms of energy, other than thermal and external stresses on the mechanical behavior of materials, and to identify critical technical issues which must be addressed to make a headway to understand the mechanisms involved in these effects and exploit this emerging technology. The program started with the considerations of the fundamental mechanisms relevant to the physical effects to be discussed, followed by the discussion of the mechanisms involved in specific mechanical effects and a full session on the materials processing. The spirit of this workshop is to exclude from its scope the thermally and mechanically induced effects.</p>			
20. DISTRIBUTION/AVAILABILITY OF ABSTRACT <input type="checkbox"/> UNCLASSIFIED/UNLIMITED <input type="checkbox"/> SAME AS RPT. <input type="checkbox"/> DTIC USERS		21. ABSTRACT SECURITY CLASSIFICATION Unclassified	
22a. NAME OF RESPONSIBLE INDIVIDUAL		22b. TELEPHONE (Include Area Code)	22c. OFFICE SYMBOL

90 03 06 05 4

Proceedings
ARO-Sponsored Workshop

**HIGH-INTENSITY ELECTRO-MAGNETIC AND ULTRASONIC EFFECTS ON
INORGANIC MATERIALS BEHAVIOR AND PROCESSING**

July 17-18, 1989
North Carolina State University
Raleigh, NC 27695

Co-Chairmen: H. Conrad, North Carolina State University
I. Ahmad, U. S. Army Research Office

CONTENTS

Introduction

Program

List of Attendees

Submitted Papers

Issues and Opportunities

R. Rosenberg
D. Kuhlmann-Wilsdorf and H. Conrad
H. Conrad

Accession For	
NTIS CRA&I	<input checked="" type="checkbox"/>
DTIC TAB	<input type="checkbox"/>
Unannounced	<input type="checkbox"/>
Justification	
By _____	
Distribution/	
Availability Codes	
Dist	Avail and/or Special
A-1	



Workshop

on

**HIGH-INTENSITY ELECTRO-MAGNETIC AND ULTRASONIC EFFECTS ON
INORGANIC MATERIALS BEHAVIOR AND PROCESSING**

North Carolina State University
Raleigh, NC

July 17-18, 1989

INTRODUCTION

It is becoming increasingly clear that externally-applied, high-intensity fields (i.e., electric, magnetic, electromagnetic or ultrasonic) can have a significant **direct** influence on the properties of materials, in addition to such indirect effects as Joule heating or induced mechanical stresses. Some examples of phenomena reflecting direct effects are electromigration (1,2), electroplasticity (3,4), plastoelectricity (5), magnetoplasticity (6,7) photoplasticity (8,9) and acoustoplasticity (10,11).

Electric fields and currents have been found to influence recovery, recrystallization and grain growth (12,13) and phase transformations including solidification (14,15) crystallization of amorphous alloys (16) and aging or precipitation (17-19). Magnetic fields have been found to influence aging (20) and martensitic transformations (21) in iron alloys. Beneficial effects of electric and magnetic fields have been reported in metal working and processing, including rolling and drawing (22,23), forming (24), and consolidation of metal powders (25,26). The effects of electric and magnetic fields and electric currents become especially important in the following applications:

- (1) High energy power sources
- (2) Microelectronic circuits
- (3) Electromagnetic forming and propulsion
- (4) Advanced forming and processing techniques

Moreover, with increased application of superconductors (low- and high-temperature), the effects and applications of high electric and magnetic fields and electric currents will become increasingly important. Also, it is expected that the high magnetic field studies on solids presently underway (27) will lead to new and improved electronic and magnetic materials.

In addition to electric and magnetic fields, electromagnetic radiation, such as for example microwaves (28,29), white light (8,9,30) and lasers (31), are known to influence materials behavior. Moreover, ultrasonic oscillations applied to metals and alloys have been reported to influence mechanical behavior and phase transformations (11). Of special interest to this workshop, are the **direct** effects of such electromagnetic and ultrasonic waves on materials behavior, rather than any indirect effects resulting from the associated heating.

It was felt that the general subject of the effects of electric and magnetic fields, electric current, electromagnetic waves and ultrasonic energy on inorganic materials behavior and processing had reached a stage that a workshop was desirable to review the state-of-the-art and to identify fruitful directions of research. Bringing together theoretical and experimental investigators in this general area in the USA should lead to an exchange of ideas that would enhance our appreciation of the fundamentals of the subject and of its scientific and technological importance, and hopefully lead to: (a) a better understanding of materials behavior in general and (b) the development of new and improved processing methods.

The U. S. Army's interest in the subject matter of the workshop are discussed in the included papers by Dr. I. Ahmad of the Army Research Office and Dr. P. Cate of the Benet Laboratories, Watervliet Arsenal.

H. Conrad
North Carolina State University

I. Ahmad
U. S. Army Research Office

REFERENCES

1. **Electro- and Thermo-transport in Metals and Alloys**, ed. by R. E. Hummel and H. B. Huntington, AIME (1977).
2. F. d'Heurle and P. S. Ho, **Thin Films-Interdiffusion and Reactions**, ed. by J. M. Poate, K. N. Tu and J. W. Mayer, Wiley-Interscience, N. Y. (1978) p. 243.
3. O. A. Troiskii, Zh. ETF Pis. Red 10 18 (1969).
4. H. Conrad and A. F. Sprecher, "The Electroplastic Effect in Metals", in **Dislocations in Solids**, F. R. N. Nabarro, ed., Elsevier Science, Bv (1989) p. 497.
5. J. C. M. Li, **The Mechanics of Dislocations**, E. C. Aifantis and J. P. Hirth, eds. ASM (1985) p. 85.
6. L. R. Motowidlo, P. V. Goldman and J. M. Galligan, Scripta Met. 15 787 (1981).
7. J. M. Galligan, Scripta Met. 18 653 (1984).
8. S. A. Varchenya, G. P. Upit and I. D. Manika, in **The Science of Hardness Testing and Its Research Applications**, J. H. Westbrook and H. Conrad, eds. ASM (1973) p. 440.
9. H. P. Leighly and R. M. Oglesbee, *ibid.* p. 445.
10. G. Blaha and B. Langenecker, Naturwiss. 42 556 (1955).
11. Anton Puskar, **The Use of High-Intensity Ultrasonics**, Elsevier (1982).
12. H. Conrad, A. F. Sprecher, W. Cao and X. Lu, in **Homogenization and Annealing of Al and Cu Alloys**, H. D. Merchant, J. Crane and E. H. Chia, eds. TMS-AIME (1988) p. 227.
13. H. Conrad, Z. Guo and A. F. Sprecher, Scripta Met. 23 821 (1989).
14. A. K. Misra, Met. Trans. A 16A 1354 (1985).
15. T. Bryskiewicz, C. F. Boucher, J. Lagowski and H. C. Gatos, "Bulk GaAs Crystal Growth by Liquid Phase Electro-epitaxy", submitted J. Crystal Growth.

16. Z. H. Lai, H. Conrad, Y. S. Chao, S. Q. Wang and J. Sun, *Scripta Met.* **23** 305 (1989).
17. F. Erdman-Jesnitser, D. Mrówka and K. Ouvrier, *Archiv. f.d. Eisenhüttenwesen* **30** 31 (1959).
18. Y. Onodera and K. Hirano, *J. Met. Sci.* **11** 809 (1976).
19. M. C. Shine and S. R. Herd, *Appl. Phys. Lett.* **20** 217 (1972).
20. G. Sauthoff and W. Pitsch, "Orienting of $Fe_{16}N_2$ Particles in α -iron by an External Magnetic Field", submitted to *Phil. Mag.*
21. Kakeshita, K. Shimizu, S. Funada and M. Date, *Acta Met.* **33** 1381 (1985).
22. O. A. Troitskii, V. I. Spitsyn, N. V. Sokolov and V. G. Ryzhkov, *Phys. Stat. Sol. (a)* **52** 85 (1972).
23. O. A. Troitskii, *Mat. Sci. Engr.* **75** 37 (1985).
24. D. F. Brower, "Electromagnetic Forming", *ASM Metals Handbook* Vol. 4 8th Ed. (1969) p. 256.
25. K. Okazaki, D. Kim and H. Pak, in *Proc. 2nd Int. Conf. Rapidly Solidified Materials*, ASM (1988) p. 183.
26. H. L. Marcus, D. L. Bourell, Z. Eliezer, C. Persad and W. Weldon, *Jnl. Met.* (Dec. 1987) p. 6.
27. D. L. Mitchell, *Sci. Info. Bull. ONR/AFOSR/ARO* **13** No. 2 65 (1988).
28. M. K. Krage, *Cer. Bull.* **60** 1232 (1981).
29. B. Swain, *Adv. Mat. Proc.* (Sept. 1988) p. 76.
30. J. M. Galligan and P. Hansen, *phys. stat. sol. (a)* **109** K19 (1989).
31. *Laser-Solid Interactions and Transient Thermal Processing of Materials*, ed. by J. Narayan, W. Brown and R. A. Lemon, North-Holland (1983).

Program
ARO-Sponsored Workshop
titled

**HIGH-INTENSITY ELECTRO-MAGNETIC AND ULTRASONIC EFFECTS ON
INORGANIC MATERIALS BEHAVIOR AND PROCESSING**

held at the

Brownstone Hotel
1707 Hillsborough Street
Raleigh, NC
Telephone: (919)828-0811

Sunday, July 16, 1989

Registration: 5:00 - 8:00 p.m.
Social: 6:00 - 7:00 p.m.
Dinner: 7:00 - p.m.

Monday, July 17, 1989

7:00 - 8:20 Continental Breakfast

INTRODUCTORY REMARKS

8:20 *I. Ahmad*, U. S. Army Research Office
"The U. S. Army's Interest in the Workshop Topic"

8:40 *G. Mayer*, Institute for Defense Analysis
"A Survey of Research into Electro-Magnetic and Acoustic
Effects on Mechanical Behavior and Processing of Materials"

FUNDAMENTAL CONSIDERATIONS

Chairman: *I Ahmad*, U. S. Army Research Office

9:00 *B. Klein*, Naval Research Laboratory
"Electron Theory of the Solid State"

9:40 *A. C. Anderson*, University of Illinois
"Phonons, Electrons and Defects"

10:20-10:40 COFFEE

ARO-Sponsored Workshop (Continued)

- 10:40 *A. Brailsford*, Ford Motor Company
"Electronic Contribution to the Dislocation Drag Coefficient"
- 11:20 *H. B. Huntington*, Rensselaer Polytechnic Institute
"Electromigration-Caused Deterioration of Metallic Strips –
A Computer Simulation"
- 12:00 LUNCH

Monday Afternoon

- 1:00 *D. Kuhlmann-Wilsdorf*, University of Virginia
"Electric Field Effects Observed Through High Resolution X-Ray
Diffraction" by K. Lal and Coworkers of NPL, India
- 1:40 *R. Green*, Johns Hopkins University
"Interaction of High-Intensity Ultrasonic Waves with Solids"

DISLOCATIONS AND MECHANICAL BEHAVIOR

Chairman: *G. Mayer*, Institute for Defense Analysis

- 2:20 *J. C. M. Li*, University of Rochester
"Plastoelectric Effect in Crystals"
- 3:00 – 3:20 COFFEE
- 3:20 *J. Galligan, C. S. Kim and T. J. Garosshen*, University of
Connecticut
"On the Interaction of Charge Carriers with Mobile Dislocations
in Metals and Semiconductors"
- 4:00 *H. Conrad, A. F. Sprecher, X. P. Lu and W. D. Cao*, North
Carolina State University
"Effects of Electric Fields and Currents on Mechanical
Properties of Metals-Electroplasticity"
- 4:40 *K. Salama*, University of Houston
"High Power Ultrasound on Mechanical Properties of Solids-
Acoustoplasticity"
- 6:00 DINNER

ARO Sponsored Workshop (Continued)

ANNEALING AND PHASE TRANSFORMATIONS

Chairman: B. Rath, Naval Research Laboratories

7:00 A. F. Sprecher and H. Conrad, North Carolina State University
"Effects of Electric Fields and Currents on Annealing of Metals"

7:40 R. F. Hochman, Georgia Institute of Technology and N. Tselesin, Duratech, Inc.
"The Effect of Pulsed Magnetic Fields on Metallurgical Properties". (In the written version this paper was combined with that by N. Tselesin, below. Another paper was substituted titled "Photomechanical and Ultrasonic Radiation Effects in Materials".)

8:20 GENERAL DISCUSSION

Chairman: A. C. Anderson, University of Illinois

Tuesday Morning, July 18, 1989

7:00 - 8:20 Continental Breakfast

ANNEALING AND PHASE TRANSFORMATIONS (Continued)

Chairman: B. Rath, Naval Research Laboratories

8:20 W. Morris, University of California, Berkeley
"Magnetic Effects in Martensitic Transformations"
(unable to attend)

9:00 R. Rosenberg, T. J. Watson Research Center, IBM
"Effects of Electric Fields and Currents on Phase Changes in Thin Film Alloys"

9:40 H. Conrad, A. F. Sprecher, W. D. Cao and X. P. Lu
North Carolina State University
"Effects of Electric Fields and Currents on Phase Transformations in Bulk Alloys"

10:00-10:15 COFFEE

ARO Sponsored Workshop (Continued)

MATERIALS PROCESSING

Chairman: H. Conrad, North Carolina State University

- 10:15 *N. Tselesin*, Duratech Inc.
"Review of Soviet Work on the Effect of Electric and Magnetic
Fields on Materials Behavior"
- 10:55 *A. F. Sprecher and H. Conrad*, North Carolina State University
"Application of Electroplasticity in Metal Forming and Working
- Review of Soviet Work"
- 11:20 *K. Okazaki*, University of Kentucky
"Electric Current Effects in the Sintering of Powder Materials -
Electro-Discharge Compaction"
- 12:00 LUNCH
- 1:00 *P. J. Cote*, Benet Laboratories, Watervliet Arsenal
"Potential Army Applications for Electric Field and Current
Effects on Material Properties"
(unable to attend)
- 1:20 *H. D. Kimery*, Oak Ridge National Laboratory
"Effects of High Intensity-High Frequency Microwaves in
Materials Processing"
- 2:00 *J. Narayan*, North Carolina State University
"Photon-Solid Interactions and Processing of Materials"

2:40 PANEL DISCUSSION

Chairman: H. Conrad, North Carolina State University

3:30 END OF WORKSHOP

REGISTRATION LIST July 16-18, 1989

NAME	TITLE / COMPANY / ADDRESS
DR. D. KUHLMANN -WILSDORF	UNIVERSITY OF VIRGINIA DEPT. OF MATERIALS SCIENCE CHARLOTTESVILLE, VA 22401
DR. RALPH ADLER	US ARMY MATERIALS TECH LAB ATTN: SLCM WATERTOWN, MA 02172-0001
DR. IGBAL AHMAD	US ARMY RESEARCH OFFICE PO BOX 12211 RTP, NC 27709
DR. A.C. ANDERSON	UNIVERSITY OF ILLINOIS DEPT. OF PHYSICS URBANA, IL 61801
DR. ALAN BRAILSFORD	FORD MOTOR COMPANY PO OX 2053/SCIENTIFIC RES LAB DEARBORN, MI 48121-2053
WEI-DI CAO	STUDENT NC STATE UNIVERSITY MATERIALS SCIENCE/ENGINEERING RALEIGH, NC 27695-7907
DR. RONALD N. CARON	METAL RESEARCH LAB/OLIM. CORP. 91 SHELTON AVE. NEW HAVAN, CT 06511
DR. H. CONRAD	NC STATE UNIVERSITY MATERIALS SCIENCE/ENGINEERING RALEIGH, NC 27695-7907
JULIUS FRANKEL	US ARDEC, SMCAR-CCB-RP WATERVLIET ARSENAL WATERVLIET, NY 12189-4050
DR. JAMES M. GALLIGAN	UNIVERSITY OF CONNECTICUT DEPT. OF METALLURGY STORRS, CT 06268
DR. ROBERT GREEN, JR.	THE JOHNS HOPKINS UNIVERSITY MATERIALS SCIENCE & ENGINEER. BALTIMORE, MD 21218
DR. ROBERT F. HOCHMANN	GEORGIA INST. OF TECHNOLOGY SCHOOL OF MATERIALS ENGINEER. ATLANTA, GA 30332-0245

COURSE REGISTRATION LIST

NAME	TITLE / COMPANY / ADDRESS
DR. H.B. HUNTINGTON	RENSSELAER POLYTECHNIC INST. PHYSICS DEPT TROY, NY 12181
DR. H.D. KIMREY	OAK RIDGE NATIONAL LAB PO BOX 2009 OAK RIDGE, TN 37831-8071
DR. BARRY KLEIN	NAVAL RESEARCH LABORATORIES CODE 4690 WASHINGTON, DC 20375
DR. MICHAEL KOTYK	USS TECHNICAL CENTER 4000 TECH CENTER DRIVE MONROEVILLE, PA 15146
DR. J. C. M. LI	UNIVERSITY OF ROCHESTER COLLEGE OF ENGR & APPLIED SCI ROCHESTER, NY 14627
DR. GEORGE MAYER	INSTITUTE FOR DEFENSE ANALYSIS 1801 N. BEAUREGARD STREET ALEXANDRIA, VA 22311
DR. LAWRENCE MEISEL	MATLS ENGR BR, SMCAR CCB-RM, RES. DIV. BENET LABS. ARMY ARMAMENT RD&E CENTER WATERVLIET, NY 12189-4050
DR. JAY NARAYAN	NC STATE UNIVERSITY MATERIALS SCIENCE/ENGINEERING RALEIGH, NC 27695-7907
MR. LINUS J. O'CONNELL	ALUMINUM COMPANY OF AMERICA 174 THORN HILL ROAD WARRENDALE, PA 15086
DR. KENJI OKAZAKI	UNIVERSITY OF KENTUCKY METALLURGICAL ENGR/MAT. SCI. LEXINGTON, KY 40506-0046
DR. BHAKTA B. RATH	ASSOC. DIR./RMSCT NAVAL RESEARCH LABORATORY CODE 6000, BLDG. 43, RM 212 WASHINGTON, DC 20375-5000
DR. ROBERT ROSENBERG	IBM MAT. PROCESSING SCIENCES T.J. WATSON RESEARCH CENTER YORKTOWN HEIGHT, NY 10598

COURSE REGISTRATION LIST

NAME	TITLE / COMPANY / ADDRESS
DR. KAMEL SALAMA	UNIVERSITY OF HOUSTON UNIVERSITY PARK/MECH. ENGR. HOUSTON, TX 77004
DR. A. FRITZ SPRECHER	NC STATE UNIVERSITY MATERIALS SCIENCE/ENGINEERING RALEIGH, NC 27695-7907
DR. JOHN SWARTZ	ALCOA TECHNICAL CENTER ALCOA LAB ALCOA CENTER, PA 15069
DR. N. TSELESIN	DURATECH, INC. 2900 LOOKOUT PLACE ATLANTA, GA 30305

US Army Interest in the Electrical, Magnetic, Acoustic and Photonic
Effects on the Mechanical Behavior of Materials and Processes *

Iqbal Ahmad
US Army Research Office
Research Triangle Pk N.C. 27709

ABSTRACT

A brief historical perspective of the research on the electrical, magnetic, and photonic effects on the mechanical behavior of materials and processes followed by a discussion of the objectives and the scope of the workshop are presented.

INTRODUCTION

One of the important functions of the Army Research Office is to identify new fundamental concepts and emerging technologies relevant to the mission objectives of the DoD R&D program in general and the Army needs in particular. The topic of this workshop is in the area of an emerging technology, which has considerable potential for application in the mechanical metallurgy of hard to work materials of importance both to the defense and industrial sector. In the following, a brief overview of the effects of the electrical current and field, and magnetic, acoustic and photonic fields on the mechanical behavior of materials followed by a discussion of the objectives and scope of the workshop and potential applications of this rather unexplored technology in future Army materiel are presented.

HISTORICAL

The phenomenon of the effect of various kinds of force fields on the behavior of materials has been known for more than a century. For Example Geradin (1) as early as 1861 reported electromigration of constituents of liquid solder alloy. Since early 1960 it has been recognized that conduction electrons exert a drag on motion of dislocations in metals. The enhancement of dislocation mobility by the irradiation of a zinc single crystal under tensile stress, with directed electron beam was reported by Troitskiy and Likhtman in 1963 (2). Electrons with energy level lower than the threshold of the atomic dislocations, when the true radiation hardening could occur, were used. They found that when the electron beam was parallel to the slip plane the flow stress was lower and the fracture strain was higher than when it was normal to the plane (Figure 1).

* Presented at the workshop on the "Effect of Electric Current and Intense Electrical, Magnetic, Acoustic and Photonic Fields on the Mechanical Behavior of Materials" held on July 16-17, 1989 at the North Carolina State University, Raleigh, North Carolina.

A few years later USSR scientists, mainly Troitskiy and his group at the Institute of Physical Chemistry of USSR Academy of Sciences started studying the effect of electron state of metals on their mechanical properties (3). The use of pulsed current (instead of continuous) made it possible to achieve high current density but leave the metal practically cold. In this manner the effect of electric current on the ductility and deformation of a number of metals uncomplicated by heating of the sample was studied. It was shown that the application of high density electric current pulses increased the low temperature ductility of metals including Zn, Pb and In. Figure 2 shows this so called "electroplastic effect" in a Zn single crystal specimen deformed under uniaxial tension at 78K. At each application of the electric current pulse the load dropped. The load drop occurred only during the plastic deformation (region A), and none in elastic range or following appreciable stress relaxation. Furthermore the load drop increased with the increase in current density. The effect was explained to be due to the interaction of drift electrons with dislocations, in that the electron wind provided additional force on dislocations enhancing their mobility. Similar effect was discovered, when metals were exposed to acoustic energy. Blaha and Langanecker (5) reported in 1955 that ultrasound field reduced the apparent shear stress necessary for plastic deformation of metals such as Zn, Al, Cu steels. Langanecker et al successfully achieved almost 100% reduction even in hard to deform metals when ultrasonic energy density was sufficiently high. He exhibited a macroscopic wire drawing machine at the 4th International Wire Exhibition in Basle in 1974. Semen P. Kundas et al (6) reported a Vacuum Hot Ultrasonic Flattening (VHUF) method shown in Figure 3a, where in heated wires of tungsten (0.1-0.3 mm) and molybdenum (0.1-0.8mm) could be flattened by subjecting them to ultrasonic energy (0.4-4.5 KV depending on the diameter of the wire, with resonance frequency of 18-44 kHz), without damaging the wire. In fact as Figure 3b and 3c show the microstructure of the VHUF wire was much superior to that obtained by conventional rolling. The process has been patented in USA, Japan and many European Countries. Troitskiy and his group (7,8) also designed a mill to flatten tungsten wires, in which high density electric current pulses were supplied to the high roll stand (Fig 4). The wire after passing through these rolls passed through the ultrasonic station for flattening. In one pass the experimental mill produced about a 75% deformation of a 0.41mm diameter work hardened tungsten wire into a ribbon 0.1x 1.5 mm in size with shape factor of 11, achieving complete satisfactory ductility. The ribbon had a strength of 260 kg/mm sq. and could be wound on rollers having 1 mm radius. Without applying the electric current and ultrasonic flattening the ribbon delaminated and broke. There is a threshold effect of current induced ductility. The maximum ductility was achieved at 1500-2000 A/mm sq. The great potential of this process can be appreciated from Figure 6, which shows a transverse section of high temperature-high strength wires of thoriated tungsten used for the reinforcement of superalloys (9). These wires, made by the state of the art process, have radial cracks in as received condition. Under the stresses induced during the composite fabrication and during the thermal cycling in service, these cracks propagate and are one of the causes of the failure of the turbine blades made from these composites. Conceivably use of the electro-acoustic process can enable the fabrication of relatively high quality crack free high strength W alloy wires. The same technology can be applied to molybdenum wires, ribbons and sheets. The USSR workers also reported beneficial use of electric current and fields as well as magnetic and acoustic fields in

the heat treatment processes and improvement of fatigue and creep behavior of metallic materials. A number of papers in this workshop will describe these contributions.

In view of these interesting results reported in the USSR literature and their potential application in thermomechanically processing of difficult to form metals, ARO has been sponsoring research in the area of the effect of electric current pulses and fields on the mechanical behavior of metals for the last six years. Professor Conrad and co-workers have summarized their results in an excellent review published recently (4). They will report the results of their more recent work at this workshop.

During recent years there have been papers on the effect of magnetic field and radiations. Again most of them were from the USSR school. The first Soviet work was published in 1937 by A.V. Alekseev, who reported hardening of high strength steel by magnetic treatment. Since then hundreds of articles and three monographs have been published in USSR. The beneficial effects reported (10) include strengthening of materials, controlling or retarding of cracks, and improved wear resistant and machine tool life. Dr. Naum Tselesin, who has translated some of the Soviet literature on the subject will review them. Professor Hochman who has recently completed an ARO supported study will discuss the effect of the magnetic field on the stress relaxation in welds.

The photomechanical effect is the variation in hardness, as measured by microindentation tests, with illumination of the surface of a semiconductor. Original experiments demonstrating photoplasticity in semiconductors were carried out by Osipyan and Savachenko (11). They found that when CdS was irradiated with visible light, the stress for plastic deformation under indentation increased by as much as 25% at 70°C. Holt (12) in 1965 reported a large increase in hardness (Figure 5) with illumination in GaAs, GaP and PbS. Under other conditions illumination can also induce softening. These changes have been attributed to the interaction between charged dislocations in the material and the electronic defects generated by the illumination. However, the nature of these interactions is a subject of much controversy. Photo-mechanic effects are of considerable concern in the electronic packages. Electromagnetic radiations and nuclear radiations can cause similar effects.

There are a number of other mechanical effects such as piezoelectricity, electrostriction and magnetostriction which may be weaker than the more dramatic electro or magneto mechanical effects, but they are also important. In general the basic mechanisms of all these effects are not very well understood. In Table I an effort is made to summarize the influence of various force fields, excluding thermal and external stresses, on the mechanical behavior of materials.

In other disciplines also field effects are opening up exciting new applications. Sonochemistry and plasma chemistry are such examples. Plasma assisted CVD has made possible the synthesis of diamond films. Crystals with predetermined crystallographic orientation can be grown by applying magnetic field in appropriate direction. For example Figure 7 shows growth of iron whiskers aligned in the direction of the applied field. Those without the field grow in random directions (13).

Table II summarizes potential applications of this exciting emerging technology which are of interest to the DoD.

The above clearly indicates new opportunities of not only fundamental contributions to the theory of solid state, but also potential improvements in the processing technology and new ways to enhanced performance of important materials. These considerations have prompted ARO to hold this workshop.

The objectives of this workshop are to review the ongoing work on the effects of the various forms of energy, other than thermal and external stresses on the mechanical behavior of materials, and to identify critical technical issues which must be addressed to make a headway to understand the mechanisms involved in these effects and exploit this emerging technology. The program will start with the considerations of the fundamental mechanisms relevant to the physical effects to be discussed, followed by the discussion of the mechanisms involved in specific mechanical effects and a full session on the materials processing. The spirit of this workshop is to exclude from its scope the thermally and mechanically induced effects.

There will be a general discussion at the end of the first day and a Panel discussion at the end of the workshop. These are important forums to bring out the salient issues and make recommendation for future research.

REFERENCES:

1. M. Geradin, *Compt. Rend.*, 53 (1861), p 727.
2. O.A. Troitskiy and V.I. Likhtman, *Dokl. Acad. Nauk SSSR* 148 (1963), p 332; O.A. Troitskiy and A.G. Ronzo, "Electroplastic Effect In Metals", *FIT*, 1970, vol 12(1), p 203.
3. O.A. Troitskiy, "The Electromechanical Effect In Metals", *Pis'ma v ZhETP* (1969) vol 10(1) p 18; V.I. Spitsyn and O.A. Troitskiy, "Electroplastic Effect In Metals", *Vestnik AN SSSR*, (1974), 11.
4. Hans Conrad and Arnold F. Sprecher, "Electroplastic Effects In Metals", In *Dislocation In Solids*, Ed. F.R.N. Nabarro, Elsevier Science Publishers B.V., 1989, p 499-541.
5. F. Blaha and B. Langanecker, *Z. Naturwiss.*, vol 20 (1955) pp 556-557; B. Langanecker and O. Vodep: *Ultrasonics International*, 1975 Proceedings, pp 202-204.
6. Semen P. Kundas et al, Minsk Radioengineering Institute, Minsk. Pat. No 2716769 (FRG).
7. K.M. Kalimov, I.I. Novikov and G.D. Shnyrev, "Electric Current Induced Ductility In Heat Resistant Metals and Alloys For Rolling Wire Into Strip" *Fiziko-mechanicheskiye i teplofizicheskiye svoystva metallov. Sbornik k 60 - letiyu I.I. Novikova*, Moscow, Nauka (1976), p 183; "Tungsten and Tungsten Alloys-An Assessment", R.C. Technical Research Corporation, P.O.B. 7242, McLean VA 22106, TRC 89-0001 TR, March 1989, p 3-39.
8. V.I. Spitsyn, A.V. Kop'yev, V.G. Ryzkhov, M.G. Sokolov, and O.A. Troitskiy, "Mill For Finest Tungsten Spring Band Using Ultrasonic and Electric Current Induced Ductility", *Dokl. AN SSSR* (1977) vol 236, (4), p 861.
9. I. Ahmad and J. Barranco, "W-2% Thoria Filament Reinforced Cobalt Base Alloys", in "Advanced Fibers and Composites For Elevated Temperatures", Eds I. Ahmad and B. Noton, TMS-AIME Proceedings, 1979, p 195.
10. Naum Tselesin, this Workshop.
11. Yu A. Osip'yan and I.B. Savachenko, *ZhETF Pis'ma* 7, 130 (1968).
12. D.B. Holt, "Photo and Electromechanical Effects In Semiconductors", in *Proceedings of the Metallurgical Society Conference 35, "Environment-sensitive Mechanical Behavior"*, Baltimore, Md June 7-8, 1965, Eds. A.R. Westwood and N. Stoloff, p 269-292.
13. I. AHMAD, "Process of Forming of Iron Whiskers of Uniform Quality", US Pat. No. 3607451, (1971).

TABLE I: SUMMARY OF THE FIELD EFFECTS ON MECHANICAL BEHAVIOR OF MATERIALS (THERMAL AND MECHANICAL STRESS EXCLUDED)

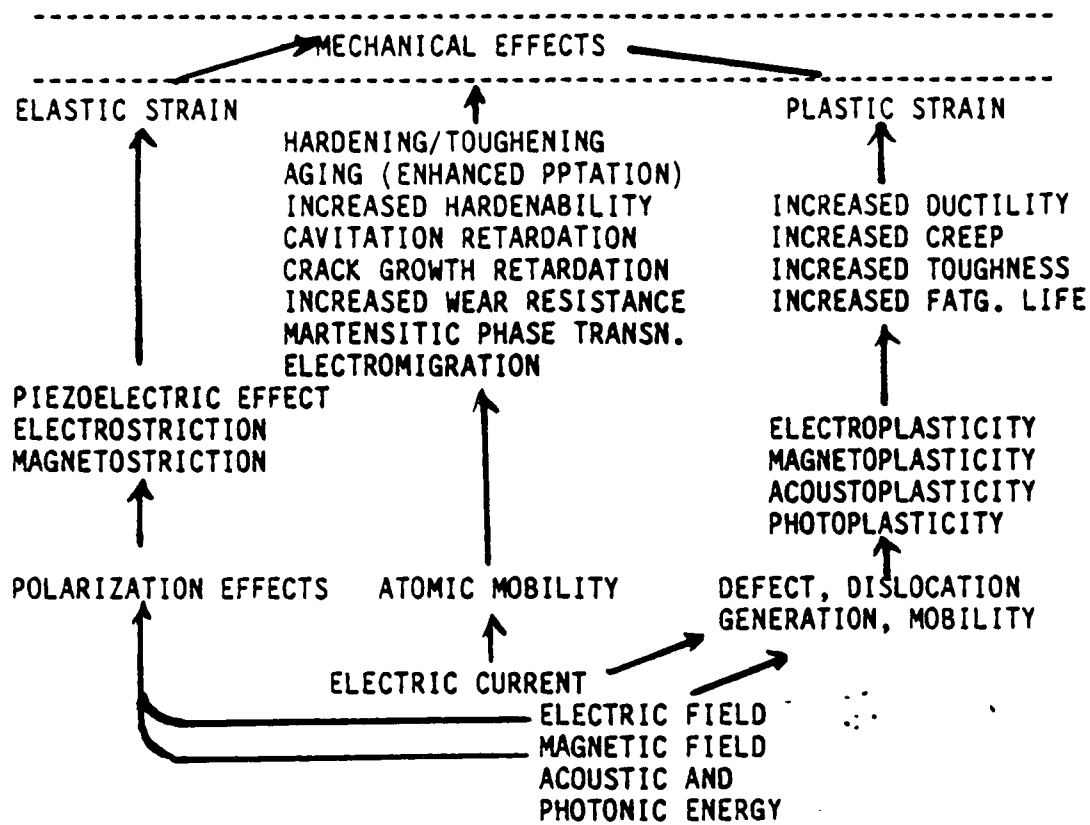


TABLE II. POTENTIAL PAYOFFS

APPLICATION	MATERIAL	PAYOFF
SHAPING OF HARD TO WORK MATERIALS (ARMAMENTS, HI TEMP COMPONENTS, ROTORCRAFT)	W, Mo, CR, Ti INTERMETALLICS	IMPROVED QUALITY IMPROVED PERFORMANCE LOW COST
THERMOMECHANICAL PROCESSING (ARMAMENTS, VEHICLES, TOOLS)	FERROUS AND NON-FERROUS ALLOYS, INTERMETALLICS, CERAMICS	IMPROVED QUALITY ENERGY SAVING IN HT TREATMENT PROCESSES
NOVEL MATERIALS AND SYSTEMS (ARMAMENTS, VEHICLES, ROTORCRAFT, RAILGUN, ELECTROTHERMIC GUN)	FERROUS/NON FERROUS ALLOYS, INTERMETALLICS, CERAMICS ELECTRONIC MATLS	INCREASED FTG LIFE INCREASED WEAR RESIST REDUCED CREEP SUPERIOR WELDS SUPERIOR LAUNCHERS
MECHANISMS	NEW THEORIES OF VARIOUS FIELD EFFECTS ON THE MECH BEHAVIOR OF MATERIALS	

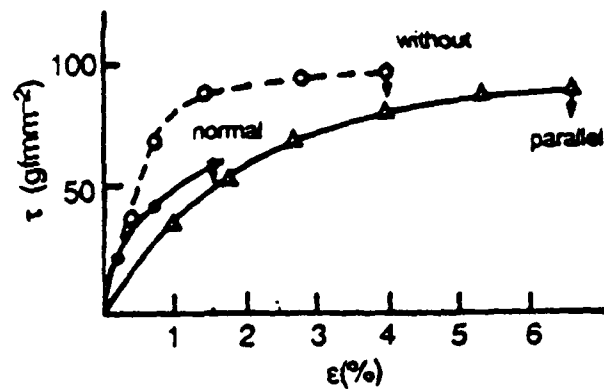


Figure 1: Stress-elongation curves for Zn single crystal specimen irradiated with directed electrons beam during plastic deformation at 77K. (Δ) parallel to the glide plane; (\bullet) normal to the glide plane; (\circ) without irradiation.

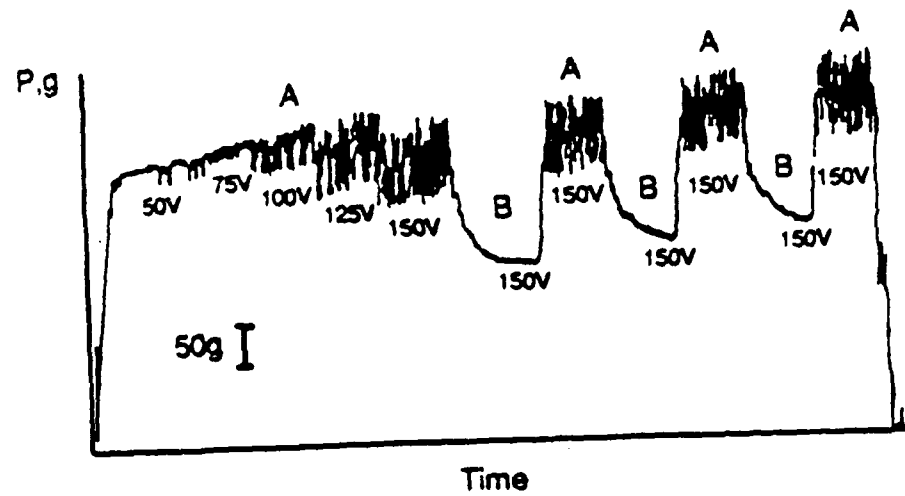


Figure 2: Load vs time diagram for a Zn crystal in uniaxial tension at 78K and strain rate of $1.1 \times 10^{-4} \text{ s}^{-1}$ showing load drops resulting from the application of $1.5 \times 10^5 \text{ A/cm}^2$ dc pulses. Regions A correspond to constant extension rate, regions B to stress relaxation.

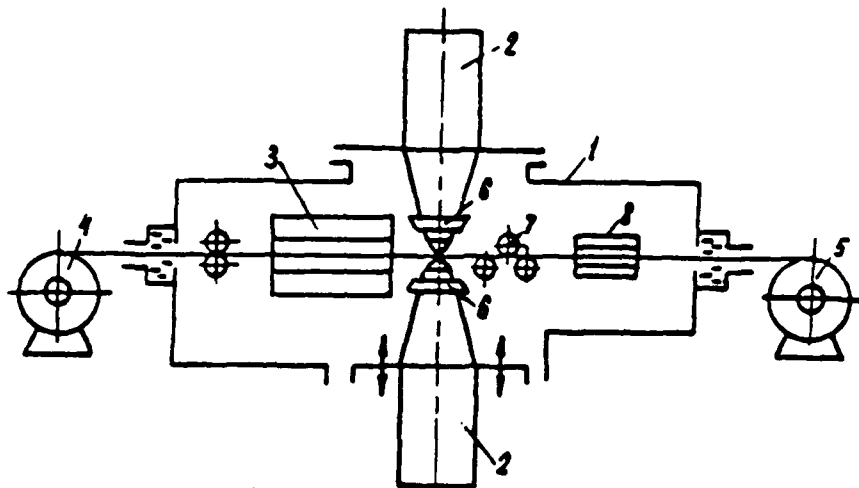


Figure 3(a): Schematic of VHUF method of flattening of Mo and W wires. 1-Vacuum chamber; 2-Ultrasonic source-magnetostrictive transducers with 0.4-4.5KV power with resonance frequency in 18-44 kHz range; 3-Wire heater (800-1600K); 4 and 5-Pay-off and take-up reels; 6-Unit to measure ultrasonic amplitude; 7-Wire tensiometer; 8-Thickness gauge.



Figure 3(b): Ultrasonically flattened Mo strip (x70) after recrystallization anneal at 1400K for 30 minutes.



Figure 3(c): Rolled Mo strip (x120) after recrystallization anneal at 1400K for 30 minutes.

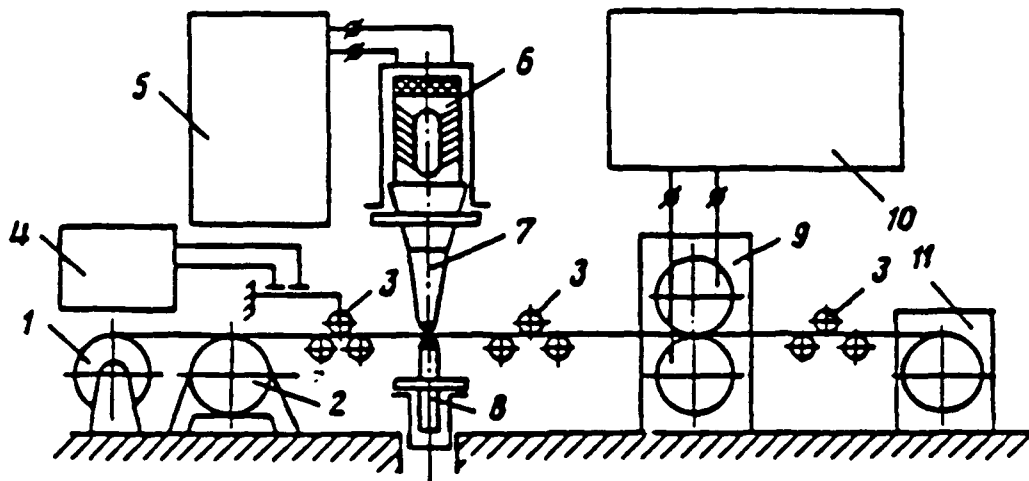


Figure 4: Schematic of experimental mill for flattening a wire into strip: 1-Unwinding reel; 2-Direct current motor; 3-Tension gauge; 4-Strain station; 5-Ultrasonic generator; 6-Transformer; 7-Concentrator; 8-Reflector; 9-Double-roll stand; 10-Electric current source; 11-Take-up reel.

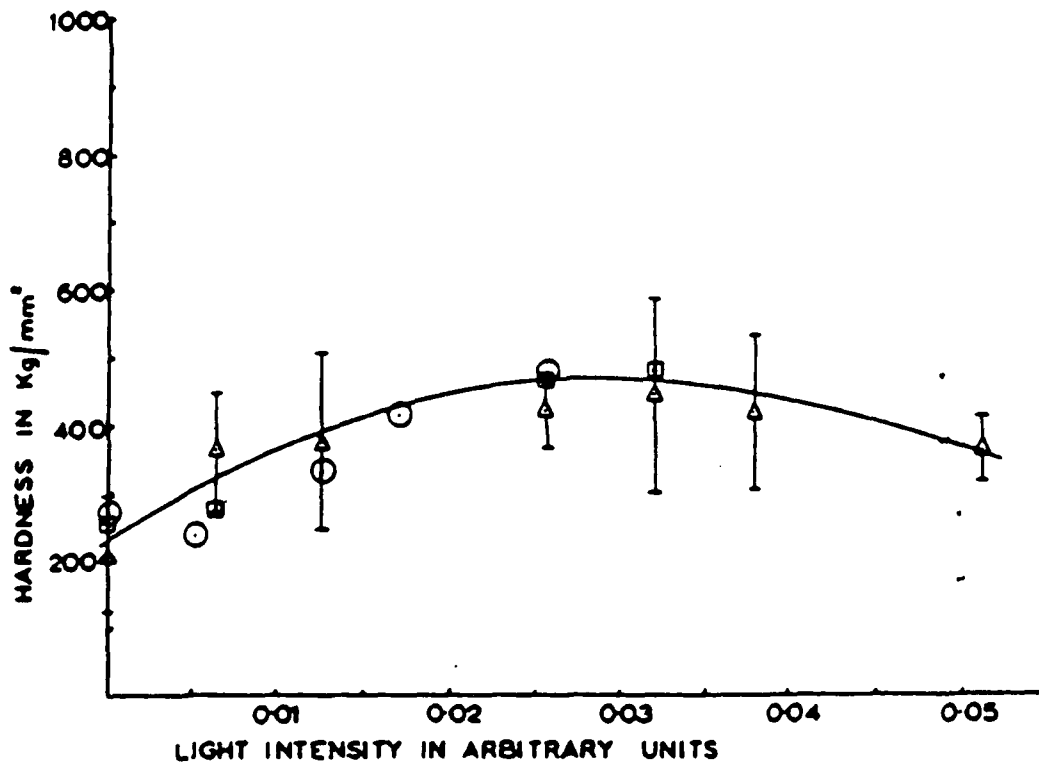


Figure 5: Hardness versus light intensity measurements on the arsenic face (○ specimen 1, △ specimen 2) and the gallium face (□) of semi-insulating GaAs. 95 pct confidence limits are indicated by vertical bars. (12)

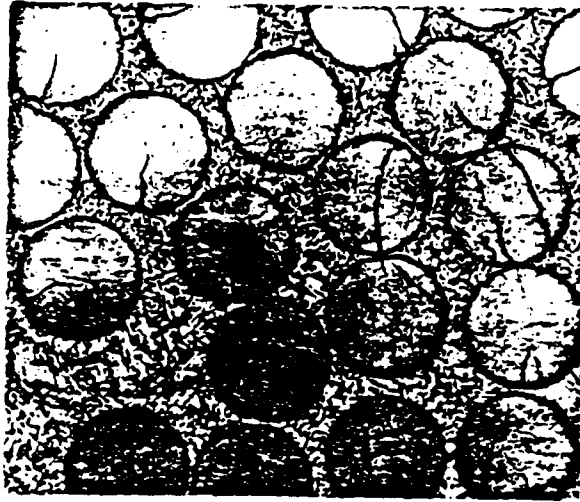
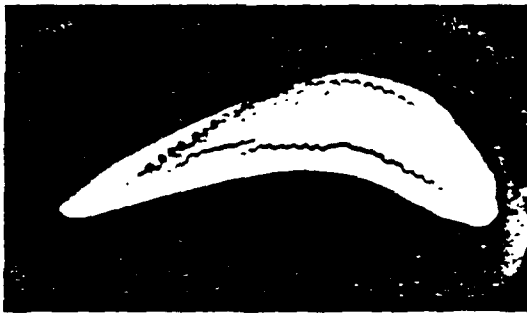
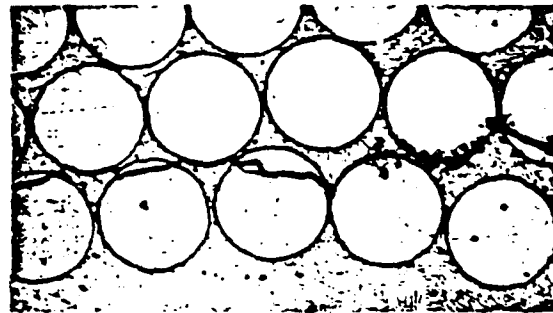


Figure 6(a): Cross-section of a composite containing
.40 V_f W-2% ThO_2 filaments (x 20).



(b)

Figure 6(b): Transverse section of cast JT9D composite
blade (x 3).



(c)

Figure 6(c): Showing connecting pattern of cracks, some
initially present in the filaments (x 20).



(a)



(b)

Figure 7: Showing whiskers of iron grown by CVD.

- (a): Without superposition of magnetic field, growing in a random fashion.
- (b): With superposition of magnetic field. Note all of these are aligned parallel to the field.

**A SURVEY OF RESEARCH INTO ELECTROMAGNETIC AND
ACOUSTIC EFFECTS ON MECHANICAL BEHAVIOR AND
PROCESSING OF MATERIALS**

by

**George Mayer
Institute for Defense Analyses**

A literature search has been conducted into the roles of electrical, magnetic, acoustic and microwaves in influencing the physical properties and forming of inorganic materials. Activities in these areas and trends in research over the last three decades are reviewed.

Electron Theory of the Solid State

Barry M. Klein

Complex Systems Theory Branch
Code 4690
Naval Research Laboratory
Washington, D. C. 20375-5000

It is now possible to give a good first-principles description of many properties of condensed matter systems based on modern techniques of electronic structure theory. Utilizing advances in the theoretical framework, such as the local density approximation (LDA) for exchange and correlation, sophisticated algorithms and supercomputers, theoreticians can now simulate many aspects of the experimental environment. Examples include predictions of crystal structural parameters and elastic constants; superconducting properties; dynamic behavior such as crystal growth and surface reconstruction; lattice dynamics; and transport properties. As examples of the accuracy of such calculations, predicted structural parameters and mechanical properties (e.g. lattice and elastic constants) are, in general, accurate to 1% and 10%, respectively. Electronic structure theory, besides adding insights into the interpretation of experimental observations, has a predictive capability which is a useful adjunct to experimental searches for new, better materials. In this paper I will describe several of the methods used, and some illustrative results of electronic structure theory. Some of the future developments needed to address aspects of the Workshop topics will also be discussed, including the need for more efficient quantum mechanical basis sets and computer algorithms for large, complex systems; and the need for improvements beyond the LDA to treat excited states and magnetic materials.

INTRODUCTION

Modern electronic structure theory has evolved over the past few decades to the point where "real" materials properties may be determined theoretically and compared with experiment. This not only adds interpretation and insights into observed phenomena, but also offers the possibility of predicting new materials with enhanced desirable properties. Especially in the past ten years, theories and computer codes have reached highly sophisticated levels, with a firm understanding of the reliability and accuracy of calculated phenomena, and a closer matching of theoretical and experimental "conditions". In what follows, I give a brief discussion of the formal underpinnings of these approaches, some examples of the kinds of results that may be obtained, and some prognostications of where this theoretical/computational research is going.

DENSITY FUNCTIONAL THEORY

On the intuitive level, knowing the atomic positions and the electronic charge density of a condensed matter system provides a wealth of information about many of the physical properties. The theorems of Hohenberg, Kohn and Sham [1] formalize this by showing that the ground state total energy of a system of nuclei is a unique functional of the electronic density --- e.g., if you know the density you know the total energy. Using their formalism, one can show that the following system of equations follows:

$$E_{\text{tot}}[n(\mathbf{r})] = E_{\text{H}}[n(\mathbf{r})] + E_{\text{xc}}[n(\mathbf{r})]$$

$$[-\nabla^2 + v_{\text{eff}}(\mathbf{r}) - \epsilon_i] \psi_i(\mathbf{r}) = 0$$

$$n(\mathbf{r}) = \sum_i^{\text{occ}} |\psi_i(\mathbf{r})|^2 .$$

Here, E_{H} is the Hartree contribution to total energy, containing electron-nucleus and electron-electron coulombic terms. E_{xc} is the exchange-correlation contribution for the electrons (fermions). The electron density, $n(\mathbf{r})$, is determined from the occupied one-electron orbitals, $\psi_i(\mathbf{r})$, which are in turn determined from the Schrodinger equation with an effective potential, $v_{\text{eff}}(\mathbf{r})$.

The above equations represent a well-defined approach for determining the self-consistent electron density, the mean potential that the electrons move in, and the ground state total energy of the system of nuclei and electrons. Magnetic and/or electric fields may be included or not, with paramagnetic or spin-polarized calculations for the electron system. The one-electron equation for the electron orbitals contains energy parameters ϵ_i which, strictly speaking, are not rigorously the one-electron energies that are seen experimentally, but in practice there is a "practical" relationship, and often good quantitative agreement between the ϵ_i and experiment. The key "unknown" ingredient in these procedures is the precise form of the exchange-correlation energy and its

derivatives, but the local density approximation form has proven to be entirely adequate in most cases. In this approach, the E_{xc} is obtained from results of the homogeneous electron gas, with the value of E_{xc} at the density $n(r)$ being that of the homogeneous electron gas at that density. This local potential is straight forward to implement, in practice.

It is important to recognize that this is a ground state theory, with the only rigorously determined quantities being the ground state charge density and total energy. In practice, though, the one-electron eigenenergies have a good deal of quantitative relevance, with one of the most glaring counter examples being the lack of agreement between theory and experiment for the band gap in semiconductors and insulators. Examples of ground state properties that can be determined are: structural parameters, elastic constants, and phonon spectra; some examples are discussed below. Also, defect problems can be tackled using "supercell" methods. A recent review of applications to the high- T_c oxide materials has been given by W. Pickett [2].

The most rigorous, but computer intensive, approach for solving the Kohn-Sham equations is to do self-consistent loops until the input and output charge densities match, and the total energy converges (there is a variational principle operating so that convergence tends to be smooth and systematic). Generally, these approaches are very robust, with a host of methods used to solve the effective one-electron Schrodinger equation for the solid in question. Using Bloch's theorem is, generally, crucial for computational viability for the "bulk" calculations, although cluster methods are gaining increasing favor for certain kinds of problems. A paper by M. Pederson, J. Harrison and B. Klein illustrates these latter methods [3]. For the Bloch periodic systems, one deals with a unit cell of several atoms, and chooses some convenient basis set for expanding the one-electron orbitals --- e.g. plane waves, gaussians, etc. --- and proceeds in solving the set of equations in a straight forward, but very computer intensive manner.

The fully *ab initio* self-consistent method that we favor is the full-potential linearized-augmented-plane-wave (LAPW) method [4] which makes no approximations as to the shape of the charge density or potential in solving the Kohn-Sham equations. This is a workhorse electronic structure method for many of the groups working in this field, although other approaches, when properly implemented, converge to the same result. In the LAPW method, one expands the single-particle orbitals in a dual representation: atomic-like functions near the nuclei (in the so-called muffin-tins) and by plane waves in the interstitial region where the potential and charge density are rather slowly varying. Appropriate matching of the dual representation at the muffin-tin boundaries are performed to ensure continuity of the wavefunction.

Alternatively, with less rigor but several orders of magnitude less computation, one can use model charge densities in one pass of the equations and bypass the self-consistency procedures. These generic "constrained density models", which are physically/chemically motivated, have proven to be very useful and accurate in many cases [5]. Some examples are given below. Other methods, such as the embedded atom approach [6] also make an *ansatz* for the potential/density, but have the advantage of being able to deal with much larger systems, such as extended defects.

Structural and Elastic Properties of Ordered Intermetallics

The ability to calculate structural parameters, stability or instability of phases, and elastic properties, etc., can be a big asset in programs to develop better high-temperature alloys, for instance. We are embarked on such a program at NRL, and we show several examples which illustrate the state-of-the-art. We refer the reader to a recent article by Chubb, Papaconstantopoulos, and Klein [7], on Ti-Al alloys for details of the method, etc. Some results are shown in Figures 1 and 2. The structural parameters are determined by finding the global minimum of the total energy, using the above procedures, as a function of all of the internal parameters of a given structure. The bulk modulus is related to the second derivative of the total energy at the minimum; other elastic constants are determined by straining the theoretical crystal about the ground state structural minimum. Various structures can be tested to see which one has the lowest total energy. As can be seen, these LAPW studies predict the structural parameters to of order 1%, and the elastic behavior (where known experimentally) to about 10% accuracy. Discrepancies are usually ascribed to the local density approximation or, in some cases, to experimental uncertainties. It should be noted that these are true theoretical predictions, as experimental information is not used in the calculations. We note that phonons can be calculated using similar techniques, freezing in the phonon displacements and using the total energy second derivatives to determine the force constants.

Cluster Methods

As remarked above, local density methods can also be applied to systems without using Bloch periodicity, to clusters, for instance. As an example, consider work done by M. Pederson, J. Harrison and B. Klein on lithium clusters using a gaussian basis set [3]. As can be seen from Figure 3, it is possible to extrapolate from finite clusters to the infinite bulk using rather modest sized clusters, with quite good agreement with experiment. One advantage of these cluster methods is that they can often be done in a computationally more efficient way than bulk LAPW, especially for the cases of treating defect structures. Speeding up methods and codes is a very active field of research right now with the potentially big payoff of being able to treat "larger" systems.

Magnetic Systems

The electronic structure calculations can also be done in a spin-polarized mode or in the presence of external electric or magnetic fields. For the magnetic case, discrepancies with experiment are significantly larger than for paramagnetic calculations due, it is believed, to the inadequacy of the local spin density approximation. See [8] for a good, relatively recent discussion. Major efforts are underway by a number of groups to go "beyond the local density approximation" with improvements to be expected in the coming years. Motivated by the unusual new results discussed at this conference, perhaps many of these limitations can be eliminated soon.

Constrained Density Models

The first two examples were fully *ab initio* self-consistent studies which were extremely computer intensive. Although "guessing" at the right density in the Kohn-Sham equations circumvents the great majority of the computational burden, it requires physical/chemical insight into the specific nature of the bonding in the materials in question. For ionic materials, for instance, it is a good approximation to choose the model of the self-consistent charge density to be that of overlapping ionic charge densities obtained from isolated-ion atomic structure calculations which can be done quite rapidly on the computer. Allowing the radial charge densities to "breathe" in response to the ambient crystal field greatly improves these calculations for many materials (the "potential induced breathing", PIB, model [5]). L. Boyer and colleagues at NRL have shown that this approximation for ionic materials, such as alkali halides, works very well in studies of equations of state, melting, thermal conductivity, elastic behavior, etc. Figure 4. shows results of elastic constants using the PIB approach with very good agreement with experiment. PIB works very well for many ionic systems, so well that comparisons of the charge density and electronic structure using PIB and LAPW are often close to indistinguishable!

CONCLUSIONS

Modern electronic structure theory and computational approaches offer the opportunity of addressing "real" materials properties. Where the methods have been compared with experimental results, agreement has usually been very good for ground-state related properties. There are many remarkable opportunities ahead as theoreticians hone their tools to address increasingly complex phenomena such as extended defects (grain boundaries, dislocations, etc.), and the effects of large electromagnetic fields. A major challenge for the future is to develop new computational methods built on the current successes that are computationally viable for these extended systems. In a sense, the fully self-consistent *ab initio* methods act as a theoreticians experiment, enabling the development of simpler physically and chemically motivated models of the materials world.

ACKNOWLEDGMENTS

The work discussed here involved collaborations between members of the Complex Systems Theory Branch of the Naval Research Laboratory. Support for parts of this work came from the Office of Naval Research and the NSF-supported Pittsburgh Supercomputer Center and the National Center for Supercomputer Applications.

REFERENCES

- [1] Excellent reviews of density functional theory can be found in: W. E. Pickett, *Comments on Solid State Phys.* 12, 1 (1985); *ibid.* 59 (1986); W. Kohn and P. Vashista, in Theory of the Inhomogeneous Electron Gas, S. Lundqvist and N. H. March, editors (Plenum Publishing Corporation, 1983).
- [2] W. E. Pickett, *Reviews of Modern Phys.* 61, 433 (1989).
- [3] M. R. Pederson, J. G. Harrison, and B. M. Klein, *Mat. Res. Soc. Symp.* 141, 153 (1989).
- [4] A good exposition of the method and references is given in: E. Wimmer, H. Krakauer, M. Weinert, and A. J. Freeman, *Phys. Rev. B* 24, 864 (1981).
- [5] L. L. Boyer, *Phys. Rev. Lett.* 42, 584 (1979); L. L. Boyer, M. J. Mehl, J. L. Feldman, J. R. Hardy, J. W. Flocken, and C. Y. Fong, *Phys. Rev. Lett.* 54, 1940 (1985).
- [6] M. S. Daw and M. I. Baskes, *Phys. Rev. B* 29, 6443 (1984).
- [7] S. R. Chubb, D. A. Papaconstantopoulos, and B. M. Klein, *Phys. Rev.* 38, 12 120 (1988).
- [8] C. S. Wang, B. M. Klein, and H. Krakauer, *Phys. Rev. Lett.* 54, 1852 (1985).
- [9] R. E. Cohen, *Geophys. Res. Lett.* 14, 37 (1987).

FIGURE CAPTIONS

1. Structural parameters and elastic constants of $L 1_0$ structure TiAl from [7].
2. Unpublished structural parameters and elastic constants of B1 structure SbY.
3. Elastic constants of Al_2O_3 from [9].
4. Results for simulation of crystal growth using cluster methods from [3]. A_0 is the atomic separation, B is the bulk modulus, and U is the cohesive energy.

First-principles study of $L1_0$ Ti-Al and V-Al alloysS. R. Chubb,^{*} D. A. Papaconstantopoulos, and B. M. Klein*Condensed Matter Physics Branch, Condensed Matter and Radiation Science Division, Naval Research Laboratory,
Washington, D.C. 20375-5000*

(Received 11 May 1988; revised manuscript received 25 July 1988)

TiAl (AuCu I structure) ($L1_0$)**Theory Experiment****Lattice constants (\AA)**

a	3.94	3.99
c	4.02	4.07
c/a	1.02	1.02

Bulk Modulus (MBar)

1.95

Elastic moduli (MBar)

$C_{11}+C_{12}$	5.8
C_{13}	2.01
C_{33}	1.95

Figure 1.

SbY (Sodium Chloride structure) (B1)

Theory Experiment

Lattice constant (\AA)

a 6.12 6.11

Bulk modulus (Kbar)

670 660

K_0' 3.5

Elastic constants (KBar):

C_{11} 1800

C_{12} 100

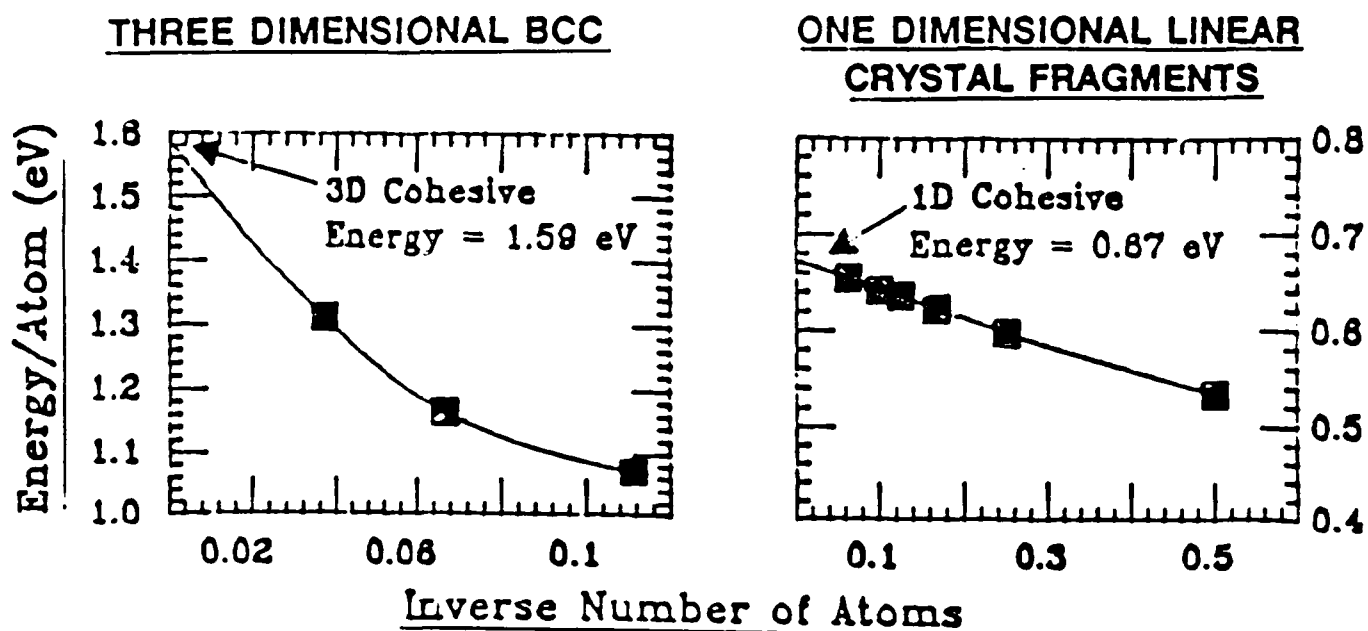
C_{44} 260

$\langle G \rangle$ 430 405

Figure 2.

A SIMULATION OF CRYSTAL GROWTH

By studying successively larger crystal fragments, the transition from atomistic to bulk phenomena may be observed:



<u>No. of Atoms</u>	<u>A_0 (au)</u>	<u>B (Mbar)</u>	<u>U (eV)</u>
9 atoms	5.62	0.15	1.07
15 atoms	6.36	0.11	1.17
27 atoms	6.16	0.13	1.31
<u>Infinity</u>			<u>1.59</u>
Bulk-KKR-MT	6.42	0.15	1.65
Bulk-LOGO	6.52	0.14	1.65
Bulk-LAPW	6.36	0.15	1.77
<u>Bulk-Expt.</u>	6.58	0.12	<u>1.63</u>

Figure 3.

**Static elastic constants (in GPA)
and pressure derivative at zero
pressure for Al_2O_3 (corundum).**

	Elastic Constants		P Derivatives	
	PIB	Exp.	PIB	Exp.
C_{11}	540	498	5.78	6.17
C_{12}	157	163	3.44	3.28
C_{13}	130	117	3.56	3.65
C_{14}	-48	-23	0.18	0.13
C_{33}	455	502	4.36	5.00
C_{44}	157	147	1.62	2.24
C_{66}	191	168	1.17	1.45
K	261	254	4.06	4.32

Experimental data: Gleske and Barsch (1968)

Figure 4.

DISCUSSION OF BARRY M. KLEIN'S PAPER

H. Conrad:

1. What fundamental properties of the electrons are needed to carry out the calculations which you discussed?
2. Can you calculate the effect of an external magnetic or electric field on the energy E_f^v to form a vacancy? If so, what is the nature of the relationship between E_f^v and the magnetic or electric field?

B. Klein:

1. Phonon spectra are calculated from first principles. The self-consistent electron densities and total energies are determined as a function of the nuclear locations — for "small" displacements from their equilibrium positions. The phonons are found from the coefficients of the second derivative of the total energy with displacement.

In these "all-electron" methods, all the electrons are treated from first principles.

2. Vacancy formation energies can be calculated for the case of applied EM fields, but I'm not aware of any previous calculations. I see no impediment to doing such calculations in the future.

D. Wilsdorf:

1. Can you calculate the coefficient of thermal expansion?
2. How do your methods relate to the "embedded atom" method?

B. Klein:

1. Temperature-dependent properties, such as thermal expansion, can be calculated but are very computer intensive. Most of the work done has been performed using constrained density approaches with very good agreement with experiment. More can and will be done in the future.

Klein's paper (Continued)

2. The first-principles, self-consistent methods I described do not "model" the potential as the embedded atom method does. The first-principles results can be used as "input" to determine the embedded atom potential parameters. This is being done. Of course the embedded atom method is much faster (but less accurate) on the computer and, hence, can deal with much larger systems than the first-principles methods. The strategy of using the full-blown methods to benchmark more approximate approaches is expected to continue.

H. B. Huntington:

1. Can you distinguish between two phases of the same material? In particular two phases with the same number of nearest neighbors, such as fcc vs hcp?
2. Is the basic approximation of the Local Density Approximation (LDA) the choice of the $V_{\text{ex-cor}}$ potential?

B. Klein:

1. We can distinguish between different phases, including fcc vs hcp if the energy differences are ~ 1 mRyd or more. That's the scale of accuracy of these first-principles calculations.
2. There are two aspects to the local density approximation: (1) the exchange-correlation potential depends on the **local** electron density at the point being sampled; and (2) this potential is that of a homogeneous electron gas of the same density as the point being sampled. The first is a fundamental aspect of LDA, and the second is the practical prescription for determining the potential.

PHONONS, ELECTRONS, AND DEFECTS

A. C. Anderson

Department of Physics
and
Materials Research Laboratory
1110 West Green Street
Urbana, IL 61801

The introduction of either a finite electrical current or a finite strain rate to a metal or dielectric solid will, with few exceptions, cause an accumulation of thermal energy in that solid. The subsequent behavior of the solid depends critically on how efficiently the thermal energy is removed. The purpose of my presentation is to review some of the physics intrinsic to these thermal transfer processes. Much of the experimental work in this field has been carried out at cryogenic temperatures, since the individual energy transfer processes can be studied more readily at reduced temperatures.

For most practical devices, heat is removed via phonon transport. For one not familiar with phonon physics, it may be helpful to keep in mind the close analogy with photon physics. Phonons exhibit a black-body frequency spectrum peaked near the energy kT and with a width at half maximum of $\approx kT$. The Stefan-Boltzmann law indicates that the rate of energy exchange Q between two solids in intimate contact and at temperatures T_1 and T_2 is proportional to $T_2^4 - T_1^4$ or, if $T_1 - T_2 = \Delta T$ is not large, $T^3 \Delta T$. Hence one may define a thermal boundary resistance between two solids, $R_B = \Delta T / Q \approx 1 / AT^3$ where A is the area of contact between the two solids. The thermal resistance R_B is important when the phonon mean free path $\ell \gg D$, a dimension of the solid. Hence R_B is generally of little importance at room temperature except for very small devices. The theory of R_B is under control and depends only on the acoustic properties of the two solids.¹⁾

The acoustic behavior of any crystal is extremely anisotropic. The most vivid evidence of this anisotropy, and a phenomenon relevant to thermal transport, is phonon focusing. If a small heater is placed at the center of one face of a cube, the arrival pattern of phonons on the other five faces of the cube is highly localized in a manner which depends sensitively on the ratios of elastic constants.²⁾ This anisotropy must be considered in any discussion of phonon transport, or in phonon interactions with electrons or defects.

When an energy flux is introduced to a metal or semiconductor by an electrical current, the effective temperature of the charge carriers (here called electrons for convenience) must increase with time unless that energy is transferred to the phonons. In brief, we are here interested in the electron-phonon interaction. An early theory gives acoustic attenuation varying roughly as $\beta\omega$ where ω is the phonon frequency.³⁾ If, then, the electron gas is heated to a temperature of $T + \Delta T$ through application of an electric field, a thermal resistance R_V may be defined between the hot electrons and the phonon bath at temperature T , $R_V \approx 1 / \beta VT^4$. Here V is the volume of sample in which Joule heating occurs. R_V is of little importance for metals except for very small devices.⁴⁾ However, if the electron density is decreased (i.e. β is decreased), R_V can become a problem. Examples are alloys near the metal-insulator transition⁵⁾, metals near the superconducting transition, and semiconductors in general, especially in devices where one or two dimensions of V are constrained.⁶⁾

A consequence of strain is the introduction and acceleration of dislocations. Since the dislocation-dislocation interaction is weak (compared, for example, to the electron-electron interactions), one cannot ascribe an effective temperature to the dislocations. Nevertheless, the energy absorbed by the dislocations is transmitted to the local phonon (and electron) populations. This interaction with *thermal* phonons can be measured directly in cryogenic heat-transport experiments. In ionic and metallic crystals the phonon-dislocation interaction is dynamic in character and can be described by the simple "fluttering dislocation" model.⁷⁾ The most beautiful evidence for fluttering dislocations is derived from ballistic-phonon (heat-pulse) measurements in which all details of the data, including the extreme anisotropy of the interaction, is found to agree with theory.⁸⁾

The interactions of phonons with a variety of other defect or excitation systems have been studied, including the tunneling states of glasses⁹⁾ and the excitations of superionic conductors.¹⁰⁾

In summary, we see that the application of a stress or electric field to a solid can excite defects, or localized excitations, with an energy which must be passed through the phonon bath to the environment of the solid or device. A variety of thermal resistances can hinder this transfer of thermal energy resulting in an effective heating of the excitations.

References

1. A. C. Anderson, in *Nonequilibrium Superconductivity, Phonons, and Kapitza Boundaries*, Ed. by K. E. Gray (Plenum, New York, 1981) p. 1.
2. J. P. Wolfe, *Phys. Today* **33**, 44 (1980).
3. A. B. Pippard, *Phil. Mag.* **46**, 1104 (1955).
4. A. C. Anderson and R. E. Peterson, *Phys. Lett.* **38A**, 519 (1972).
5. M. Osofsky, M. LaMadrid, J. B. Bieri, W. Contrata, J. Gavilano and J. M. Mochel, *Phys. Rev.* **B38**, 8486 (1988).
6. F. T. Vas'ko, *Soc. Phys. Solid State* **30**, 1207 (1988).
7. S. G. O'Hara and A. C. Anderson, *Phys. Rev.* **B10**, 574 (1974).
8. G. A. Northrop, E. J. Cotts, A. C. Anderson and J. P. Wolfe, *Phys. Rev.* **B27**, 6395 (1983).
9. A. C. Anderson, in *Amorphous Solids*, Ed. by W. A. Phillips, (Springer, Berlin, 1981) p. 65.
10. P. J. Anthony and A. C. Anderson, *Phys. Rev.* **B14**, 5798 (1976).

DISCUSSION OF A. C. ANDERSON'S PAPER

D. Wilsdorf:

Is there a strong effect of an adsorbed atomic layer on the thermal boundary resistance at interfaces?

A. C. Anderson:

When the acoustic mismatch between the two materials is large, as for Cu and He, there is an additional mechanism of energy transfer at $T > 1^\circ\text{K}$ which is not understood. This second mechanism does depend strongly on surface conditions, including adsorbed atoms.

ELECTRONIC CONTRIBUTION TO THE DISLOCATION DRAG COEFFICIENT

A.D. Brailsford

Research Staff, Ford Motor Company
Dearborn, MI 48121

ABSTRACT

A formal theory of the motion of a dislocation in a visco-elastic medium will be outlined. By this means it will be demonstrated that the linearly velocity - dependent drag force acting on the dislocation may be expressed in terms of certain phenomenological viscosities of the medium. The latter will then be shown to be derivable from straightforward generalizations of the theory of the acoustic attenuation arising from either electronic or vibrational degrees of freedom. The result for the electronic contribution that is determined by this procedure is shown to be identical to the classical result of Holstein and Kravchenko. The outcome can also be paraphrased as a kinetic theory-type viscosity result, but the number of carriers that contributes effectively to the drag is significantly less than the total number, because only those electrons moving parallel to the dislocation deformation wave fronts extract energy from the associated internal electric field.

Alternative expressions to the Holstein-Kravchenko form for the electronic drag that have appeared since the seminal work of these authors will be discussed. In addition, a brief overview will be given of effects that have been suggested to be of importance in metals with substantially non-spherical Fermi surfaces and in the change in the dislocation drag coefficient that accompanies a transition to the superconducting state.

ELECTRONIC CONTRIBUTION TO DISLOCATION DRAG

When a dislocation glides at moderate velocity in an otherwise defect free crystal, it experiences a viscous drag force due mainly to the influence of its motion on the elementary excitations of the body (phonons and electrons or quasiparticles). Such motion causes inelastic (dissipative) processes to occur within the system of excitations, thereby necessitating the input of energy from an external source in order to sustain that motion. Such inelastic events are contributory processes to the dissipative function [1] of the body, specifically to certain generalized (non-local) viscosities [2] in terms of which, along with strain rate variables, this function is determined. As a result, it is natural to anticipate the existence of some functional relationship between the drag coefficient and these same viscosity parameters, and in fact the precise nature of this connection has been known for some time [2,3]. Adaptation of the latter affords the most general approach to the drag problem. Once the geometry of the dislocation has been specified, the determination of the generalized viscosities of the host medium leads immediately (by quadrature) to the contribution to the dislocation viscous drag coefficient arising from the particular elementary excitations considered.

The generality alluded to above is manifest in the fact that some years ago it proved possible [2] to derive a unified description of the many mechanisms that had been separately proposed earlier as contributors to the drag (specifically, those to be attributed to lattice, rather than electronic effects). In particular, the comparative insignificance of thermoelastic effects relative to anharmonic scattering effects could then be established within one and the same formalism. A similar discussion of electronic effects was given shortly thereafter [3]. Basically, all that was required to arrive at this formalism was a certain generalization of the standard Boltzmann equation theories of the electronic and lattice anharmonic contributions to ultrasonic attenuation. Essentially only one single change of substance was required: namely, the dispersion relation of the lattice distortion appropriate to a sound wave needed to be replaced by that corresponding to each Fourier component of the deformation appropriate to a dislocation moving (in a first approximation uniformly) through the host dissipative medium. Specific applications of the foregoing theory to electronic and lattice processes, and for different dislocation geometries, may be found in the two references just cited.

Subsequent discussions of the same problem that have been presented by Russian investigators [4-7] have generally questioned, but never more than in passing, the applicability of the Boltzmann equation approach to this problem. In response, and for lack of more substantive criticism, one might observe first that to question the method is, simultaneously, to question the standard theory of ultrasonic attenuation. Second, it should be stated that the use of quantum mechanical perturbation theory, as advocated in these later works, had already been shown to be equivalent (for the case that the mean free path of the appropriate excitation is greater than the wavelength of the lattice distortion) to the other more general method in the case of the calculation of the sound attenuation in metals [8], the electronic contribution to dislocation drag [9-11] and lattice anharmonicity contributions to the same phenomenon [2]. And third, a recent appraisal of all theoretical models [7], while clearly sympathetic to the views of the Russian school, nevertheless comes to the conclusion that there is no substantial difference in prediction in the shared common ground between the earlier work and the later expositions. Such a conclusion is important, because as more sophisticated modern techniques (e.g. Local Density Functional Theory, in the electronic case) are brought to bear on the problem of determining how the energies of the elementary excitations are affected by strain, it will clearly remain useful to have a formalism at one's disposal for translating these results into the different

realms of dislocation drag without the necessity of re-developing the whole of the latter from first principles.

Turning now exclusively to electron drag, it appears that the fundamental similarity of mechanism in this effect and in ultrasonic attenuation in metals at low temperatures might still be explored to greater advantage than has been done to date. Thermoelastic contributions to the drag have been shown to be negligible [3], while the Boltzmann equation approach in each case is known to give the same result as quantum mechanical perturbation theory when the mean free path is sufficiently large (pure materials), as already indicated. Thus we may take the standard result for the attenuation, α , in this limit [8], as obtained from free electron (FE) theory and isotropic continuum elasticity, compare it with the formula for the electronic drag coefficient, B_e , [9-11] in the same model, and so obtain the following final expression of B_e in terms of directly measurable quantities:

$$\alpha_q = \frac{\tau}{6} \frac{\omega_q}{\rho c_t^2} n_0 m v_F : B_e = \left(\frac{1 - 2\nu}{1 - \nu} \right)^2 \frac{n_0 m v_F b^2 q_D}{96} \quad (1)$$

$$\therefore B_e = \frac{1}{2\sqrt{2}} \left(\frac{c_t}{c_l} \right)^2 G b \left(\frac{\alpha}{\omega} \right)$$

In the intermediate steps above, ν is Poisson's ratio, n_0 is the electron density, m the electron mass, q_D the Debye radius and v_F the Fermi velocity. Note, however, that the final result depends only upon the ratio of the transverse to longitudinal sound velocity, the shear modulus, G , and Burgers vector, b , and the attenuation per unit frequency, α/f , (ω is the angular frequency). In order of magnitude, B_e for a free electron metal of density similar to that of Cu is of the order 10^5 dyne.sec/cm². That magnitude also follows from the above analysis upon using the experimental values for the real material, as given in Table 1, which is reproduced from the work of Rayne and Jones [12]. However, what we consider more instructive here is the extent of the discrepancy between FE theory and experiment for the attenuation, since there must surely be discrepancies of comparable magnitude (or larger?) between FE and experimental values of B_e . Further, it should be noted that the deviations can be of either relative sense, greater or smaller. Similar calibrations can also be formed for divalent metals and so forth by more detailed perusals of ref [12] than we here have the space to pursue. It may be helpful to note, however, for any who wish to consider this theme further, that the above discussion presumes the attenuation to be linear in the frequency. For sufficiently impure metals this is not observed; instead the attenuation varies as the square of the frequency rather than the first power [8]. While for this different regime the theoretical result can still be used to eliminate the Fermi velocity, as carried out above, the ultimate expression for B_e in this case depends non-linearly upon the electrical resistivity of the material as well as on the attenuation, and so the essential attractive simplicity of eq. (1) is lost.

Though there have been attempts in the literature to boost the numerical estimate of B_e by one ruse or another using some manipulation of free electron theory and isotropic continuum elasticity, none have earned any degree of credulity. To advance the theory to any significant extent, it is necessary at the least to include the complexities of ultrasonic attenuation for real metals [12]. Moreover, it would seem equally important to consider the discrete atomic nature of the solid and use the body force distribution corresponding to such an object, instead of that for a continuum. In this context, there seems no compelling logic behind the use of arbitrary core cut-off procedures that are occasionally invoked [5], and model excitation spectra that incorporate the

associated dispersion in the spectra of excitations appear to have mainly illustrative value until justified more closely. An example which reinforces these remarks is that of the interaction between two vacancies. In continuum elasticity, this is zero at any finite separation. Within the framework of lattice statics, however, it varies inversely as the fifth power of the separation [13]. Continuum elasticity theory, but with the appropriate body forces distributed at discrete lattice sites, reproduces this dependence but gives an interaction of magnitude too large by a factor of $(4/3)$, [14]. The reason for this discrepancy is that the phonon dispersion inherent in a true lattice model is not properly included in the latter treatment. The moral for the present problem is apparent therefore: the correct dislocation form factor [2], the correct dispersion, the proper lattice-electron deformation coupling at the Fermi surface and the appropriate Fermi surface topology all require careful attention if significant improvement over eq.(1) above is to be attained.

Much detailed work remains to be done. However, by now there appears to be fairly universal agreement that the independent approaches (but common result) developed by Holstein and Kravchenko are basically correct. An early attempt [15] to link the drag with the kinetic theory (local) viscosity, and hence with the conductivity for spatially uniform electric fields, is no longer considered tenable. An alternative approach [16], which seeks to link the power dissipation associated with the drag force acting on moving dislocations to the Joule heating produced by the resistive flow of an electron gas through a stationary dislocation distribution, still receives some mention [17], even though it suffers from the same basic flaws as the kinetic theory local viscosity model. The correct description of Joule heating is to be found via the theory of ultrasonic attenuation in metals [8,11], where it is shown that the appropriate conductivity is the non-local rather than the uniform field value. Additionally, the dissipation itself is concentrated near the dislocation core rather than spread uniformly throughout the entire body. Attention to both these factors converts the result of ref. [16] to that of eq. (1). Accordingly, we conclude that forms of the drag force that supposedly follow directly from the dislocation contribution to the electrical resistivity [16,18] are theoretically unjustified.

A.D. Brailsford
Research Staff
Ford Motor Company
Dearborn, MI 48124

July 25, 1989

Table 1

Metal	Propagation Direction	Attenuation/Frequency (dB /cm. MHz)		Ratio Expt/FE
		Expt	FE*	
Copper	[001]	0.186	0.0985	1.88
	[110]	0.072	0.0691	1.03
	[111]	0.051	0.0747	0.68
Silver	[001]	0.095	0.0811	1.17
	[110]	0.062	0.0603	1.02
	[111]	0.050	0.0649	0.77
Gold	[001]	0.122	0.0531	2.29
	[110]	0.093	0.0445	2.09
	[111]	0.031	0.0464	0.67

* Computed for one electron per atom and the appropriate sound velocity. (After ref. 12).

References

1. L.D. Landau and E.M. Lifshitz, *Statistical Physics*, 2nd ed., p. 378, Addison - Wesley Publishing Co. Inc., Reading (1969).
2. A.D. Brailsford, *J. Appl. Phys.* 43, 1380 (1972).
3. A.D. Brailsford, *Internal Friction and Ultrasonic Attenuation in Crystalline Solids*, (edited by D. Lenz and K. Lucke), Vol. II, p.1, Springer - Verlag, New York (1975).
4. V.I. Alshits and A.G. Malshukov, *Sov. Phys. JETP* 36, 978 (1973)
5. V.I. Alshits and V.L. Indenbom, *Sov. Phys. USP* 18, 1 (1975).
6. V.I. Alshits and V.L. Indenbom, *Dislocations In Solids*. (edited by F.R.N. Nabarro), Vol. 7, p. 43, Elsevier Science Publishers, Amsterdam (1986).
7. E. Nadgornyi, *Dislocation Dynamics and Mechanical Properties of Crystals*, p. 231 (1989).
8. C. Kittel, *Quantum Theory of Solids*, p. 326, John Wiley and Sons, Inc., New York (1963).
9. T. Holstein, Appendix to B.R. Tittman and H.E. Bommel, *Phys. Rev.* 151, 178 (1966).
10. V.Ya. Kravchenko, *Sov. Phys. Sol. State* 8, 740 (1966).
11. A.D. Brailsford, *Phys. Rev.* 186, 959 (1969)
12. J.A. Rayne and C.K. Jones, *Physical Acoustics*, (edited by W.P. Mason and R.N. Thurston), Vol.VII, p. 149, Academic Press, New York (1970).
13. J.R. Hardy and R. Bullough, *Phil. Mag.* 15, 237 (1967).
14. A.D. Brailsford, *J. Appl. Phys.* 40, 3087 (1969).
15. W.P. Mason, *J. Appl. Phys.* 35, 2779 (1964).
16. F.R.N. Nabarro, *Theory of Crystal Dislocations*, p. 529, Clarendon Press, Oxford (1967).
17. H. Conrad and A.F. Sprecher, *Dislocations in Solids*, (edited by F.R.N. Nabarro), Vol. 8, p. 497, Elsevier Science Publishers, Amsterdam (1989).
18. A.M. Roshchupkin, V.E. Miloshenko and V.E. Kalinin, *Sov. Phys. Sol. State* 21, 532 (1979).

DISCUSSION OF A. BRAILSFORD'S PAPER

D. Wilsdorf:

What is the absolute magnitude of the electron drag force (coefficient) for Cu?

A. Brailsford:

The drag coefficient B as a function of temperature (in Cu) was obtained a number of years ago by Alers and Thompson, who measured the ultrasonic attenuation of specimens before and after neutron irradiation. (Defects pin the dislocations, and so remove the (dislocation) contributions).

Their analysis showed that B was consistent with a temperature-independent electronic part (B_e) and a temperature-dependent component (B_{PH}) arising from vibrational degrees of freedom.

A somewhat similar result has been obtained by Elbaum et al, using a somewhat different technique, in Al.

In the above experiments it is easily established that the dislocations do not move over large distances and so experience only "essentially pure" matrix. (These experimental results and theoretical considerations given in my manuscript give $B_e \approx 10^{-5}$ dyn-s/cm²).

H. Conrad:

1. Do you expect an electron push coefficient to have the same magnitude as an electron drag coefficient?
2. Does an electron-phonon-dislocation effect occur when an electric current (drift electrons) is passed through a metal specimen?

A. Brailsford:

1. In a free electron gas and a dislocation in an isotropic elastic continuum the force should depend only upon the relative velocity of the dislocation and the gas.
2. In higher order perturbation theory there may be processes linking BraBra

Brailsford's Paper (Continued)

electronic and vibrational processes. I do not know of any work directed towards this topic.

Electromigration—Caused Deterioration of Metallic Stripes—
A Computer Simulation

H.B. Huntington

Physics Department

Rensselaer Polytechnic Institute, Troy, New York

Electromigration as an observed phenomenon dates back to 1871, well over a century ago. It is commonly restricted to current induced mass motion in metals and semi-conductors, materials which ordinarily conduct by electrons or holes. If the mass motion is that of an impurity, the effect can be observed through chemical analysis, but the motion of the matrix atom can be followed by the use of radioisotopes or the study of specimen shape changes.

The basic mechanism for the transport of matter consists in the momentum exchange between the charge carriers (electrons and holes) and the ions of the material. It has become customary to resolve the force exerted by the electric field on the ions into two components the above-mentioned "wind" force, arising from the momentum exchange, and the "direct" force arising from the electrostatic interaction with the charge of the ions. This is a simplistic view (1,2) of quite a subtle theoretical problem which has challenged several outstanding theorists (Friedel (3), Peierls, Sorbello (4), Landauer (5), Sham (6), Shaich (7), and Gupta (8)) to employ sophisticated treatments to attain a more complete and basic understanding of the problem.

Various measurements have been employed to obtain the strength of the electromigration driving force for bulk materials, usually expressible in terms of a Z^* , the effective charge number that the moving ion would appear to have in the applied electric field for the observed force. The technological interest in the bulk behavior was limited to specimen purification (9) and filament failure (10). The development of thin film integrated circuitry, however, revealed a really serious technological problem related to the failure through thin-films, electromigration of the connecting metal stripes of the component networks (11). Initially the metal stripes were aluminum. From the temperature dependence of the failure rate it was immediately apparent that grain boundary motion rather than bulk diffusion was the avenue for mass transport. The problem attracted wide attention and intense technical effort.

To prevent regions of void formation and alternatively mass accumulation, uniformity of morphology in the stripe was valuable. Grain boundary intersections were possible sources of trouble. Increasing grain size helped but going to the limit of bamboo structure (chains of single crystals with boundaries roughly perpendicular to the stripe) may improve the average strip lifetime but also lowered the time of first failure by increasing the variation in strip lifetime (12). The most effective remedial measure of a decade ago was to alloy the aluminum with 2-4% copper (13). Although impurities tend, in general, to increase bulk diffusivity, the opposite is true for grain boundary diffusion. Of the several alloying agents (14) tried in aluminum, copper appears to be perhaps the most effective agent in slowing diffusion. Ten to hundred-fold increase in stripe lifetime can result. However, the electromigration failure problem has a way of resurfacing and this has been particularly true in the present trend toward greater miniaturization. If 1 μm wide lines are under development today, it will be 0.5 μm lines for tomorrow. Presently other

higher melting point materials than aluminum, such as noble metals and silicides, are being explored and in particular composite films are under investigation. A low melting-point, high conductivity metal is combined with a high melting-point metal sublayer, which supplies electrical continuity at the failure regions of the good conductor (15).

The problem of adequate pretesting the lifetime of a particular set of stripes lies in the need for an accelerated procedure. This can be accomplished by performing the testing at elevated temperature and electric field so that electromigration damage equivalent to several months or year of actual use can be simulated by a few hours of testing. For quantitative scaling one needs to know a reliable value for the activation energy for the diffusion mechanism involved and the exponent in the power dependence of the damage on electric field (16). The diffusion activation energy is around 0.5 eV but really has to be measured independently for each metal alloy. It has been customary to take the damage

rate to be proportional to E^n where E is the electric field and n is the before-mentioned exponent. Customarily n is thought to be about 2 but values of 5 and 6 have been observed in cases of high over-voltage. The National Bureau of Standards is developing an apparatus and procedure for obtaining a standardized stripe lifetime. The question as to the best value for n has proved troublesome. Another approach to predicting long term reliability, which has shown promise, is to measure the low frequency electrical noise ($\sim 1/f$) in the stripes (17). Apparently the cause of this noise is in many cases microscopic events such as the jumping of an atom in a grain boundary and the extent to which these occur is a good indicator of incipient stripe instability.

Because of the considerable technological importance of stripe stability, any approach which promised a better understanding of the action of electromigration has appeared worth pursuing. With this in mind there have been several investigations (18-21) using computer simulation. In the effort that we have developed, our approach has tried to involve the actual grain boundary structure and to avoid gross approximations.

The first task was the generation of a suitable grain boundary structure. We assumed the stripes are essentially two dimensional structures with pronounced (111) textures and widths varying over a wide range. The grain boundary network was constructed by the Voronoi method (22). This method consists of laying down a set of random points to act as nucleation centers for the grains. One then constructs the perpendicular bisectors of lines joining neighboring points. These lines are the grain boundaries. The orientations of the respective grains are then randomly assigned and the intergranular mismatch noted since these will be taken into account in arriving at the grain boundary diffusivities.

The next stage was to simulate a sort of annealing by allowing the vertices (grain corners) to move so as to decrease the resultant surface tension. A simple dislocation model was employed for the grain boundaries to calculate the diffusivities and grain boundary energies. This procedure had some effect on the susceptibility to damage by electromigration, since both surface tension and diffusivity increase with intergranular misorientation. These highly misoriented grain boundaries are those whose extent are most directly reduced by stress minimization. Overall we shall see that stress relaxation does reduce the damage caused by electromigration.

Next the actual process for electromigration is simulated first for a specimen with a free surface and then for the more important case of a specimen with a covering passivating layer which prevents diffusion of matter over the surface. The first situation results in a steady transfer of matter from the voids to the free surface of the stripe and the second ends in a static situation wherein the matter flows become balanced out. Electromigration causes stripe failure by open circuits resulting from voids or short circuits caused by hillocks. We do not follow our simulation into the later stages of deterioration when voids have made the current density inhomogeneous and temperature and diffusivity are no longer uniform. We prefer to concentrate on the earlier stages of the process where one is concerned with the prediction of final failure rather than its occurrence.

The grain boundary network is made of connecting segments and vertices which are the points of segment joining. It is at the vertices that transport of electromigration is unbalanced. At some the net flux of matter will be positive and at the others the net flux will be negative (outward) resulting in voids. Since matter can not concentrate at a point. the positive vertices will feature an outward diffusional flux. Electromigration will also function along the segments but its influence will be appreciably smaller than the diffusional flow. The model envisions strong electromigration effects at the vertices and diffusion only down the segments. The basic equation for matter flow is

$$\frac{dc(\vec{r},t)}{dt} = \nabla D \left\{ \nabla c(\vec{v},t) - A c(\vec{r},t) \right\}$$

where A is a constant related to the electromigration force.

We now apply this model to the case of the free surface. After a short transient period a steady state develops in the segments where D is constant and $\nabla^2 c = 0$. The concentration $c(x,z)$ shows a hyperbolic function in x, the coordinate along these grain boundary, but varies as $\sin \pi z/2d$ where z is measured perpendicular to the free surface and d is the thickness of the stripe film. Some of this matter flow spills over into these (-) vertices, where the voids are developing, but in general this flow is insufficient to halt the increase of the voids. The picture is one of uniformly increasing matter on the free surface and increasing voids. Eventually the model breaks down because of the assumption of homogeneity of temperature and current density. Monitoring the total void volume after a fixed time gives a good measure for comparative purposes. For example the equilibrated stripe showed only about 60% of the total void volume developed in the untreated Voronoi. run under otherwise the same conditions.

Electromigration for the passivated stripe involves a considerable more complicated analysis than for the free surface, principally because the matter builds up near the (+) vertices instead of extruding to the surface as in the preceding case. We chose to construct our solution from combinations of the function, $(\frac{x}{L})^3 + 6D t \frac{x}{L^3}$ which is a solution of the diffusion equation. Nevertheless our solution can not be exact and we must decide what aspect it should clearly display. It is important that matter be conserved., that the excess matter in the segments equal the void volume. In each case the change of excess matter void volume per unit time equals

$$\sum_i F_i - \sum_j S.O._j,$$

where F_i is the inward electromigration flux at the ith vertex and SO_j is the flux of matter which spills over into the jth void. In pursuing the time-wise development of the simulation we find that initially many small voids are formed but are later filled by the diffusion flow from nearly (+) vertices.

In summary we face the question as to what basic insight the simulation affords that could not have been deduced initially. We should like to point out that these are still many promising avenues that the simulation has open for future pursuit - effect of fracture of the passivation, development of short circuiting extrusions, pulsing and a.c. operation, and void motion under electromigration. Even at this stage, however, at least two interesting results have been developed. As in the preceding paragraph it has been shown why some voids appear and then disappear. A second result, demonstrated so far only for the free surface, is that annealing can improve resistance to electromigration more effectively than could be expected simply from the grain growth.

We thank the Southeastern Center for Electrical Engineering Education and the Texas Instruments Company for the support of this research.

References

1. F.B. Fiks, Sov. Phys - Solid State (English Trans) 1, 14 (1959).
2. H.B. Huntington and A.R. Grone, J. Phys. Chem. Solids 20, 76 (1961),
H.B. Huntington and S.C. Ho, J. Phys. Soc. Japan Suppl. II 18, 202 (1963).
3. C. Bosvieux and J. Friedel, J. Phys. Chem. Solids 23, 123 (1962).
4. R.S. Sorbello, J. Phys. Chem. Solids 34, 937 (1973).
5. R. Landauer and J.W.F. Woo, Phys. Rev. B10, 1266 (1974).
6. L.J. Sham, Phys. Rev. B12, 3142 (1975).
7. W.L. Schaich, Phys. Rev. 13B, 3350, 3360 (1976).
8. R.P. Gupta, J. Phys. Chem. Solids 47, 1057 (1986).
9. D.T. Peterson and F.A. Schmidt, J. Less-Common Metals 18, 111 (1969).
10. R.P. Johnson, Phys. Rev. 54, 459 (1938).
11. I.A. Blech and E.S. Meieran, Appl. Phys. Lett. 12, 201 (1968).
12. E. Kingsbron, Appl. Phys. Lett. 36, 968 (1980).
13. I. Ames, F.M. d'Heurle and R. Horstman, IBM J. of Res. Develop 4, 461 (1970).
14. A. Gangulee and F.M. d'Heurle, Appl. Phys. Lett. 19, 73 (1971); Thin Solid Films 16, 227 (1973).
15. T. Kwok, P.S. Ho and H.-C.W. Huang, J. Vac. Soc. Tech. A 2 241 (1984); P.S. Ho, T. Kwok and H.-C. W. Huang, Proc. of 16th Int'l Conf. on Solid State Devices and Materials (1984), p. 55.
16. J.R. Black, IEEE Trans. ED-16, 338 (1969); Proc. IEEE 57, 1587 (1969).
17. P.M. Chen, D.P. Jeu and R.D. Moore, International Symposium on Reliability Physics (1985).
18. N.J. Attardo, R. Rutledge and R.C. Jack, J. Appl. Phys. 42, 4343 (1971).
19. J.D. Venables and R.G. Hye, IEEE. Proc. 10 IRPS, 159 (1972).
20. J.M. Schoem, J. Appl. Phys. 51, 513 (1980).
21. K. Nikata, Reliability Physics Symposium 19, 175 (1981).
22. D. Weaire and N. Rivier, Contemp. Physics 25, 59 (1984).

HBHP1.T3V

DISCUSSION OF H. B. HUNTINGTON'S PAPER

H. Conrad:

What effect on electromigration can one expect when the specimen is exposed to an external electrostatic field compared to an electric field applied by electrode attachments directly to the specimen which gives an electric current?

H. B. Huntington:

Since I have no experience with external electric field on IC interconnects, I really have no basis for prediction. It might be an interesting experiment.

Workshop on High Intensity Electro-Magnetic and Ultrasonic
Effects on Inorganic Materials Behavior and Processing
July 16-18, 1989, N. Carolina State U., Raleigh, H. Conrad

ELECTRIC FIELD EFFECTS OBSERVED THROUGH HIGH RESOLUTION X-RAY DIFFRACTION

BY K. LAL (Natl. Physical Laboratory, New-Delhi, India) AND COWORKERS

reported by

D. Kuhlmann-Wilsdorf
Department of Materials Science
University of Virginia, Charlottesville, VA 22901

Since before 1981, K. Lal and co-workers have studied effects of electric fields on non-conductor crystals, employing an ultra-high resolution X-ray diffraction technique developed in the Indian National Physical Laboratory (1-6). The studies have been conducted principally on silicon single crystal wafers of high perfection (7-12) but also have involved LiF and CdS crystals (7,12).

Mostly, the observed effects of electric fields on the crystals can be explained in terms of (i) heating effects and (ii) the establishment of filamentary rather than homogeneously distributed current flow (due no doubt to the fundamental mutual attraction of parallel current flow lines). However, a more subtle effect suggested by the results is that of reorientation of atoms whose electron charge distribution is not spherically symmetrical (13).

REFERENCES

- 1) K. Lal and B. P. Singh, Solid State Commun., 22 71 (1977).
- 2) K. Lal, B. P. Singh and A. R. Verma, Acta Cryst., A35 286 (1979)
- 3) K. Lal and B. P. Singh, Acta Cryst., A36 178 (1980)
- 4) K. Lal and B. P. Singh, J. Crystal Growth, 54 493 (1981)
- 5) K. Lal, Indian J. Pure Appl. Phys., 19 854 (1981)
- 6) K. Lal, Proc. Indian Natn. Sci. Acad., 47A 20 (1981)
- 7) K. Lal and P. Thoma, Solid State Commun., 40 637 (1981).
- 8) K. Lal and P. Thoma, Phys. Stat. Sol., (a)80 491 (1983).
- 9) K. Lal and P. Thoma, Solid State Commun., 53 107 (1985).
- 10) K. Lal and S. N. N. Goswami, in "Physics of Semiconductor Devices" (Eds. S. C. Jain and N. Radhakrishna, Proc. 3rd. Int. Workshop, Madras (India) Nov.27 -Dec. 2, 1985), WSPC - Costed Series in Emerging Technology.
- 11) K. Lal and S. N. N. Goswami, Mater. Sci. engg., 85 147 (1987).
- 12) K. Lal, The Rigaku J., 5 11 (1988).
- 13) V. S. Bhasin, L. S. Kothari. K. Lal and M. P. Srivastava, Phys. Lett. A, 133 438 (1988).

INTERACTION OF HIGH-INTENSITY ULTRASONIC WAVES WITH SOLIDS

Robert E. Green, Jr.
Materials Science and Engineering Department
The Johns Hopkins University
Baltimore, MD 21218

Introduction

The fact that ultrasonic waves of sufficient intensity influence the physical properties of solid materials has been known for many years. However, it was not until Blaha and Langenecker (1), in 1955, reported that the superposition of high-intensity ultrasonic vibrations caused a marked decrease in load on zinc crystals which were undergoing tensile elongation, that modern scientific investigation of the influence of high-intensity ultrasound on metal deformation was initiated. They constructed an apparatus which permitted zinc single crystals to be exposed to high intensity ultrasound during a tensile test. The zinc crystals, tensile grips, and specimen holding frame were suspended in a glass tank filled with carbon tetrachloride. The bottom of the tank was coupled to an ultrasonic generator operating at 800 kHz with a maximum power output of 25W (2 W/cm^2). The results of these first experiments are shown in Fig. 1. Curve A shows that intermittent application of high intensity ultrasound reduced the tensile stress by about 40% and that upon termination of the ultrasound the tensile stress returned to the value it had prior to ultrasound application.

During the following years high-intensity ultrasound has found practical application in welding, machining, drawing, forming, grain refinement during solidification, diffusion enhancement, accelerated fatigue testing, and stress relieving. However, explanations are still necessary as to how the proper application of high-intensity ultrasound causes three major effects on the mechanical deformation of metals, namely work softening, work hardening, and reduction of friction between tool and workpiece. Of particular interest to metal deformation processes is the phenomenon that metal single crystal and polycrystalline specimens undergoing tensile deformation experience a "softening" effect resulting from superimposed high-intensity ultrasound.

Literature Survey

In 1975 Green (2) published a review article which summarized the experimental observations of the ultrasonic "softening" effect up to that time. The conclusions reached with respect to the "softening" effect are as follows. The amount of stress reduction experienced by a specimen undergoing uniaxial tensile elongation was observed to be directly proportional to the intensity of the ultrasound and independent of frequency over the range 15 Hz through 1.5 MHz. More thermal energy than ultrasonic energy is required to produce the same stress reduction. The effect is independent of test temperature over the range 30 through 500 deg C. Most investigators agreed that the "softening" effect is more pronounced after yield in the plastic region of the stress-strain curve. Upon removal of the ultrasonic vibrations, the applied tensile stress returns to the value it would have attained in the absence of ultrasound. However, the elasticity involved does not always appear to be linear, since the reduction in tensile stress and return to the non-vibration value is often not instantaneous and indicates a time dependence.

A number of mechanisms were set forth to explain the "softening" effect. The most prevalent explanation among the various investigators is that of simple superposition of alternating ultrasonic stresses on the externally applied static stress. Investigators holding this view have used mechanical calculations based on linear elasticity theory to account for the magnitude of the stress reduction. These theoretical calculations show that the ultrasonic stress amplitude is a function of Young's modulus, which is assumed to remain constant throughout the course of the experiment. Some investigators have also assumed that the ultrasonic vibration amplitude, vibration frequency, and velocity of sound in the test specimen also remain constant.

However, Langenecker and associates claimed that the observed effects are due to the creation and movement of dislocations caused by the additional energy supplied by the high-intensity ultrasonic field. Although the conventional mechanisms of resonance, relaxation, and hysteresis by which dislocations can absorb energy from an ultrasonic wave were rejected for various reasons, Langenecker suggested that the actual mechanism was localized heating in regions around dislocations and other imperfections when the ultrasonic waves are scattered. Moreover, he stated that acoustic heating and high-temperature fracture of metals present strong evidence for drastic changes in Young's modulus during application of high-intensity ultrasound.

Theoretical Considerations on High-Intensity
Ultrasound Softening of Metals

In order to determine some possible explanations for the observed experimental results, Green (2) considered the relatively simple case of a metal specimen subjected to a tensile test at a constant rate of elongation. Following Gilman (3), he regarded this type of test to be such that a rigid crosshead moves at a fixed speed and one end of a test specimen is attached to it and pulled. The other end of the specimen is attached to a load-cell which contains a stiff spring whose calibrated linear elastic deflection is measured and used to determine the axial force acting on the test specimen. An equation describing the behaviour of the machine-specimen interaction was derived by considering the various displacements of the system at a given time. The final equation for the axial stress on the specimen subjected to the tensile stress is

$$\sigma = \frac{St - \epsilon_p l}{A/K + l/E^*}$$

where S = crosshead speed, t = time, ϵ_p = plastic strain, l = specimen length, A = cross-sectional area of specimen, K = compliance of load-cell spring and frame of tensile test machine, E^* = effective Young's modulus for specimen.

For a constant displacement tensile test St always increases with time and K remains constant, while the cross-sectional area A can only decrease; therefore, in order for there to be a stress decrease, one or more of the following must occur:

- (a) l increases
- (b) E^* decreases
- (c) ϵ_p increases

Let us consider the possibility of each of these events in turn.

Increase in Length:

Since we are considering a constant crosshead displacement tensile test, the relative motion between the crosshead and the load cell determines the length of the specimen. In the event that the superposition of high-intensity vibrations causes the length to increase, while the crosshead is moving at a speed too slow to accommodate this increased length, then the force on the load cell

spring would be decreased and a stress drop would be indicated on the stress-strain curve.

Decrease in Effective Young's Modulus:

Green (4) published a review of the low-intensity ultrasonic investigation of the mechanical properties of solid materials, which included a detailed account of both linear and non-linear elastic wave propagation. In this publication equations were given for the velocity of propagation of both low-intensity longitudinal and transverse ultrasonic waves propagating in a homogeneous, isotropic solid material in a direction which coincided with the direction of an externally applied tensile stress. Using these equations an expression for the effective Young's modulus of the solid in the stressed state was derived. This expression showed that, based on non-linear elastic considerations alone, the effective Young's modulus varies in a linear fashion with the applied tensile stress. Moreover, since for all common metals the third-order elastic moduli are negative and from 3 to 10 times larger than the second-order moduli, non-linear elastic theory predicts that the effective Young's modulus should decrease in a linear fashion with increasing applied tensile stress.

Using typical values of the second- and third-order elastic moduli for the case of polycrystalline copper, the numerical value for the effective Young's modulus in the unstressed state was calculated. A numerical value for the imposed tensile stress was chosen which was identical in magnitude to the stress reduction observed by Pohlman and Lehfeldt (5) during the fourth application of high-intensity ultrasound in their work. For this case the percentage decrease in the effective Young's modulus for the specimen in the stressed state was calculated to be 0.7%.

Another factor which can cause a decrease in the effective Young's modulus is an increase in temperature of the test specimen. Consideration of the case of polycrystalline copper showed that a temperature increase of 20.6 deg K is required to decrease the effective Young's modulus by 0.7%.

A third factor which can cause a marked decrease in the effective Young's modulus of a metal is the non-linear effect associated with the motion of dislocations which can take place at very low stress levels, even in the macroscopic elastic region of a conventional stress-strain curve. It should be pointed out here that the term macroscopic elastic range is used because, if sensitive enough detectors are used, it is found that the region of the tensile stress-strain curve normally considered to be linear elastic actually contains non-linear elastic and even plastic contributions. Numerous experimental investigators

have shown that deformation of a metal specimen either by a continuously applied stress or by alternating stresses above a certain threshold amplitude causes a marked decrease in the experimentally measured effective second-order elastic moduli, including the effective Young's modulus.

Increase in Plastic Strain:

It has been amply documented in the literature that the application of stresses of sufficient amplitude will cause dislocation motion, multiplication, and permanent plastic deformation. All papers and books published on plastic deformation of metals since 1930 amply attest to this fact. The exact mechanism or mechanisms as to how high-intensity ultrasonic waves interact with dislocations and cause them to move, multiply, and interact, is unknown. However, there is no question that ultrasonic waves of sufficient amplitude to cause permanent plastic deformation can no longer be regarded as linear elastic waves and theories based purely on linear elasticity will not satisfactorily explain the observed experimental results.

Summary of Theoretical Considerations:

Several possible mechanisms have been discussed which may result in a stress reduction caused by the superposition of high-intensity ultrasonic vibrations on a metal specimen subjected to a constant displacement rate uniaxial tensile test. In some cases the experimental results suggest that the effects observed are actually elastic in origin and due simply to stress superposition, that is the ultrasonic vibrations cause the specimen length to increase lowering the force measured by the load cell, which in turn, indicates a reduction in the applied tensile stress. However, the elasticity involved, even in these cases, does not always appear to be linear, since the reduction in tensile stress and return of the tensile stress to the non-oscillatory value is often not instantaneous and indicates a time dependence either due to non-linear elastic or plastic effects.

The effective Young's modulus (the actual modulus of a real material) of metal is far from actually being a constant and during mechanical deformation non-linear elastic effects occur causing elastic moduli to decrease even in defect free materials. The presence of crystalline lattice defects, such as dislocations, causes an even greater non-linear decrease in the elastic moduli and a decrease (usually linear) may also be caused by a temperature increase in the test specimen.

Ample experimental evidence exists which shows that ultrasonic waves of sufficient intensity can interact with, move, multiply, and cause dislocations to interact. The

fact that all of these effects occur in certain regions of a test specimen and not at others is simply a manifestation of the inhomogeneous nature of plastic deformation of metal specimens which has been extensively documented in the literature. This interaction between ultrasonic waves and dislocations can cause a non-linear change in the elastic moduli and tensile stress reduction by increasing the amount of plastic strain.

Experimental Investigation of High-Intensity Ultrasonic Softening Mechanisms

Mignogna and Green (6-9) developed a multiparameter system which permitted simultaneous measurement of a number of quantities to test the proposed mechanisms for the influence of high-intensity ultrasound on the mechanical properties of metals. The parameters, which were either controlled or measured during tensile elongation and/or high-intensity insonation, were applied tensile load, specimen elongation, electrical power supplied to high-intensity ultrasonic (20kHz) horn, contact force between ultrasonic horn and test specimen, insonation time, specimen temperature distribution, vibrational amplitude of the test specimen, low-intensity ultrasonic (8MHz) wave velocity (directly related to elastic moduli) and attenuation (directly related to dislocation motion).

A block diagram of the entire multiparameter system is shown in Fig. 2 and a schematic diagram of the specimen test configuration is shown in Fig. 3. A steel cage served to grip the upper end of the test specimen and couple it to the load cell of a tensile test machine. A second steel cage, which was bolted to the moving crosshead of the tensile test machine, gripped the lower end of the test specimen and also contained the mount for the high-intensity ultrasonic horn converter assembly. Control and measurement of the applied tensile load was accomplished with standard instrumentation incorporated with the tensile test machine.

The high-intensity ultrasonic horn converter assembly was mounted in the lower steel cage in such a manner that it had freedom of movement along the tensile axis within the confines of the cage itself. Positioning of the horn assembly was accomplished with two steel guide tubes and a screw, which was threaded into the bottom plate of the lower grip cage and passed through the tensile test machine crosshead. The screw was attached to the horn assembly mount by a shoulder bolt which permitted the screw to turn freely while moving the mount either up or down. Once the test specimen was in place in the cage grips, the high-intensity ultrasonic horn converter assembly was positioned so that the tip of the catenoidal horn was in contact with the bottom of the test specimen. On the lower side of the crosshead a pulley fastened to the horn assembly positioning

screw, combined with a system of additional pulleys and a weight pan, permitted a constant torque to be applied to the screw. The screw, in turn, converted this torque into a constant contact force between the ultrasonic horn tip and the bottom of the test specimen.

The insonation period of the high-intensity ultrasonic unit was controlled by a timing circuit inserted in the power supply, which permitted the insonation period to be continuously varied from 0.03 to 6.03 sec. Longer insonation periods were obtained by switching to manual control. An x-cut quartz transducer, possessing a resonant frequency of 8 MHz, was acoustically coupled to the flat upper end of the test specimen with a light oil and clamped in place. The clamping fixture maintained constant contact pressure between the transducer and specimen end face. The transducer was electrically connected through an impedance matching network to an ultrasonic pulse-echo system. Measurements of elastic wave velocity directly yielded information on the variation of the effective Young's modulus as a function of tensile elongation and application of high-intensity ultrasound. The same system permitted simultaneous measurement of ultrasonic attenuation, which served as a monitor of dislocation motion.

In the early experiments the temperature of the test specimens was monitored by attaching thermocouples to the central region of the specimen gauge length. In later experiments the temperature distribution over the entire gauge length was continuously monitored with an infrared radiometric television system.

Confirmation of Previous Work:

One of the first tests was to essentially reproduce the type of experiment reported by most previous investigators, namely to apply high-intensity ultrasound to a metal specimen which is undergoing tensile elongation. Figure 4 presents load decrease data obtained from an aluminum single crystal. Each load drop was produced by an 0.03 sec application of high-intensity ultrasound at constant horn power. Comparison of the dashed curve drawn through the minimum loads attained during the high-intensity insonation and the "conventional" curve obtained during tensile elongation reveals that they diverge. This divergence shows that the high-intensity ultrasound caused load drop was not constant for constant ultrasonic horn power and insonation time, but increased with increasing plastic strain.

Low-Intensity Ultrasound Measurement of Effects of High-Intensity Ultrasound:

In order to attempt to separate the combined effects of tensile loading and application of high-intensity ultrasound some of the parameters enumerated above were monitored during application of high-intensity ultrasound to a test specimen, without simultaneous tensile elongation. As shown in Fig. 5, an aluminum single crystal subjected to high-intensity ultrasound for various insonation time periods exhibited changes in specimen length and low-intensity ultrasonic velocity and attenuation each time the high-intensity ultrasound was applied to the test specimen. However, in the case of some polycrystalline aluminum alloys, although an apparent softening occurred during similar tests, a drastic decrease in ductility was observed and found to be a function of the intensity of the high-intensity ultrasound, decreasing to as little as one percent in some cases. Scanning electron microscopy revealed a significant difference between the fracture surface of specimens loaded in tension only and those with superimposed tensile and high-intensity ultrasound loading.

The ultrasonic attenuation results, as shown in the lower portion of Fig. 5, provide strong evidence for the ability of sufficiently high-intensity long wavelength ultrasound to physically interact with and move dislocations. Figure 6, taken from the work of Sachse and Green (10), is typical of the results obtained by many researchers illustrating the extreme sensitivity of low-intensity ultrasonic attenuation measurements to dislocation motion. This figure shows the results of an experiment with an aluminum single crystal, which was loaded to 180 kg, well into the plastic region of the stress-strain curve, and unloaded. Then the crystal was reloaded to 60 kg and maintained at this load for one minute, unloaded to 45 kg and maintained for one minute, unloaded to 30 kg and maintained for one minute, unloaded to 15 kg and maintained for one minute, and finally unloaded completely. Upon subsequent reloading to 70 kg and unloading, the ultrasonic attenuation displayed dips at those load values which had been maintained for the one minute periods during the previous load-unload cycle. Note that even though the ultrasonic attenuation "remembered" the discontinuous nature of the prior load-unload cycle, the load-time curve (or equivalently the stress-strain curve) gave no indication of it. The observed results were attributed to the pinning of dislocation loops by point defects which were preferentially located at the position they occupied when the load was maintained constant for the one minute intervals. Upon reloading, these point defects pinned the dislocation loops again when the dislocations arrived at the location of the point defects thus causing the dips in attenuation. These results show that ultrasonic attenuation measurements are

extremely sensitive to dislocation motion as well as the interaction of dislocations with point defects. The similarity of the first change of ultrasonic attenuation versus time plot in the lower left portion of Fig. 6 and the change in ultrasonic attenuation versus time plot in the lower part of Fig. 5 provides strong indirect evidence that both results are due to dislocation motion.

Infrared Thermography:

As shown schematically in Fig. 7, infrared thermography scans of the test specimens' surfaces revealed extremely rapid temperature increases at the point of attachment of thermocouples to the specimens' surfaces, which cast doubt on most past temperature measurements and which has undoubtedly led to misunderstanding about the mechanism causing specimen heating (11).

Half-wavelength single crystal and fine-grained polycrystalline specimens exhibited pronounced heating at displacement nodes, while similar specimens of non-resonant length were observed to heat only at the horn/specimen interface. High-intensity ultrasonic insonation also induced localized heating at displacement nodes in brass, copper, and steel specimens of resonant length. These observations are in agreement with elasticity theory. Localized hot regions were also detected at saw-cuts, drilled holes, fatigue cracks, and grain boundaries (11).

Subsequently, several large-grained zinc specimens subjected to high-intensity ultrasound were observed to heat excessively at certain large grains. One specimen bent plastically into a curved shape as a result of the interaction of the high-intensity ultrasound with the grain microstructure (7).

X-ray Diffraction Topography:

X-ray topography is the name given to several x-ray diffraction techniques which permit direct observation of lattice defects both on the surface and in the bulk of single crystals. Defects ranging in size from dislocations upward may be imaged over large areas of crystal specimens. These techniques have been reviewed in several publications (12-13). One of the primary advantages of x-ray topography is that not only can crystal surfaces be examined in the reflection mode, but relatively thick crystal specimens can be investigated in the transmission mode, particularly with the use of synchrotron sources. Moreover, x-ray topography can be used to examine materials which are damaged by the electron beam in conventional electron microscopy and unlike electron microscopy the specimens can be examined in air or other atmospheres.

Although these techniques are unique in that they yield information about the defect structure, down to the size of individual dislocations, throughout the volume of fairly thick crystals, the exposure times required when using conventional x-ray generators and techniques often run to hours or even days for recording a single image.

Synchrotron X-ray Topography:

The Synchrotron Topography Project (STP) was established in 1979 as a Participating Research Team (PRT), with the present author serving continuously since that time on the executive committee. The goal to construct an x-ray topography station on the 2.5 GeV National Synchrotron Light Source (NSLS) at Brookhaven National Laboratory was attained on beam-line X-19C (14). This station is the only one at NSLS fully dedicated to synchrotron topography with general purpose peripheral equipment suitable for in-situ experiments. The two principal instruments consist of a white beam camera and a multiple crystal monochromatic beam camera. Recent use of this synchrotron source for x-ray topography has permitted film exposure times to be reduced to seconds and replacement of film with state-of-the-art electro-optical detectors has permitted exposure times to be reduced even further to milliseconds (15-18).

In order to obtain more direct evidence of high-intensity ultrasound interaction with dislocations, an aluminum single crystal of resonant length was subjected to high-intensity ultrasound so that a displacement node, and hence strong plastic deformation, would be expected to occur at the mid-section. Subsequently, white beam transmission x-ray topographic images of the mid-section were obtained at the National Synchrotron Light Source at Brookhaven National Laboratory (19). The extreme asterism and inhomogeneity observed in the resulting x-ray diffraction images clearly indicated that high-intensity ultrasound caused severe plastic deformation and lattice bending throughout the volume of the mid-section (Fig. 8).

Summary of Experimental Results:

Hot zones detected at saw-cuts, drilled holes, fatigue cracks, and grain boundaries, coupled with the bending of the large grain polycrystalline zinc specimen, the ultrasonic attenuation measurements, the scanning electron microscope observations, and the white beam synchrotron x-ray topographic images clearly indicate that high-intensity ultrasound can interact with material inhomogeneities many orders of magnitude smaller than the ultrasonic wavelength, e.g. dislocations.

Conclusions

Although many practical applications of high-intensity ultrasound for mechanical deformation and stress relieving of metals have been reported, no completely satisfactory theory explaining all details of the experimental observations has yet appeared. This paper has reviewed some theoretical considerations, has described some of the experimental observations, and has shown that ultrasonic waves of sufficiently high-intensity can definitely interact with and move dislocations causing plastic deformation of metals. Moreover, it has been shown that the interaction of high-intensity ultrasound with the microstructural features of metals causes localized heating to occur.

Although, some progress has been made, additional experimental and theoretical research is necessary in order to fully understand the interaction of high-intensity ultrasound with metals and as a result optimize practical applications of high-intensity ultrasound to metal forming, joining, and stress (strain) relieving operations.

References

1. F. Blaha and B. Langenecker, "Dehnung von Zink-Kristallen unter Ultraschall einwirkung", *Naturwissenschaften* 42, 556 (1955).
2. R.E. Green, Jr., "Non-linear Effects of High-Power Ultrasonics in Crystalline Solids", *Ultrasonics* 13, 117-127 (1975).
3. J.J. Gilman, Micromechanics of Flow in Solids, McGraw Hill, New York, p. 215 (1969).
4. R.E. Green, Jr., Ultrasonic Investigation of Mechanical Properties, *Treatise on Materials Science and Technology*, Vol. 3, Academic Press, New York (1973).
5. R. Pohlman and F. Lehfeldt, "Influence of Ultrasonic Vibrations on Metallis Friction", *Ultrasonics* 4, 178 (1966).
6. R.B. Mignogna and R.E. Green, Jr., "Multiparameter System for Investigation of the Effects of High-Power Ultrasound on Metals", *Rev. Sci. Instrum.* 50, 1274-1277 (1979).
7. R.B. Mignogna and R.E. Green, Jr., "Changes in Ultrasonic Attenuation, Velocity and Other Parameters Resulting from High-Power Insonation of Metals", Proceedings of Ultrasonics International 79 Conference, pp. 215-220, IPC Science and Technology Press Ltd., Guilford, England (1979).

8. R.B. Mignogna and R.E. Green, Jr., "Nondestructive Evaluation of the Effects of Dynamic Stress Produced by High-Power Ultrasound in Materials", in Mechanics of Nondestructive Testing, W.W. Stinchcomb (Ed.), pp. 231-248, Plenum Publishing Corp., New York (1980).
9. R.B. Mignogna and R.E. Green, Jr., "Effects of High Frequency Loading on Materials", Ultrasonic Fatigue, pp. 63-85, The Metallurgical Society of AIME, Warrendale, Pennsylvania (1982).
10. W. Sachse and R.E. Green, Jr., "Deformation Rate Effects on the Attenuation During Loading, Unloading, and Reloading of Aluminum Crystals", J. Phys. Chem. Solids 31, 1955-1961 (1970).
11. R.B. Mignogna, R.E. Green, Jr., E.G. Henneke II, and K.L. Reifsnider, "Thermographic Investigation of High-Power Ultrasonic Heating in Materials", Ultrasonics 19, 159-163 (1981).
12. R.W. Armstrong and C.C. Wu, "X-ray Diffraction Microscopy", in Microstructural Analysis: Tools and Techniques, J.L. McCall and W.M. Mueller (Eds.), pp. 169-219, Plenum Press, New York (1973).
13. B.K. Tanner, X-ray Diffraction Topography, Pergamon Press, New York (1976).
14. J.C. Bilello, H.Chen, A.B. Hmelo, J.M. Liu, H.K. Birnbaum, P.J. Herley, and R.E. Green, Jr., "The Synchrotron Topography Project (STP) at the National Synchrotron Light Source," Nuclear Instruments and Methods, 215, pp. 291-297 (1983).
15. R.E. Green, Jr., "Electro-Optical Systems for Dynamic Display of X-ray Diffraction Images," in Advances in X-ray Analysis, C.S. Barrett, J.B. Newkirk, and C.O. Ruud (Eds.), 14, pp. 311-337, Plenum Press, NY (1971).
16. R.E. Green, Jr., "Direct Display of X-ray Topographic Images," in Advances in X-ray Analysis, H.F. McMurdie et al. (Eds.), 20, pp. 221-235, Plenum Press, NY (1977).
17. R.G. Rosemeier and R.E. Green, Jr., "A New Miniature Microchannel Plate X-ray Detector for Synchrotron Radiation," Nuclear Instruments and Methods, 195, pp. 299-301 (1982).
18. J.M. Winter and R.E. Green, "Rapid Imaging of X-ray Topographs," in Applications of X-ray Topographic Methods to Materials Science, S. Weissmann, F. Balibar, and J-F Petroff (Eds.), pp.45-58, Plenum Press, NY (1984).

19. R. Green, "Real-Time X-Ray Diffraction Investigation of Metal Deformation", Metallurgical Trans. A, 20A, 595-604 (1989).

FIGURE CAPTIONS

- Figure 1. Effect of superimposed high-intensity 800 kHz ultrasound on the tensile deformation of a zinc crystal.
A-intermittent application of ultrasound
B-continuous application of ultrasound
[after Blaha and Langenecker (1)]
- Figure 2. Block diagram of multiparameter measurement system.
[after Mignogna and Green (6)]
- Figure 3. Schematic diagram of specimen test configuration
A-moving crosshead, B-bottom grip cage, C-upper grip cage, D-mount for ultrasonic horn converter assembly, E-guide tubes, F-horn positioning screw, G-lower plate of bottom grip cage, H-pulley, I-converter, J-booster, K-catenoidal horn, L-specimen, M-split conical clamps, N-LVDT fixture and positioner, O-8Mhz quartz transducer, P-transducer holder.
[after Mignogna and Green (6)]
- Figure 4. Effect of superimposed 20kHz high-intensity ultrasound on the tensile deformation of an aluminum crystal. The load drops were caused by a sequence of 0.03 sec insonation periods at the same ultrasonic power level.
[after Mignogna and Green (7,9)]
- Figure 5. Change in specimen length (Δl), % change in low-intensity ultrasonic velocity ($\Delta v/v$), and change in low-intensity ultrasonic attenuation ($\Delta \alpha$) as a function of time for insonation of an aluminum single crystal subjected to high-intensity 20kHz ultrasound for various time periods.
I-0.03 sec, II-0.63 sec, III-1.23 sec
IV-1.83 sec, V-2.43 sec, VI-3.63 sec.
[after Mignogna and Green (7-9)]
- Figure 6. Load versus time and change of ultrasonic attenuation versus time plots obtained during a load-hold-unload-hold sequence (left) followed by a reload-unload sequence (right) conducted on an aluminum single crystal.
[after Sachse and Green (10)]
- Figure 7. Schematic diagram showing heat generated at a thermocouple epoxied to the surface of a non-resonant fine-grained polycrystalline aluminum specimen caused by high-intensity ultrasound.
[after Mignogna et al. (11)]

Figure 8. Optically enlarged image of a synchrotron white beam x-ray diffraction spot showing evidence of plastic deformation in an aluminum single crystal caused by high-intensity ultrasound.
[after Green (19)]

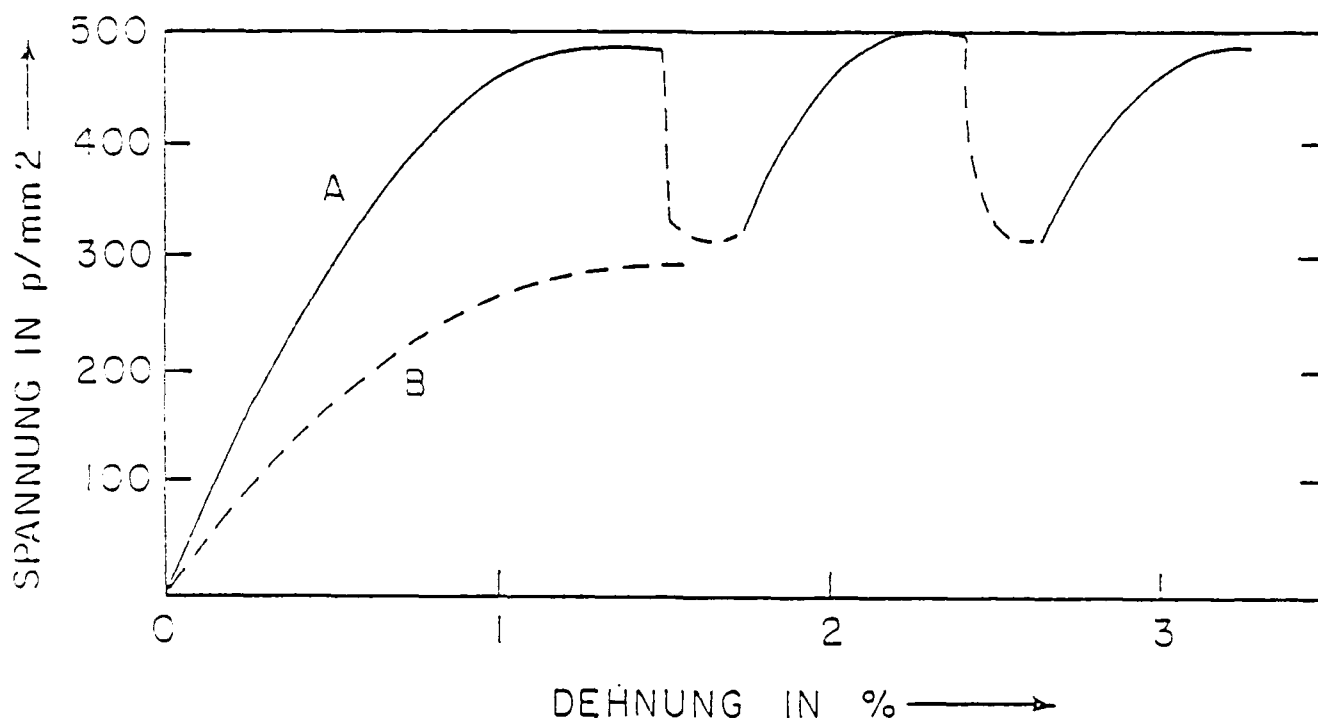


Figure 1. Effect of superimposed high-intensity 800 kHz ultrasound on the tensile deformation of a zinc crystal.
 A-intermittent application of ultrasound
 B-continuous application of ultrasound
 [after Blaha and Langenecker (1)]

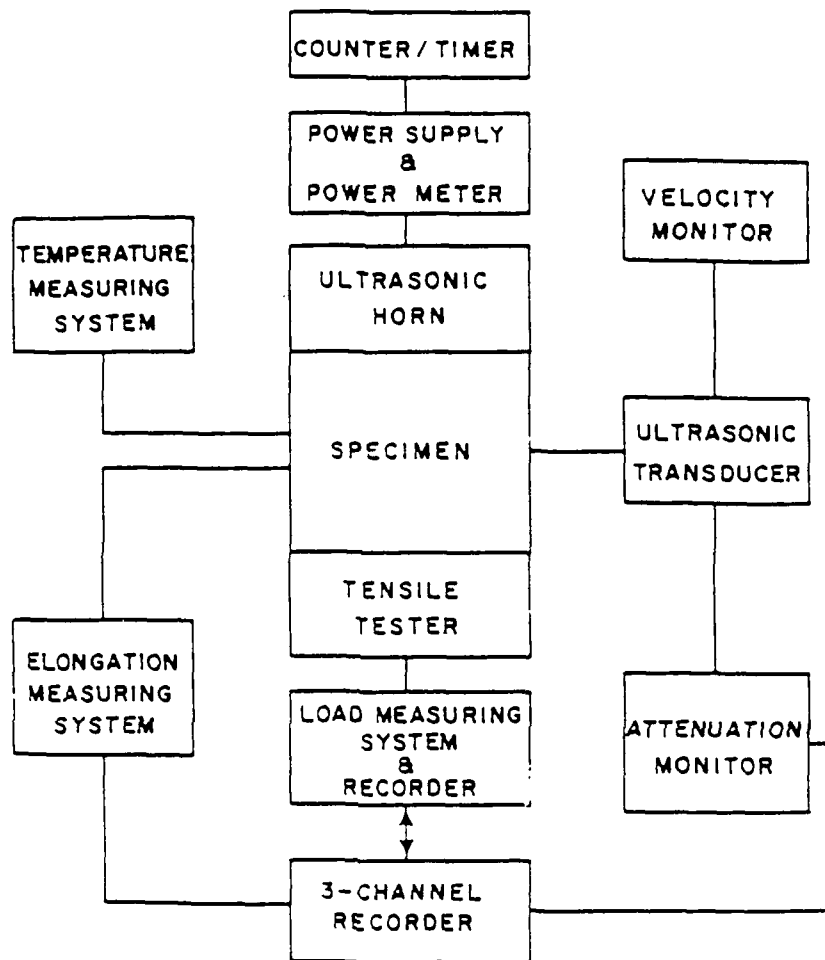


Figure 2. Block diagram of multiparameter measurement system.
 [after Mignogna and Green (6)]

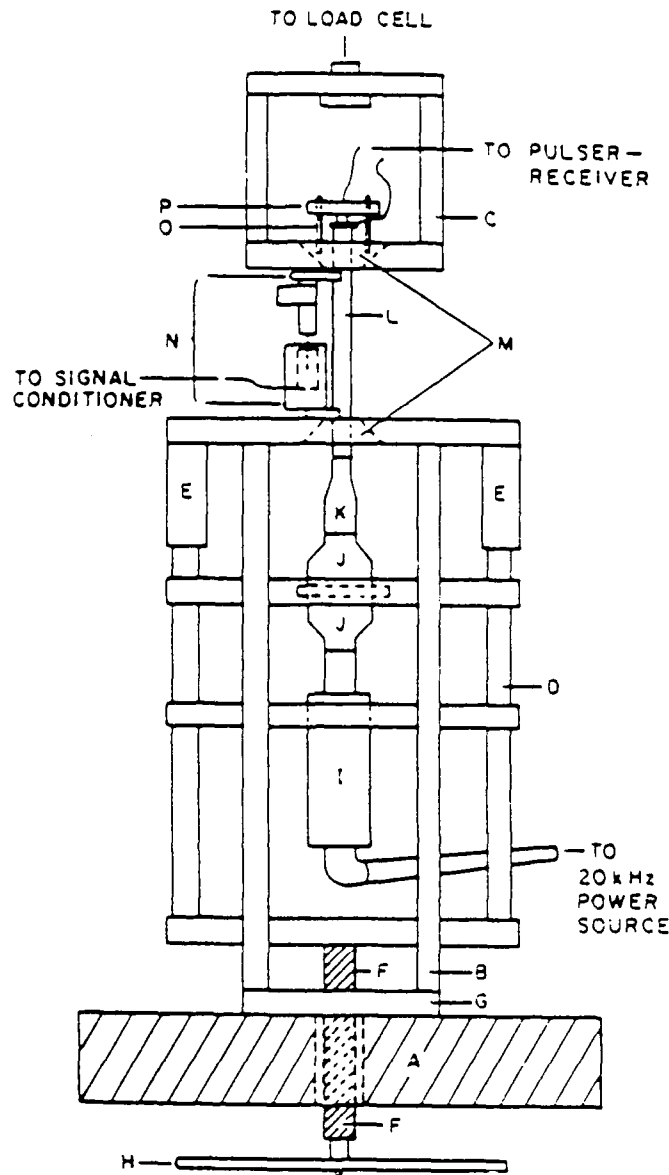


Figure 3. Schematic diagram of specimen test configuration A-moving crosshead, B-bottom grip cage, C-upper grip cage, D-mount for ultrasonic horn converter assembly, E-guide tubes, F-horn positioning screw, G-lower plate of bottom grip cage, H-pulley, I-converter, J-booster, K-catenoidal horn, L-specimen, M-split conical clamps, N-LVDT fixture and positioner, O-8Mhz quartz transducer, P-transducer holder. [after Mignogna and Green (6)]

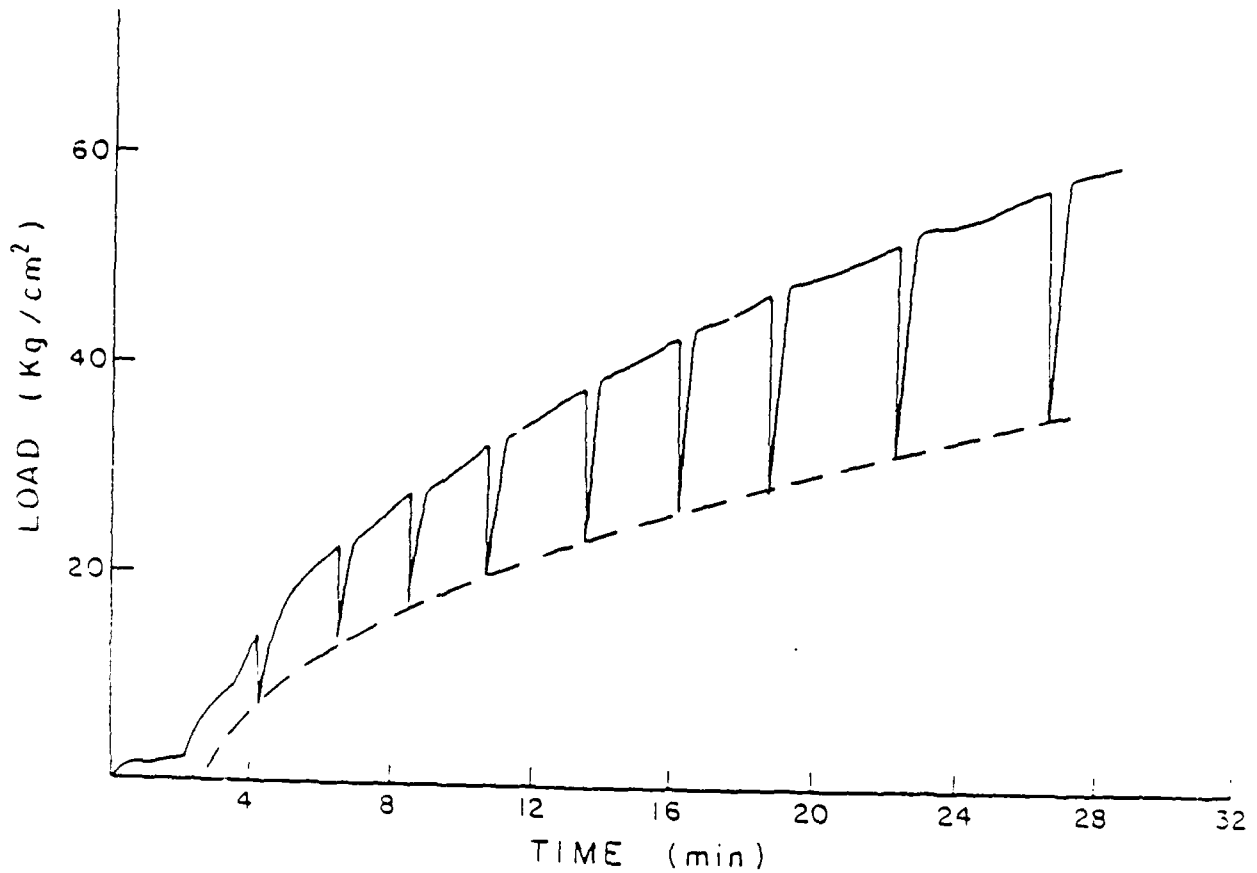


Figure 4. Effect of superimposed 20kHz high-intensity ultrasound on the tensile deformation of an aluminum crystal. The load drops were caused by a sequence of 0.03 sec insonation periods at the same ultrasonic power level. [after Mignogna and Green (7,9)]

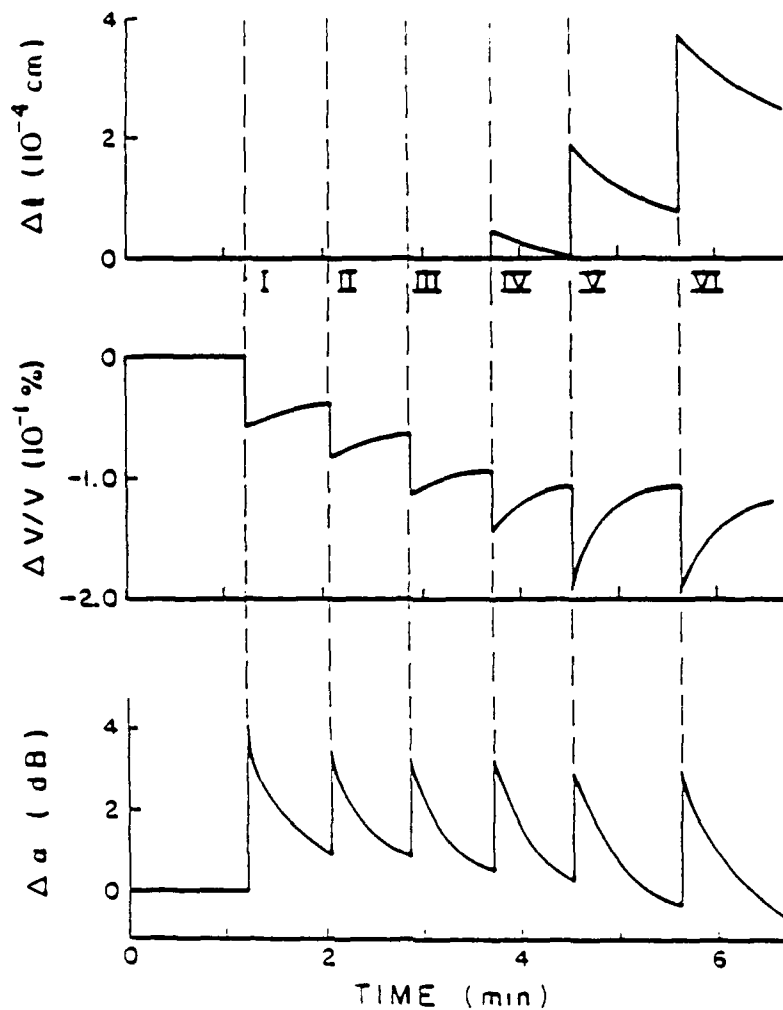


Figure 5. Change in specimen length (Δl), % change in low-intensity ultrasonic velocity ($\Delta v/v$), and change in low-intensity ultrasonic attenuation ($\Delta \alpha$) as a function of time for insonation of an aluminum single crystal subjected to high-intensity 20kHz ultrasound for various time periods.
 I-0.03 sec, II-0.63 sec, III-1.23 sec
 IV-1.83 sec, V-2.43 sec, VI-3.63 sec.
 [after Mignogna and Green (7-9)]

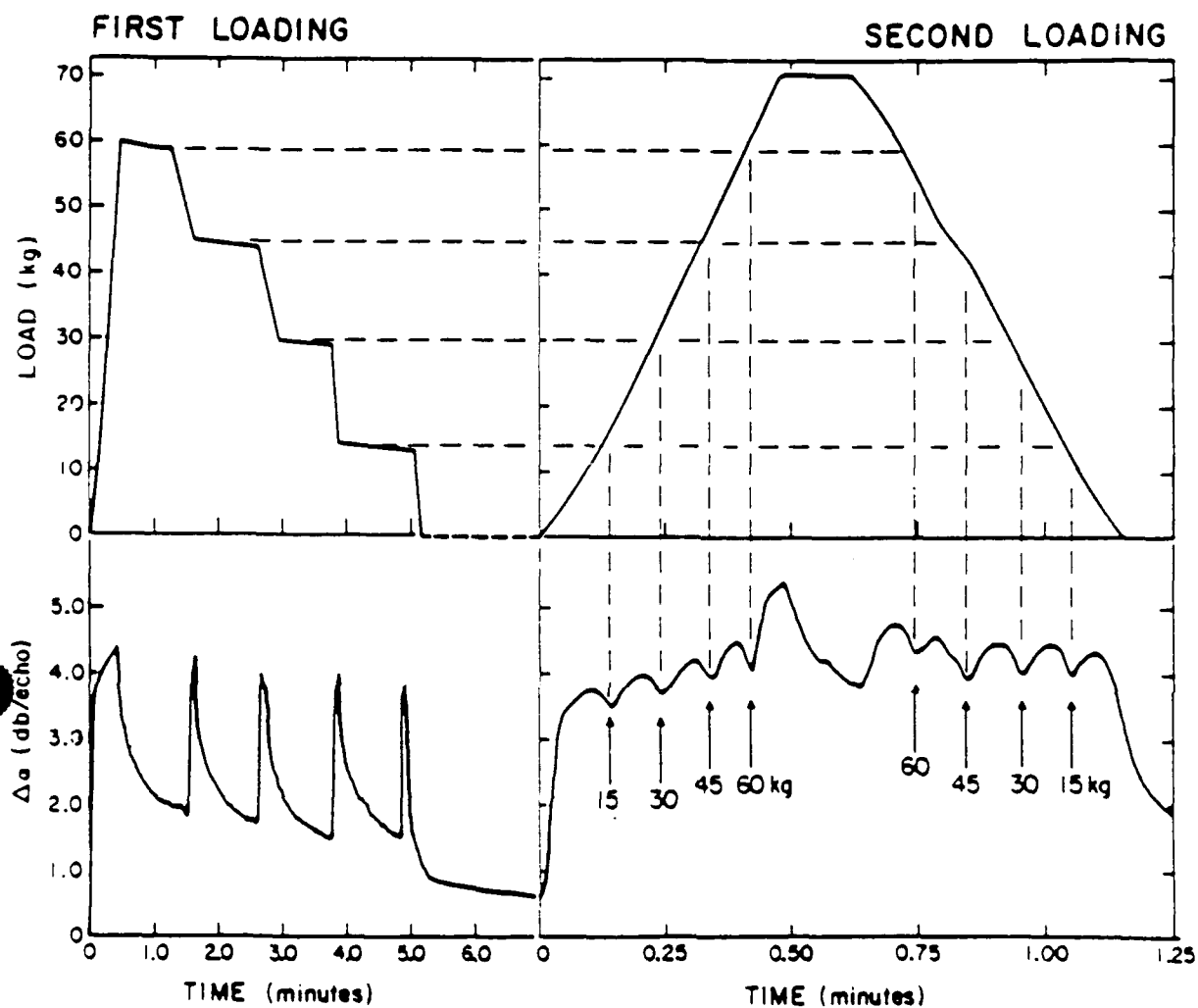


Figure 6. Load versus time and change of ultrasonic attenuation versus time plots obtained during a load-hold-unload-hold sequence (left) followed by a reload-unload sequence (right) conducted on an aluminum single crystal. [after Sachse and Green (10)]

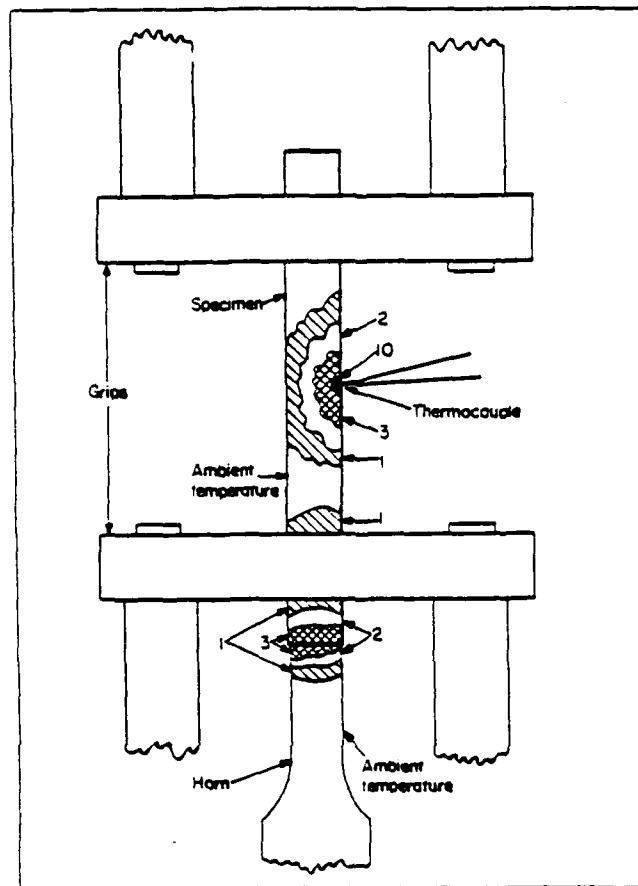


Figure 7. Schematic diagram showing heat generated at a thermocouple epoxied to the surface of a non-resonant fine-grained polycrystalline aluminum specimen caused by high-intensity ultrasound. [after Mignogna et al. (11)]



Figure 8. Optically enlarged image of a synchrotron white beam x-ray diffraction spot showing evidence of plastic deformation in an aluminum single crystal caused by high-intensity ultrasound. [after Green (19)]

PLASTOELECTRIC EFFECT IN CRYSTALS

J.C.M. Li

Department of Mechanical Engineering
University of Rochester, Rochester, NY 14627

1. The electroplastic effect:

It is known that dislocations carry electric charges in ionic crystals. As a consequence, an externally applied electric field can move dislocations and hence produce plasticity. This is called the electroplastic effect.

Measurements of electric charges on dislocations by direct observation of etch pit movements in a d.c. field have been attempted in the past, but all seem to have involved some uncertainties. For example, Zagoruiko, Savenko and Bekkauer¹ measured the lengths of rays (bands of etch pits) of dislocation rosettes produced by a micro-indentation on a (001) surface of a NaCl single crystal, both with and without the presence of an electric field along [100]. While the lengths of screw bands were about the same (30 and 29 μm) with or without a d.c. field of 2.6 MV m^{-1} indicating that the screw dislocations are probably not charged, the lengths of edge bands were about 20% longer (81 and 67, and 79 and 66 μm) towards the cathode and about 2% longer (68 and 67, and 67 and 66 μm) towards the anode. By using the external stress needed to produce the same elongation of the bands, they estimated for the edge dislocations either a positive charge of $2.8 \times 10^{-11} \text{ C m}^{-1}$ or a negative charge of 10% of that magnitude. It is seen that the difficulty involved in extending the bands only slightly is that the effect of dislocation interactions within the indentation rosette may modify or distort the effect of the electric field.

To avoid this difficulty² we made an indentation first on the (001) surface of a KCl crystal containing nominally 88 ppm Ca^{+} . Then a d.c. field of up to 15 MV m^{-1} along [100] was applied. Only edge dislocation bands appeared, extending from the indentation towards the anode and forming an asymmetric rosette pattern. From the minimum field needed to produce such edge bands and the yield stress of the crystal, a charge of $-7 \times 10^{-11} \text{ C m}^{-1}$ was obtained for the edge dislocations. Since no screw dislocation bands appeared, the charge on screw dislocations in KCl was probably zero.

2. The plastoelectric effect:

If the dislocations in ionic crystals carry electric charges, plastic deformation which produces a net dislocation flux in one direction will result in an electric potential difference in that direction. This is called the plastoelectric effect.

Measurement of such potential difference could determine the charges on dislocations^{3,4}. To do this a KCl single crystal was compressed in the [010] direction between tilted plates. The dislocation charge was found negative in Ca^{++} doped KCl and its magnitude increased with Ca^{++} concentration as well as temperature. For comparison, the dislocations produced at the surface scratch were moved by the sole action of an electric field larger than a certain value. The dislocation charges were

obtained from such critical field and from the critical resolved shear stress at yield. The results agreed well with those obtained by the plastelectric effect. A sweep-up mechanism for the edge dislocations to collect K^+ vacancies with thermally activated adsorption and desorption processes was proposed and found consistent with experimental observations.

3. The density of mobile dislocations:

In 1934, Orowan⁵ proposed his famous equation

$$\dot{\epsilon} = \phi \rho b v \quad (1)$$

between the macroscopic strain rate $\dot{\epsilon}$ and the microscopic parameters of dislocations, namely, their Burgers vector b , the density ρ , and the average velocity v . The geometric factor ϕ resolves the shear strain produced by the dislocation motion onto the measuring direction. If there are several systems operating, the macroscopic strain rate is the sum of the contributions of all the operating systems. In the half century following his proposal, many progresses have been made. These include the measurement of individual dislocation velocities as a function of stress⁶ and temperature⁷; the measurement of dislocation density as a function of tensile strain and the relationship between such density and the flow stress⁸. Also in this period, direct observations of dislocation arrangements have advanced from optical to electron microscopy⁹ and dislocation tangling and cell formation were frequent findings during deformation. Such findings suggested that some dislocations may not be mobile and that the Orowan equation (1) should be applied only to the mobile dislocations. As a result, attempts have been made to deal with the problem of how to identify the mobile ones from the immobile ones, but none was very successful. The main difficulty seems to be the lack of an experimental technique to differentiate between the mobile and immobile dislocations.

The usual way of avoiding this problem is to do interrupted tests with the hope that, by suddenly changing one test variable, the microstructural state of the material including the density of mobile dislocations may be the same before and after the change. These include the following:

Temperature change tests to obtain the activation enthalpies for dislocation motion.¹⁰

Pressure change tests to obtain the activation volumes for dislocation motion.¹¹

Stress change tests to obtain the stress-velocity exponents or the activation strain volumes.¹²

However, all these tests involve the assumption that the density of mobile dislocations remain the same so that the variation of strain rate reflects only the variation of the dislocation velocity. In some cases, such as the temperature and pressure change tests, the validity of the assumption is generally accepted because there is a strong correlation between the activation parameters obtained and those for self diffusion. In the other two cases the validity is still questionable.

It is seen that the state of affairs is not very satisfactory. Without a good measurement of the density of mobile dislocations, it is difficult to employ the Orowan equation to the various deformation conditions so as to predict the material

processing behaviors. The lack of such measurement can be considered a major roadblock in the advance of dislocation plasticity. To see what can be done, it is reviewed here a recent attempt in measuring directly the density of mobile dislocations in ionic crystals by taking advantage of the fact that the edge dislocations carry electric charges in these crystals.

By using the plastelectric effect and by knowing the electric charges on the dislocations, it was possible to determine the density of mobile dislocations during deformation^{14,15}. This method has the advantage over direct observations which could not differentiate between mobile and immobile dislocations.

By using this method it was found that the density of mobile dislocations increases during constant strain rate compression, remains the same during the strain rate cycling, and decreases to a steady value during stress relaxation. Such information could not be obtained before.

By using the same method¹⁶, the density of mobile dislocations in gamma-irradiated LiF was determined by measuring the potential difference developed between the side surfaces of a specimen while compressing it between tilted plates. It was found that the density of mobile dislocations in the latent deformation was about one half of that in the primary deformation and the density in the soft deformation was about twice that in the latent deformation. Stress-relaxation tests were performed on unirradiated as well as irradiated LiF single crystals during primary, latent, and soft deformations. It was found that 90% of latent hardening was due to an increase in effective stresses. Similarly, when the slip directions were reversed, softening was mainly due to the lower internal stresses.

4. Acknowledgement:

This work was supported by USDOE, BES Division, through DE-FG02-85ER45201.

5. References:

- 1) N.V. Zagoruiko, V.I. Savenko and N.N. Bekkauer, Soviet Phys. JETP Lett. **14**, 186 (1971).
- 2) L. Colombo, T. Kataoka and J.C.M. Li "Movement of Edge Dislocations in KCl Single Crystals by Large Electric Fields" Phil. Mag. A **46**, 211-215 (1982).
- 3) T. Kataoka, L. Colombo and J.C.M. Li "Dislocation Charges in Ca²⁺-Doped KCl in the Temperature Range from 82 to 294 K" Radiation Effects **75**, 227-234 (1983).
- 4) T. Kataoka, L. Colombo and J.C.M. Li "Dislocation Charges in Ca²⁺-Doped KCl: Effects of Impurity Concentration and Temperature" Phil. Mag. A **49**, 409-423 (1984).

- 5) E. Orowan, Z. Phys. **89**, 634-659 (1934).
- 6) W.G. Johnston and J.J. Gilman, J Appl. Phys. **30**, 129 (1959).
- 7) D.F. Stein and J.R. Low, J Appl. Phys. **31**, 362 (1960).
- 8) A.S. Keh "Direct Observation of Imperfections in Crystals" AIME Symposium (Ed. by J.B. Newkirk and J.H. Wernick, Interscience, New York, 1962) pp. 213-238.
- 9) P.B. Hirsch, R.W. Horne and M.J. Whelan, Phil. Mag. **1**, 677 (1956).
- 10) J.E. Dorn "Creep and Recovery" (Am. Soc. Metals, 1957) p.255.
- 11) J.C.M. Li "Dislocation Dynamics" (Ed. by A.R. Rosenfield, G.T. Hahn, A.L. Bement, Jr. and R.I. Jaffee, McGraw-Hill, 1968) pp. 87-116.
- 12) W.G. Johnston and D.F. Stein, Acta Met. **11**, 317 (1963)
- 13) J.C.M. Li Can. J Phys. **45**, 493-509 (1967).
- 14) T. Kataoka and J.C.M. Li "Mobile Dislocation Density During the Deformation of KCl Single Crystals" Phil. Mag. A **51**, 1-14 (1985).
- 15) J.C.M. Li "A Measurement of the Density of Mobile Dislocations During Deformation" in "The Mechanics of Dislocations" (Ed. by E.C. Aifantis and J.P. Hirth, Am. Soc. Metals, Metals Park, Ohio, 1985) pp. 85-91.
- 16) T.K. Chaki and J.C.M. Li "Mobile Dislocations and Internal Stresses in the Latent Hardening of LiF Crystals" Phil. Mag. A **55**, 317-327 (1987).

DISCUSSION OF J. C. M. LI'S PAPER

D. Kuhlmann-Wilsdorf:

Do the dislocations drag their vacancy atmospheres? If so, they transport charge and are subject to an electric force, but in that case the experiments do not pertain to ordinary dislocation glide.

J. C. M. Li:

Instead of forming a vacancy atmosphere, we think the vacancies are condensed onto the dislocation core and form jogs. These jogs can be glissile so that no diffusion is involved for dislocation motion at low temperatures.

H. Conrad:

Your results are for purely ionic crystals. Would you expect similar effects if you have crystals of mixed ionic and covalent bonding, or for metallic bonding?

J. C. M. Li:

I expect similar results if the dislocations are charged or effectively charged and can carry the charges during motion. Crystals with mixed ionic and covalent bonds may have charged vacancies which can be absorbed by dislocations. Vacancies in metals may have effective charges because their motion is affected by a dc current. As a result, dislocations in metals may be charged also.

THE INFLUENCE OF CHARGE CARRIERS ON DISLOCATION MOTION IN METALS AND SEMICONDUCTORS

J.M. Galligan, C.S. Kim and T.J. Garosshen
Department of Metallurgy and Institute of Materials Science
University of Connecticut
97 North Eagleville Road, Storrs, CT 06269-3139

Plasticity is at the heart of a multitude of production processes and usages of materials. This extends from the successful production of high temperature superconductors to light related failures of electrooptic devices. In the following we present experiments which delineate the role that charge carriers - electrons or holes - play in the plasticity of materials. We focus on three basic problems of plasticity of materials:

1. The influence of magnetic fields on dislocation motion. As we shall see this allows us to establish instantaneous dislocation velocities, a major, and previously unfilled goal.
2. A method of establishing the influence of viscosity on thermally activated processes. Experimental evidence on the nature of the influence of damping on the surmounting of a barrier is supplied in the case where dislocations are underdamped. These experiments fill a gap in treating thermal activation.
3. The influence of excess charge carriers on the plasticity in semiconducting crystals. In this case we provide evidence for charged dislocations in specific crystals.

Consider a mobile dislocation at low temperatures, where the electrons determine its viscous drag(1). As a dislocation moves it emits phonons and these phonons are scattered by electrons. The more the phonons are scattered the slower the dislocations move, since more phonons must be emitted for continued motion. An interesting and instructive way to demonstrate this is by rotating a magnetic field through the plane in which dislocations move.

A magnetic field restricts the motion of electrons to helical paths, changing the energy states of the electrons. By aligning a magnetic field such that it is parallel to a mobile dislocation we alter the scattering process. This alignment is carried out by rotating the field, at constant magnitude, through the plane containing the moving dislocations. The arrangement is illustrated in Fig. 1. The geometry of this problem has been treated by Grishin, Kaner and Fel'dman(2) who show that two dislocation velocity regimes are possible, Fig. 2. For slowly moving dislocations a change in stress, $\Delta\sigma$, occurs due to the interaction of the dislocation with the electrons in a helical path. For slowly moving dislocations this change in stress takes the form of a single peak in stress versus the angle, θ , that the magnetic field makes with respect to the slip plane. If the dislocations move rapidly then $\Delta\sigma$ exhibits two peaks equidistant from $\theta = 0^\circ$.

In order to observe two peaks, displaced from $\theta = 0^\circ$, the following conditions must prevail, Fig. 1. When a dislocation moves with velocity V it emits phonons which travel through a distance $X = V/\Omega$ where Ω is the cyclotron resonance frequency (given by eH/mc where e is the electronic charge, m the mass, H the magnetic field and c the speed of light). If at the same time an electron moving in a helical path scatters the dislocation phonons then this electron will have moved a distance $(V_f/\Omega)\theta\cos\delta$ in the direction of dislocation motion, where V_f is the Fermi velocity of the electron. A large amount of scattering occurs when $(V_f/\Omega)\theta\cos\delta = V/\Omega$ or $\theta = V/V_f\cos\delta$. We know V_f to better

than 1% and we can measure θ to better than 1%, so that we can readily measure V , the dislocation velocity. Fig. 3 presents the observed change in stress versus angle θ . Quite clearly the data demonstrate that there are a number of maxima showing that more than one velocity is involved in the plastic deformation process. The measured velocities range from 1×10^3 m/sec to 3×10^3 m/sec. These observed peaks are only observed under the following conditions:

1. First the dislocations must be moving, i.e. no peaks are observed in the elastic region.
2. The phonon drag must be small relative to the electron drag; to achieve this the experiments are carried out at low temperatures.
3. The field must be rotated through an angle including the slip plane.

These experiments prove that we are measuring dislocation velocities. Further these measurements are instantaneous values, values which are appropriate to the plastic deformation process.

Another aspect of electrons interacting with mobile dislocations concerns the influence of viscosity on thermal activation(3). Standard treatments of thermal activation consider a particle, in free flight, going over a barrier whose energy is consistent with a Boltzmann distribution of thermal energies. What is neglected in this process is the coupling of the activated particle to the heat bath, and this coupling affects the particle surmounting the barrier. If there is no coupling of the particle to the heat bath, then the particle does not get over. If the coupling is extremely strong the particle is too heavily damped to surmount the barrier without an extensive outside force. We demonstrate below the influence of viscosity on dislocations surmounting barriers; in this experiment a single variable is changed, the viscosity, while all other state variables are held constant.

The experiment which demonstrates the influence of viscosity on thermal activation concerns the stress relaxation of a plastically deformed crystal. This relaxation process, at low temperatures, occurs as single particle process and involves two modes, Fig. 4. The first mode is found to be independent of the dislocation pinning point concentration, Fig. 5. Furthermore, this first mode is affected by the drag a dislocation experiences. This is shown by performing two relaxation experiments, Fig. 6. As shown in Fig. 6, when a crystal relaxes in the superconducting state the first mode of relaxation is different than when the same crystal relaxes in the normal state. The only difference in these two tests is the state of the electrons which only affects the drag on a dislocation.

The third area of research concerns the influence of charge on the motion of dislocations in semiconductors. In these experiments we inject electrons and holes into a plastically deforming crystal and observe the change in flow stress, the so-called photoplastic effect(4). We have carried out experiments for two types of semiconductors, wide band gap materials, such as CdS and narrow band gap materials such as (Hg, Cd)Te.

In the case of CdS we have measured the temperature dependence of the decay of the photoplastic effect after irradiation with laser light, which is incidentally of energy less than the band gap energy. This experiment is carried out such that we pulse the light for 10 seconds or so and measure two time constants. In Fig. 7 we show the temperature dependence of the time delay. The first time constant involves the increase in stress, $\Delta\sigma_+(T)$ as a function of temperature, T , while the second involves the decrease in stress, $\Delta\sigma_-(T)$ as a function of temperature. The activation energies for these processes are about the same and surprisingly low, about 0.07 eV.

We have also measured the charge associated with dislocation motion for edge dislocation moving in the basal plane and in the prismatic plane. In the case of dislocations moving in the basal plane there is first a measurable charge associated with dislocation motion. Further when irradiated with light the dislocation charge goes to a very small value if not zero. Irradiating with light substantially reduces motion of the dislocation. In contrast for edge dislocations moving on the prismatic plane there is very little dislocation charge observed. This is in agreement with the idea that charge carriers, introduced by light, interact with charged dislocations. Furthermore, there is an extremely small photoplastic effect, consistent with this effect being related to dislocation charge.

In the case of (Hg, Cd)Te, a narrow band gap semiconductor, we also observe a photoplastic effect, but this effect has a temperature dependent time delay, $t(T)$. Fig. 8 shows a typical example while Fig. 9 shows the temperature dependence of this time delay. A simple diffusive model(5) suggests that the activation energy associated with this time delay is about 0.4 eV for mercury cadmium telluride.

In summary we have illustrated how charge carriers affect the basic aspects of plasticity in metals and in semiconductors. These experiments provide information on the motion of dislocations in a variety of materials and provide a method of checking on the basic aspects of thermal activation in materials. The research on dislocation velocities and drag processes has been supported by the National Science Foundation, Division of Materials Research.

REFERENCES

1. J.M. Galligan, P.D. Goldman, L. Motowidlo and J. Pellegrino, Journal of Applied Physics 59 3747 (1986).
2. A.M. Grishin, E.S. Kaner and E.P. Fel'dman, Soviet Physics J.E.T.P. 43 753 (1976).
3. H.A. Kramers, Physical (Utrecht) 7 824 (1940).
4. Y.A. Osipyan, et al. Advances in Physics, Vol. 35, No. 2, p 115, 1986.
5. J. Pellegrino and J.M. Galligan, Journal of the Materials Research Society 1 3 (1986).

FIGURES

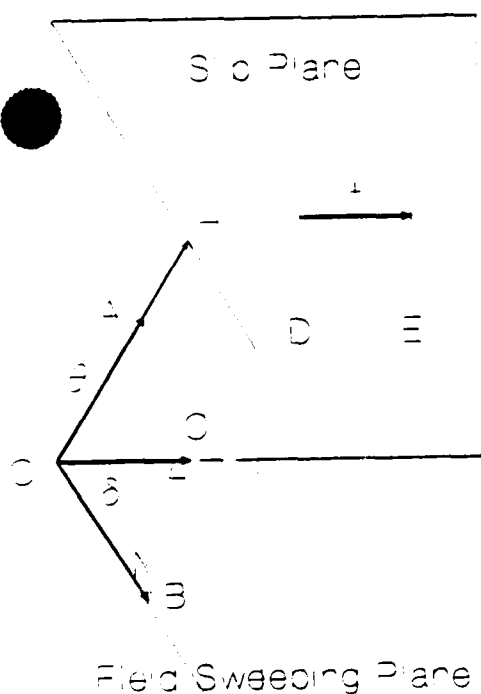


FIG. 1.

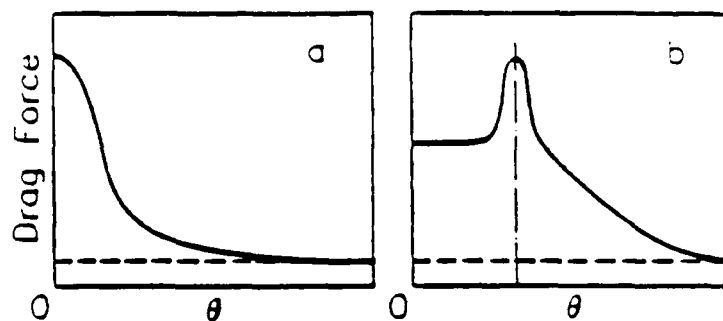


FIG.2.

- FIG. 1. Geometry used in experiment involving the rotation of a magnetic field.
 FIG. 2. The expected change in force acting on a moving dislocation for two dislocation velocity regimes. a) for slowly moving dislocations, b) for rapidly moving dislocations

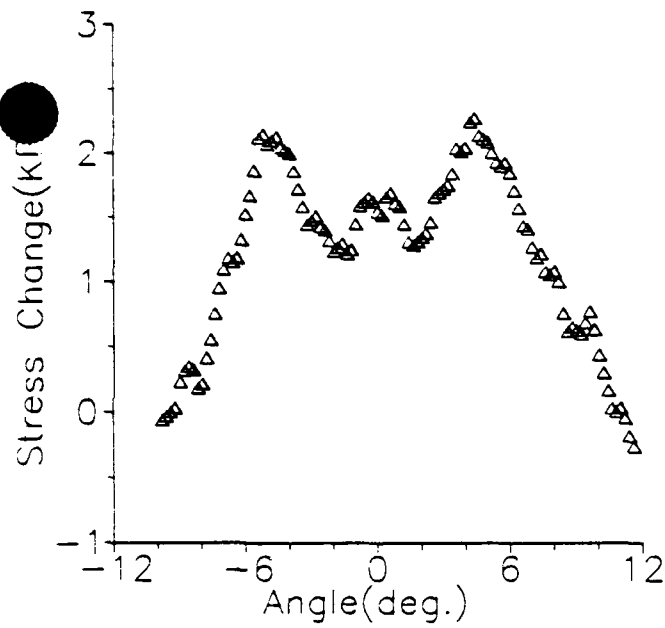


FIG. 3.

FIG. 3. The observed change in stress as a function of the angle θ (θ is defined in the text).

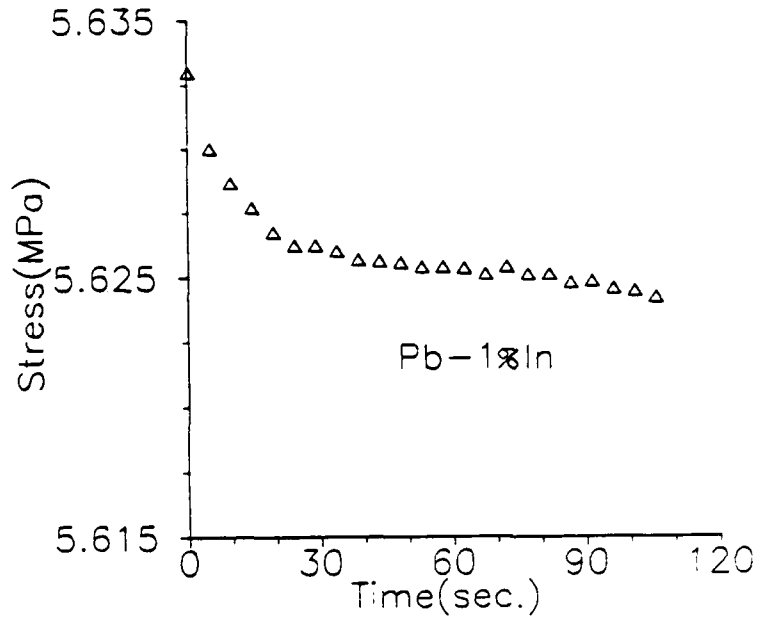


FIG. 4.

FIG. 4. Stress relaxation for a Pb 1% In alloy, relaxed at 4.2K.

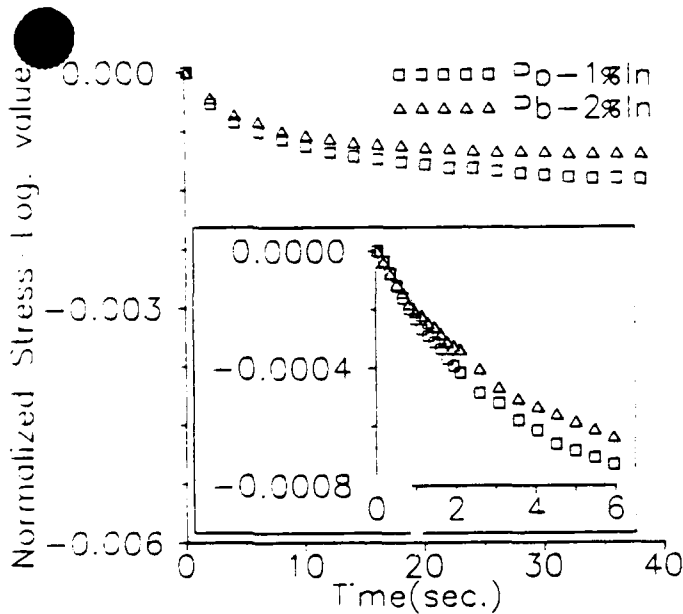


FIG. 5.

FIG. 5. In this figure we show the presence of two relaxation modes for crystals of different composition. Note that for short times - for both alloys - the first mode of relaxation is the same. Experiments carried out at 4.2K.

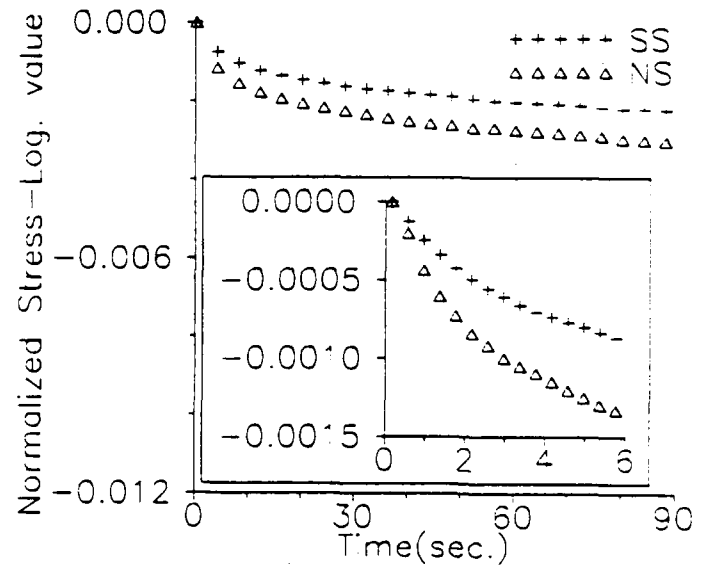


FIG. 6.

FIG. 6. The first mode of relaxation is affected by the drag it experiences, as shown in this figure. Temperature during experiments 4.2K. SS: Superconducting state, NS: Normal state.

EFFECTS OF ELECTRIC CURRENT AND EXTERNAL ELECTRIC FIELD ON THE MECHANICAL PROPERTIES OF METALS—ELECTROPLASTICITY

H. Conrad, A. F. Sprecher, W. D. Cao and X. P. Lu
Materials Science and Engineering Department
North Carolina State University
Raleigh, NC 27695-7907

Abstract

The paper reviews the available information on the effects of electric current and an external electric field on the mechanical properties of metals, including recent unpublished results by the authors.

The experimental results on the effects of an electric current on dislocation mobility and mechanical properties at **low homologous temperatures** ($T < 0.5 T_m$) reveal a polarity effect and yield the following expression for the effect of current density j on the plastic strain rate $\dot{\epsilon}$

$$\dot{\epsilon}_j / \dot{\epsilon} = (j/j_c)^n$$

where $\dot{\epsilon}_j$ is the strain rate with the current and $\dot{\epsilon}$ that without, $n \approx 3$ and j_c a critical current density, which increases with electron concentration n_e according to

$$j_c = C n_e^q$$

where $q \approx 2/3$ at 300 K and $2/5$ at 77 K. The experimental results were evaluated in terms of thermally-activated motion of dislocations, which gives

$$\ln \dot{\epsilon}_j / \dot{\epsilon} = \ln (\dot{\epsilon}_{o,j} / \dot{\epsilon}_o) - \left(\frac{\Delta G_j^* - \Delta G^*}{kT} \right) + \left(\frac{(A_j^* - A^*) b \tau^*}{kT} \right) + \log \left\{ 2 \cosh \left(\frac{A^* F_{ew}}{kT} \right) \right\}$$

where $\dot{\epsilon}_o$ is the pre-exponential, ΔG^* the Helmholtz free energy, A^* the activation area, τ^* the effective shear stress and F_{ew} the electron wind force per unit length of dislocation. The subscript j refers to the value with current. The magnitudes of

the derived values of F_{ew} were in reasonable agreement with theoretical predictions. However, they decreased with decrease in temperature, which is not predicted. The observed effects of j on the remaining parameters of the above listed equation need explanation. Limited data at **high homologous temperatures** suggest that the influence of j increases appreciably with increase in temperature above $0.5 T_m$.

An external d.c. electric field has been reported to influence the creep rate of unalloyed metals at **high homologous temperatures** and during the superplastic deformation of the 7475 Al alloy such a field has been found to: (a) decrease the flow stress, (b) reduce strain hardening, (c) increase strain rate hardening and (d) reduce grain boundary cavitation. The effects of the field were influenced by polarity and extended to the center of 1–2 mm thick specimens. Work by the present authors revealed that no significant effect of the field on the flow stress occurred at **low homologous temperatures**. This suggests that the field influences atomic mobility through vacancy generation and/or migration. The occurrence of an uneven electron density at the interfaces between phases and at grain boundaries has been proposed, but this idea is questionable.

EFFECTS OF ELECTRIC CURRENT AND EXTERNAL ELECTRIC FIELD ON THE MECHANICAL PROPERTIES OF METALS—ELECTROPLASTICITY

1. Introduction

The effects of electric fields and currents on atomic mobility in metals are rather well known. However, less is known regarding the influence of such fields and currents on dislocation mobility, which has been termed **electroplasticity**. The present paper reviews some of the pertinent aspects of the subject of electroplasticity, including recent work by the present authors. A more detailed review of the effects of an electric current is given in [1].

2. Electric Current Effects

2.1 Low Homologous Temperatures

2.1.1 *Soviet Work*

Troitskii and Likhtman [2] in 1963 were the first to propose that directed electrons could influence dislocation mobility. Upon irradiating Zn crystals with 1–3 MeV electrons while being deformed in uniaxial tension at low temperatures they found that when the electron beam was parallel to the slip plane the flow stress was less than when it was perpendicular to the plane. Based on these results they concluded that the mobility of dislocations might also be enhanced by the directed (drift) electrons associated with the passage of an electric current. To evaluate this, Troitskii and other Soviet workers [3–33] carried out an extensive number of studies into the effects of high density ($10^3 - 10^7$ A/cm²) electric current pulses (~ 100 μ s duration) on the flow stress and other mechanical properties of metals and alloys. High current densities j were employed to enhance the effect of the electrons, short pulse times t_p to keep Joule heating to a minimum.

An example of the effect of current pulses on the load-elongation behavior of a ~ 1 mm dia. Zn crystal deformed in uniaxial tension at 78 K is given in Fig. 1. A sudden drop in load occurred at each application of a current pulse, the magnitude of the load-drop increasing with increase in voltage (current density). A significant load drop only resulted when the crystal was being plastically deformed (Region A); none occurred in the initial elastic loading of the crystal, nor following appreciable stress relaxation (Region B).

Strong support that a major influence of the current resulted from the interaction of drift electrons with dislocations is provided by the experiments shown in Figs. 2 and 3, illustrating polarity effects. In Fig. 2a single crystal spheres (~ 2×10^{-2} cm radius) of Cu, Au and W were first compressed slightly between parallel plates establishing a contact radius of ~ 5×10^{-4} cm. They were then subjected to a single current pulse of 5 to 30 A ($j \approx 10^7$ A/cm²) and 10^{-2} s duration, which produced a difference in the contact areas at the two electrodes. The influence of the magnitude of the current I on the difference is presented in Fig. 2b. For the n-type conductors Au and Cu, the contact area at the positive pole was larger than that at the negative pole, whereas the reverse was the case for the p-type conductor W.

Fig. 3 shows the effect of current polarity ($j = 7.3 \times 10^3$ A/cm², $t_p = 200$ μ s) on $(11\bar{2}2) \langle 11\bar{2}3 \rangle$ dislocation velocity (determined by etch pits) in Zn crystals as a function of applied mechanical stress. The current pulse produced an increase in dislocation velocity for both the parallel and antiparallel directions; however, the increase is larger for the parallel direction, again indicating a vectorial effect of the current, i.e. an electron wind effect. The fact that an increase in velocity over that for $j = 0$ occurred when the current was antiparallel to the dislocation velocity suggests a scalar effect of the current in addition to an electron wind. The

scalar effect cannot be attributed to macroscopic Joule heating, since the temperature rise resulting from the current pulse was only of the order of 0.5 K.

2.1.2 Authors' Work

Theoretical estimates of the electron wind force exerted by drift electrons on dislocations are of two types: (a) those based on consideration of the specific dislocation resistivity [34–36a] and (b) kinetic or quantum mechanics considerations of the interaction between conduction electrons and dislocations [37–39]. The former yield for the electron wind force per unit length of dislocation

$$F_{ew} = \rho_D e n_e j / N_D \quad (1)$$

and the latter give

$$F_{ew} = \alpha b p_F (j/e - n_e v_D) \quad (2)$$

where ρ_D/N_D is the specific dislocation resistivity, e the electron charge, n_e the electron density, j the current density, α a constant ranging between 0.25 and 1.0 depending on the details of the Fermi surface and the calculations, b the Burgers vector, p_F the Fermi momentum and v_D the dislocation velocity. Knowing the electron wind force one can obtain the electron wind push constant $K_{ew} = F_{ew}/j$ and the electron wind push coefficient $B_{ew} = K_{ew} e n_e$ [1].

Eq. 1 yields $B_{ew} \approx 10^{-4}$ dyn-s/cm², whereas Eq. 2 gives $B_{ew} \approx 5 \times 10^{-5}$ dyn-s/cm² for the FCC metals Cu, Ag and Au with $\alpha = 0.25$. Employing the free electron theory and isotropic continuum elasticity, Brailsford (this volume) obtains B_{ew} of the order of 10^{-5} dyn-s/cm² for a free electron metal similar to Cu.

Monotonic Stressing: A major objective of our work was to perform careful experimental tests whereby the electron wind force (and other direct effects of the drift electrons) could be separated from the usual side effects of the current such as Joule heating, pinch, magnetostrictive and skin effects. Details regarding the experimental procedure are given in [40]. The experiments were similar to those of Troitskii in Fig. 1, whereby the effects of a single, high density ($\sim 10^5$ A/cm²)

($\sim 10^5$ A/cm²) current pulse (~ 100 μ s) on the flow stress of metals was determined. The metals considered (Ag, Al, Cu, Ni, Nb, Fe, W and Ti) varied in purity from 99.9 – 99.999 wt.%, were polycrystalline in form and represented a range of crystal structures, stacking fault energies and electronic properties.

Examples of the effect of current density j at 300 K on the ratio $\dot{\epsilon}_j/\dot{\epsilon}_{j=0}$, where $\dot{\epsilon}_j$ is the strain rate with the current pulse and $\dot{\epsilon}_{j=0}$ is that prior to the pulse, are given in Fig. 4. Included are results by Troitskii on Zn single crystals at 77 K for a single pulse on the flow stress and for multipulses ($\nu_p = 100$ Hz) on creep and stress relaxation rates. The results of Fig. 4 give

$$\dot{\epsilon}_j / \dot{\epsilon}_{j=0} = (j/j_c)^q \quad (3)$$

where j_c is the critical current density ($10^3 - 10^4$ A/cm²) and q is an exponent of ~ 3 . For the various metals j_c was found to increase with electron density n_e , giving

$$j_c = An_e^p$$

where $p \approx 2/3$ at 300 K and $2/5$ at 77 K; see Fig. 5.

Since the strain rates produced by a current pulse were $< 1s^{-1}$, the electroplastic results were analyzed employing the approach of thermally activated overcoming of obstacles to dislocation motion shown in Fig. 6. This gives the following expression for the resolved shear rate $\dot{\gamma}$ [1]

$$\ln \dot{\gamma}_j / \dot{\gamma} = \ln (\dot{\gamma}_{oj} / \dot{\gamma}_o) - \left(\frac{\Delta G_j^* - \Delta G^*}{kT} \right) + \left(\frac{(A_j^* - A^*) b \tau^*}{kT} \right) + \ln \left\{ 2 \cosh \left(\frac{A^* F_{ew}}{kT} \right) \right\} \quad (4)$$

where $\dot{\gamma}_o$ is the pre-exponential factor, ΔG^* the Helmholtz free energy, A^* the activation area, τ^* the resolved effective stress and kT has the usual significance. The subscript j indicates the value with the current; omission of this subscript indicates the value prior to the application of the current.

The magnitudes of the parameters of Eq. 4 derived from experimental data for the FCC metals Al, Ag and Cu and for BCC Nb are presented in Table 1.

Evident is that the greatest contribution is through the effect of j on $\dot{\gamma}_0$, the effects on the other parameters being much less. Since $\dot{\gamma}_0 = N_{D,m} b \bar{s} v^*$, where $N_{D,m}$ is the mobile dislocation density, b the Burgers vector, \bar{s} the average distance the dislocation segment l^* has moved per successful thermal fluctuation and v^* the frequency of vibration of the dislocation segment, the current is considered to have influenced one or more of these components of $\dot{\gamma}_0$. Since $N_{D,m}$ is generally of the order of 0.1 the total dislocations density $N_{D,t}$, it is expected that the increase in $\dot{\gamma}_0$ from the effect of j on $N_{D,m}$ is at most of the order of 10. Moreover, the observed effect of j on the velocity of dislocations in Zn crystals by the etch pit technique provides additional support that the effect of j on $\dot{\gamma}_0$ is not entirely through its effect on $N_{D,m}$. This then leads to the conclusion that a significant effect of j is on either \bar{s} or v , or both. Additional work is needed to ascertain the extent to which each of these parameters may be affected by the current.

A comparison of the value of B_{ew} for Cu determined experimentally as a function of temperature with that predicted from Eqs. 1 and 2 is presented in Fig. 7. There is reasonable agreement in the magnitude of the experimental value with the predicted one at 77K. However, the experimental B_{ew} increases with increase in temperature, whereas no clear temperature dependence is included in the theory. Results similar to those in Fig. 7 were obtained for the other FCC metals Ag and Al. In the case of BCC Nb, the experimental values of B_{ew} were about an order of magnitude larger than those predicted. The difference may lie in the accuracy of the experimental electronic parameters employed to calculate F_{ew} from Eqs. 1 and 2.

Fig. 8 shows that B_{ew} decreases with increase in stacking fault energy γ_{sf} for the FCC metals Ag, Cu and Al, the effect being slightly larger at 300 K compared to 77 K. Considered in terms of the separation distance d^* of the partial

dislocations, B_{ew} increases with d^* , again the effect being slightly larger at the higher temperature.

Cyclic Stressing: Concurrent application of high density electric current pulses ($\sim 10^4$ A/cm² for 100 μ s and 2 Hz) during rotating bending tests on polycrystalline Cu produced a 2-3 fold increase in fatigue life; see Fig. 9. Although the magnitude of the effect of electropulsing does not appear to be large, it should be pointed out that the current was "on" only 2×10^{-4} fraction of the total time. Associated with the increase in fatigue life was an increase in the linear density of persistent slip bands (PSBs) and a decrease in this width, Fig. 10. TEM observations suggested that the dislocations in the walls and cells were also somewhat less dense. In addition to increasing fatigue life, the electropulsing reduced the amount of intergranular compared transgranular cracking.

The experimental results indicated that the increased fatigue life from electropulsing is due to both an increase in the number of cycles for microcrack initiation and a decrease in macrocrack growth rate. The retardation in microcrack initiation and the reduction in grain boundary cracking were attributed to the increased slip homogenization produced by the electropulsing. The decrease in fatigue crack growth rate was concluded to result from the effect on crack closure of an observed increase in oxidation of the crack surface.

2.2 High Homologous Temperatures

Only few studies have been carried out on the effects of an electric current on the mechanical behavior of metals at high homologous temperatures, i.e. at $T/T_m > 0.5$. The investigations [41-44] known to the present authors employed a continuous current, rather than current pulses. Fig. 11 shows the influence of a small continuous d.c. current of 1.6×10^2 A/cm² on the stress relaxation of polycrystalline Cu, the effect of the current becoming appreciable as the temperature approaches $0.5 T_m$ [41,42]. Similar behavior was noted for Al. An

increase in stress relaxation rate also occurred for an a.c. current of the same magnitude, but the effect was smaller than for the d.c. current. Further, it was found that the d.c. current altered the dislocation arrangement in the Cu specimens; i.e. there occurred a partial destruction of the cell structure [43].

A continuous d.c. current of $2.5 \times 10^3 \text{ A/cm}^2$ was found to increase the creep rate of the intermetallic compound V_3Si compared to indirect heating [44]; see Fig. 12. Moreover, heating with d.c. current gave a higher creep rate than with a.c.

No theoretical analyses have been published to-date on the mechanisms by which the current influences the deformation of metals at high homologous temperatures. It is expected that atomic mobility plays a role in the behavior.

3. External Electric Field

3.1 Soviet Work

As a follow-up on the work by Troitskii on the effects of electric current pulses on mechanical properties of metals, Kishkin and Klypin [45] in 1973 presented results on the influence of an external electrostatic d.c. field on the creep rate of Cu and Co. They reported that the application of an electric field $E = 100 \text{ V/cm}$ during the creep of these metals at high homologous temperatures produced an order of magnitude increase in the creep rate. They suggested that the increase in creep rate at the instant the electric field was applied was possibly associated with electrostriction, while the continuation of the effect with time was related to the effect of the field on dislocation motion. In a subsequent paper, Klypin [46] reported that small changes in creep rate occurred in Cu at voltages as low as 0.01 V at 400°C and in Al at 20°C for voltages of 2 to 6 V. He concluded that these results reflected the existence of a charged surface layer and its interaction with crystal defects.

3.2 Authors' Work

It was found that an external field of 2 kV/cm had no significant effect on the stress-strain curve of ~ 1 mm thick high purity Al or a 7475 Al alloy at room temperature, i.e. at **low homologous temperatures**. However, significant effects occurred for the 7475 Al alloy at ~ 520°C, i.e. at **high homologous temperatures**. To investigate these effects, two lots of 7475 Al alloy were employed. Alloy I was a commercial alloy of nominal composition, whereas Alloy II had Fe and Si contents well below the nominal specification of 0.08 wt.%. The general effects of the field were similar for the two lots.

Figs. 13-15 show that the application of an external d.c. electric field E during the superplastic deformation of the 7475 Al alloy produced the following effects [47]: (a) decreased the flow stress σ at all strain ϵ levels, (b) reduced the rate of strain hardening $\theta = d\sigma/d\epsilon$ and (c) increased the strain rate hardening exponent $m = d \ln \sigma / d \ln \dot{\epsilon}$. Moreover, as shown in Fig. 16, the concurrent application of the field during superplastic deformation significantly reduced the amount of grain boundary cavitation produced by the deformation. The degree of reduction was found to increase with E . Noteworthy is that the effects of the electric field extended to the center of the 1.2 mm thick specimens. Also, it was found that polarity had an influence on the effect of the field. In the case of the flow stress, connecting the specimen to the positive terminal of the power supply gave a decrease in the flow stress, the magnitude of which increased with E , whereas connecting the specimen to the negative terminal gave an increase in the flow stress. The electric current flowing in the electrostatic circuit was of the order of 1 mA.

These effects of an external electric field on the mechanical behavior of the 7475Al alloy are not clear. Since they only occurred at high homologous temperatures, it is concluded that diffusion plays a controlling role and that the

effects of the electric field are on the diffusion process, notably the generation and/or migration of vacancies. If we assume that the effects of the electric field result entirely from a charged surface layer, then one must account for the fact that these effects extended to the center of 1.2 mm thick specimens. Starting with the relation

$$x = \sqrt{Dt} \quad (5)$$

where x is the diffusion distance, $D = D_0 \exp(-\Delta H/kT)$ the diffusion coefficient and t the time of the test and taking the values $x = 6 \times 10^{-2}$ cm and $D = 0.2 \exp - 11,500/RT$ (vacancy diffusion in Al [48,49], one obtains $t = 25$ s. Considering the strain rates employed, this time is short enough that any changes in vacancy concentration at the surface could diffuse into the interior and thereby influence mechanical behavior. An alternative explanation for the fact that the electric field extends to the center of relatively thick specimen was proposed by Klypin [50]. He suggested the possibility of an uneven electron density at the interfaces between phases and at grain boundaries. The reduction in cavities produced by the field might be a reflection of this, since the cavitation occurred mainly along the grain boundaries.

The observed effect of polarity of the field on the flow stress suggests that a deficiency of electrons in the specimen reduces the flow stress, whereas an excess of electrons increases it.

References

1. H. Conrad and A. F. Sprecher in **Dislocations in Solids**, Chapt. 43, ed. F. R. N. Nabarro, Elsevier Science (1989) p. 497.
2. O. A. Troitskii and V. I. Likhtman, Dokl. Akad. Nauk SSSR 148 (1963) 332.
3. O. A. Troitskii, Pis'ma v Zh. Eksp. & Teor. Fiz. 10 (1969) 18.
4. O. A. Troitskii and A. G. Rozno, Fiz. Tverd. Tela 12 (1970) 203.
5. O. A. Troitskii, Fiz. Met. & Metalloved. 32 (1971) 408.
6. O. A. Troitskii, Probl. Proch., July (1975) p. 14.
7. V. I. Spitsyn and O. A. Troitskii, Dokl. Akad. Nauk SSSR 220 (1975) 1070.
8. O. A. Troitskii, Fiz-Khim. Mekh. Mater. 13 (1977) 46.
9. O. A. Troitskii, V. I. Spitsyn and V. I. Stashenko, Dokl. Akad. Nauk SSSR 241 (1978) 349.
10. O. A. Troitskii and V. I. Stashenko, Fiz. Met. & Metalloved. 47 (1979) 180.
11. O. A. Troitskii, V. I. Spitsyn and P. U. Kalymbetov, Dokl. Akad. Nauk SSSR 253 (1980) 96 [Sov. Phys.-Dokl. 25 (1980) 5581].
12. O. A. Troitskii and P. V. Kalymbetov, Fiz. Met. & Metalloved. 51 (1981) 1056 [Phys. Met. & Metallogr. 51 (1981) 134].
13. O. A. Troitskii and V. I. Stashenko, Fiz. Met. & Metalloved. 51 (1981) 219 [Phys. Met. & Metallogr. 51 (1981) 191].
14. O. A. Troitskii, V. I. Stashenko and V. I. Spitsyn, Izv. Akad. Nauk.SSSR Met. 1 (1982) 164.
15. V. I. Stashenko, O. A. Troitskii and V. I. Spitsyn, Phys. Status Solidi a 79 (1983) 549.
16. Yu. I. Boiko, Ya. E. Geguzin and Yu. I. Kinchuk, Pis'ma v Zh. Eksp. & Teor. Fiz. 30 (1979) 168.
17. Yu. I. Boiko, Ya. E. Geguzin and Yu. I. Klinchuk, Zh. Eksp. & Teor. Fiz. 81 (1981) 2175.
18. L. B. Zuev, V. E. Gromov, V. F. Kurilov and L. I. Gurevich, Dokl. Akad. Nauk SSSR 239 (1978) 84.

19. V. I. Spitsyn, O. A. Troitskii and P. Ya. Glzunov, Dokl. Akad. Nauk SSSR 199 (1971) 810.
20. O. A. Troitskii, I. L. Skobtsov and A. V. Men'shikh, Fiz. Met. & Metalloved. 33 (1972) 392.
21. Yu. I. Golovin, V. M. Finkel and A. A. Sletkov, Probl. Prochn. 2 (1977) 86.
22. G. V. Karpenko, O. A. Kuzin, V. I. Tkachev and V. P. Rudenko, Dokl. Akad. Nauk SSSR 227 (1976) 85.
23. V. I. Spitsyn, O. A. Troitskii, E. V. Gusev and V. K. Kurdiukov, Izv. Akad. Nauk SSSR Met. 2 (1974) 123.
24. O. A. Troitskii, Stal. 5 (1974) 450.
25. K. M. Klimov, G. D. Shnyrev and I. I. Novikov, Dokl. Akad. Nauk SSSR 219 (1974) 323.
26. V. I. Spitsyn, O. A. Troitskii, V. G. Ryshkov and A. S. Kozyrev, Dokl. Akad. Nauk SSSR 231(1976) 402.
27. V. I. Spitsyn, A. V. Kop'ev, V. G. Ryzhkov, N. V. Sokilov and O. A. Troitskii, Dokl. Akad. Nauk SSSR 236 (1977) 861.
28. O. A. Troitskii, V. I. Spitsyn, N. V. Sokolov and V. G. Ryshkov, Dokl. Akad. Nauk SSSR 237 (1977) 1082.
29. O. A. Troitskii, V. I. Spitsyn and V. G. Ryshkov, Dokl. Akad. Nauk SSSR 243 (1978) 330.
30. K. M. Klimov and I. I. Novikov, Russ. Metall. 6 (1978) 127.
31. O. A. Troitskii, V. I. Spitsyn, N. V. Sokolov and V. G. Ryshkov, Phys. Status Solidi a 52 (1978) 85.
32. K. M. Klimov, A. M. Morukhovich, A. M. Glezer and B. V. Molotilov, Russ. Metall. 6 (1981) 68.
33. O. A. Troitskii, Mater. Sci. & Eng. 75 (1985) 37.
34. F. R. N. Nabarro, Theory of Crystal Dislocations (Clarendon Press, Oxford, 1967) p. 529. Reprinted 1987 (Dover, New York).
35. A. M. Roshchupkin, V. E. Miloshenko and V. E. Kalinin, Fiz. Tverd. Tela 21 (1978) 90-9 [Sov. Phys.-Solid State 21 (1979) 532].
36. V. B. Fiks, Zh. Eksp. Theor. Fiz. 80 (1981) 2313.

- 36a. H. Conrad, "Electromigration, Electroplasticity and Other Effects of Electric Current on the Behavior of Metals", North Carolina State University Seminar, April 24, 1987 (1987).
37. V. Ya. Kravchenko, Zh. Eksp. & Teor. Fiz. 51 (1966) 1676 [Sov. Phys.-JETP 24 (1967) 1135].
38. M. I. Kaganov, V. Ya. Kravchenko and V. D. Natsik, Usp. Fiz. Nauk 111 (1973) 655 [Sov. Phys.-Usp. 16 (1974) 878].
39. K. M. Klimov, G. O. Shnyrev and I. I. Movikov, Dokl. Akad. Nauk SSSR 219 (1974) 323 [Sov. Phys.-Dokl. 19 (1975) 787].
40. A. F. Sprecher, S. L. Mannan and H. Conrad, Acta Metall. 34 (1986) 1145-1162.
41. V. L. A. Silveira, M. F. S. Porto and W. A. Mannheimer, Scr. Metall. 15 (1981) 945.
42. V. L. A. Silveira, R. A. F. O. Fortes and W. A. Mannheimer, Proc. 7th Int. Am. Conf. on Materials Technology, Mexico, 1981 (Southwest Institute, San Antonio, TX, 1981) p. 722.
43. V. L. A. Silveira, R. A. F. O. Fortes and W. A. Mannheimer, Beitr. Electronenm. Direkt. Oberfl., 15 (1982) 217.
44. A. San Martin, D. M. Nghiep, P. Paufler, K. Kleinstruck, U. Krämer and N. H. Guyen, Scripta Metall. 14 (1980) 1041.
45. S. T. Kishkin and A. A. Klypin, Dokl. Akad. Nauk SSSR 211 (1973) 325-327.
46. A. A. Klypin, Problemy Prochnosti, No. 7 (July, 1975) 20-26.
47. H. Conrad, W. D. Cao, X. P. Lu and A. F. Sprecher, Scripta Met. 23 697 (1989).
48. P. G. Shewmon, **Diffusion in Solids**, McGraw-Hill, N. Y. (1963) p. 74.
49. R. A. Johnson, **Diffusion**, ASM (1973) p. 25.
50. A. A. Klypin, Metallov i Termich Obradbotra Metallov. No. 3 (1979) 12.

TABLE I. CONTRIBUTIONS TO THE ELECTROPLASTIC EFFECT(1)

Metal	T (K)	$\sigma^{*(2)}$ (MPa)	$\dot{\epsilon}_j/\dot{\epsilon}$	$\dot{\epsilon}_{0j}/\dot{\epsilon}_0$	$\frac{-(\Delta G_j^* - \Delta G^*)}{e}$ kT	$\frac{(A_j^* - A^*)b\sigma^*}{e}$ kT	$\frac{-(\Delta G_j - \Delta G)}{e}$ kT	$\frac{A_j^* F_{ew}}{kT}$
Al	300	9.5	8.8×10^3	7.1×10^3	1.55	0.54	0.84	1.48
Cu		27.0	5.8×10^3	3.4×10^3	2.10	0.69	1.45	1.17
Ag		26.5	5.0×10^3	3.9×10^3	2.01	0.53	1.07	1.21
Nb		42.0	68.2×10^3	10.9×10^3	8.98×10^2	5.20×10^{-3}	4.67	1.34
Al	78	27	26.9×10^3	9.9×10^3	5.64	0.47	2.65	1.03
Cu		40	29.1×10^3	4.1×10^3	17.29	0.36	6.22	1.14
Ag		39	25.1×10^3	4.9×10^3	14.88	0.28	4.17	1.20
Nb		584	324.5×10^3	10.2×10^3	2.92×10^{11}	1.03×10^{-10}	30.08	1.06

Notes: (1) Calculations for lower bound case; $j = 5.5 \times 10^5$ A/cm² for FCC metals, 4.2×10^5 A/cm² for BCC Nb.

(2) σ^* for FCC metals at $\epsilon_p = 0.8\%$ and $\epsilon_j = 0 = 1.67 \times 10^{-4}$ s⁻¹; for BCC Nb at $\epsilon_p = 2\%$ and $\epsilon_j = 0 = 1.67 \times 10^{-5}$ s⁻¹. For these conditions, F_{ew} makes the largest observed contribution to the ratio $\dot{\epsilon}_j/\dot{\epsilon}$.

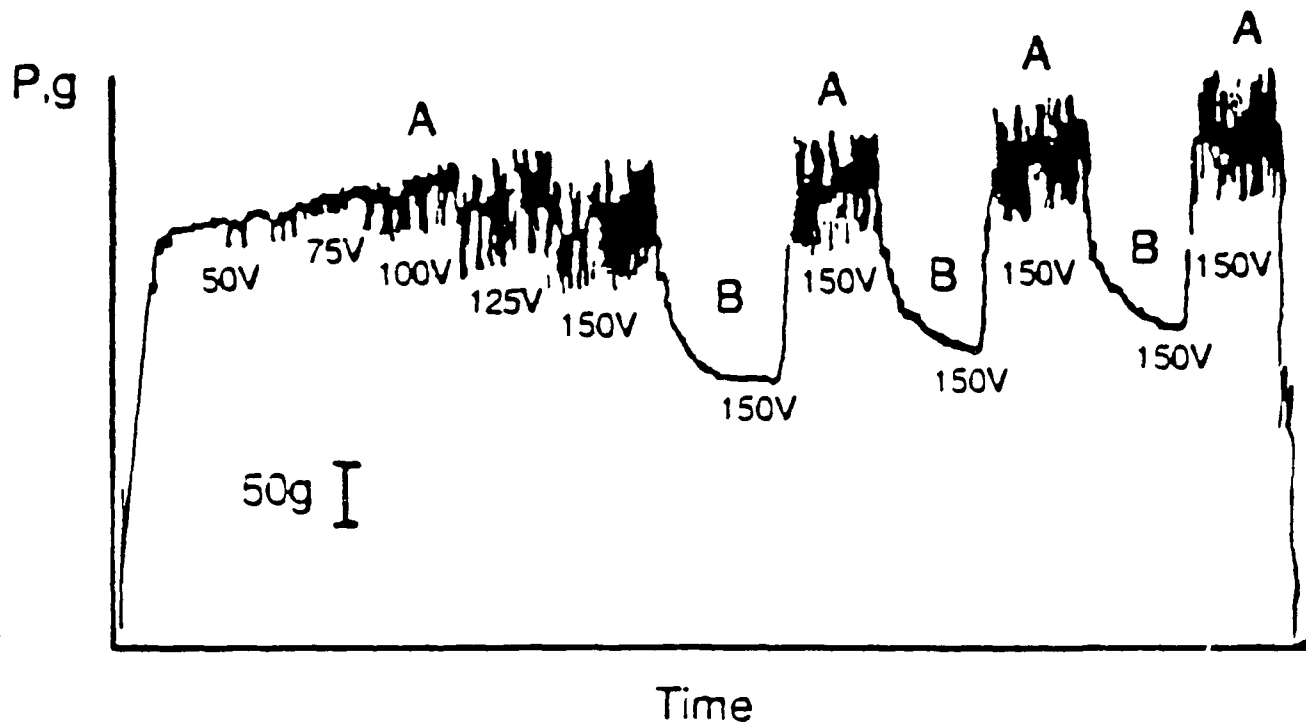
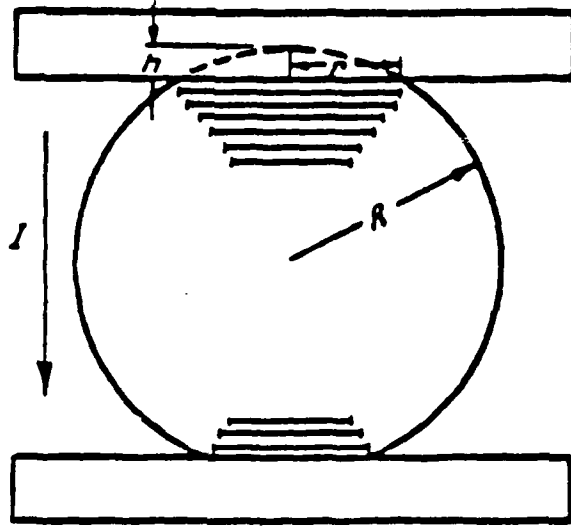
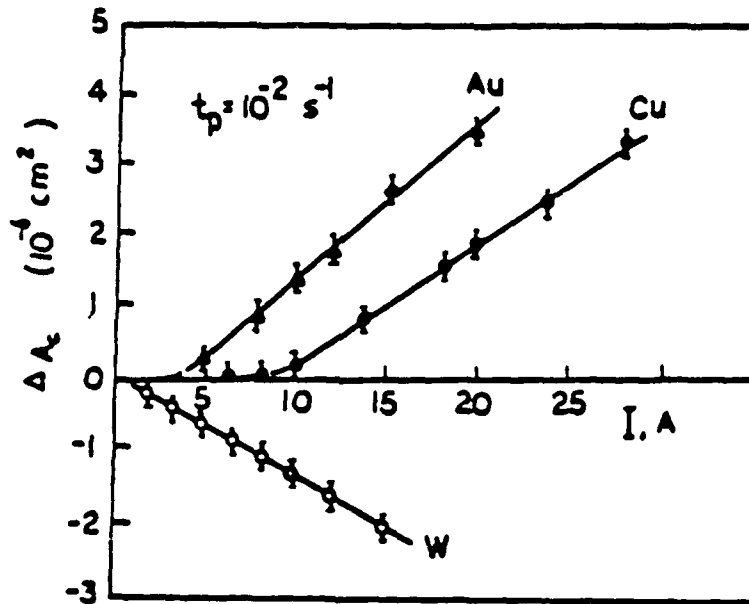


Fig. 1. Load vs extension diagram for a Zn crystal in uniaxial tension at 78 K and strain rate of $1.1 \times 10^{-4} \text{ s}^{-1}$ showing load drops resulting from the application of dc pulses produced by discharging capacitors with the voltages V indicated ($100\text{V} = 1.5 \times 10^5 \text{ A/cm}^2$). Regions A correspond to constant extension rate, regions B to stress relaxation, i.e. the test machine was shut off. From Troitskii [3].



(a)



(b)

Fig. 2. Electroplastic studies by Boiko et al [16,17]: (a) Schematic of procedure employed. (b) Effect of electric current on the difference in contact area at the two electrodes for Au, Cu and W single crystal spheres compressed between two parallel plates.

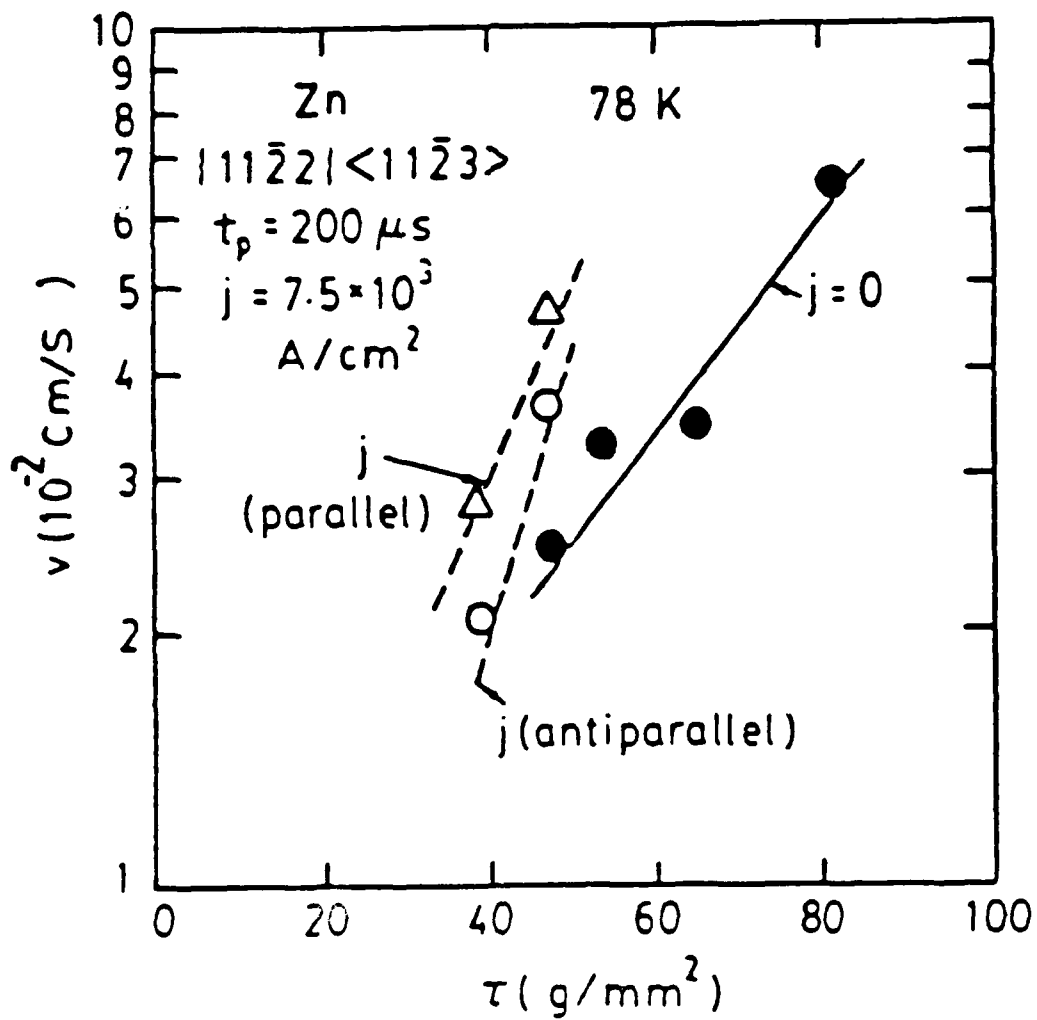


Fig. 3. Effect of a single current pulse ($j = 0.75 \times 10^4 \text{ A/cm}^2$, $t_p = 200 \mu s$) on the velocity of $\{11\bar{2}2\} \langle 11\bar{2}3 \rangle$ dislocations in Zn parallel and antiparallel to the electron current as a function of the mechanically applied stress τ . Data from Zuev et al. [18].

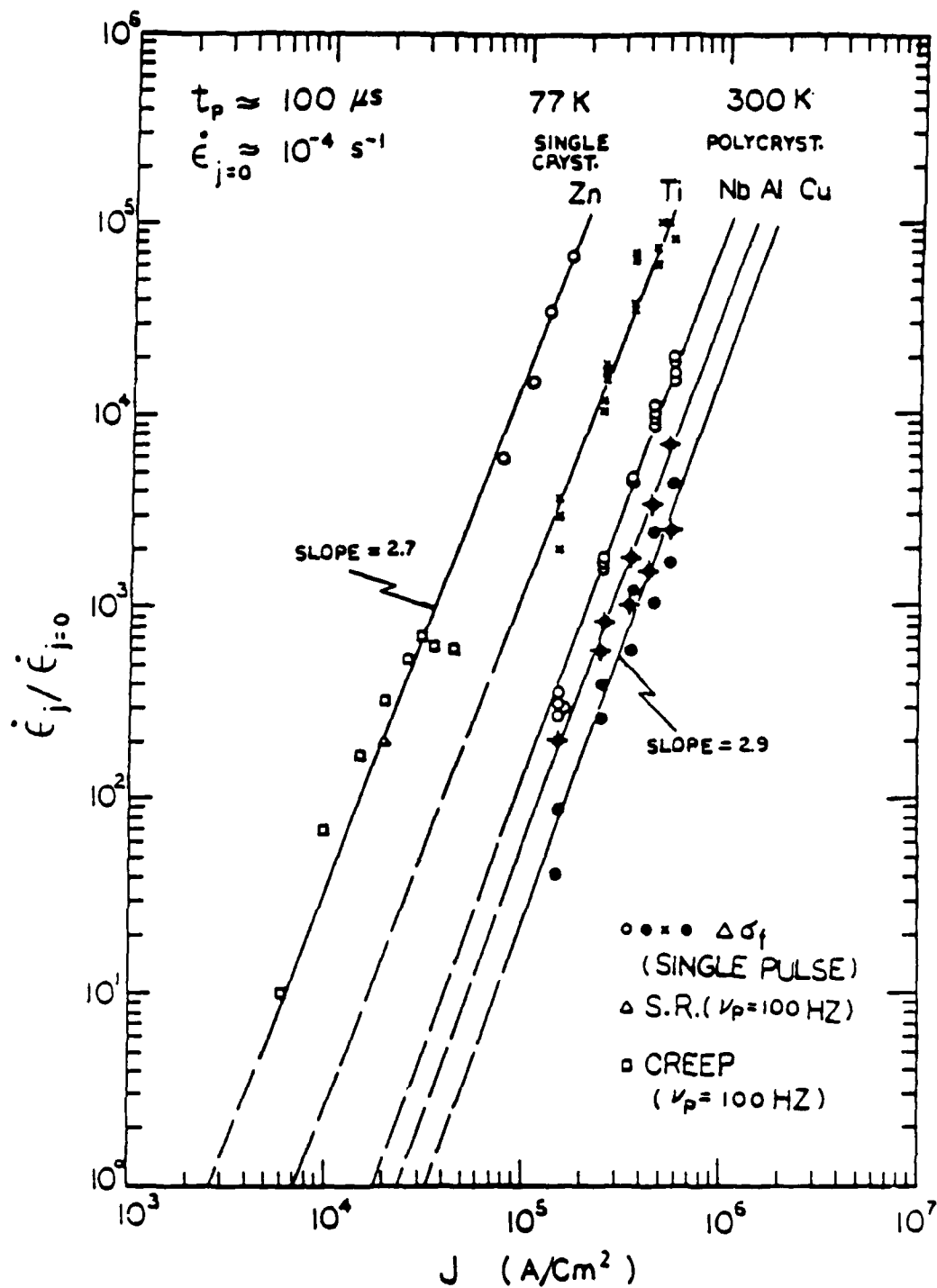


Fig. 4. Log-log plot of the ratio of the plastic strain rate $\dot{\epsilon}_j$ produced by an electric current pulse to the applied strain rate $\dot{\epsilon}_{j=0}$ prior to the pulse for Zn single crystals at 78K and a number of polycrystalline metals at a 300K. Test methods include constant strain rate test to yield the drop in flow stress for a single pulse $\Delta\sigma_f$, stress relaxation S.R. and creep tests with 100 pulses per second. From Conrad and Sprecher[1]

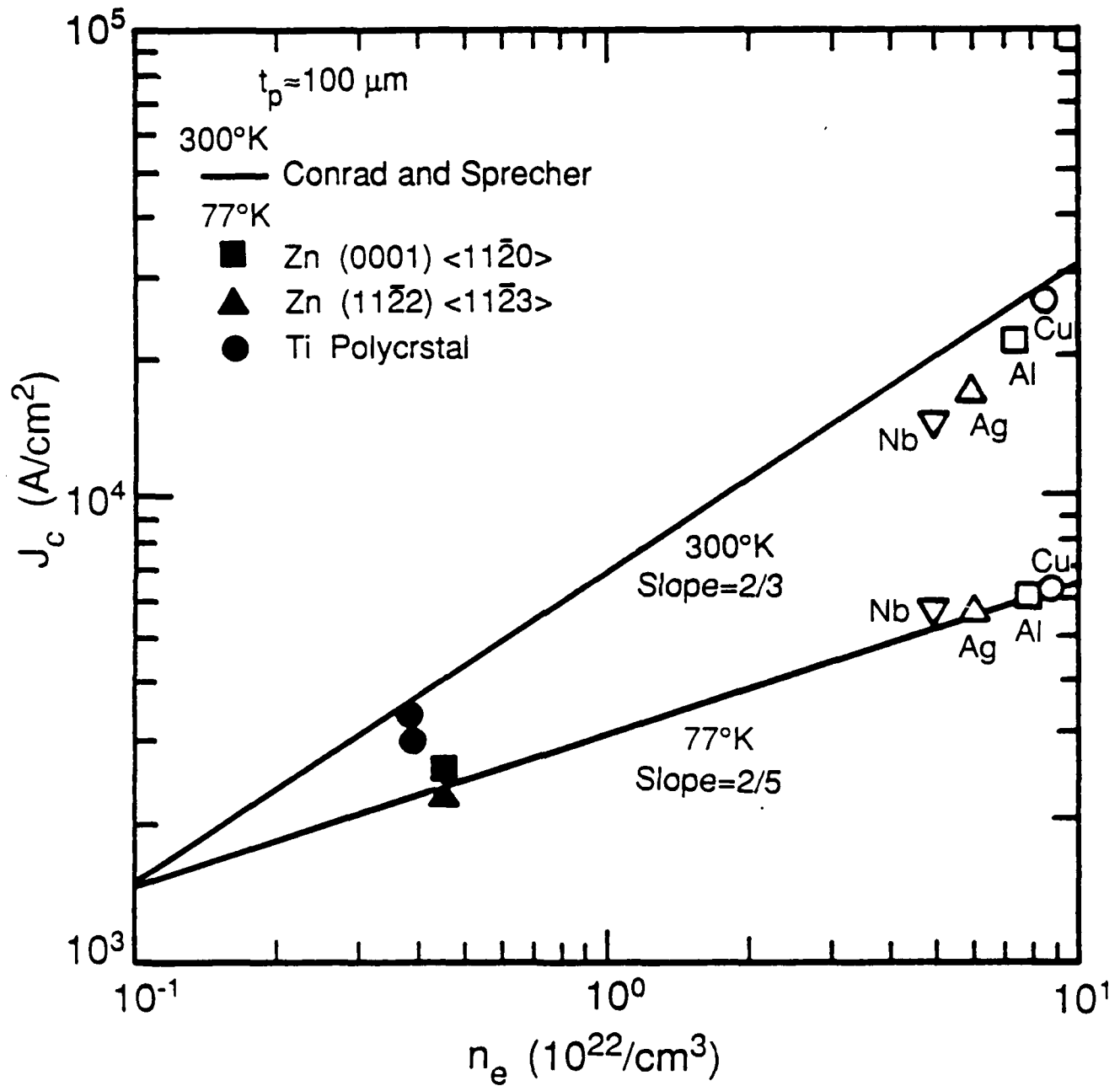


Fig. 5. Log-log plot of the critical current density j_c at 77 and 300 K vs the electron density n_e .

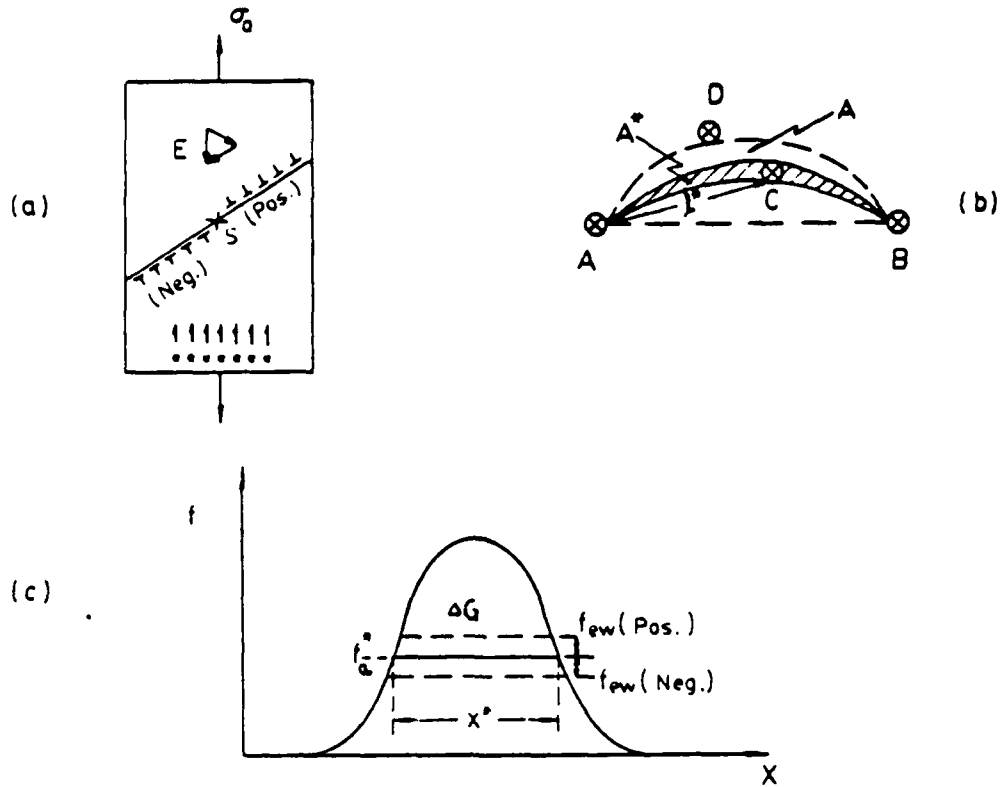


Fig. 6. Schematic pertaining to the effect of an electric force (in the opposite direction to the current) on dislocation velocity: (a) Specimen subjected to the combined action of a mechanical stress σ_0 and an electric force, with dislocations moving on the glide plane with a velocity parallel (pos.) and antiparallel (neg.) to e (e indicates direction of drift electrons; E the electric field). (b) Dislocation segment of length $2l^*$ overcomes obstacle C by combined action of total applied force and thermal fluctuations. (c) Force-distance curve for overcoming the obstacle C . ΔG = Gibbs free energy of activation. $f_a^* = \tau_0^* b l^*$, $f_{ew} = F_{ew} l^*$, x^* = activation distance, $A^* = l^* x^*$, $\tau_0^* = (\sigma_0 - \sigma_i) / M$, where σ_i is the long-range internal stress and M the orientation factor.

$$\dot{\gamma} = \dot{\gamma}_0 \exp - \left[\frac{\Delta G^* - A^* b \tau^*}{kT} \right] \quad (1)$$

$$\dot{\gamma}_j = \dot{\gamma}_{0,j} \exp - \left(\frac{\Delta G_j^* - A_j^* b \tau^*}{kT} \right) \left[\exp \frac{A_j^* F_{ew}}{kT} + \exp \frac{-A_j^* F_{ew}}{kT} \right] \quad (2)$$

$$\ln \left(\frac{\dot{\gamma}_j}{\dot{\gamma}} \right) = \ln \left(\frac{\dot{\gamma}_{0,j}}{\dot{\gamma}_0} \right) - \left(\frac{\Delta G_j^* - \Delta G^*}{kT} \right) + \frac{(A_j^* - J^*) b \tau^*}{kT} + \ln \left[2 \cosh \left(\frac{A_j^* F_{ew}}{kT} \right) \right] \quad (3)$$

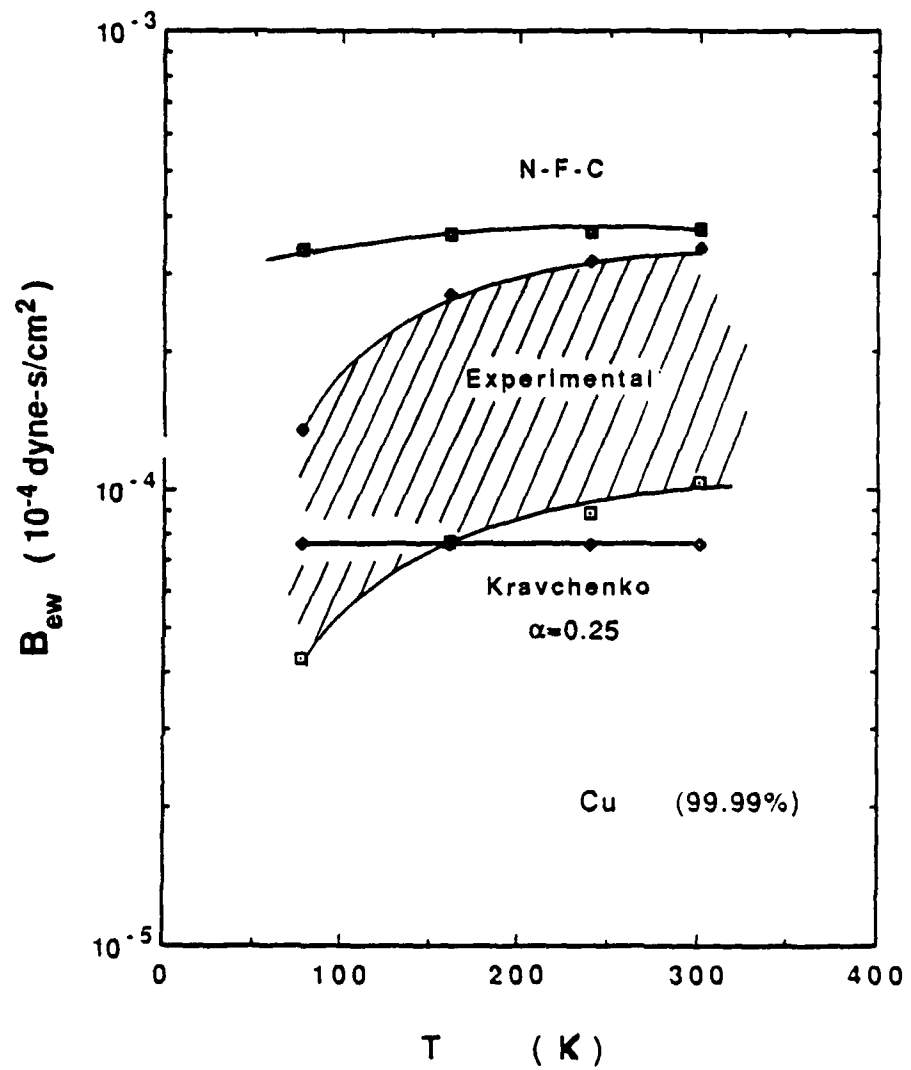


Fig. 7. Comparison of experimental value of B_{ew} for Cu with the theoretical values $B_{ew} = 0.25 b p_F j/e$. (Kravchenko) and $B_{ew} = \rho_D e n_e j / N_D$ (N-F-C).

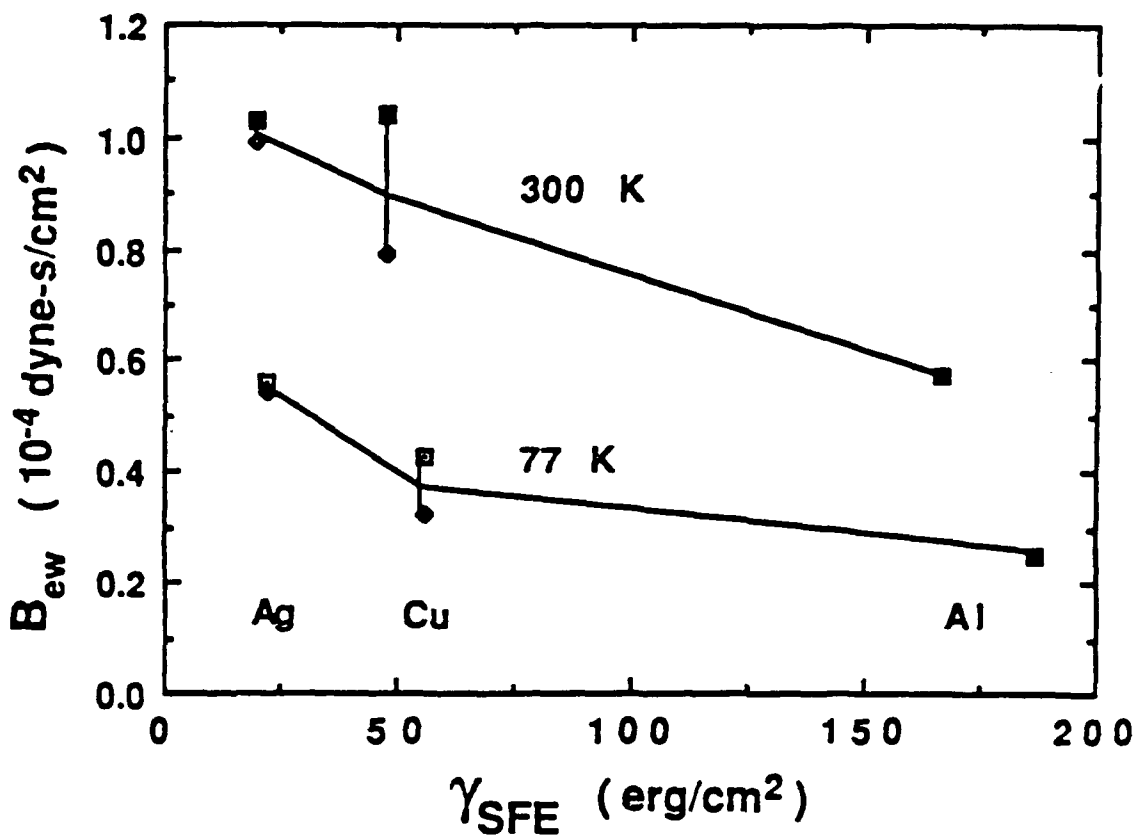


Fig. 8. Effects of stacking fault energy in FCC metals on the electron wind push coefficient B_{ew} as a function of temperature.

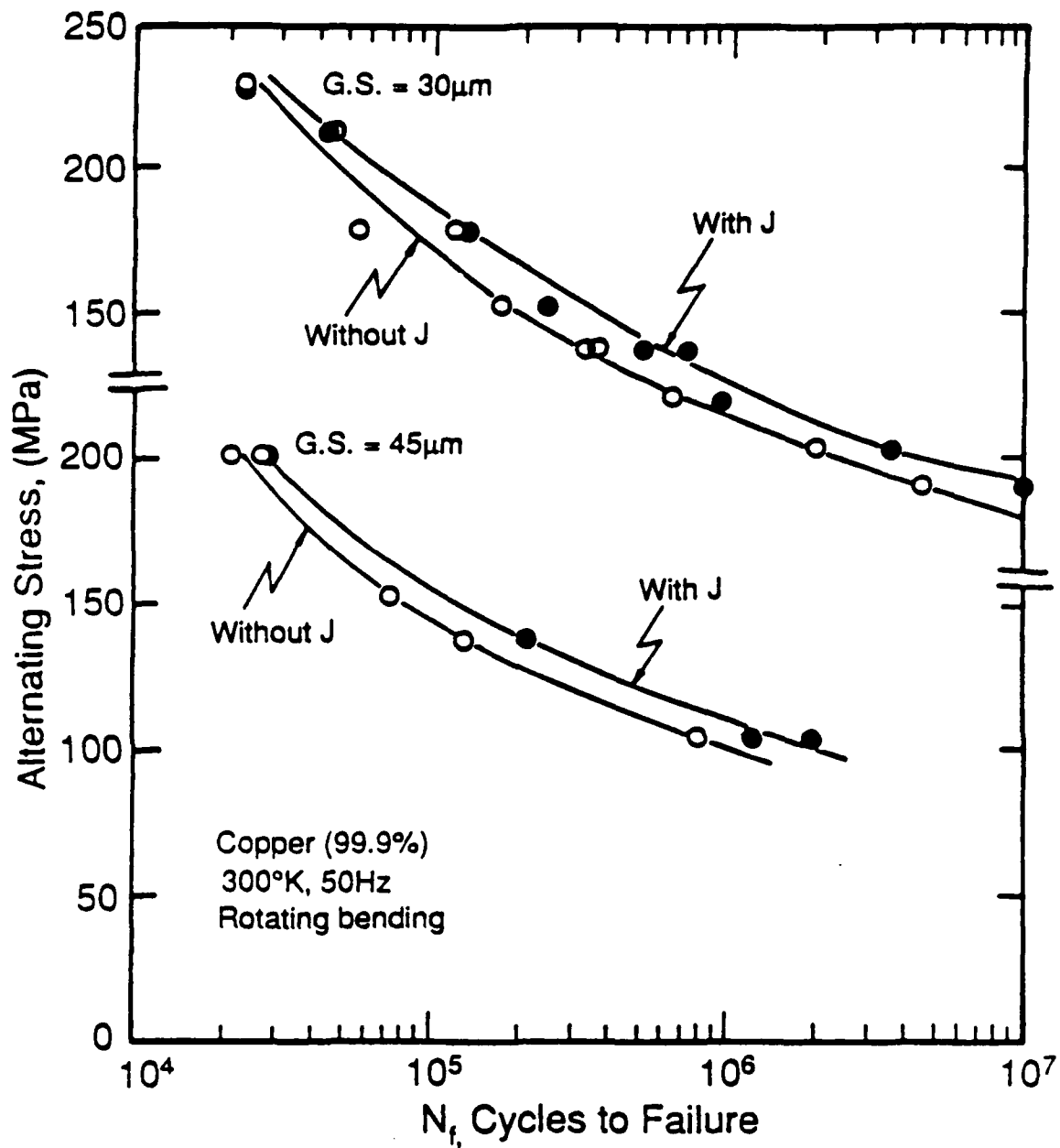


Fig. 9. S- N_f curves as a function of grain size for tests with, and without, current pulsing. ($j = 1.3 \times 10^4 \text{ A/cm}^2$, $t_p = 100 \mu\text{s}$, and $\nu_p = 2 \text{ Hz}$)

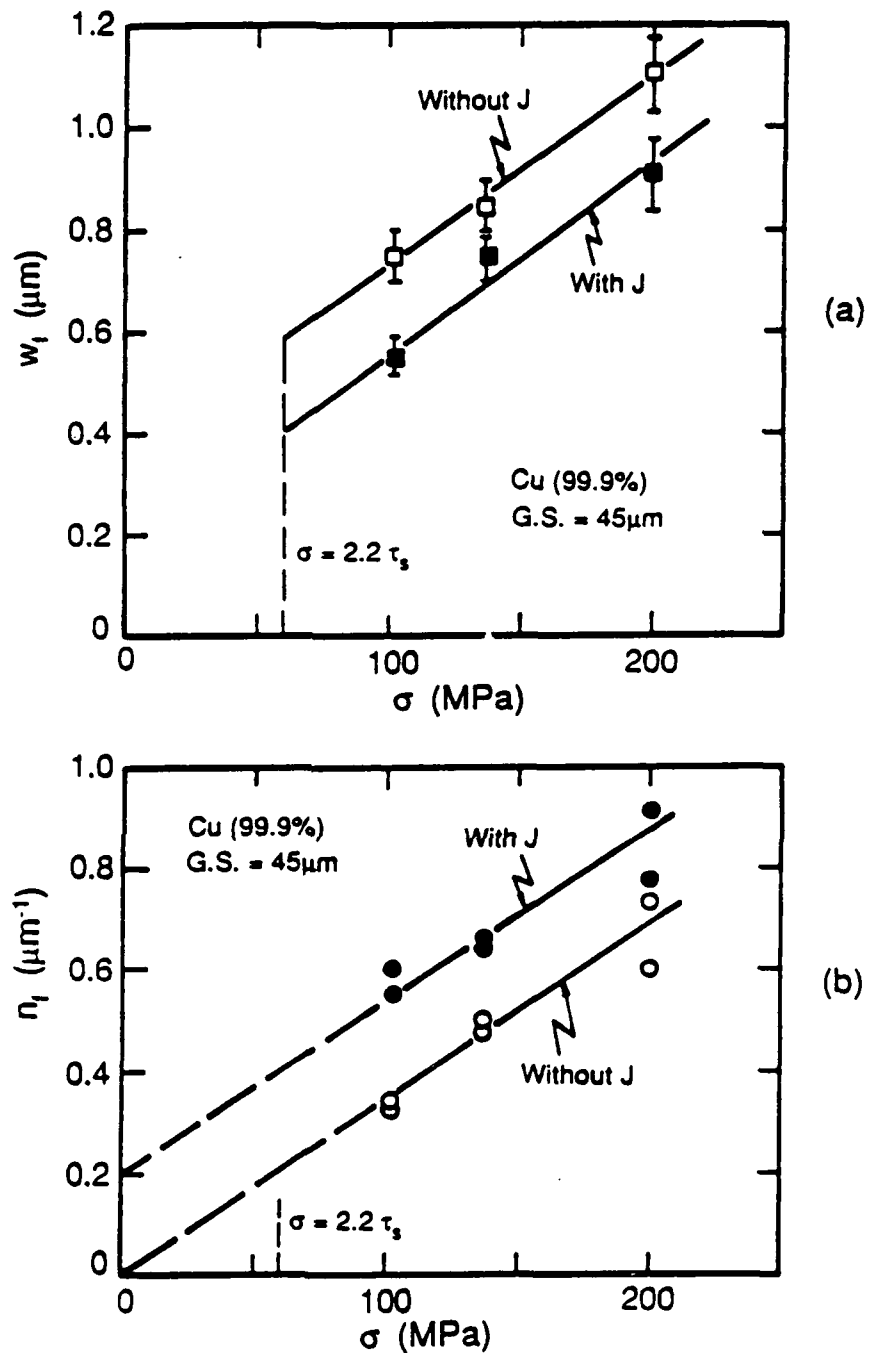


Fig. 10. Effect of electropulsing on PSB characteristics at fracture as a function of stress: (a) width and (b) linear density. $\tau_s = 28$ MPa is the plateau resolved shear stress (Stage B) in the fatigue of Cu single crystals. The factor 2.2 is the Sachs orientation factor.

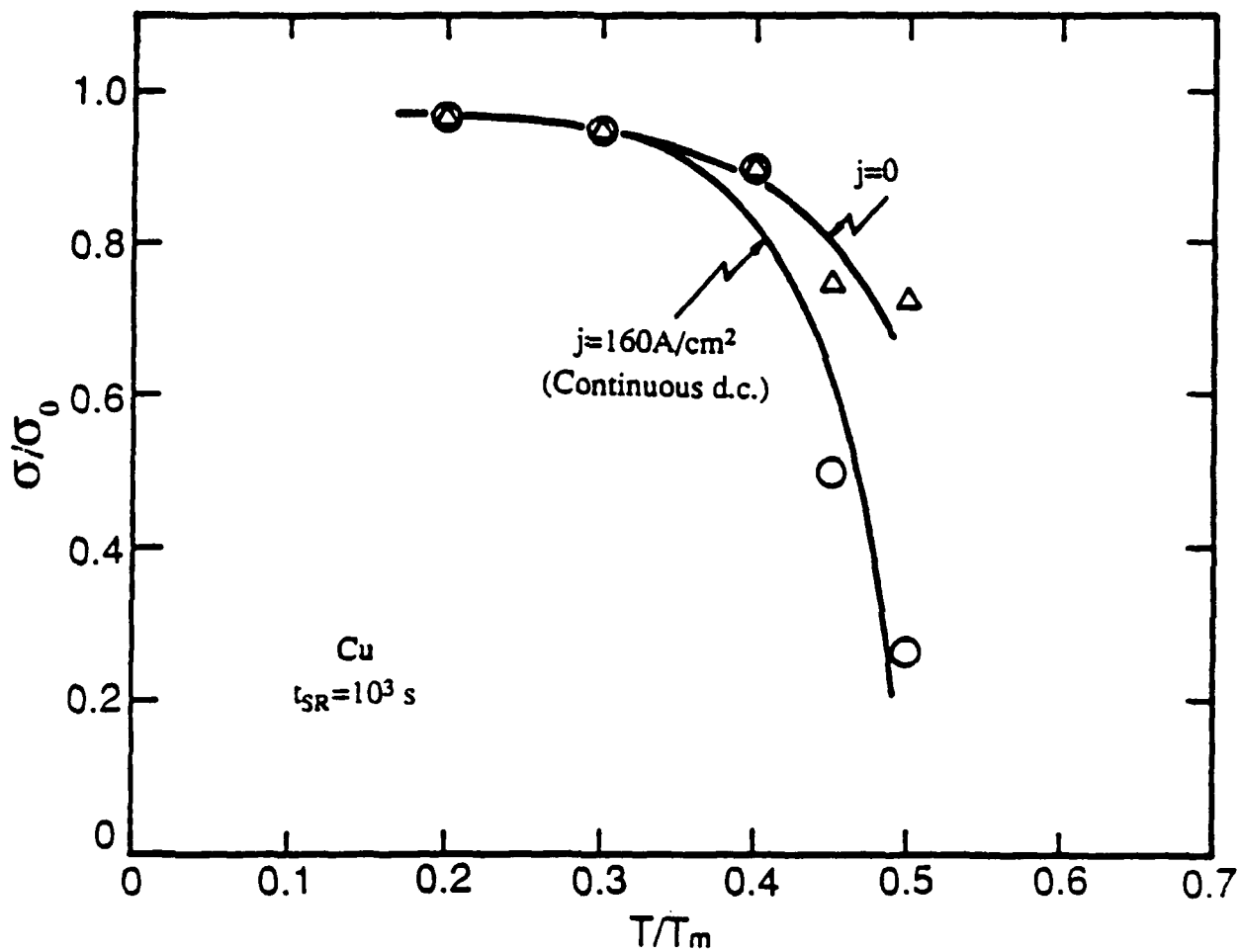


Fig. 11. Fraction of stress relaxed in 10^3 s vs homologous temperature for stress relaxation tests on polycrystalline Cu specimens tested with, and without, the concurrent application of a continuous d.c. current of 1.6×10^2 A/cm². Data from Silveira et al [41, 42].

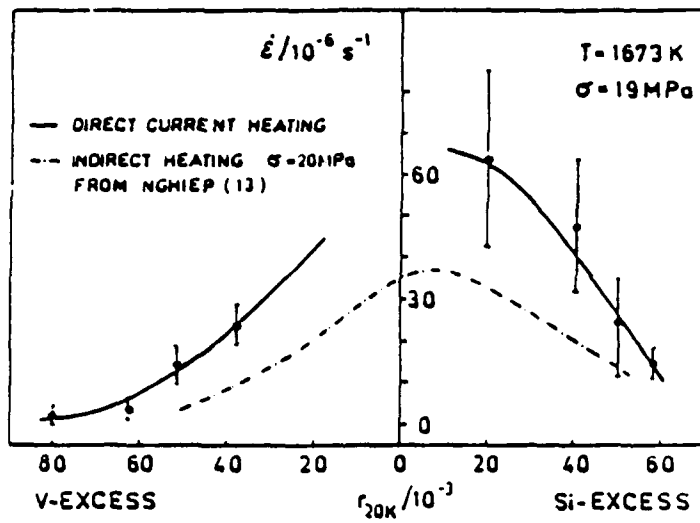


Fig. 12 Effect of a continuous d.c. current of $2.5 \times 10^3 \text{ A/cm}^2$ on the steady-state creep rate of V_3Si as a function of stoichiometry. From San Martin et al [44].

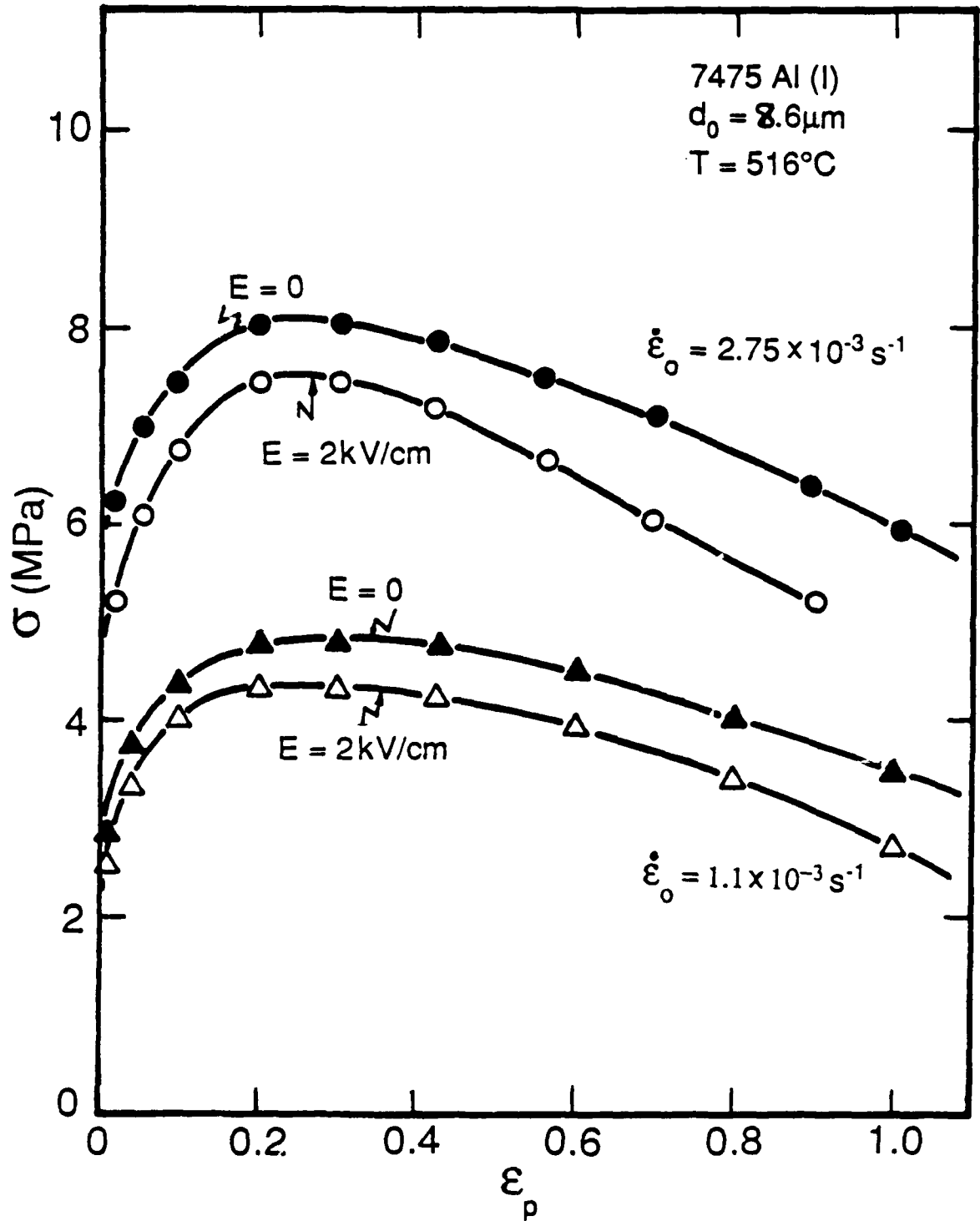


Fig. 13. Effect of external electric field E on the true stress vs true strain curves for the superplastic deformation of 7475 Al at two strain rates.

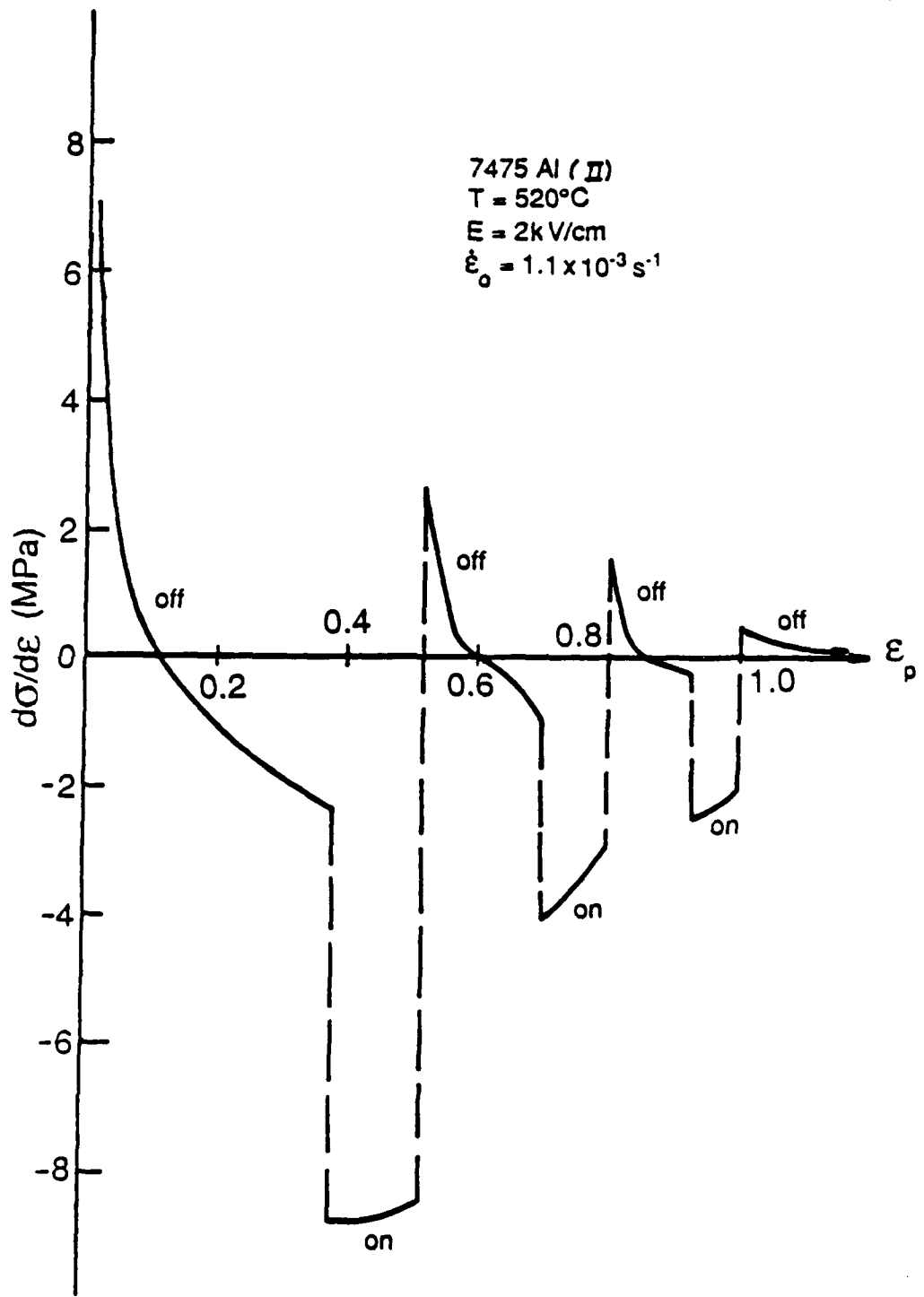


Fig. 14. Changes in the rate of strain hardening when a continuous d.c. electric field $E = 2 \text{ kV/cm}$ is turned "on" and "off" during superplastic deformation of 7475 Al alloy. From Conrad et al [47].

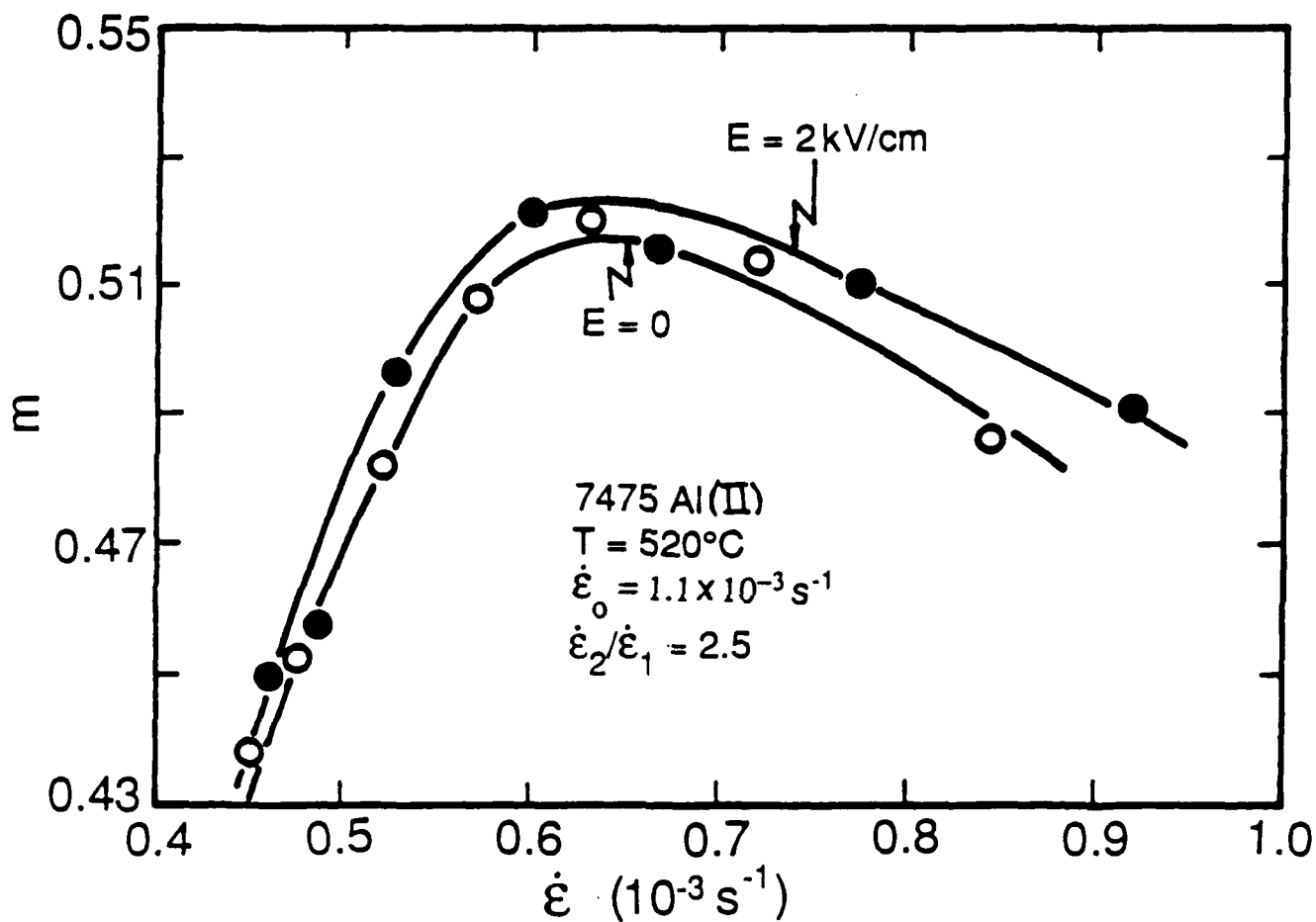
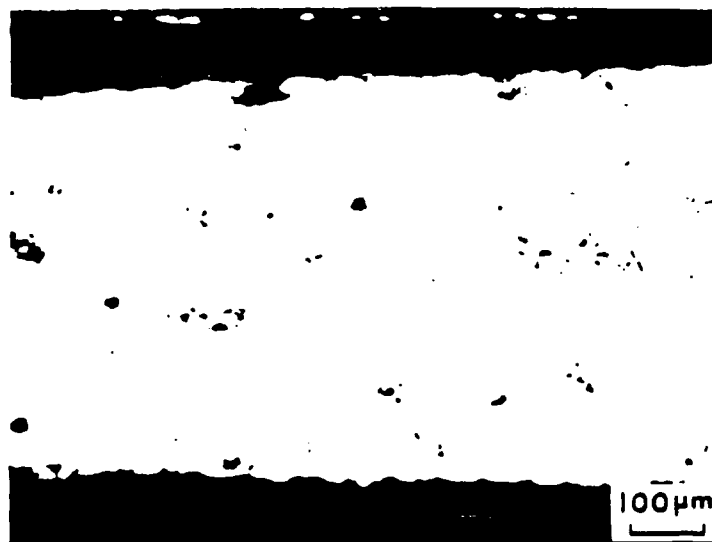


Fig. 15. Effect of a continuous d.c. electric field $E = 2 \text{ kV/cm}$ on the strain rate hardening parameter $m = \ln \sigma / \ln \dot{\epsilon}$ vs strain rate $\dot{\epsilon}$ during superplastic deformation of 7475 Al alloy. The variation in $\dot{\epsilon}$ results from the elongation of the specimen during plastic deformation at a constant crosshead speed. From Conrad et al [47].



(a)



(b)

Fig. 16. Effect of an electric field E on the amount of cavitation which occurred during superplastic deformation of 7475 Al at 516°C : (a) $E = 0$, elongation = 334% and (b) $E = 2$ kV/cm, elongation = 455%. From Conrad et al [47].

THE USE OF HIGH-POWER ULTRASOUND TO STUDY MECHANICAL PROPERTIES - A REVIEW

Kamel Salama

Mechanical Engineering Department
University of Houston
Houston, Texas 77004

The application of high-power ultrasound has been found to affect mechanical properties which are characteristic of plastic deformation such as yielding, ductility, fatigue and wear¹⁻³. During the application of ultrasound, the static shear stress necessary for deformation is significantly reduced and the ductility is considerably increased. These softening effects are interpreted to be caused by the activation of dislocations which can be set mobile during the superposition of the ultrasound. The effect of ultrasonic energy is to reduce the stress required for dislocation movement by supplying energy to dislocation sites. When these dislocations receive sufficient additional energy to surmount the potential barriers between their equilibrium positions, they break free from their solute atmosphere and cause the reduction of the flow stress and the increase of deformation. The movements of these dislocations by slip will yield microcracking which lead to fatigue and wear processes. In this review, we will present three examples where high-power ultrasound have proven to be a powerful technique to study mechanical behavior of solids and mechanisms responsible for this behavior.

1. Hydrogen Embrittlement

In this work, the high-power ultrasound was used to study the role of dislocations in the embrittlement of group VA metals with hydrogen. The effects of 20 kHz high-power ultrasound of strain amplitude 10^{-4} superimposed on static loading, on the yielding and the ductility of hydrogenated niobium, have been studied in the temperature range between 373 and 78K. A special holder is designed to allow for the direct application of the ultrasonic vibrations to the specimen while it is subjected to the static loading. In order to ensure that only a negligible amount of ultrasonic power is dissipated in the Instron Machine after the specimen is attached, the displacement amplitude at both ends of the specimen are measured before and after the application of static stress. For tensile tests performed with ultrasound, both the crosshead and the ultrasonic generator are started in motion simultaneously, and the load-elongation relationship is plotted on the recording system. Desired sub-ambient temperatures were obtained by means of controlled evaporation of liquid nitrogen throughout a copper coil immersed in an isopentane liquid. Above room temperature, the desired temperature was obtained by heating water by means of an immersion heater equipped with a temperature control system.

The results obtained in this study show that in pure niobium, the application of ultrasound has no effect at temperatures above 150K, and has small reducing effect below this temperature. When hydrogen is dissolved, however, the yield stress is considerably reduced at all temperatures by the application of ultrasound. The reduction in stress is larger at lower temperatures when the hydride phase is expected to be present. The reduction in the yield stress varies between 30 MPa at

300K, and 270 MPa at 78K. The precipitation of hydride is found to result in the formation of dislocations punched out into the matrix of the alloy⁴, and yields more reduction in the yield stress. At higher hydrogen concentration (170 ppm wt), the effect of ultrasound on the yield stress is less pronounced, and about half that exhibited when the niobium specimens contain 70 ppm wt H. The number of dislocations which can be set free from hydrogen barriers when ultrasound is applied, is expected to be larger at lower hydrogen concentrations.

On the other hand, the effect of ultrasound on the temperature dependence of ductility indicates that the ductility in the presence of hydrogen is considerably lowered at all temperatures used in the tests. This decrease in the ductility is also manifested by an increase of approximately 50K in the ductile-brittle transition temperature. This embrittlement effect of ultrasound is contrary to what would be expected when dislocations are set free to move and cause an increase in the ductility^{5,6}. The loss of ductility in the presence of hydrogen when ultrasound is applied, may then be interpreted as due to the rapid transport of hydrogen to the highly stressed area of the crack tip⁷⁻⁹. In this case, dislocations set mobile by ultrasound, will drag the clouds of hydrogen atmosphere around them, and result in deeper penetration of the hydrogen, than that allowed by random walk diffusion. The rapid dislocation transport of hydrogen will provide the necessary hydrogen enrichment at the crack tip for the continuation of the crack growth process.

2. Ultrasonic Fatigue

Fatigue failure at low or high frequency originates from dislocation sources¹⁰ and their interactions when subjected to stress cycles. Point defects also play an important part in the early stages of deformation.^{11,12} The character of these mechanisms may be studied by the observation of slip line structures on the surface of electropolished specimens when they are subjected to stress. Observations of surface slip lines or bands have proven to be a powerful technique to study mechanisms which affect mechanical properties, especially those occurring¹³ before fracture. Slip zone for microcracks are also formed before fracture occurs and found to be sensitive to both frequency and strain amplitude.¹⁴ The present work was undertaken to determine the characteristics of slip line structures of face-centered cubic materials when subjected to high strain amplitudes at ultrasonic stress cycles.¹⁵ Ductile metals, copper and aluminum, were chosen for this study because the mechanisms of fatigue in these metals are not well understood. The results obtained were used to test theories developed to describe crack growth in conventional fatigue.

Fundamentally, the initiation of cracks in ductile fatigue occurs at the slip bands created during the cyclic loading. These bands can lead to the localization of plastic strain by the creation of discontinuities on a previously featureless surface. Regions beneath these fatigue bands are softer than the adjacent matrix¹⁶ and within them, further dislocation motion is easier. Cross slip and climb are suggested to be involved in this process,¹⁶ where their presence indicate favorable conditions for nucleation. Once the crack is initiated at a slip band on the surface, it will continue to advance along the primary slip planes involved in the creation of this band. This is usually referred to as Stage I growth. In polycrystalline metals, Stage I crack growth usually terminates when the slip band crack encounters a grain boundary. As the specimen is subjected to longer intervals of insonation, the crack growth enters into Stage II, which is characterized by advances of finite increment in each loading cycle.¹⁷ Stage II is also characterized by the appearance of striations on the fracture surface, which provide a record of the passage of the fatigue crack front. Both effects are involved in establishing a balance between the applied stress and the amount of plastic

deformation at the crack tip. Stage II continues until the remaining cross section area can no longer support the applied load.

There is no simple relationship between the rate of crack growth defined as (dc/dN) , and the stress intensity factor $K = \sigma\sqrt{\pi c}$ where $2c$ is the length of the crack. In Stage II, however, the following relationship has been found to hold in conventional fatigue for a large variety of materials,¹⁸

$$\frac{dc}{dN} \propto (\sigma\sqrt{c})^4 \quad (1)$$

but with a wide variation in the resistance to fatigue growth. The analysis of crack growth based on continuum dislocation model of plastic yielding at a notch¹⁹ resulted in expressing equation [1] as

$$\frac{dc}{dN} \propto \frac{(\sigma\sqrt{c})^4}{\delta G \sigma_y^2} \quad (2)$$

where δ is the surface deformation energy, G is the shear modulus and σ_y is the yield stress. Equation [2] has been further modified to incorporate the effects of strain hardening,²⁰ as

$$\frac{dc}{dN} \propto \frac{(\sigma\sqrt{c})^4}{[(\sigma_y + \sigma_u) / 2] E \sigma_u^2 \epsilon_u} \quad (3)$$

where σ_u and ϵ_u are respectively the stress and the strain at necking.

In order to test the application of equation [3] to ultrasonic fatigue, the quantity $[(\sigma_y + \sigma_u) / 2] E \sigma_u^2 \epsilon_u$ is computed using the results of tensile tests undertaken on specimens similar to those used in the ultrasonic fatigue experiments. The values of $[(\sigma_y + \sigma_u) / 2] E \sigma_u^2 \epsilon_u$ computed for copper and aluminum are respectively $24.6 * 10^{18}$, and $0.05 * 10^{18}$, which suggest that the rate of crack growth in aluminum is much larger than that in copper. In the present study, failure in the aluminum specimen occurred after less than 17 minutes of insonation, while the copper specimen did not fracture even after 30 minutes of insonation. This result shows the importance of strain-hardening in ultrasonic fatigue as a mechanism affecting crack propagation in Stage II.

3. Fretting Wear

Fretting wear is defined as oscillating low amplitude sliding surface contact between two solid bodies. Wear caused by fretting is a severe materials process. In order to explore the possibility of utilizing ultrasonic techniques in fretting wear tests, the wear characteristics of one ferritic^{21,22} and one stainless steel²³ have been studied using high-power ultrasound of frequency 20 kHz. In these tests, wear rates were measured as functions of applied load, displacement amplitude, and number of cycles. The test program was designed to explore the influence of number of cycles, slip amplitude and load load on fretting wear with like metals in contact. The magnitude of the wear damage was estimated for each specimen by measuring the minor diameter

of the wear scar and calculating the volume of material removed. The results of tests with varied normal load and slip amplitude at a constant duration are summarized by three-dimensional graphs.

From these tests, one can see that for low loads and amplitudes, low wear rates are recorded. In addition, it is also found that wear is little affected by changing only one parameter. On the other hand, if either a high load or a high amplitude is applied, the wear rate is strongly affected by a change in any of these two parameters. This means that a mild and a severe wear regime seem to be present in the fretting of these materials, and the boundary line is a function of the combination of load and amplitude. The occurrence of an inner and an outer contact zone in the wear scars was confirmed by metallographic studies.

Since the contact area increases due to plastic deformation, the contact conditions will gradually change during each test, with a concomitant reduction in contact pressure. Eventually, the real area of contact may approach the nominal area. This corresponds to seizure, and precludes interfacial sliding. Then, if a tangential force is applied, the relative motion of the vibrating specimen will be accomplished by shearing of the material in a zone adjacent to the initial contact area. This condition of total surface contact, with shear stresses exceeding the shear yield stress will most likely result in the formation of a friction weld at the contact area.

The high cyclic tensile-compressive stresses, generated along the edge of the contact area, will cause the formation of transverse microcracks, which are observed experimentally after 10^4 cycles. This will only partly reduce the high stresses, and therefore the cracks will continue to propagate. Finally, several cracks will run together, resulting in the transfer and loss of material. A loose particle however, cannot be removed as a whole since it is entrapped between the mating specimens. Instead, it is gradually worn away, probably by oxidation and subsequent crushing of the brittle oxide. The formation of a loose particle in the central region will also result in a reduced contact pressure. Consequently, the total area of contact must increase by plastic deformation outside the original contact area. In principle, the same process can now be repeated, i.e. crack formation, oxidation of cracks and crushing and removal of oxides. At this point, however, the individual points of contact are smaller, and thus the stress generated at the edge of the weld region is reduced. The resulting cracks will no longer propagate to the same depth as earlier, and the pits will become shallower.

It is still interesting to note, however, that the wear mechanisms found at low frequencies correspond well with those found in ultrasonic fretting. The observed wear mechanisms also exhibit many features which agree with some of the most accepted models for fretting in the literature.^{24,25} The main differences between ultrasonic fretting and low frequency fretting seems to lie in the increased severity of the initial adhesive stage at ultrasonic frequencies. In general, it seems that ultrasonic testing appears to be a promising technique for accelerated fretting wear testing, although more experimental work is required to further evaluate the method.

REFERENCES

1. B. Langenecker, ATAA Journal, 1963, Vol. 1, pp. 80.
2. D.R. Culp and H.T. Gencsoy, Proc. Ultrasonic Symposium, 1973, pp. 195.
3. D. Oelschlagel and B. Weiss, Acta Phys. Austr., 1965, Vol. 20, pp. 363.
4. J.C. Williams, Proc. AIME Symposium on "Effects of Hydrogen on Behavior of

- Materials", A.W. Thompson and I.M. Bernstein, eds., 1976, pp. 367.
5. A.R.C. Westwood, C.M. Preece and M.H. Kamdar, Trans. Am. Soc., 1967, Vol. 60, pp. 723.
 6. A. Kelly, W.R. Tyson and A.H. Cottrell, Phil. Mag., 1967, Vol. 15, pp. 567.
 7. J.K. Tien, Proc. AIME Symposium on "Effects of Hydrogen on Behavior of Materials", A.W. Thompson and I.M. Bernstein, eds., 1976, pp. 309.
 8. J.K. Tien, A.W. Thompson, I.M. Bernstein and R.J. Richards, Met. Trans., 1976, Vol. 7A, pp. 821.
 9. J.K. Tien, R.J. Richards, O. Buck and H.L. Marcus, Scripta Met., 1975, Vol. 9, pp. 1097.
 10. W.P. Mason, Proceedings of the First Ultrasonic Symposium 1970, I.P.C. Science and Technology Press Ltd., London.
 11. B. Weiss, Proceedings of the First Ultrasonic Symposium 1970, I.P.C. Science and Technology Press Ltd., London.
 12. D. Mclean, Vacancies and Other Point Defects in Metals and Alloys, Institute of Metals, London, 1968.
 13. K. Salama, and J. M. Roberts, Materials Science and Engineering, 1972, Vol. 9, pp. 50.
 14. N. Thompson, Advances in Physics, 1958, Vol. 7, pp.72.
 15. A. Tulyanon and K. Salama, Proc. IEEE Ultrasonics Symposium, 1976, pp.644,
 16. O. Helgeland, J. Inst. Metals, 1965, Vol. 93, pp.570.
 17. P.J.E. Forsyth, Acta. Met., 1963, Vol. 63, pp. 703 .
 18. J. Weertman, J. Proc. Int. Conf. of Fracture, Sendai, Japan, 1966.
 19. A. J. McEvey, and T. L. Johnston, J. Proc. Int. Conf. of Fracture, Sendai, Japan, 1966.
 20. S.S. Mason, Exp. Mech., 1965, Vol. 5, pp. 193.
 21. S. Soderberg, T. Colvin, D. Nikoonezhad, O. Vingsbo, and K. Salama, Proc. Ultrasonics International, 1985, pp.929.
 22. S. Soderberg, T. Colvin, K. Salama, and O. Vingsbo, J. Materials and Technology, 1986, Vol.108, pp.153.
 23. S. Soderberg, D. Nikoonezhad, K. Salama, and O. Vingsbo, J. Ultrasonics, 1986. Vol. 24, pp. 348.
 24. R. B. Waterhouse and D. E. Taylor, Wear, 1974, Vol.29, pp.337.
 25. E. S. Sproles and D.J. Duquette, Wear, 1978, Vol.49, pp. 339.

EFFECTS OF AN ELECTRIC CURRENT AND EXTERNAL ELECTRIC FIELD ON THE ANNEALING OF METALS

A. F. Sprecher and H. Conrad
Materials Science and Engineering Department
North Carolina State University
Raleigh, NC 27695-7907

ABSTRACT

This paper reviews recent investigations into the influence of an electric current and an external electric field on the annealing response of cold worked Al, Cu, α -Ti and Ni₃Al. A low density ($\sim 10^3$ A/cm²) continuous dc current has been reported to decrease the recrystallized grain size of Cu and α -Ti. High density ($\sim 10^5$ A/cm²) current pulses enhanced the rates of recovery and recrystallization and decreased the recrystallized grain size of Al, Cu and Ni₃Al. The effects of both levels of current on recrystallization appear to be on the nucleation rate. Regarding grain growth, electropulsing significantly decreased the rate of grain growth immediately following recrystallization at low temperatures. Experimental evidence indicates that this reduced grain growth rate results from a decreased residual dislocation density in the electropulsed specimens. The effects of current on grain growth at higher annealing temperatures is not clear, a low level continuous dc current produced a smaller grain size in Cu, but a larger grain size in α -Ti.

An external dc electric field retarded the rates of recovery and recrystallization in Al and Cu, but enhanced them in Ni₃Al. The polarity of the field was important in Cu, but not in Ni₃Al. The influence of the field on the annealing response extended to the center of specimens up to 0.8 mm thick. The mechanism by which this occurs is not clear.

EFFECTS OF AN ELECTRIC CURRENT AND EXTERNAL ELECTRIC FIELD ON THE ANNEALING OF METALS

1. INTRODUCTION

It is well recognized that electric fields and currents affect point defect mobility (1,2), which is known as electromigration. Moreover, it has been found that line defect (dislocation) mobility can also be affected by high density electric currents (3-6), which is termed **electroplasticity**. Since the phenomena of recovery, recrystallization and grain growth are governed by point and line defect interactions, it is expected that electric fields and currents may in turn affect these processes. This paper reviews the work to date on the effects of electric current and electric field on the annealing of metals. Specifically, the effects of simultaneously passing an electric current or applying an external dc electric field during annealing (**electroannealing**) of cold worked Al, Cu, Ti, and the intermetallic compound Ni₃Al will be presented. Since most of the work on the subject has been by the present authors and their coworkers, the paper will mainly cover our studies.

2. EXPERIMENTAL

The experimental arrangement used by the authors for annealing with an electric current is shown in Fig. 1a. Wire specimens (\approx 1mm diameter) were generally employed to minimize Joule heating. Thermocouples were attached to the specimens and temperatures were kept to $\pm 2^\circ\text{C}$. In the annealing with current, the resulting Joule heating was used in part to heat the sample. Under these circumstances, the set temperature of the furnace was adjusted to compensate for this heating so that the specimen temperature was maintained at the desired level. With the arrangement shown in Fig. 1a, Joule heating resulted in a steady state temperature increase of only 1° to 2°C for the Al and Cu specimens (7-9). The larger copper electrical contacts

acted as isothermal blocks, thereby allowing both specimens with and without current to be annealed simultaneously at nearly the same temperature. Temperature rises were somewhat higher for Ti (7) and Ni₃Al (10) so that the arrangement of Fig. 1a could not be employed for these materials. Therefore separate tests with, and without current were performed.

Joule heating was not a concern when the effects of an external dc electric field were investigated. The experimental arrangement for these studies is shown in Fig. 1b. Two specimens were annealed side by side; one was connected to the positive terminal of a high voltage power supply and the other to the negative terminal. Electrically, the samples formed a parallel wire capacitor. For comparative purposes, separate tests were performed using the same arrangement but without applying a field.

3. RESULTS

3.1 Continuous Low Density Current

No effect of a low density, continuous dc current (up to 31 A/mm²) was found by the present authors [7] on the isochronal (15 min) annealing response (hardness vs temperature) of 99.99 Cu wire which had been cold drawn either 22% or 76%. However, other investigators [11] reported that the recrystallized grain size of commercial purity Cu cold worked ~ 40% and annealed for 1 h at 400°C decreased continually from 29 to 22 μm as the current density (continuous dc) was increased from 0 to 15.5 A/mm². A refinement in the recrystallized grain size of α-Ti cold worked 64% was also found for a low density dc (or ac) current of 10 A/mm² when the annealing (1 hr) temperature was held below 550°C [12]. At 600°C however a coarsening of the grain size occurred for the dc current; see Fig. 2. The reason for the difference in behavior at the two temperatures was not completely clear. It was suggested that the more rapid rise to the test temperature produced by the concurrent application of the

dc or ac current could possibly account for the grain refinement at the lower temperature and that at the higher temperature the dc current may have influenced grain boundary mobility through its effect on impurity migration rate.

3.2 High Density Pulsed dc Current

High density electric current pulses ($j \approx 10^3$ A/mm², pulse duration time $t_p \approx 100$ μ s and frequency of pulse application $\nu_p \approx 2$ Hz) were found to have a significant effect on the annealing response of cold worked Cu [8], Al [9] and the intermetallic compound Ni₃Al [10]; see Fig. 3. For all three materials current pulsing reduced the recovery and recrystallization temperatures, i.e., enhanced the rates of these processes. In the case of Cu and Al the magnitude of the reduction in recrystallization temperature (12°–25°C for Cu and 18°–35°C for Al) was not sensitively dependent on the purity level, but declined with increase in amount of prior cold work.

Isothermal annealing studies (Fig. 4) into the effect of electropulsing on the kinetics of the recrystallization process in Cu revealed that the current pulsing mainly influenced the pre-exponential A_x of the rate equation

$$t_{50}^{-1} = A_x \exp(-Q_x/kT) \quad (1)$$

where t_{50} is the time at which the hardness decreases by 50% and Q_x is the apparent activation energy. The electropulsing produced a two-fold increase in A_x . Considering that the current was "on" only $\sim 10^{-4}$ fraction of the total annealing time, this increase in A_x is indeed significant. Along with the enhanced rate of recrystallization produced by the electropulsing there occurred a decrease in the recrystallization grain size, a reduction in annealing twin frequency and a sharpening of the recrystallization texture [8].

In contrast to enhancing the rates of recovery and recrystallization, electropulsing retarded grain growth (Fig. 5) in the temperature or time regime immediately following completion of recrystallization. This retarding influence on grain growth increased with the frequency of pulsing ν_p (number of pulses per second), but was relatively

independent of the pulse duration time t_p in the range of 50 to 200 μs [9]; see Fig. 6. Plots of the rate of grain growth $d\bar{D}/dt$ vs the grain size \bar{D} (Fig. 7) reveal that the influence of the electropulsing on grain growth rate diminished with increase in impurity content.

3.3 External Electric Field

The influence of an externally applied electric field on the annealing response of Cu and Al wire is shown in Fig. 8. The effects of the field are just opposite those for electropulsing in that the field increased the recovery and recrystallization temperatures (i.e. retarded their rates), and the magnitude of the increase became larger with increasing amounts of prior cold work. Neither the dielectric environment (vacuum, air, silicone oil) nor the field strength (2.4–8.0 kV/cm) made any substantial difference. However, polarity was most important in that an effect of the field only occurred in the Cu when the specimen was connected to the positive terminal of the power supply. Similar to what was observed for electropulsing, the field had no significant effect on the hardness following complete recrystallization. Noteworthy is that the hardness values shown in Fig. 8 were taken near the center of the ~ 1 mm dia. specimens, i.e. the effects of the field did not just occur near the surface of the specimens, but extended to their center.

The annealing response of Ni_3Al sheet specimens (0.8 x 3 x 40 mm) with an electric field is presented in Fig. 9. The effect of the field on the recovery and recrystallization temperatures of this intermetallic compound is just opposite to that for Al and Cu in Fig. 8, being more like that for electropulsing. Moreover, no polarity effect occurred for the Ni_3Al . Again, no significant effect of the field on hardness is noted once recrystallization was complete. Also, the effects of the field extended to the center of the 0.8 mm thick specimens.

4. DISCUSSION

4.1 Continuous Low Density Current

The limited results obtained to-date on the effect of a continuous, low density current on the annealing behavior of metals permit only tentative speculations. It appears that if the annealing temperature (or time) is sufficiently low the current may reduce the recrystallized grain size. One possibility for this is that increased rate of heating produced by the current leads to an increase in the rate of nucleation of new grains, as proposed by Xu, Lai and Chen [12]. At higher temperatures (or longer times) significant grain growth could mask the earlier effect of the current on the nucleation rate. The increased rate of grain growth observed at higher temperatures could result from an influence of the current on the migration rate of the impurities residing at the grain boundary [12].

4.2 High Density Pulsed dc Current

4.2.1 Recovery and recrystallization: As shown above, electropulsing enhanced the rates of recovery and recrystallization of cold worked metals. The enhancement in the rate of recovery can be attributed to an increase in the annihilation rate of dislocations through cross slip and climb. The exact mechanisms by which the current may influence cross slip and climb are however not known and need investigation. In considering the effect of electropulsing on the recrystallization rate, the nucleation of new grains and their subsequent growth must be taken into account. The fact that the effect of the current pulsing diminishes with increasing amounts of prior cold work suggests that a major influence of the current may be on the nucleation rate. This conclusion is based on the idea that the number of nucleation sites is governed both by the amount of cold work and by the current pulsing, the relative effect of the cold work becoming greater as the degree of deformation is increased. Additional support that current pulsing influences the rate of nucleation is provided by the fact that it mainly affected the pre-exponential factor A_x in

the recrystallization kinetics equation. In studies by Michalak and Hibbard [16] it was found that the effects of prior cold rolling procedure on the recrystallization kinetics of OFHC Cu were mainly on A_x , with little effect on Q_x . The variation of A_x with rolling procedure was established in this case to be associated with the nucleation period prior to the start of recrystallization.

The above considerations thus suggest that the major effect of the current on the recrystallization rate is through its influence on the nucleation rate. A plausible mechanism for the nucleation of new grains is the sequence of subgrain formation and coalescence shown in Fig. 10 [17–20]. Considering the possible effects of an electric current on the parameters involved in this process [18–19], a likely influence is on the vacancy concentration or flux at dislocation jogs.

4.2.2 Grain Growth: Considering the effect of electropulsing on the rate of grain growth, TEM micrographs [8] and hardness measurements on individual grains [9] indicated a lower residual dislocation density in the pulsed specimens. This suggests that the major driving force for the grain growth in the low temperature regime considered is the stored energy of the residual dislocations in the recrystallization grains rather than the grain boundary energy. For the case where the driving force decreases with time t due to the annihilation of dislocations, Li [19] has determined the rate of grain growth $d\bar{D}/dt$ to be given by

$$\left(\frac{d\bar{D}}{dt}\right)^{-1} = k_G^{-1} \left(\Delta F_0^{-1} + k_R t \right) \quad (2)$$

where k_G is the grain boundary mobility constant, k_R a second-order kinetics dislocation annihilation constant and ΔF_0 the driving force at $t = 0$. Fig. 11 shows that the grain growth kinetics for Cu are in reasonable agreement with Eq. 2 and that the current pulsing mainly influences the slope k_R/k_G . Subsequent studies revealed that the ratio k_R/k_G was relatively independent of pulse duration and frequency [14], but decreased with impurity content [9]. These data suggest that the decreased rate of

grain growth caused by electropulsing results to a large extent from the lowered driving force due to the increased rate of annihilation of the residual dislocations. The effects of impurity content appeared to be mainly on the grain boundary mobility. What effect the concurrent sharpened texture produced by the electropulsing had on the rate of grain growth is not known.

4.2.3 Twining and Texture: When the twining frequency was considered in terms of the grain size [21,22], no significant effect of electropulsing on twining occurred; see Fig. 12. Also, there was no effect of pulse duration and frequency, nor of purity level on the twining frequency when considered in terms of the grain size [10].

The sharper [112] texture produced by the current pulsing reflects either an influence on the orientation of the newly recrystallized grains or on their subsequent growth, or perhaps both. The mechanisms by which this might occur are not clear.

4.3 External Electric Field

Since vacancies are involved in the recovery and recrystallization of metals, a possible effect of an external electric field on these processes is through its influence on either the concentration of vacancies or their diffusion rate. According to classical electron theory of solids an electric field cannot exist within a metal. Therefore any effect of an external electric field which is observed at the center of a metal specimen should have occurred at the surface and then diffused to the center. An estimate of the time required for such diffusion to take place can be obtained from the relation [23]

$$x = \sqrt{Dt} \quad (3)$$

where x is the diffusing distance, $D = D_0 \exp - \Delta H_m / kT$ the appropriate diffusion coefficient and t the time. The times derived using Eq. 3 for the diffusion of vacancies from the surface of the test specimen to its center at temperatures where a significant change in hardness first occurred are presented in Table 1. Included in the table are the values for the diffusion constants which were employed. It is seen from Table 1 that in all cases the calculated diffusion time for any changes in concentration of

vacancies at the surface to reach the center is longer than the time of the anneal. Although the diffusion time for Ni_3Al is only 2.5 times the test time, the calculated times for Al and Cu are orders of magnitude longer than the annealing time. Thus, for these two metals either larger values of D_0 and/or smaller values for the activation enthalpy for vacancy migration ΔH_m^v must apply, or some other mechanism is responsible for the retarding influence of the electric field.

REFERENCES

1. F. M. d'Heurle and R. Rosenberg, **Physics of Thin Films**, 7, G. Hass, M. Francombe and R. Hoffman, eds., Academic Press, N. Y. (1973) 257.
2. **Electro- and Thermo- Transport in Metals and Alloys**, R. E. Hummel and H. B. Huntington, eds., TMS-AIME (1977) 1.
3. O. A. Troitskii, Zh. ETF Pis. Red. **10** 18 (1969).
4. H. Conrad, A. F. Sprecher and S. K. Mannan, **The Mechanics of Dislocations**, E. C. Aifantis and J. P. Hirth, eds., ASM (1985) p. 225.
5. A. F. Sprecher, S. L. Mannan and H. Conrad, Acta Metall. **34** (1986) 1145.
6. H. Conrad and A. F. Sprecher, "The Electroplastic Effect in Metals", Chapt. 43 in **Dislocations in Solids**, F. R. N. Nabarro ed., Elsevier Science Publishers (1989) p. 497.
7. S. K. Mannan, A. F. Sprecher and H. Conrad, unpublished research at NCSU (1987).
8. H. Conrad, A. F. Sprecher, W. D. Cao and X. P. Lu in **Homogenization and Annealing of Aluminum and Copper Alloys**, eds. H. D. Merchant, J. Crane and E. H. Chia, TMS (1988) 227.
9. H. Conrad, Z. Guo, M. Fisher, W. D. Cao and A. F. Sprecher, "Effects of Electric Current Pulses on the Recrystallization of Metals, to be publ. **Recrystallization '90**, TMS-AIME (1990)..
10. H. Conrad, Z. Guo, A. F. Sprecher, unpublished research at NCSU (1989).
11. V. L. A. Silveira, R. A. F. O. Fortes, and W. A. Mannheimer, Scripta Met. **17** (1983).
12. Z. X. Xu, Z. H. Lai and V. X. Chen, Scripta Met. **22** (1988) 187.
13. H. Conrad, N. Karam and S. L. Mannan, Scripta Met. **18** 275 (1984).
14. H. Conrad, Z. Guo and A. F. Sprecher, "Effects of Electropulse Duration and Frequency on Grain Growth in Cu", submitted to Scripta Metall.
15. H. Conrad, Z. Guo and A. F. Sprecher, Scripta Met. **23** 821 (1989).
16. J. T. Michalak and W. R. Hibbard, Trans. AIME **209** (1957) 101.
17. H. Hu, **Recovery and Recrystallization of Metals**, L. Himmal, ed. Interscience, N.Y. (1963) p. 311.
18. J. C. M. Li, J. Appl. Phys. **33** (1962) 2958.

19. J. C. M. Li, **Recrystallization, Grain Growth and Textures**, ed. H. Margolin, **ASM** (1966) 45.
20. H. Hu, **Metallurgical Treatises**, J. K. Tien and J. F. Elliott, eds., TMS-AIME (1981) p. 385.
21. O. Vöhringer, *Metall.* **11** (1972) 1119.
22. M. A. Meyers and C. McCowan, **Interface Migration and Control of Microstructure**, C. Pande, D. Smith, A. King and J. Walter, eds., **ASM** (1986) p. 99.
23. P. G. Shewmon, **Diffusion in Solids**, McGraw-Hill (1963).

TABLE 1. Comparison of the time required for vacancies to diffuse from the surface to the center of the test specimens at the indicated temperature.

Metal	Spec. Dia. or Thickness (cm)	D_0^v (cm^2/s)	Ref.	ΔH_m^v (ev)	Ref	T ($^{\circ}\text{K}$)	Approx. Diffusion Time† min.	Annealing Time min.
Al	0.05	0.2	1,3	0.60	1-3	423	650	30
Cu	0.07	0.2	1,3	0.87	1-3	473	1.6×10^5	30
Ni_3Al	0.08	1.3††	3	1.2	4,5	873	151	60

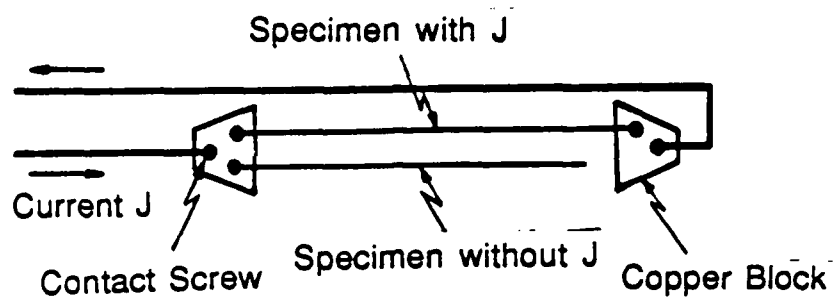
NOTES

† Time for vacancy diffusion from surface of the specimen to its center.

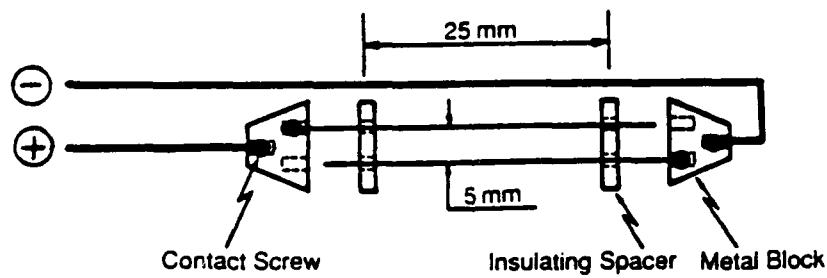
†† D_0^v is that for Ni.

REFERENCES

1. N. A. Gjostein, **Diffusion**, ASM, Metals Park, OH (1973) p. 241.
2. R. A. Johnson, *ibid.* p. 25.
3. P. G. Shewmon, **Diffusion in Solids**, McGraw-Hill (1963) p. 41-85.
4. G. F. Hancock, *Phys. Stat. Sol.* **a7** (1971) p. 535.
5. G. Gottstein, P. Nagpal and W. Kim, *Mat. Sci. Engr.* (1989).



(a)



(b)

Fig. 1. Specimen arrangement for: (a) annealing with electric current, (b) annealing with an electric field.

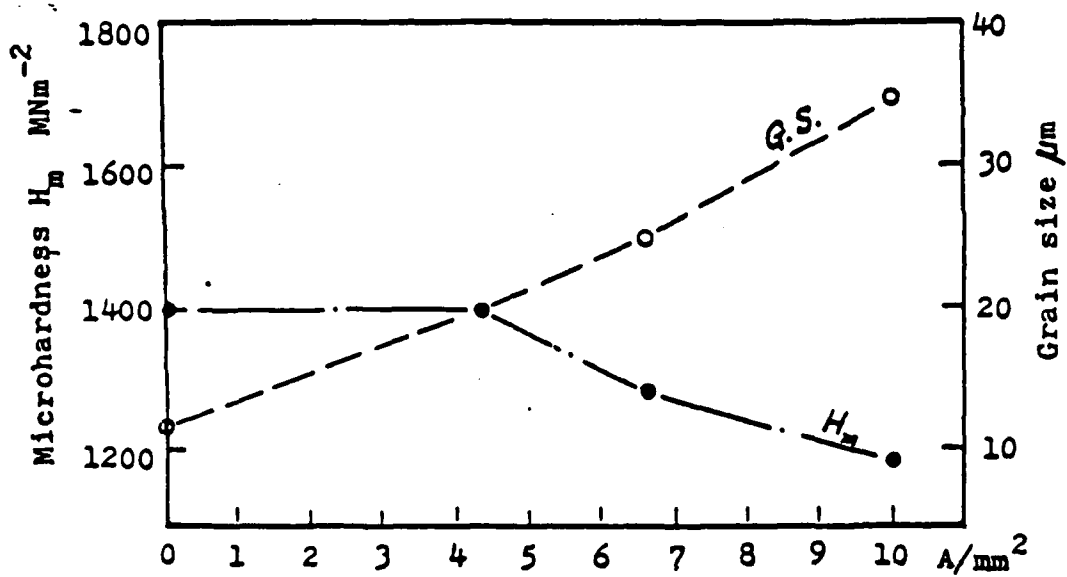
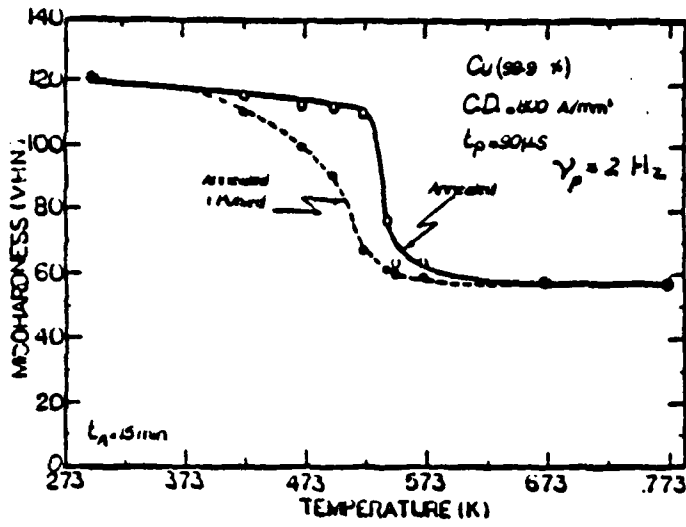
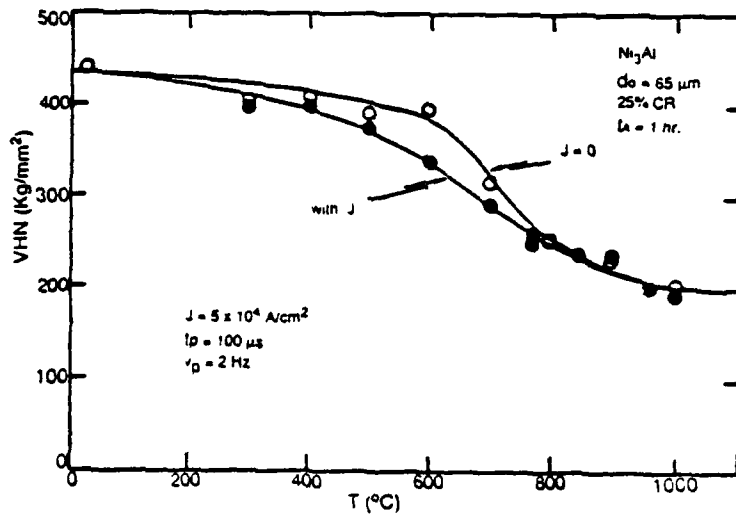
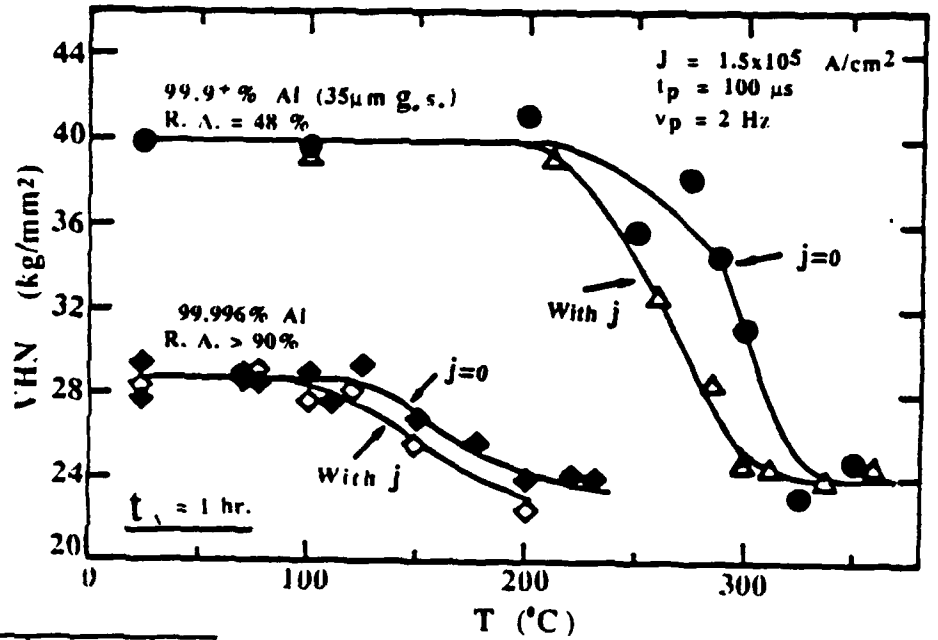


Fig. 2. Microhardness and grain size versus current density for α -Ti (cold worked 64%) annealed for 30 min. at 600°C. From [12].



(a)

(b)



(c)

Fig. 3. Effect of electropulsing on the isochronal annealing of
 a) Cu, cold work = 50% (8), b) Al annealing time = 1 hr,
 c) Ni₃Al, annealing time = 1 hr, cold work = 25%. From [8].

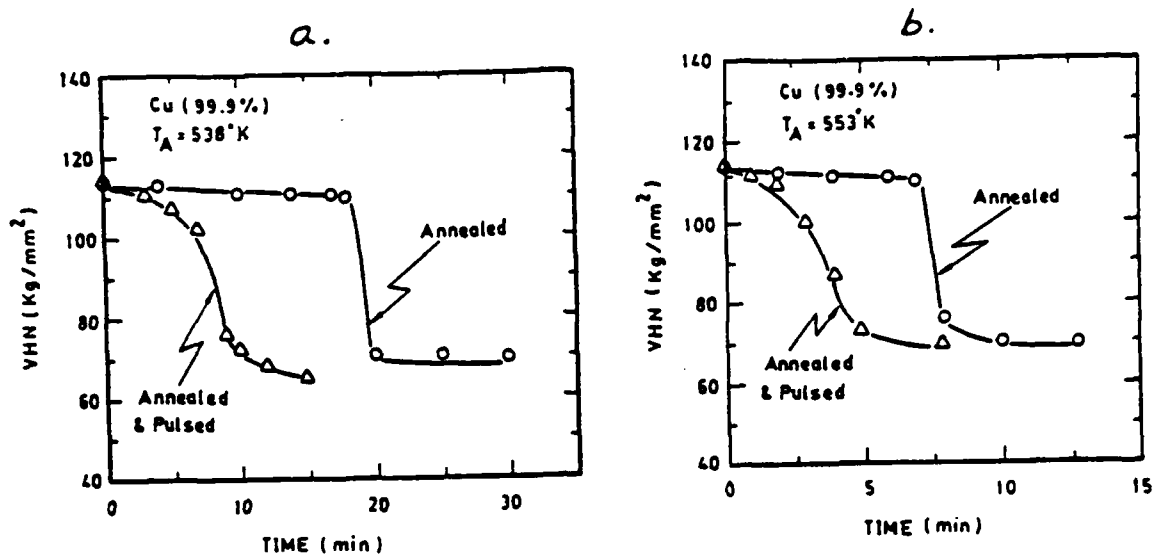


Fig. 4. Effect of high-density ($j = 8 \times 10^4 \text{ A/cm}^2$) electric current pulses ($t_p = 90 \mu\text{s}$ and $v_p = 2 \text{ Hz}$) on the hardness of cold worked ($\sim 50\% \text{ R.A.}$) copper wire vs annealing time: (a) $T_A = 538\text{K}$ and (b) $T_A = 553\text{K}$. From [13].

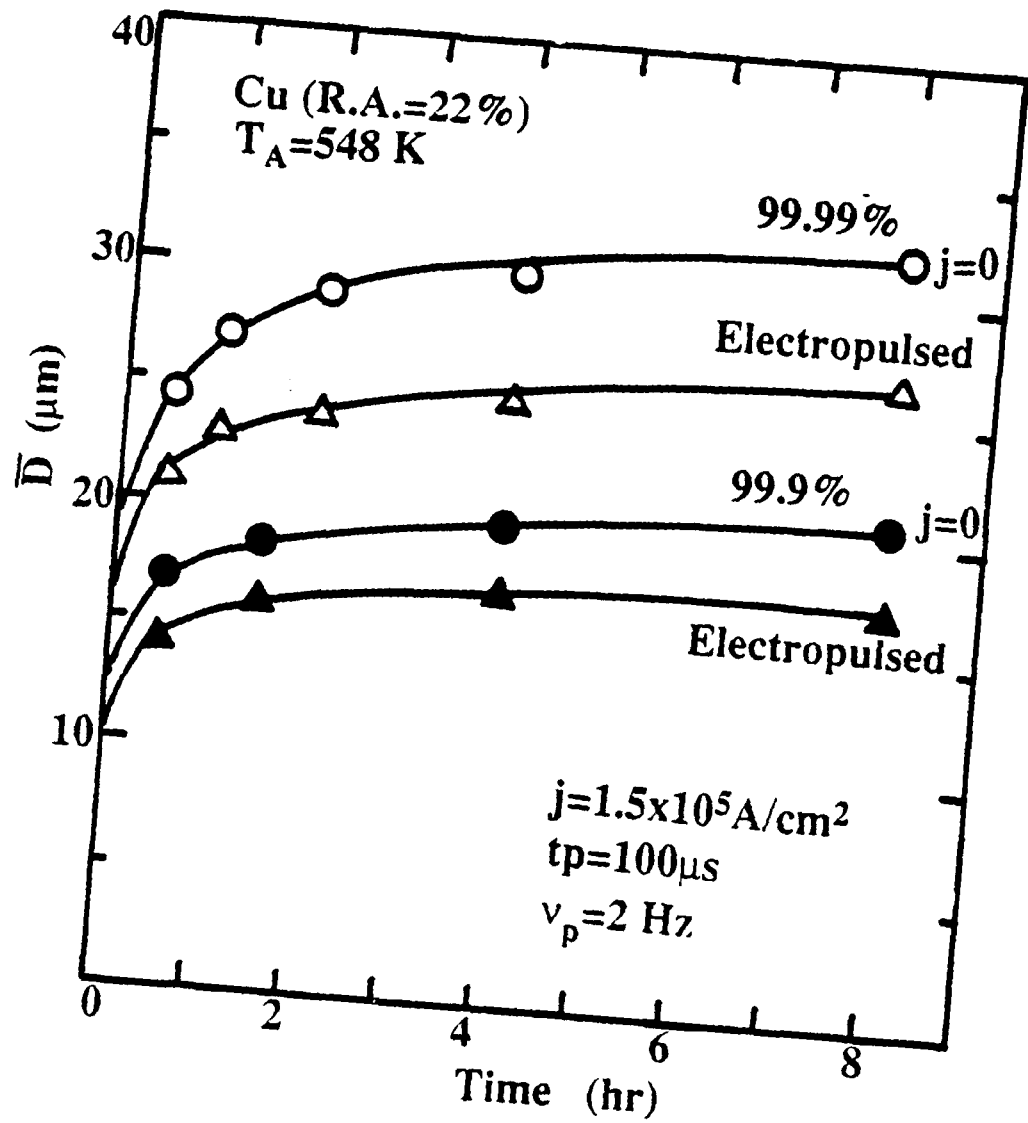


Fig. 5. Grain growth in Cu as a function of purity and electropulsing. From [9].

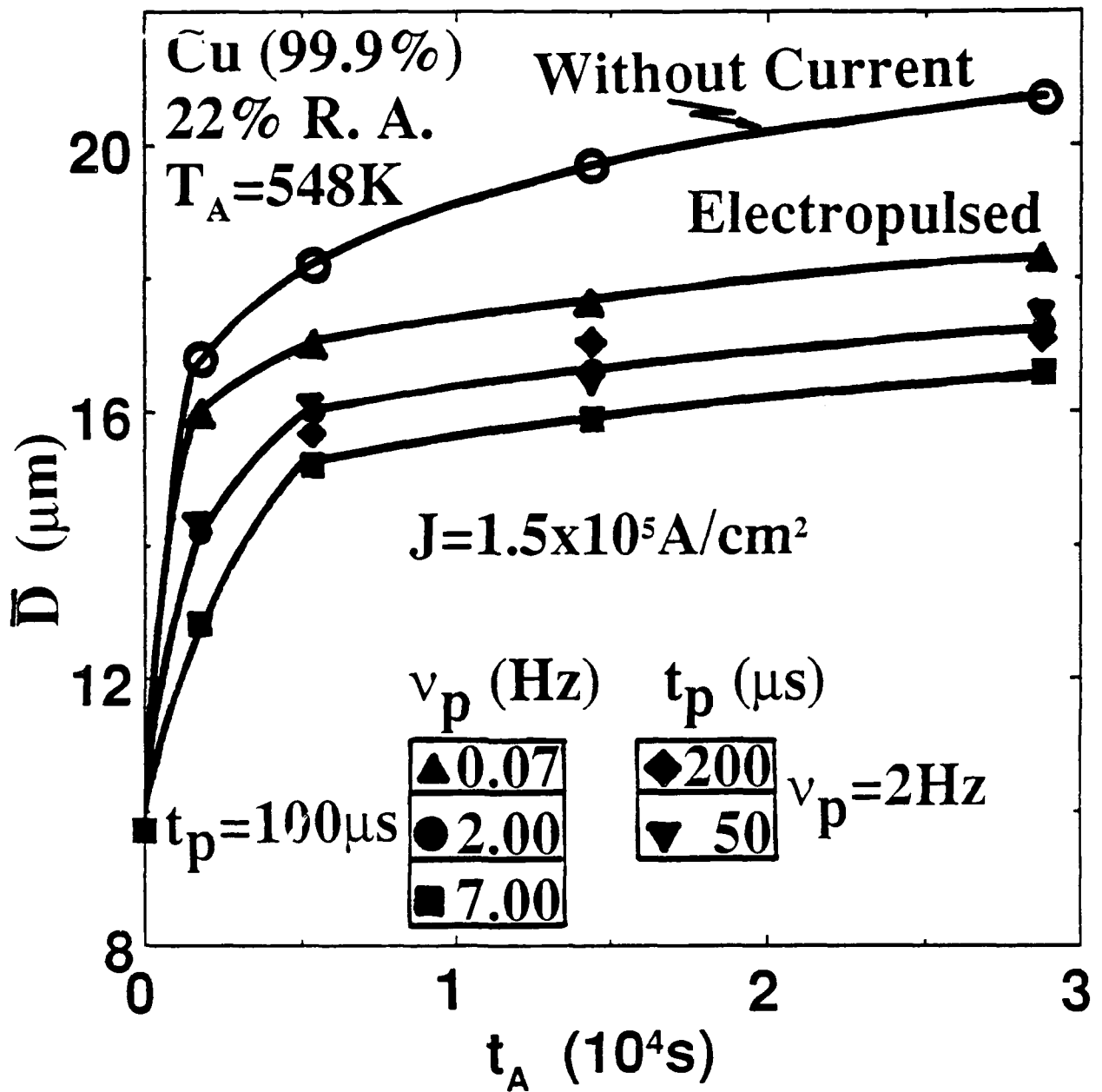


Fig. 6. Grain growth in Cu as a function of electropulse duration and frequency. From [14].

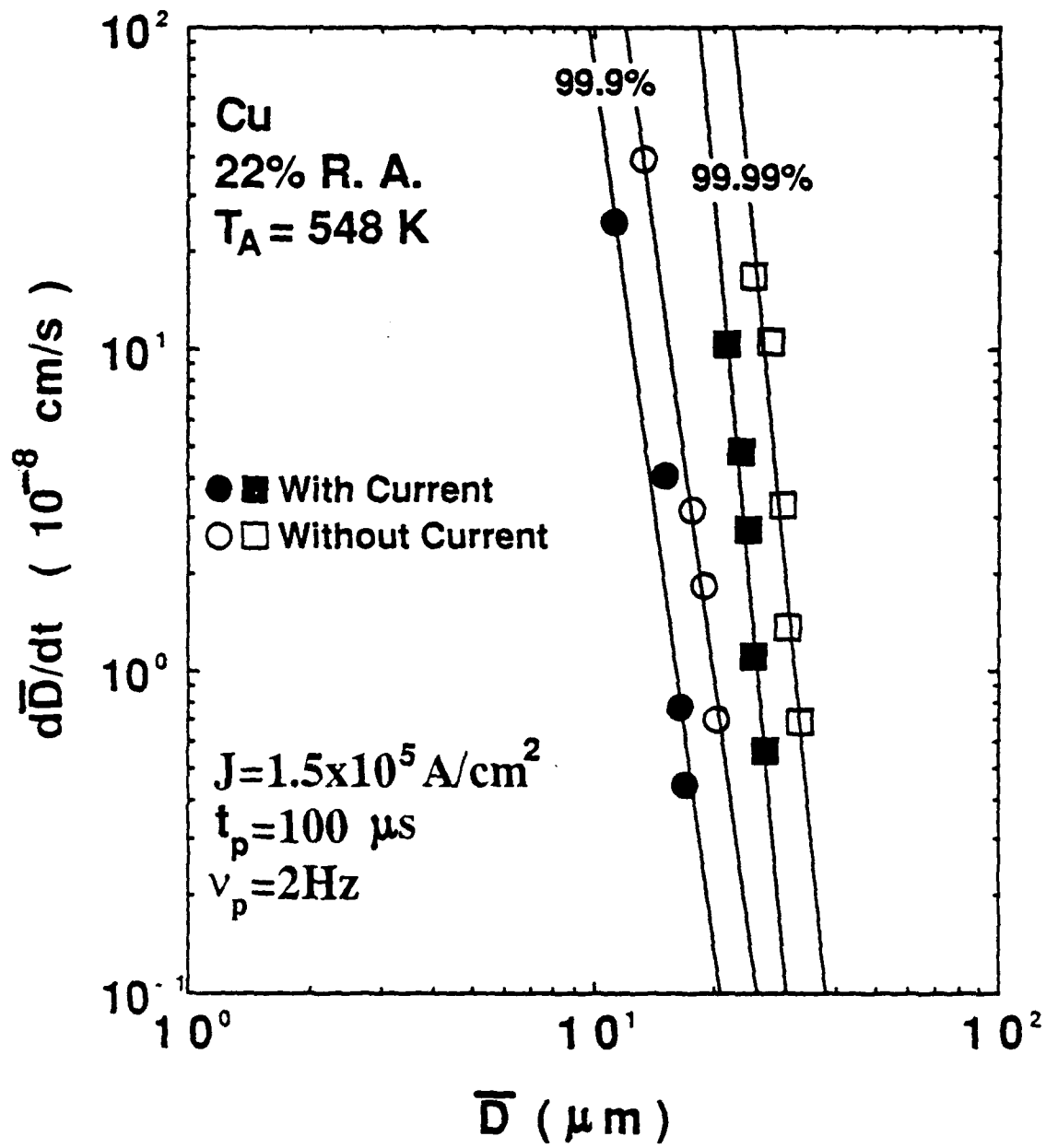
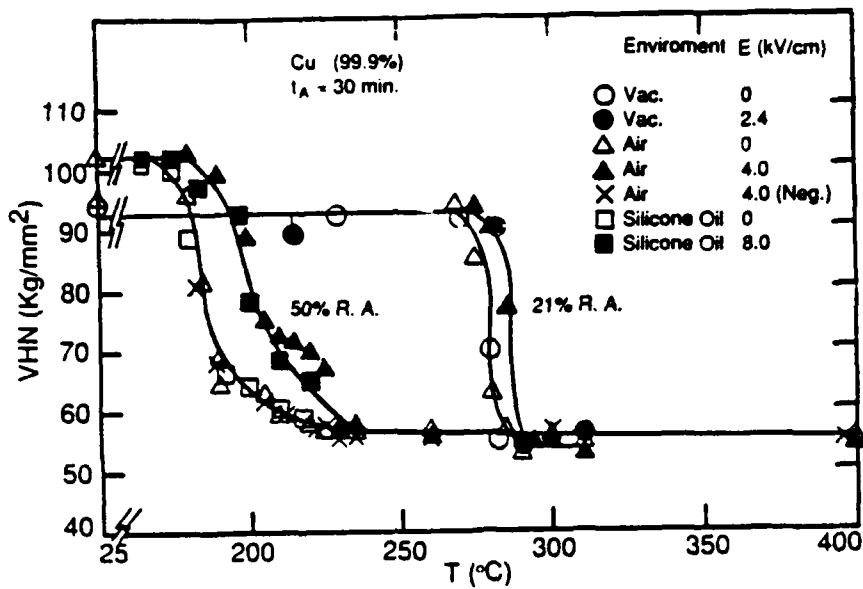


Fig. 7. Log-log plot of $d\bar{D}/dt$ vs \bar{D} derived from Fig. 5. From [9].

(a)



(b)

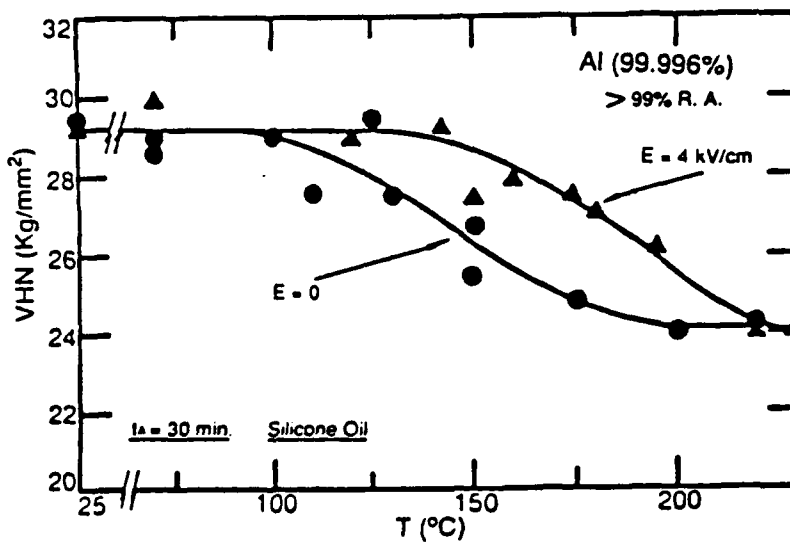


Fig. 8. Vickers hardness versus isochronal annealing temperature for a) Cu, heated in several environments, and different electric field intensities, b) Al, heated in silicone oil. From [15].

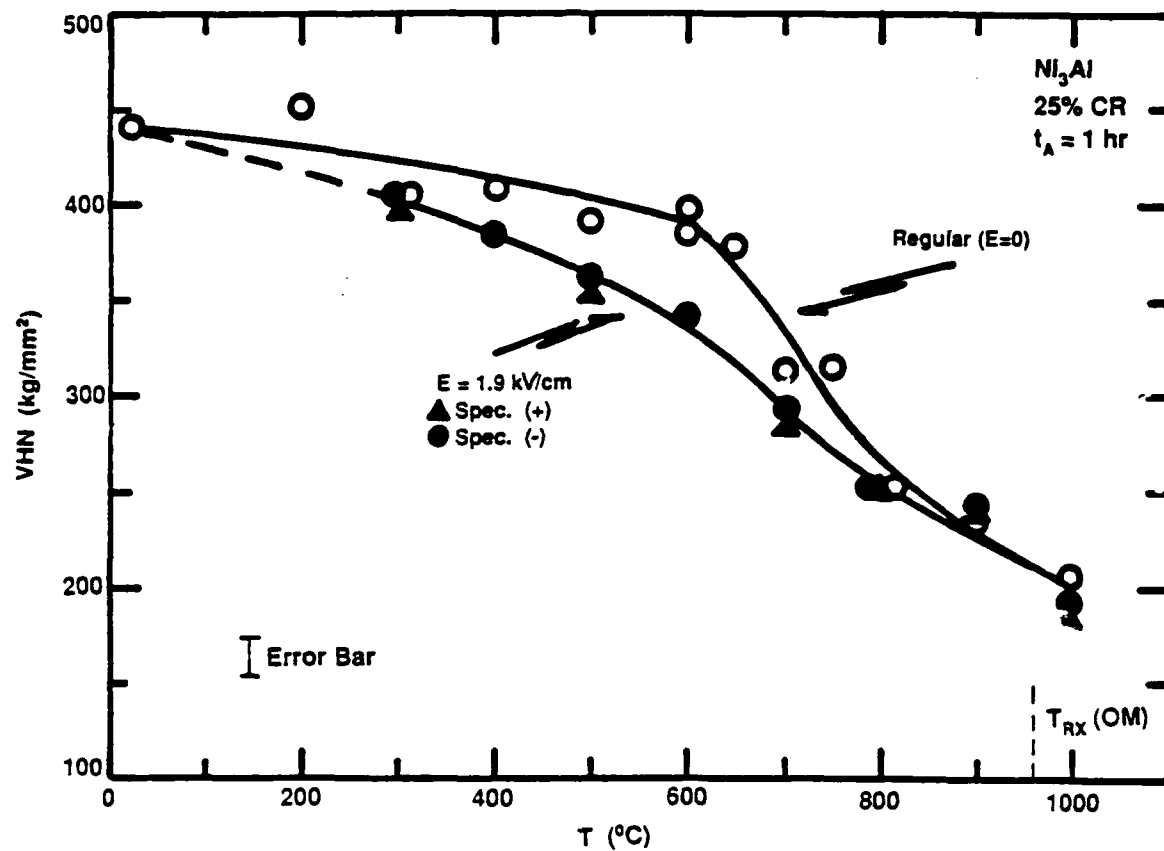


Fig. 9. Effect of an electric field of 1.9 kV/cm on the isochronal (1 hr) annealing response of Ni_3Al . From [10].

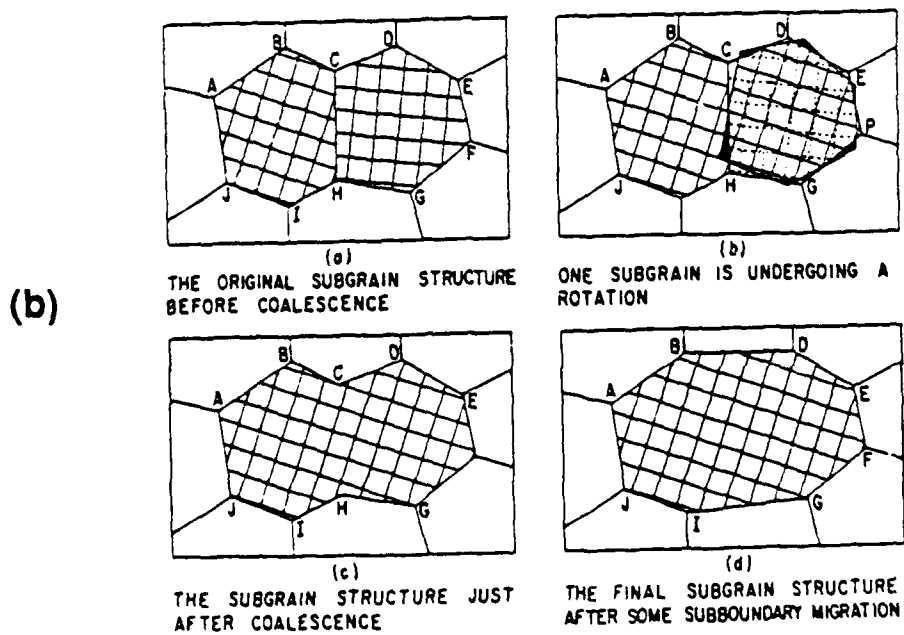
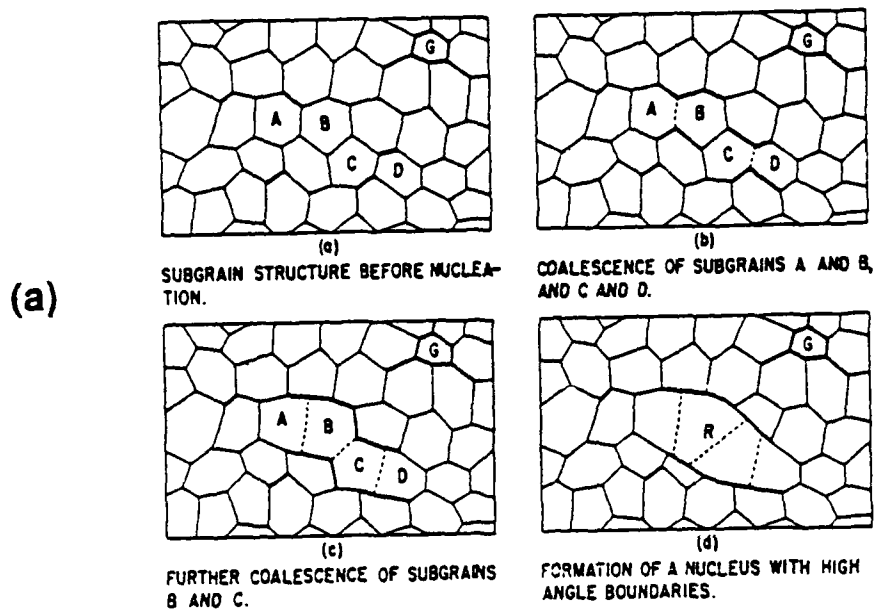


Fig. 10. Schematic of the formation of a recrystallized grain by the coalescence of subgrains. (a) From [20], (b) From [19].

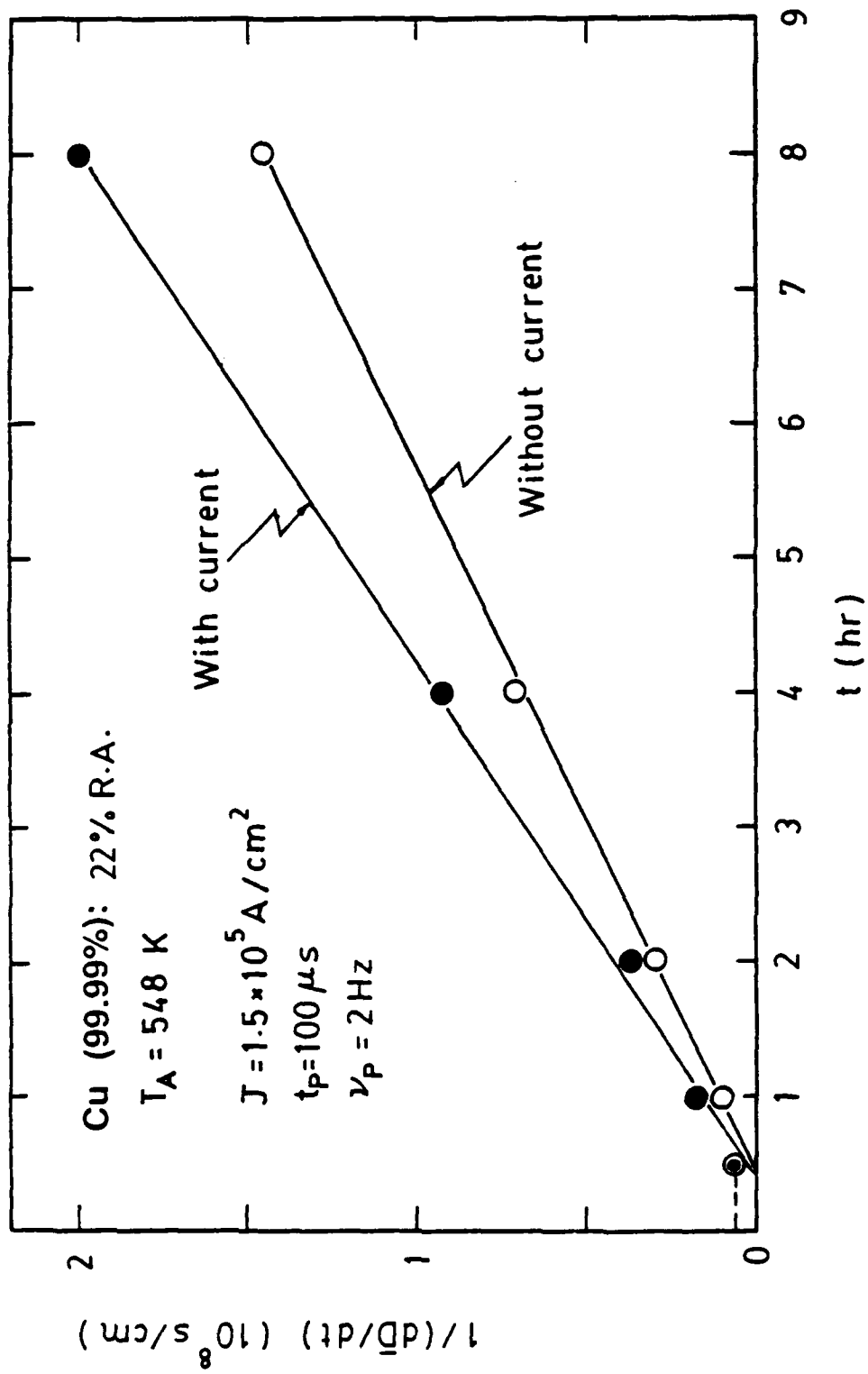


Fig. 11. Effect of electroplusing on grain growth in Cu at 548K expressed by a plot of $(d\bar{D}/dt)^{-1}$ vs t. From [8].

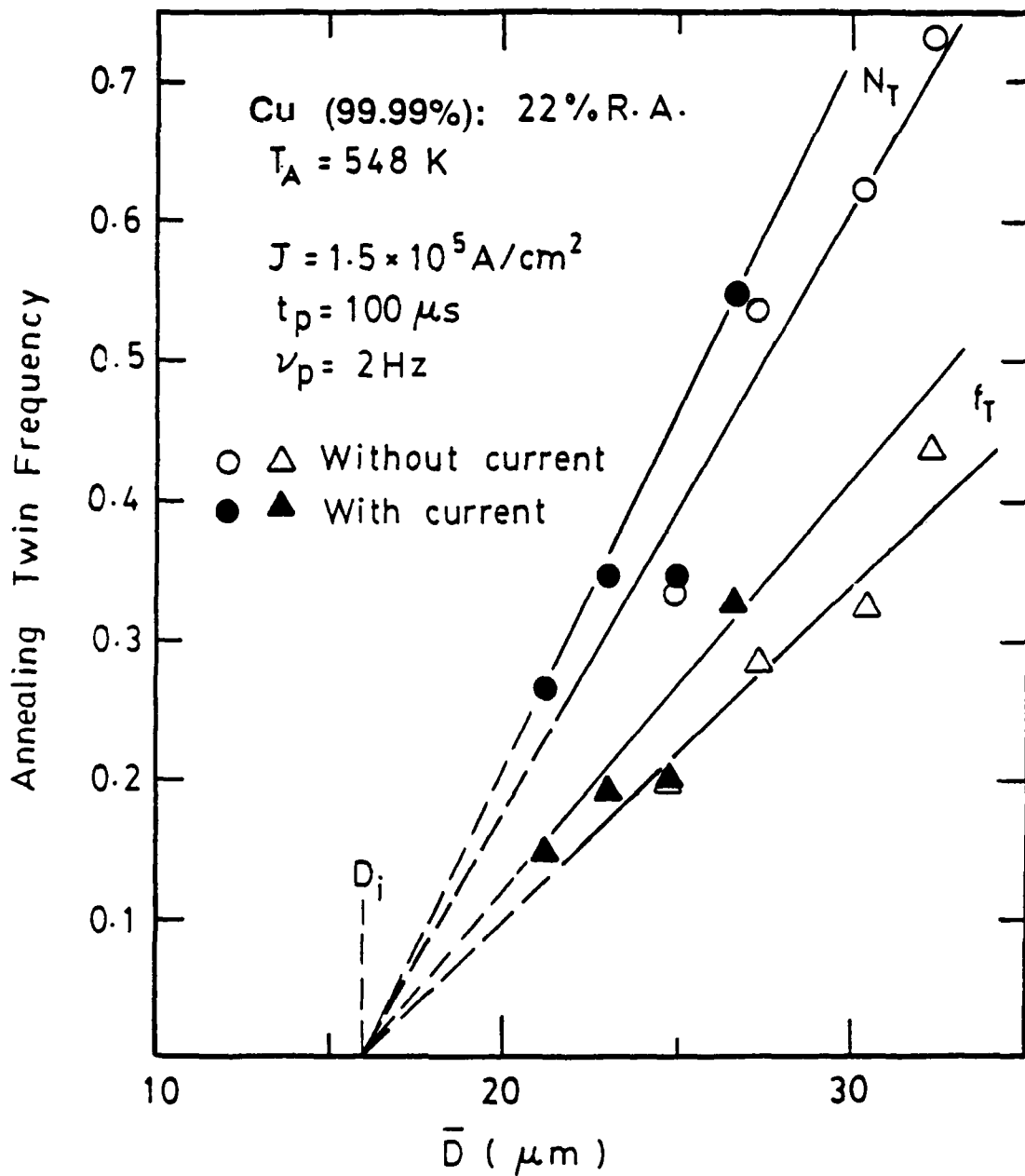


Fig. 12. Effect of electropulsing on annealing twin frequency in Cu vs the grain size \bar{D} . N_T = number of twins per grain; f_T = fraction of grains with twins. From [8].

PHOTOMECHANICAL AND ULTRASONIC RADIATION
EFFECTS IN MATERIALS

Robert F. Hochman
School of Materials Engineering
Georgia Institute of Technology
Atlanta, GA

INTRODUCTION

About three decades ago I was involved in two interesting areas of research on effect of radiation on materials. The first was work performed at Notre Dame in the 50's with Dr. G.C. Kuczynski and Dr. C.W. Allen. This work involved the effect of visible light of varying wave lengths on the hardness and mechanical properties of the surfaces of semiconductors, salts, ceramics and metals. Of these, the semiconductors were the only group of materials which showed major effects. The first section of this paper will be devoted to short review of what we termed the "Photomechanical Effect" (1,2,3).

The second area involved some studies in the early 1960's at Georgia Tech. Considering specific heat and the thermal vibration of atoms, the potential interaction of high frequency mechanical vibration or certain harmonics of high frequency vibration interaction with atomic defect structure might actually lead to local energies high enough to effect diffusion related phenomena. The second part of this paper will deal with both diffusion and sintering effects which were found in relation in ultrasonic vibration research with Dr. S.W. Freiman and R.M. Gray (4,5).

THE "PHOTOMECHANICAL EFFECT"

Background

A great deal of theoretical and experimental work has been conducted on the physical properties of semiconductors. Studies relating to dislocations in these materials have been performed particularly since investigations of this type are facilitated by the ability to easily observe dislocations as etch pits. Cognizant of these facts and the theoretical aspects of the photoelectric properties of semiconductors we considered the possibility of an effect of light radiation on the mechanical properties of semiconductors. Such an effect, which may be called a "photomechanical effect," was found by studying the microhardness of dark and illuminated semiconductor crystals. The main portion of the work was concerned with this type of experiment and the refinement of experimental procedures to more accurately measure this photomechanical effect. However, other experiments such as use of a rotating lens and a simple three point beam technique were also used to verify the existence of this effect.

Experimental

A definite softening effect was found on the surfaces of germanium crystals subjected to white light and ultra-violet illumination. Even when large errors were considered, as shown in Figure 1, The experimental results show large differences in dark and illuminated hardness. It was determined that a surface carefully polished and freshly etched with CP4 gave the largest effect and the most reproducible results. Oxidized surfaces

greatly reduced the effect. The softening or "photomechanical effect" was found to be a function of the depth of penetration of the indenter. The magnitude and depth of this effect was dependent on the carrier concentration or purity of the crystal being tested. However, both types of germanium crystals, n and p, gave similar results so that the effect appears to be independent of the type of carriers present. A complete experimental check of the available range of n-type germanium crystals of carrier concentration of 2×10^{13} (84 ohm-cm. resistivity) to 7×10^{17} (.0024 ohm-cm. resistivity) was made. Figure 2 of the experimental results, a composite of the hardness results at constant depth, indicates an illuminated hardness and an increase of photomechanical effect with increasing carrier concentration.

The effect of light intensity was studied by placing the light source at various distances from the specimen. Within the limit of experimental error, $\frac{\Delta H}{H_d}$ the fractional difference between the dark and illuminated hardness, was found to be proportional to $\frac{1}{X^2}$. This verifies that indeed the effect $\frac{\Delta H}{H_d}$ is proportional to the light intensity.

Using solid and liquid filters indicates two bands of light wave length are responsible for the effect. One band is approximately 0.2 to 0.4 microns, or in the near ultraviolet, and the other is in the infrared at 3.0 to 4.0 microns. Heating of the crystal due to radiation from the light sources was found to exercise little effect since softening was found when the samples were cooled in liquid air and liquid nitrogen. In addition, normal

photomechanical softening was shown for crystals covered with films of filter coolants such as alcohol and acetone. In these experiments the surface temperature of the sample was barely above room temperature.

Crystal orientation and differences in dislocation density seemed to have little effect on dark and illuminated hardness. Germanium is considered nearly isotropic, and therefore, the results of crystal orientation tests were important. The lack of hardness difference in different dislocation density materials is difficult to understand unless it is assumed that the nucleation of dislocations by the microhardness indenter and the movement of these newly created dislocations is more important than the movement of those already present in the crystal. Further evidence of this consideration may be gained by examination of various surface photomicrographs for example, Figure 3. A definite increase in dislocation density between the hardness imprinted disturbed and undisturbed portions of the crystal is found in these photomicrographs. A mathematical evaluation of what takes place beneath the indenter is impossible at present due to the complexity of the reaction. However, with the experimental facts in mind the previously stated assumption appears quite reasonable.

Another significant indication of the effect of light on surface dislocations is shown in Figure 4. The macrograph is of the fracture surface of a germanium crystal bar subjected to 3 point loading. The fracture occurred on the high tension side which was illuminated. Note the significant increase in

dislocations in this area of the surface.

The photomechanical effect was also found in several other semiconductors: silicon, InSb and InAs. Two other semiconductor materials did not show an effect. Selenium and Bi_2Te_3 were found to exhibit the same hardness regardless if the surface was illuminated or in darkness. However, the hardness of these two materials is inherently very low, and the depth of penetration of the hardness indenter for the smallest loads is 5 to 6 times greater than for the other semiconductor materials tested. Therefore, since the photomechanical effect appears to be restricted to a very thin layer of the semiconductor surface, the penetration of the indenter in these soft materials is apparently too deep to show a reaction.

Tests on aluminum and tungsten crystals showed no measurable effect. Negative photomechanical results were also found for fluorescent glass and aluminum oxide. Considering these results, it appears that the photomechanical effect is restricted mainly to semiconductors. However, unique effects were observed in some of the alkali salts tested.

KCl showed no effect, and if we consider the importance of available electrons to allow dislocation formation and movement, then the crystal being an insulator behaves as would be expected. In view of this, NaCl and LiF should act similarly, but not only do these materials act differently than KCl but show completely opposite photomechanical effects. NaCl softens under white and ultraviolet radiation and LiF hardens for ultraviolet but shows no

effect with white light. The softening in NaCl is also different from other photomechanical effects observed in that it appears independent of depth. This may be due to the transmission of light waves to all depths of the crystal and thereby not limiting the photomechanical effect to the surface. Since water and other coolants could not be used the possibility of some heating must be considered.

The hardening of LiF by ultraviolet light is most probably due to the creation of short lifetime color centers within the crystal. Seitz (6) has shown hardening of alkali halides due to the production of color centers by x-rays. The fact that LiF showed no effect with white light indicates that it reacts like KCl when subjected to wave lengths in the visible and infrared spectrum.

In view of the foregoing remarks, it is possible to consider that the natural reaction of salts under illumination would be to show no photomechanical effect. This is exemplified by KCl. However, other effects in NaCl and LiF come into play and tend to mask or change their reaction to light. If this is correct, then the true photomechanical softening effect is restricted principally to the semiconductors.

Discussion

Since this effect appears to be found primarily in semiconductors, it is very likely due to the electronic nature of these materials. Read (7) has shown that the energy of a dislocation in a semiconductor depends strongly upon the electron

distribution within the dislocation. The influence of light may produce a redistribution of electrons at a semiconductor surface, and subsequently a change found in mechanical properties should be expected. Detailed theory of how the redistribution of electrons was not developed but several models, all of which have some merit, were developed in my PhD thesis in 1959 (8).

DIFFUSION AND SINTERING EFFECTS

Introduction

Early work on the metallurgical applications of ultrasonics was well summarized by Kapustin (8) and Nosdreva (9) of the Soviet Union.

The first studies in the U.S. on the effects of ultrasonics on the deformation qualities of materials were performed by Langenecker (10,11,12) and his associates at the U.S. Naval Ordnance Test Station. This work was a continuation of his studies initiated at the University of Vienna and ^{with} Blaha (13,14).

Diffusion Studies

The referenced studies have indicated the effect of ultrasonics on diffusion related phenomena. Because of the importance of mercury diffusion in amalgam reactions, this system was chosen for studies of relative rates of diffusion with and without ultrasonics.

The materials used in this study consisted of annealed and machined Ag₃ Sn bars and spectrographically pure mercury. Specimens cut from the Ag₃ Sn bar were polished on one side, while the other side and edges were covered with micromask to insure that

diffusion occurred in only one direction.

The reaction system for this work consisted of a glass tube, wrapped with heating tape connected to a thermistor type temperature controller. The diffusion reaction was initiated by placing the specimen, polished side down, atop the mercury which had been brought to the required temperature. Temperatures of 40, 60, 80, and 110°C were employed and reaction times at temperature ranged from 40 minutes to 6 hours. When ultrasonic energy was applied, the glass tube containing the mercury and Ag₃ Sn specimen was placed at the focal point of a concave transducer utilizing water coupling. Because of the water couplant the maximum temperature used for ultrasonic studies was 80°C. The frequency of the ultrasonic energy was adjusted so that resonance occurred at approximately 400 kcps. The total energy of the ultrasound reaching the specimen could not be accurately determined, but was something less than 250 watts. Curves of mercury concentration versus depth of penetration were prepared for all samples and used in calculating the diffusivities of mercury in Ag₃ Sn at the different temperatures, both with and without the influence of ultrasonic energy. It is readily seen that the concentration and depth of mercury diffusion is greater under the influence of ultrasonic activation. The data for the diffusivities as a function of temperature were fitted to the Arrhenius equation and Figure 5 is the result of this analysis. The lines were drawn from a least squares fit of the data. The activation energy for nonultrasonic diffusion of mercury in Ag₃ Sn was found to be 5, 150 cal/mole and

the activation energy for ultrasonically reacted samples was found to be 7,580 cal/mole. D_0 was found to be 4.22×10^{-7} cm²/sec for nonultrasonic diffusion and 4.36×10^{-4} cm²/sec for ultrasonically activated diffusion. In analyzing this diffusion data it must be realized that this system is much more complex than a normal binary diffusion couple and several factors must be considered. When the reaction of mercury with Ag₃ Sn has proceeded for some time, the formation of a surface layer of Ag₂Hg₃ and Sn₈ Hg occurs. Furthermore, tin from the Ag₃ Sn may diffuse more readily towards the higher mercury concentration at the surface, which after some time results in a lower mercury concentration at the surface.

Discussion

Speculation based on ultrasound attenuation studies can be made. Attenuation of the ultrasound is usually caused by crystal imperfections (mainly grain boundaries, vacancies and dislocations) which produce an anharmonic restorative force in their immediate vicinity. Thus, an atom in the vicinity of a vacancy when displaced from its equilibrium position under the influence of a sonic stress wave may be subject to a much smaller restoring force in the direction of the vacancy. Thus, it may absorb energy from the sound wave and move into the imperfection, resulting in a diffusion jump.

SINTERING STUDIES

The application of ultrasonic energy to the sintering of powdered metals was initially demonstrated by Rakovski (15) by superimposing ultrasonic vibrations on conventional time-

temperature sintering conditions. However, the effect of ultrasonics on powder compacts of low melting point metals and the possibility of sintering and densifying these materials at room temperature was not explored until this work.

Lead, magnesium, zinc, tin and aluminum powders were thermally and ultrasonically sintered. After ultrasonic sintering, lead, magnesium and zinc compacts were evaluated for density and compressive strength. Additional lead compacts were sintered in the same manner, extruded into wire of 0.072" diameter, and subjected to tensile testing. It was found that all compacts, except tin, sintered by the ultrasonic treatment had higher densities, greater or equal compressive strength, and lead, when extruded into wire, had a significantly greater tensile strength than comparable material prepared by thermal sintering. The treatments and results in terms of density and strength are shown in Table 1.

Discussion

Nearly all the data indicates increased densification, and where measured, increased mechanical properties when the compact was subjected to ultrasonic sintering. Only for tin was the pattern broken and this may well have been a result of the very large particle size used in the experiment.

Our success was in part due to working with low melting metals and it was, therefore, possible to magnify the mechanisms of densification. We also used a high compacting pressure rather than the loose or loosely sintered powders. Its range was as high as

50,000 PSI in some instances. In addition, compacts were maintained under pressure during ultrasonic activation which would aid in maintaining particle to particle contact. It was, therefore, possible to enhance diffusion and/or plastic flow at these contact points which resulted in the improved densification.

ACKNOWLEDGMENT

The photomechanical studies involved the advise and direction of Dr. G.C. Kuczynski and the assistance of Dr. C.W. Allen. The ultrasonic studies were done with the capable assistance of Dr. S.W. Freiman and Mr. R.M. Gray.

REFERENCES

1. "Light Induced Plasticity in Semiconductors," Physical Review, 108, No. 4, 946-948, (1957) with G.C. Kuczynski.
2. "Light Induced Plasticity in Germanium," Journal of Applied Physics, 30, No. 2, 267 (1959) with G.C. Kuczynski.
3. "Effect of Light on Plasticity of Semiconductors," Mechanical Properties of Engineering Ceramics, pp. 495-505, Interscience Publishers, New York (1962) with G.C. Kuczynski and C. Allen.
4. "The Effect of Ultrasonic Energy on Diffusion and Sintering," Proceedings 2nd Int. Conf. on Sintering and Related Phenomena, 1965 with Freiman and Gray.
5. "A Note on the Effect of Ultrasonic Activation on Sintering and Diffusion," Int. J. of Powder Metallurgy, 2, No. 3, 1966.
6. F. Seitz, Rev. of Mod. Phys., 26, 7 (1954).
7. W.T. Read., Acta Met. 5, 83 (1957).
8. A.P. Kapustin, The Effects of Ultrasound on the Kinetics of Crystallization, USSR Academy of Sciences Press for the Institute of Crystallography, Moscow (1962).
9. B.F. Nodreva, Ultrasound in Industrial and Processing Control, State Scientific-Technical Press for Mechanical Engineering, Moscow (1959).

10. B. Langenecker, C.W. Fountain, and V.O. Jones, Metal Progress 85, 97 (1964).
11. B. Langenecker, W.H. Frandsen, C.W. Fountain, S.R. Colberg, J. Langenecker, NAVWEPS Report 8482 (1963).
12. B. Langenecker and W.H. Frandsen, Phil Mag. 7, No. 84, 2079 (1962).
13. F. Blaha and B. Langenecker, Acta Met. 7, 93 (1959).
14. F. Blaha and B. Langenecker, Z. Metallk. 49, 357 (1958).
15. V.S. Rakovski, Neue Hutte Z (12) 764-7, December (1957).

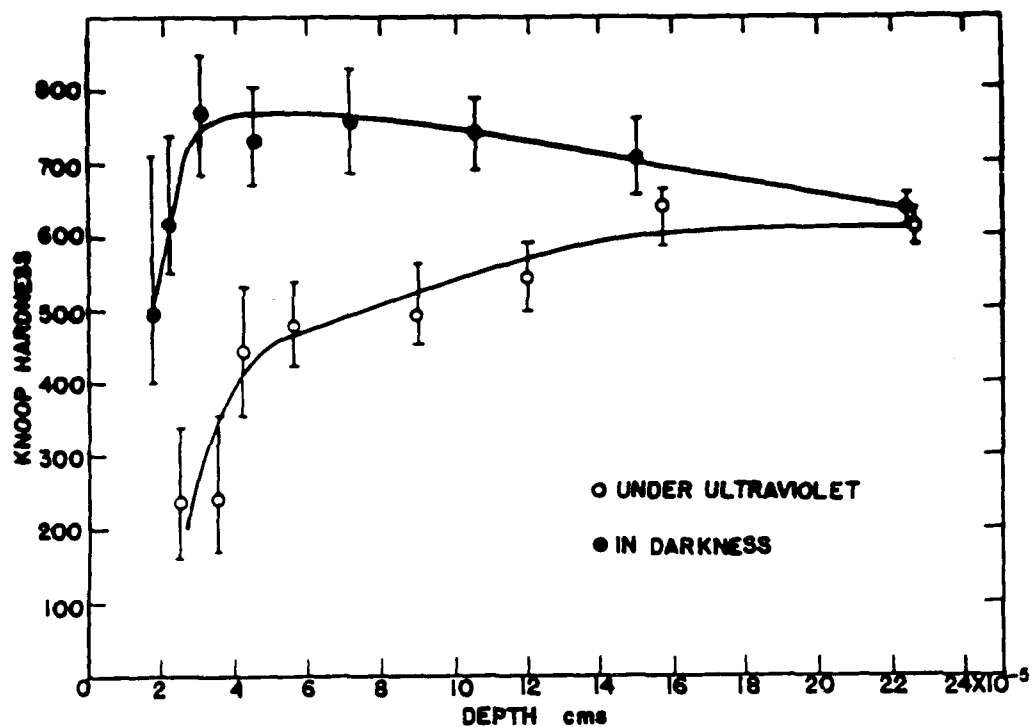


Figure 1. A plot of dark and illuminated hardness values versus depth for a 5 to 7 ohm-cm resistivity germanium crystal. The range of hardness is plotted for each set of test results.

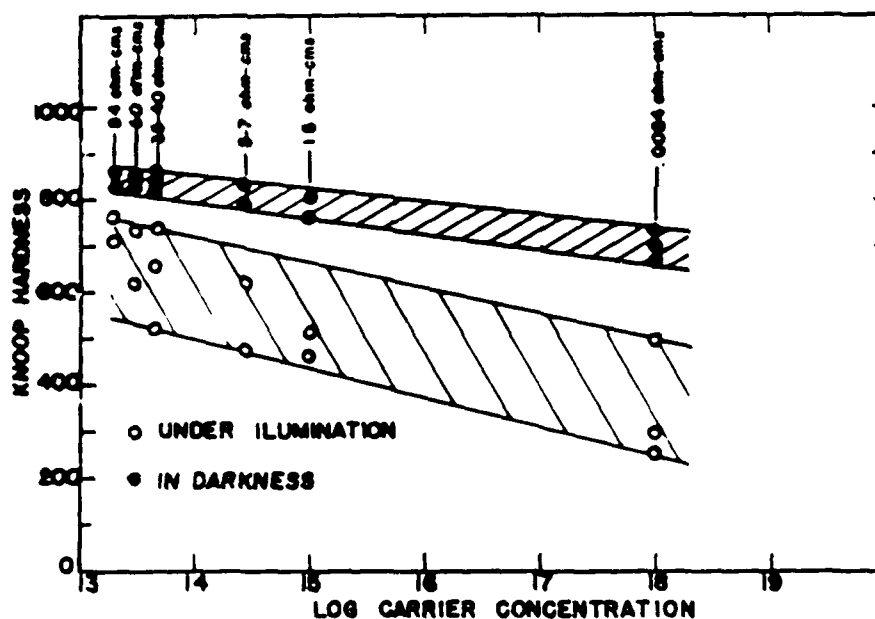


Figure 2. A plot of dark and illuminated hardness values at a constant depth of .5 microns versus the carrier-concentration of the crystals tested. Short range test data is plotted here in addition to the information taken from the previous graphs.

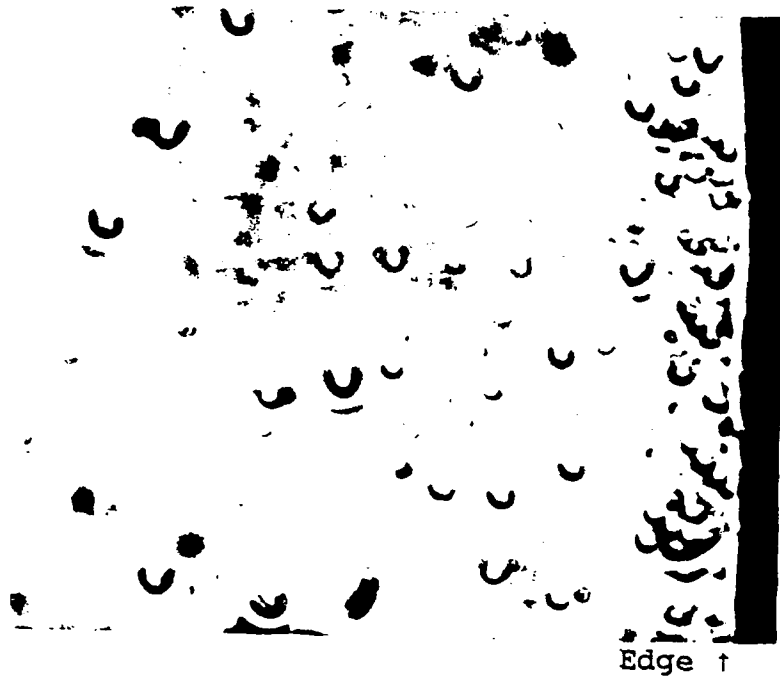


Figure 3. Note the increase in etch pit density at the high stressed surface in a 3 point beam test. This did not occur without illumination.



Figure 4. Note the large increase in dislocation etch pit density under a hardness impression made under light.

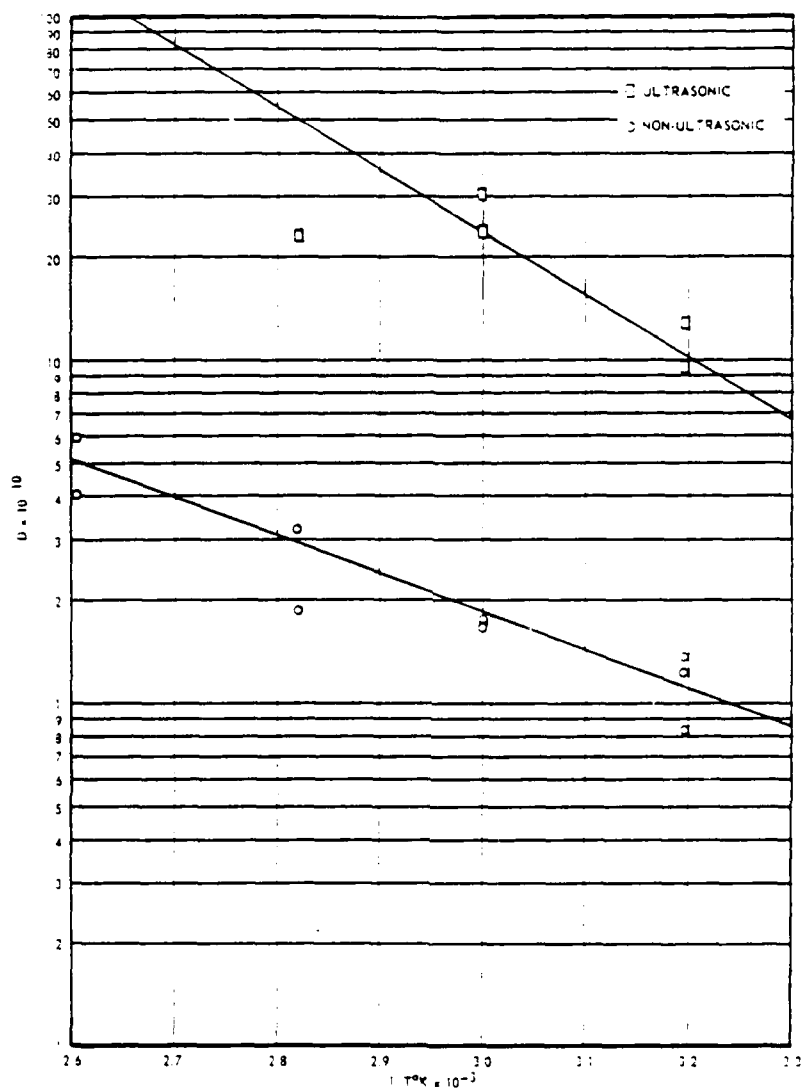


Figure 5. An Arrhenius Plot of Log Diffusivity Versus $1/T$ for Nonultrasonic and Ultrasonically Activated diffusion of Hg into $Ag_3 Sn$.

Table 1. The Effect of Ultrasonic Sintering on Density and Strength

Material	Particle Size	With Ultrasonics				Without Ultrasonics			
		Temp °C	Time Min	Density g/cc	Breaking Strength Kg/mm ²	Temp °C	Time Min	Density g/cc	Breaking Strength Kg/mm ²
Lead	-400 mesh	25	20	10.97	8.4 (compressive)	250	60	10.34	6.4 (compressive)
Lead (extruded wire)	-400 Original	25	20		7.1 (tensile)	250	60		4.5 (tensile)
Magnesium	-200 mesh	25	10	1.70	15.8 (compressive)	460	60	1.30	11.9 (compressive)
Zinc	-325 mesh	25	10	6.41	9.8 (compressive)	288	60	5.75	9.8 (compressive)
Tin	-30 mesh*	25	10	4.69		150	60	5.96	
Aluminum	-325 mesh	25	10	2.50		460	60	2.00	

*Very large particle size.

The Influence of High Magnetic Fields on the Mechanical Properties of Structural Alloys

J. W. Morris, Jr.

Center for Advanced Materials, Lawrence Berkeley Laboratory, and
Department of Materials Science, University of California, Berkeley

While there is only limited data on the influence of high magnetic fields on the mechanical properties of structural alloys, the available data suggests that significant effects occur only in metastable austenitic steels where the magnetic field influences the extent of the deformation-induced martensitic transformation. The tensile properties of metastable austenitic fields have been studied in fields up to 18T. The results show small, but measurable effects on tensile properties. In general, the work hardening rate at finite strain is increased and the tensile elongation is decreased. This behavior and the most obvious exceptions to it can be explained on the basis of the increased rate of production of deformation-induced martensite in the high magnetic field. The fracture toughness of metastable 304-type stainless steels has been measured in fields up to 8T at temperatures to 4K. Contradictory results were obtained by different investigators. Research at LBL measured an increase in K_{Ic} by a factor as large as 30% in an 8T field; research at Toshiba reported that K_{Ic} decreases by an equivalent amount. Theoretical analyses suggest that the fracture toughness should increase in the field by an amount that is difficult to predict. The only reported work on fatigue crack growth rates in metastable austenitic steels in high magnetic fields suggests that the crack growth rate is only slightly affected.

EFFECTS OF FIELD ON STRUCTURE OF ELECTRONIC MATERIALS

Robert Rosenberg
IBM Research Division
T. J. Watson Research Center
P.O. Box 218
Yorktown Heights, New York 10598

Crystal transformations, morphological changes and properties of thin layers subjected to electric and magnetic fields have been described over the years as being either necessary for property control or disastrous for component reliability. Response to fields can be considered to be in at least two regimes, electronic or non-diffusional transitions and diffusion related transitions. The former refers to such effects as changes in magnetic phase transitions produced in a magnetic field, ferroelectric transitions or superconductor field sensitivities, for example, which are important and pervasive across many technology applications. This discussion, however, will be devoted primarily to the latter, diffusional transitions, which are more closely associated with VLSI and related technologies, and to electric field effects which have produced much of the industry folklore.

Most work in this area relates to effects of either high current density or internal field gradients on structural changes, the former being associated mainly with metallic and the latter with semiconductor or dielectric components of device structures. The phenomenon of electromigration in metal films has become increasingly more important as the cell size and wiring line widths are being reduced to the point where present technology is projected to be inadequate to carry the currents necessary for circuit operation. Wiring area will dominate the ability to achieve competitive integration levels. The metallurgy of interest will remain Al-Cu alloy as conductor in conjunction with metallic under and overlayers. This is a very complicated system with respect to electromigration lifetimes, as electron flow causes change in formation and distribution of precipitates and in turn accumulation of grain boundary voids and final failure.¹ It is observed that failure of conductors may be associated with local depletion of copper, which would create a high Al electromigration flux divergence. It is also noted that the electron current has a large effect on θ CuAl₂ precipitation in quenched Al-4Cu films.² A significant retardation of grain boundary or surface precipitation is found with current densities of about 10^6 A cm⁻², although θ' bulk formation is unaffected. The retardation is evidenced by a slower reduction in resistivity during aging under field; i.e. lattice saturation seems to be maintained. Activation energies measured for electromigration failure of Al-Cu conductors vary greatly and seem to depend on whether the rate of dissolution of precipitate can compensate boundary depletion.

Electric field both externally applied and internally generated has been used to enhance crystallization and grain growth in semiconductors. For example, it has been observed that the transformation from amorphous to crystalline Si can be initiated under a field with crystallites mapping the field lines. Recently, it has been observed that the formation of TiSi_2 on polysilicon leads to large differences in the grain size of the underlying polysilicon, depending on the doping level.³ Clearly, when the polysilicon contains dopant the grain size becomes greatly increased during TiSi_2 formation over normal grain boundary migration effects encountered with intrinsic Si. The mechanism is associated with DIGM (diffusion induced grain boundary migration) where solute becomes depleted by diffusing along a moving grain boundary. In the present case, the TiSi_2 behaves as a sink for the dopant which sets up a dopant, or Fermi level, gradient across the boundary. This results in a local electric field which places a significant force on the boundary, accelerating migration and grain growth. Use can be made of this phenomenon to control grain size at reasonably low temperature. Many dielectrics, notably transition metal oxides, show bistability in resistance of orders of magnitude under field, where switching can be controlled from one stable state to the other. The switching mechanism can be explained by alternate filament formation and solution across a narrow gap.

Many variations of the above observations, including, for example, control of the grain size of deposited films by field gradients on a substrate, grain growth under electromigration forces and dislocation migration in doped semiconductors, have been or will be observed as materials and processing become more and more sophisticated. The difficulty will be to recognize when field and current effects must be considered.

REFERENCES

1. R. Rosenberg, Inhibition of Electromigration Damage in Thin Films, *J. Vac. Sci. Tech.*, 9, 263 (1971).
I. Ames, F. M. d'Heurle and R. Horstmann, Reduction of Electromigration in Al Films by Cu Doping, *IBM J. Res. Develop.* 14, 461 (1970).
Review paper: F. M. d'Heurle and R. Rosenberg, Electromigration in Thin Films, *Physics of Thin Films* 7, 257, published by Academic Press, 1973.
2. M. C. Shine and S. R. Herd, Effect of Direct Current on Precipitation in Quenched, Al + 4% Cu Thin Films, *Appl. Phys. Lett.*, 20, 217 (1972).
3. K. N. Tu and T. C. Chow, Metal and Polycrystalline Silicon Reactions, in *Polysilicon Semiconductors*, 35, 225, Editors, J. H. Werner, H. J. Muller and H. P. Strunk, Springer-Verlag Berlin, Heidelberg, 1989.

DISCUSSION OF R. ROSENBERG'S PAPER

H. Conrad:

Do you expect internal fields to occur in metal systems and of what magnitude?

EFFECTS OF ELECTRIC FIELDS AND CURRENTS ON PHASE TRANSFORMATIONS IN BULK ALLOYS

H. Conrad, A. F. Sprecher, W. D. Cao and X. P. Lu
Materials Science and Engineering Department
North Carolina State University
Raleigh, NC 27695-7907

Abstract

Since electric fields and currents can influence atomic and dislocation mobility, it is expected that they can affect phase transformations in which these defects play a role. Thus, the concurrent application of a **continuous d.c. electric current** has been reported to enhance the rate of precipitation or aging in Al and Fe alloys. Also, high-density **electric current pulses** were found to significantly reduce the crystallization temperature of rapidly-quenched, iron-base amorphous alloys. In contrast, a **continuous a.c. current** of the proper frequency has been found to retard the aging process, and in some cases stop it completely. The mechanisms by which the electric current affects these solid state transformations are not yet well understood.

Continuous electric currents applied during solidification have been found to increase the growth rate of GaAs single crystals and to reduce the grain size in a cast Pb-Sb-Sn alloy. The effect of electric current on the growth rate of the GaAs crystals is in accord with theoretical predictions based on Peltier cooling at the substrate and electromigration.

Soviet workers first reported in the late 1970's that an externally applied d.c. electric field can influence the heat treatment response of commercial Al alloys and a medium-carbon steel, leading to an increase in their respective hardness. More recently, the present authors found that the concurrent application of a d.c.

electric field of the order of kV/cm retarded quench aging in iron and increased the hardenability of steel. The effects of the field extended to the center of 1.0 to 3 mm thick specimens. Further, it was found that the application of an electric field during the superplastic deformation of 7475 Al alloy sheet (1.6–1.8 mm thick) produced the following changes in microstructure throughout the specimen: (a) significantly reduced grain boundary cavitation, (b) reduced the size of the dispersoids within the grains, but increased it at the grain boundaries, (c) reduced the grain size and (d) changed the composition of the dispersoid-free zone along the grain boundaries. The mechanism by which an external electric field affects phase transformations at the center of 2–3 mm thick specimens is not at all clear.

EFFECTS OF ELECTRIC FIELDS AND CURRENTS ON PHASE TRANSFORMATIONS IN BULK ALLOYS

1. Introduction

Since electric fields and currents influence atomic and dislocation mobility [1,2] it is expected that they will have an effect on those phase transformations in which these defects play a role. The present paper reviews available information on such effects, including recent work by the authors.

2. Effects of Current

2.1 Solid State Transformations

The first published results on the effects of an electric current on solid state phase transformations were by Erdmann-Jesnitser et al [3] in 1959, who reported that a **continuous d.c. current** of $\sim 10^3$ A/cm² enhanced the rates of quench aging and strain aging in Armco iron at 80°C; see for example Fig. 1. In contrast, a **continuous a.c. current** of 50 Hz and of the same magnitude as the d.c. retarded the aging process, so that no aging occurred in 50 hours. Subsequently, Koppelaar and Simcoe [4] studied the influence of a continuous d.c. current of $\sim 10^3$ A/cm² on the aging of an Al-4 wt.% Cu alloy at 75°C and found that the current also enhanced the aging rate in this alloy, Fig. 2. A reversal of polarity following aging under current decreased the aging rate and an a.c. current (25 Hz) significantly retarded it.

In subsequent work on the aging of Al-4 wt.%Cu at 50°-100°C, Onodera and Hirano [5] found that a constant or slightly increasing resistance of the alloy occurred for a current density $< 2 \times 10^3$ A/cm² (continuous dc), whereas for a current density higher than some critical value, the resistance decreased; see for example Fig. 3. They interpreted their results to indicate that, except for an

increased rate due to the temperature rise from Joule heating, the current retarded the precipitation reaction. The retarding effect of the current was considered to result from a sweeping of quenched-in vacancies into the grain boundaries by electromigration. They reached a similar conclusion in their studies on the effects of a d.c. current on the aging of an Al-12.5 wt.% Zn alloy [6]. Shine and Herd [7] also concluded that a d.c. current retarded the precipitation of θ Al₂Cu in their studies on quenched Al-4 wt.% Cu thin films.

In subsequent studies on the influence of the frequency ν of an a.c. current on the formation of GP zones at 30°C in the Al-12.5 wt.% Zn alloy, Onodera and Hirano [8] observed a retarding effect for $\nu = 0.25$ and 100 Hz, but no appreciable effect at 200 and 3000 Hz. These results could not be explained quantitatively in terms of their earlier model of current-assisted vacancy annihilation at grain boundaries.

In studies on the influence of high density ($\sim 10^5$ A/cm²) **electric current pulses** (pulse duration $t_p = 100$ μ s and 4-9 pulses per second) on the stability of Fe₇₅Si₁₀B₁₅ and Fe₇₉Si₇B₁₄ amorphous alloys, Lai et al [9] found that crystallization in the electropulsed specimens occurred at a temperature $\sim 150^\circ$ C lower than by normal heating, indicating an enhancement of the rate of crystallization by the electropulsing.

2.2 Solidification

Misra [10] reported that the application of 30-40 mA/cm² at 30 V (a.c. or d.c.) during the solidification of a Pb-Sb-Sn alloy produced a significant refinement of the microstructure in the casting. In subsequent work on the Cd-Sn eutectic system, Gupta et al [11] concluded that there exists a potential source inside the solidifying system itself. The origins of the potential were attributed to lie either

in the generation of a micro thermo emf caused by a small but finite temperature gradient, or the presence of a potential at the solid-liquid interface.

Brystkiewicz et al [12] investigated the growth of bulk epitaxial crystals of GaAs from the melt by passing an electric current (2–10 A/cm²) through the liquid solution and substrate. The effect of current density on the interface growth rate is illustrated in Fig. 4. Two main mechanisms were proposed [13] as being responsible for the crystal growth: (a) Peltier cooling at the substrate-solution interface leads to a change in interface temperature ΔT_p , which supercools the solution next to the substrate and (b) electromigration of solute toward the substrate, resulting in a steady-state solute flux to sustain growth. Reasonable agreement between the experimental results and theory is indicated in Fig. 4. The resulting crystals possessed both a low point defect concentration and low dislocation density, and had good electronic properties.

3. Effects of External Electric Field

3.1 Soviet Work

Klypin and coworkers [14,15] first reported in the late 1970's that an external, electrostatic field E of the order of 10 to 100 V/cm increased the hardness resulting from the heat treatment of Al alloys and a medium-carbon steel; see Figs. 5–7. The influence of the field on Al alloys was found to depend on polarity (Fig. 8), the effect being larger when the specimen was connected to the positive terminal, i.e. when the specimen was the anode. Further, the effect of the field on hardness increased linearly with the logarithm of E ; see Fig. 9. In the heat treatment of the steel, the major effect of the field occurred during the quench; very little change was noted when the field was only applied during the austenitization.

As an explanation for the effect of an electric field on phase transformations, Klypin [15] proposed that a galvanic potential exists between the phases, the magnitude of the potential being determined by: (a) the chemical potential of each phase, (b) jumps in the potential at the boundary of the solid phase and the gaseous atmosphere and (c) the difference in the work function of the electrons of each phase, i.e. the difference in Fermi levels. With application of an electric field the surface potentials will change, i.e. the external field changes the values of the galvanic potentials. These changes in potential are then compensated by changes in the chemical composition due to diffusion, including redistribution of solutes near the phase boundaries.

2.2 Authors' Work

2.2.1 Iron and Steels: Exploratory studies of the effect of an external d.c. electric field of 10 kV/cm on the quench aging of an iron indicated that the field retarded the aging process when the specimen was the anode, but had no effect when the specimen was the cathode; see Fig. 10. In other work it was found that an external field of 1 kV/cm produced a significant increase in the hardenability of a 0.9 C tool steel quenched in silicone oil; see Fig. 11. Hardness measurements and optical microscopy revealed that the influence of the field extended to the center of the 1.6–3.0 mm dia. specimens employed.

Fig. 12 shows that the influence of the field on the hardenability of 02 steel depended on the quench medium, i.e. on the cooling rate (measured by us) during the quench. The field had little, if any, effect at the two extremes in quench rate (mineral oil and still air), but had a significant effect at the intermediate cooling rate produced by the silicone oil. These results indicate that the major effect of the field was during the quench rather than during the austenitizing. This conclusion was confirmed in separate studies whereby the field was applied only

during austenitizing or only during quenching and is in accord with the results obtained by Klypin [15] for the effect of an electric field on the hardness of a medium-carbon steel quenched in water.

The major constituents of the microstructure observed by optical microscopy (1000X magnification) in the specimens quenched in the three media are presented in Table 1. The listed microconstituents for a given quench are in accord with the measured hardness values for this steel, considering data in [18,19]. Further, at the magnification of 1000X the appearance or morphology of a given constituent did not appear altered by application of the electric field during austenitizing and quenching.

Considering that the effect of the electric field depends on the cooling rate during the quench and that the resulting hardness is in accord with the observed microstructure, it is concluded that the primary influence of the field on hardenability is to shift the cooling transformation (CT) curve to longer times. An estimate of the shift based on the measured cooling rates, hardness, microstructure and data in [8,9] is presented in Fig. 13. Considering these results, it appears that the field produced a shift in the time to reach the nose from ~5s to ~50s. The cooling rate with the mineral oil quench is sufficiently high that it falls outside the nose of the CT curve both with, and without the field, giving martensite for both conditions. That for still air is so slow it falls well inside the nose for both conditions, giving mostly pearlite. The cooling rate of the silicone oil is intermediate and falls outside the nose with the field (giving martensite) and inside the nose without the field (giving pearlite plus bainite).

A shift in the CT curves to longer times requires that the electric field retards the diffusion-controlled pearlite and bainite transformations. Moreover, as mentioned above, the effect of the field extends to the center of 1.6–3.0 mm dia. specimens. To explain these effects of the field in terms of changes at the

specimen surface, which then diffuse to the center, would require an excessively large diffusion coefficient. The alternative explanation by Klypin [15] that changes in potential at the surface lead directly to rapid changes in the chemical potential of the phases in the interior is also open to question, since according to classical electron theory a field cannot exist within a metal. Thus, the mechanism by which the field shifts the CT curve to longer times is unclear at this time.

An exploratory study into the effect of an external field on the tempering of the 02 tool steel quenched in mineral oil revealed that the field increased the temperature required to attain a given reduction in hardness by about 10°–20°C in the range of 150–350°C (time of tempering, 30 min); see Fig. 14. This again indicates that an electric field retards a diffusion-controlled phase transformation.

2.2.2 7475 Al Alloy: Optical and TEM observations on superplastically deformed 7475 Al alloy sheet revealed that the application of an external electric field E during the deformation had an influence on the microstructure in addition to reducing the amount of cavitation, which is discussed by the present authors in the paper on electroplasticity in these proceedings. Fig. 15 shows the influence of the field on the dispersoid structure following a plastic strain $\epsilon = 0.7$. To dissolve the precipitates which had developed during the air cooling from the deformation temperature, the specimen in Fig. 15 was reheated to 480°C for 1–2 min and then water quenched prior to examination by TEM. To be noted in Fig. 15 is that the dispersoids are smaller within the grains, but larger at the grain boundaries when the field was applied. Also, the dislocation density within the dispersoid-free zone is lower with the field. Further, as shown in Fig. 16, the

composition of the dispersoid-free zone is different with the field compared to without; notably the Cu/Zn ratio is lower for deformation with E.

The effects of the field on the microstructure developed during the superplastic deformation of the 7475 Al alloy extended to the center of the 1.2–1.8 mm thick sheet specimens. Assuming that the changes in microstructure at the center resulted from an influence of electric field on the vacancy concentration at the specimen surface, which then diffused into the interior, one can obtain an estimate of the time t required to reach the center from the relation [20]

$$t = x^2/D \quad (1)$$

where x = one-half the specimen thickness and $D = D_0^v \exp(-\Delta H_m^v/kT)$ the diffusion coefficient for vacancy migration. Taking $D_0^v = 0.2 \text{ cm}^2/\text{s}$, $\Delta H_m^v = 0.6 \text{ eV}$ [20–22] and $T = 516^\circ\text{C}$ (test temperature), one obtains $t = 4.3 \text{ min}$. In comparison, the test time required to reach the strain indicated in Figs. 15 and 16 was 15.2 min. Thus, the changes in microstructure at the center of the superplastically deformed specimens which occurred upon application of the electric field could conceivably have resulted from a significant change in vacancy concentration at the specimen surface. Again, the alternate explanation by Klypin [15] that the galvanic potential at the specimen surface leads directly to changes in chemical potential of the phases in the specimen interior is open to question based on classical electron theory.

References

1. R. E. Hummel and H. B. Huntington, eds., **Electro- and Thermo-Transport in Metals and Alloys**, AIME, NY (1977).
2. H. Conrad and A. F. Sprecher, "The Electroplastic Effect in Metals", in **Dislocations in Solids**, Chap. 43, F. R. N. Nabarro, ed., Elsevier, (1989) p. 497.
3. F. Erdmann-Jesnitser, D. Mrówka and K. Ouvrier, *Archiv. f.d. Eisenhüttenwesen* **30** (1959) 31.
4. T. J. Koppenaal and C. R. Simcoe, *TMS-AIME* **227** (1963) 615.
5. Y. Onodera and K. Hirano, *J. Mat. Sci.* **11** (1976) 809.
6. Y. Onodera, J. Maruyama and K. Hirano, *J. Mat. Sci.* **12** (1977) 1109.
7. M. C. Shine and S. R. Herd, *Appl. Phys. Lett.* **20** (1972) 217.
8. Y. Onodera and K. Hirano, *J. Mat. Sci.* **19** (1984) 3935.
9. Z. H. Lai, H. Conrad, Y. S. Chao, S. Q. Wang and J. Sun, *Scripta Met.* **23** (1989) 305.
10. A. K. Misra, *Met. Trans.* **16A** (1985) 1354; **17A** (1986) 358; *Mat. Lett.* **4** (1986) 176.
11. T. Gupta, L. Pandey and P. Ramachandrarao, *Scripta Met.* **21** (1987) 1455.
12. T. Bryskiewicz, C. F. Boucher, J. Lagowski and H. Gatos, *J. Cryst. Growth* (1987).
13. L. Jastrzebski, J. Lagowski, H. C. Gatos and A. F. Witt, *J. Appl. Phys.* **49** (1978) 5909.
14. A. A. Klypin and E. S. Soloviev, *Tsvetnaya Metall., Izvestiya Vyschikh Uchebnykh Zaredenii*, No. 4 (1978).
15. A. A. Klypin, *Metallov. i Termich. Obrabotka Metallov.* No. 3 (1979) 12.
16. H. Conrad, "A Study into the Mechanism(s) for the Electroplastic Effect in Metals and Its Application to Metalworking, Processing and Fatigue", Final Report U. S. Army Research Office Grant #DAAL03-86-K-0015, March 10, 1989.
17. H. Conrad, Wei-di Cao, X. P. Lu and A. F. Sprecher, unpublished research NCSU (1989).

18. A. Rose, W. Peter, W. Strassburg and L. Rachenacher, **Atlas Z. Wärmebehandlung der Stähle, Teil II**, Verlag Stahleisen M.B.H., Düsseldorf (1961).
19. **Atlas of Isothermal Transformation and Cooling Transformation Diagrams**, ASM, Metals Park, OH.
20. P. G. Shewmon, **Diffusion in Solids**, McGraw-Hill (1963) p. 41-85.
21. R. A. Johnson, **Diffusion**, ASM, Metals Park, OH (1973) p. 25.
22. N. A. Gjostein, *ibid.* p. 241.

TABLE 1. Effect of electric field on the major constituents of the microstructure in 02 steel following quenching in several media.

Quench Medium	Relative Cooling Rate [†]	Microstructure ^{††}	
		E = 0	E = 1kV/cm ^{†††}
Mineral oil	1.0	M	M
Silicone oil	0.2	(P+B)+M	M
Still air	0.05	P	P

[†] Measured average cooling rate between 800° and 500°C referred to that for mineral oil.

^{††} Optical microscopy at 1000X.

^{†††} Electric field applied during both austenitizing and quenching.

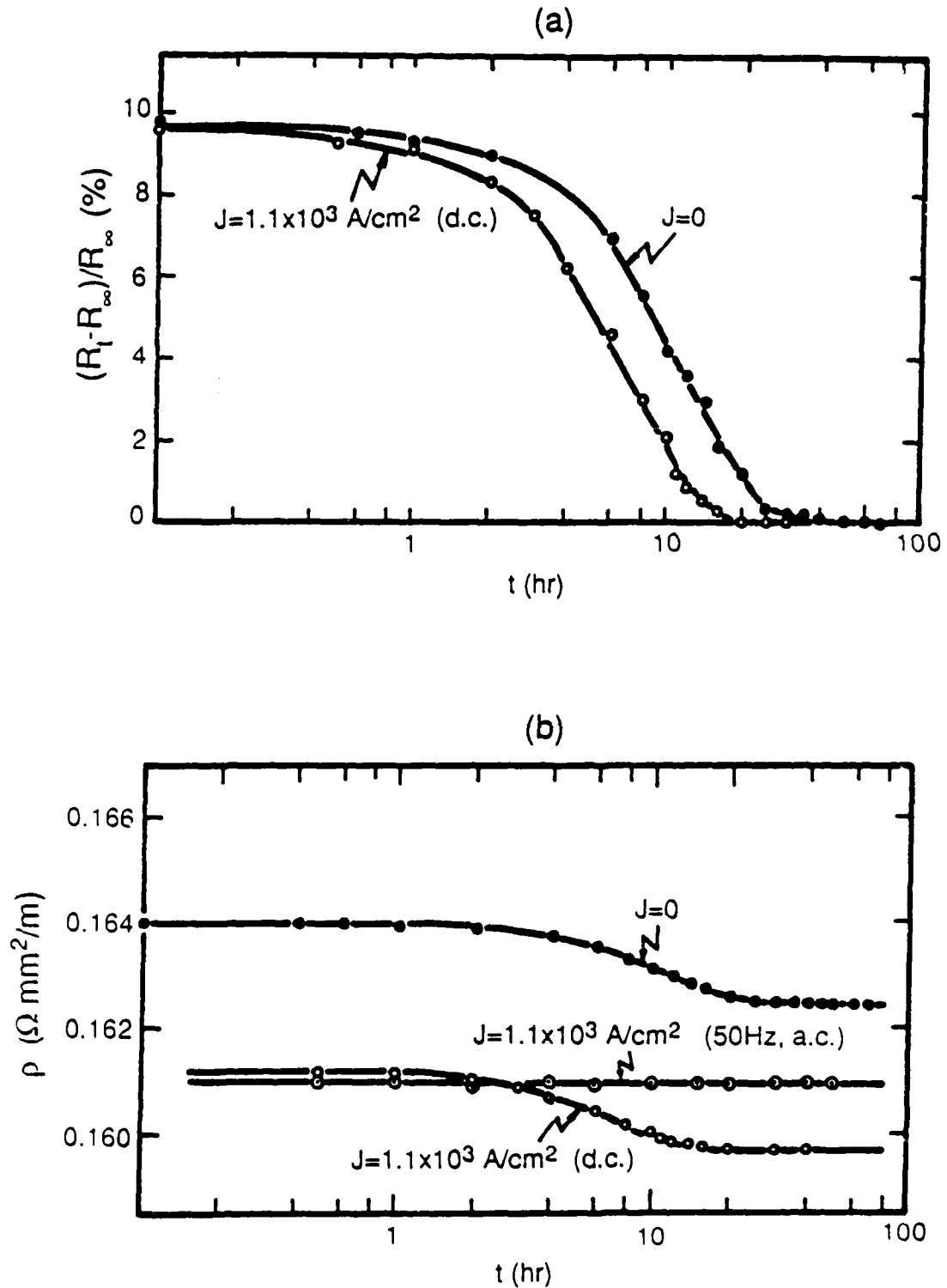


Fig. 1. Effect of continuous electric current on the quench aging of Armco iron: (a) resistivity change vs aging time as a function of d.c. current and (b) specific resistivity vs aging time as a function of d.c. current and 50 Hz a.c. current. From Erdmann-Jesnitzer et al [3].

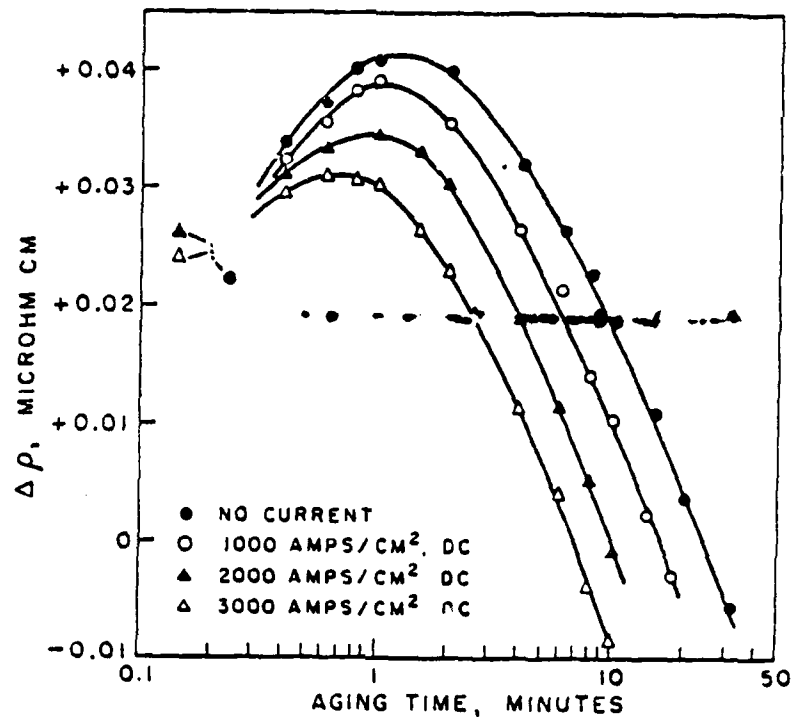


Fig. 2 Change in resistivity vs aging time at 75°C for aging an Al-4 wt.% Cu alloy under various d.c. current densities. From Koppenaal and Simcoe [4].

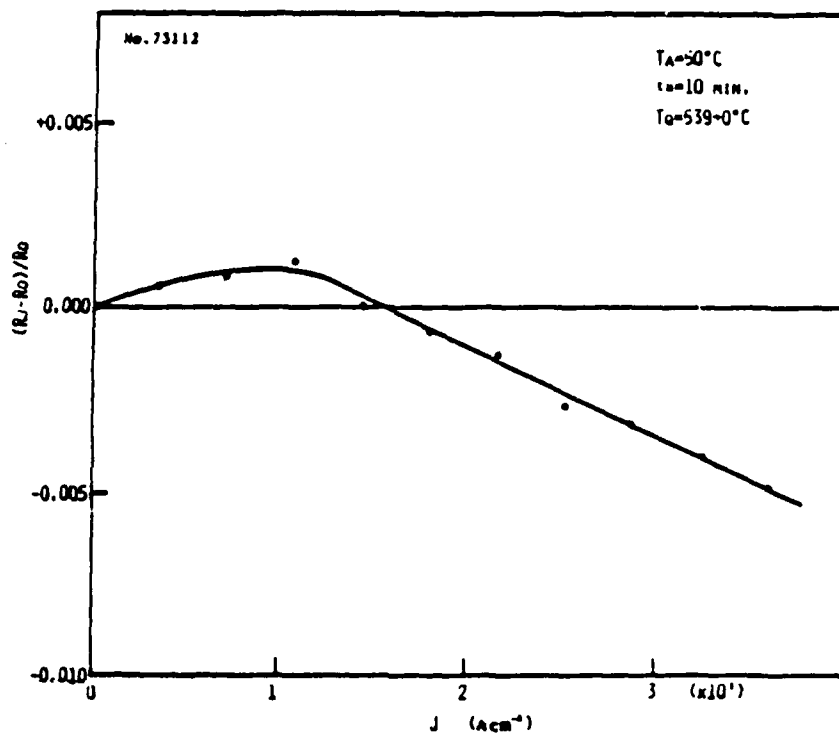


Fig. 3 Fractional change in resistance vs current density upon aging an Al-4 wt.% Cu alloy for 10 min at 50°C. From Onodera and Hirano [5].

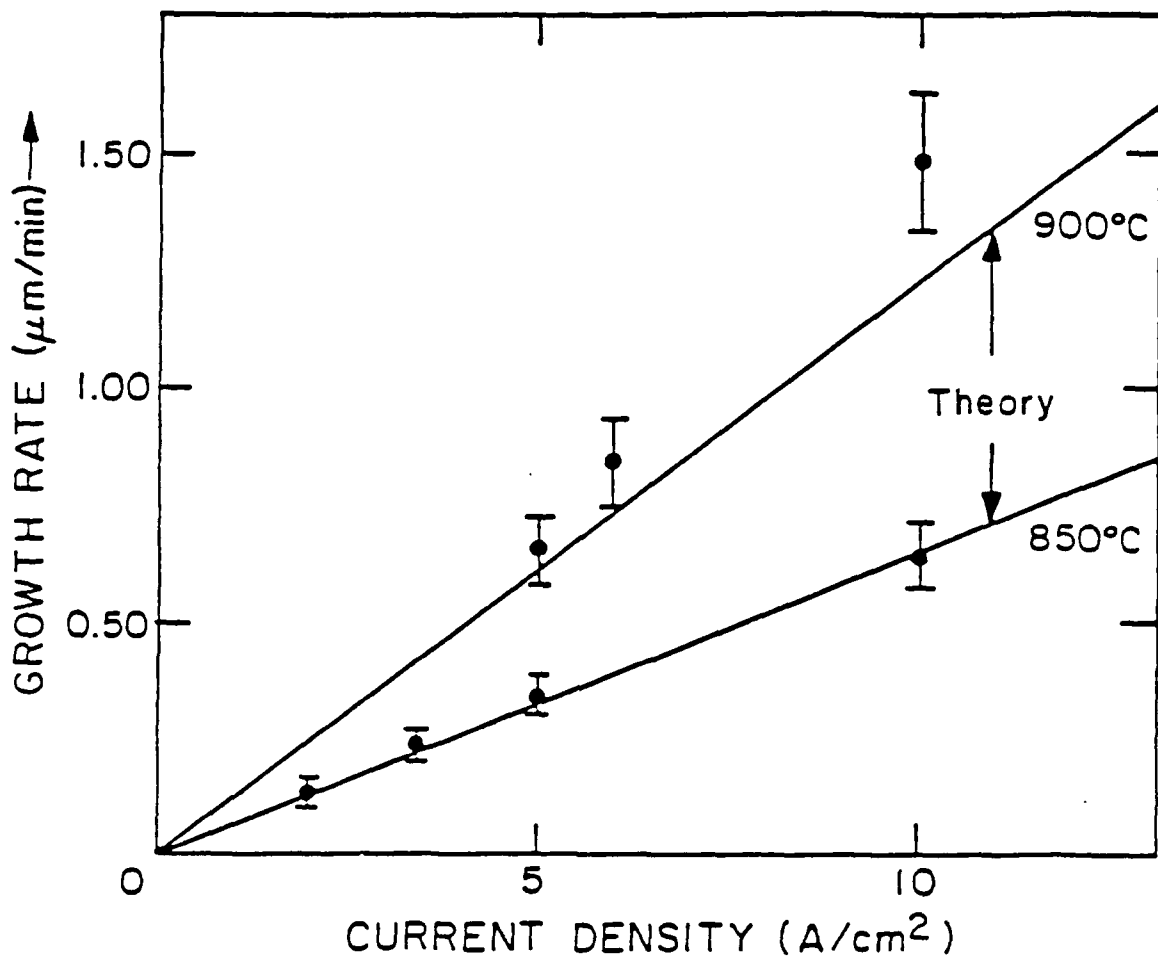


Fig. 4 Growth rate of GaAs crystals at 850° and 900°C vs current density compared with theoretical predictions (solid lines). From Bryskiewez et al [12].

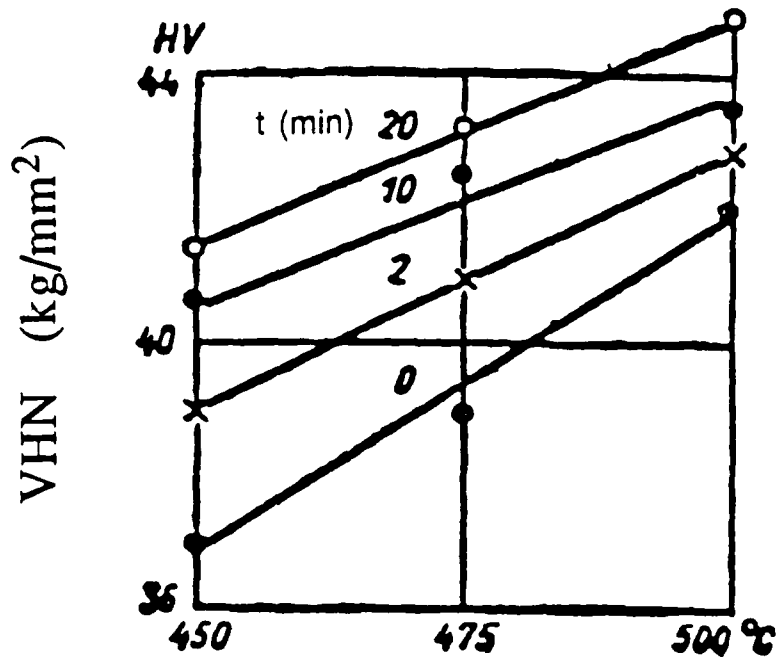


Fig.5 Effect of time (min) of application of the electric field during solutionizing at 450-500°C on the Vickers hardness of quenched 2024 Al alloy. From Klypin [15].

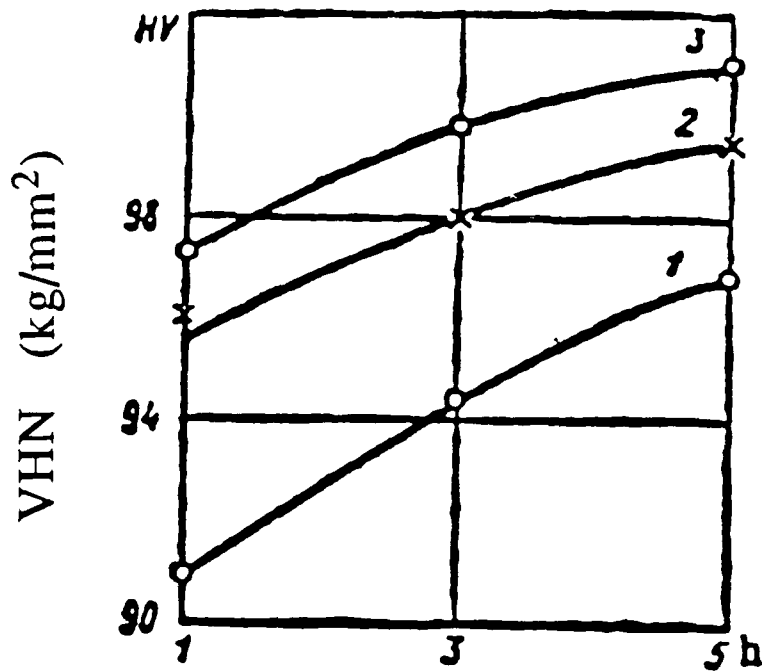


Fig.6 Vickers hardness vs aging time at 75°C of Al-Cu-Mg alloy for the following conditions:(1) quench + aging with no field, (2) quench + only aging with electric field and (3) both quench and aging with electric field. From Klypin [15].

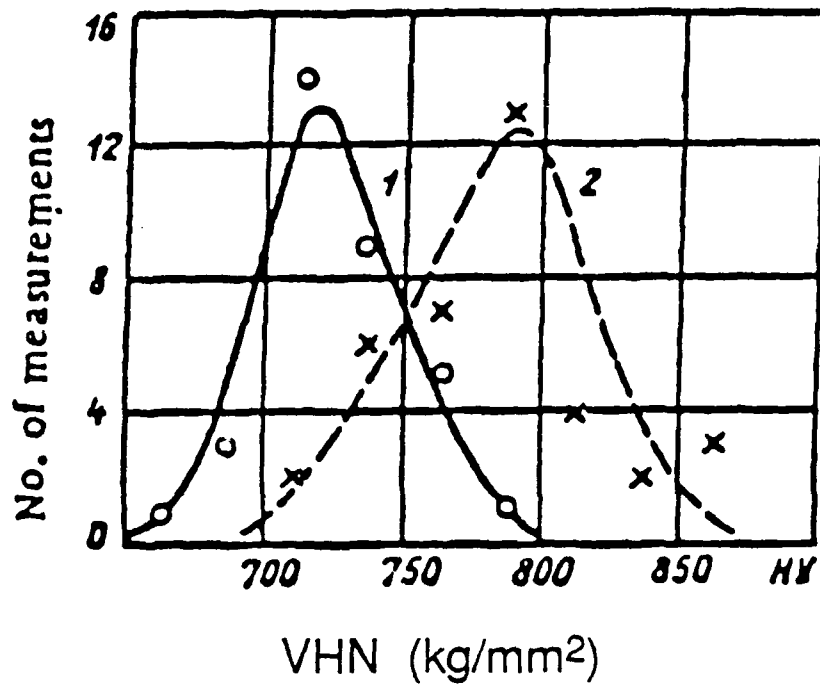


Fig. 7 Effect of an electric field on the hardness (distribution) of a medium-carbon steel quenched in water: (1) without an electric field, (2) with an electric field (50 V). From Klypin [15].

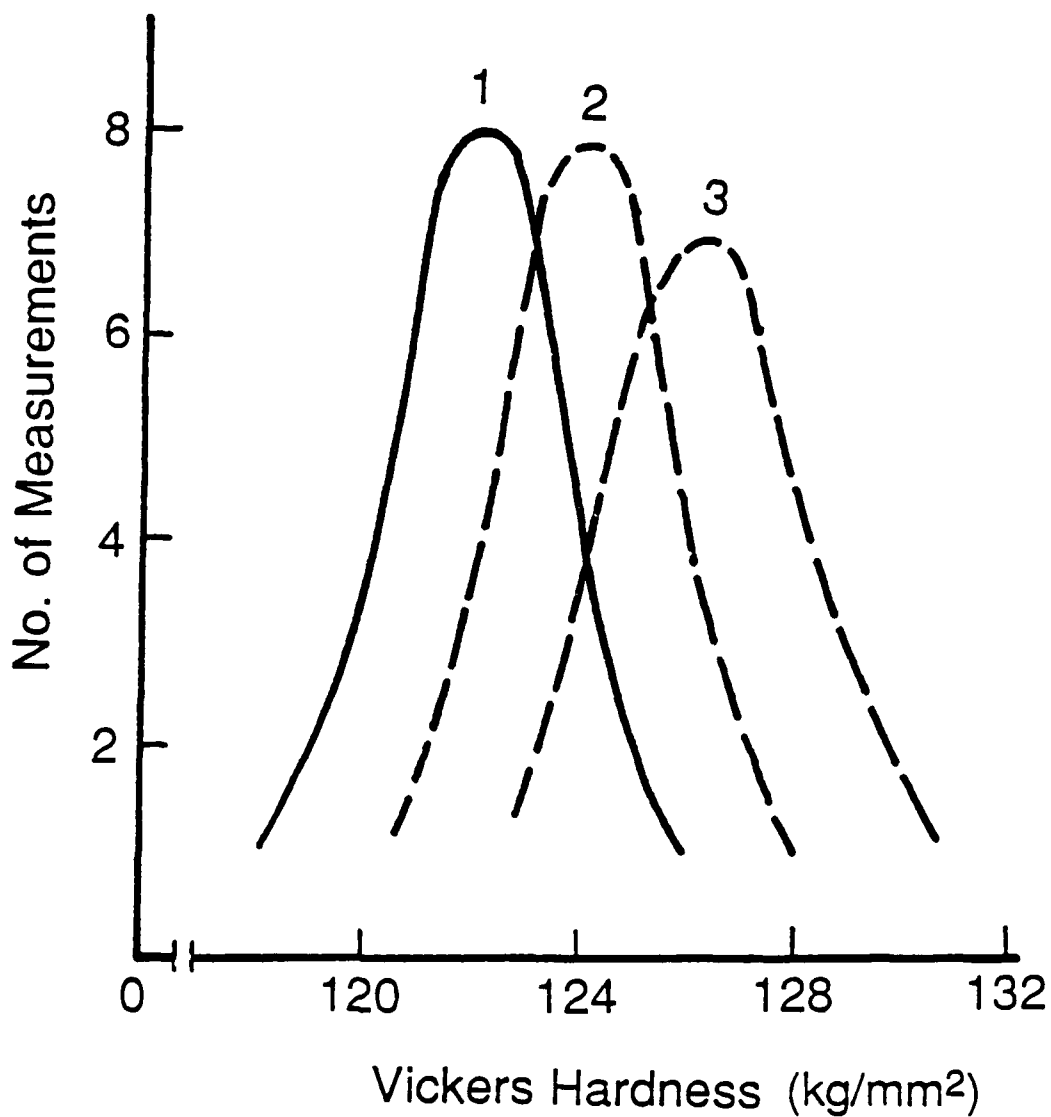


Fig. 8 Effect of polarity of electric field on the hardness distribution of quenched and aged Al-Zn-Mg-Cu alloy: (1) without electric field, (2) specimen was cathode, (3) specimen was anode. From Klypin and Soloviev [14].

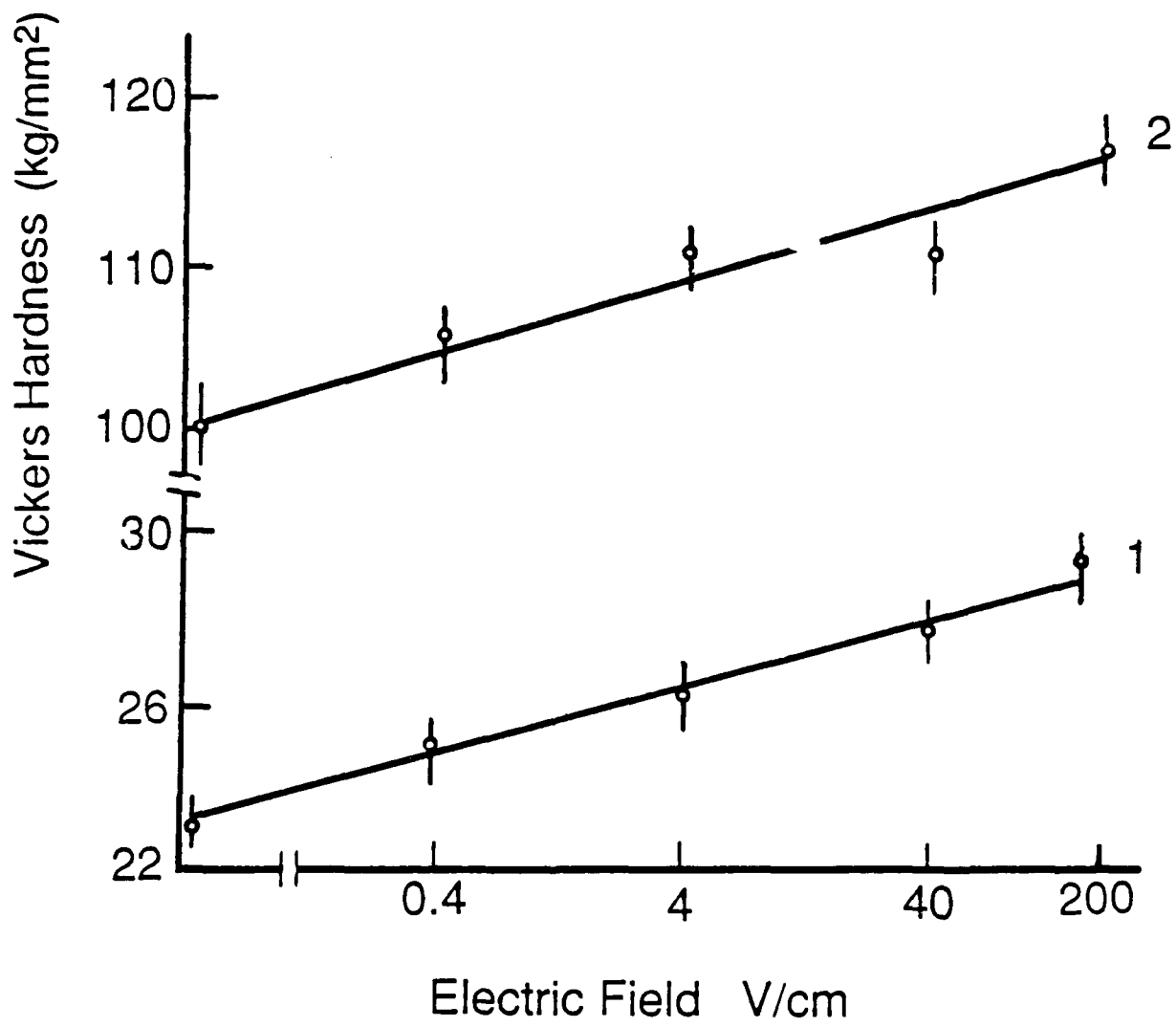


Fig. 9 Effect of electric field on the hardness of 2024 Al alloy heat treated for 30 min at 500°C and water quenched: (1) Hardness at the surface directly after quenching, (2) Hardness 0.1 mm below the surface after natural aging. From Kypin and Soloviev [14].

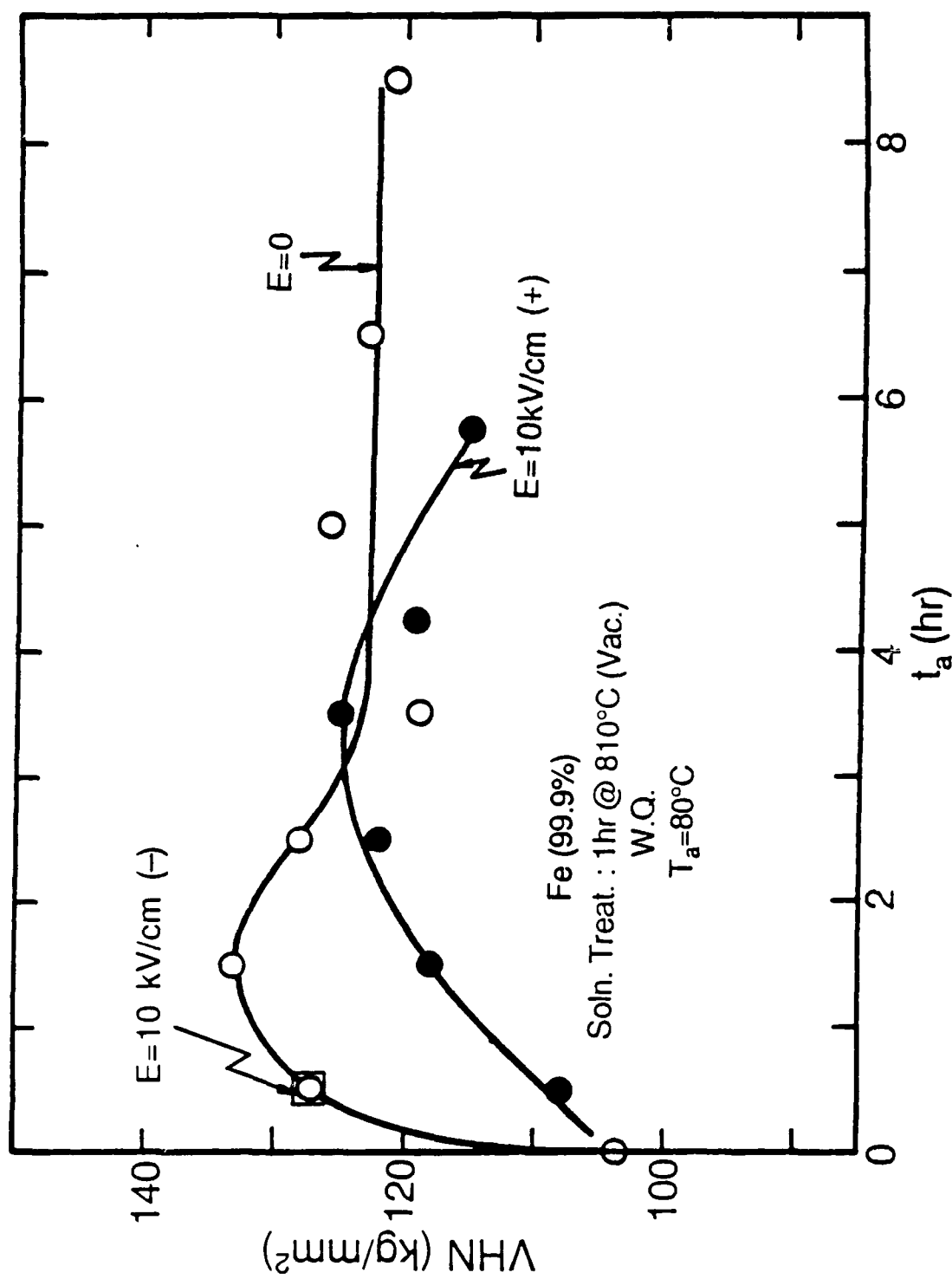


Fig. 10 Effect of a continuous d.c. electric field on the quench again of a low-carbon iron. From Conrad [16].

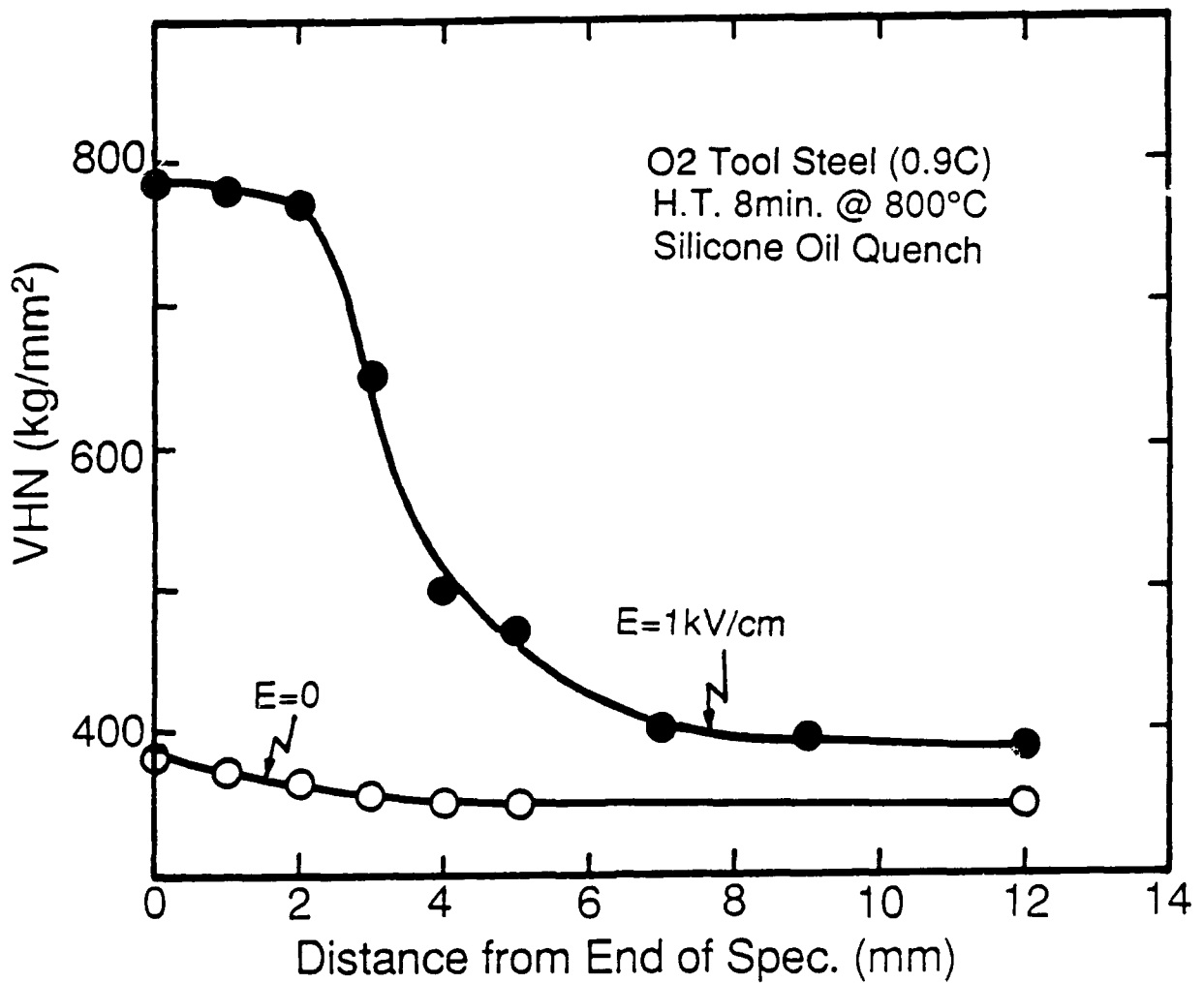


Fig.11 Effect of a a continuous d.c. **electric field** applied during austenizing and quenching on the hardenability determined in a simulated Jominy quench of an O2 tool steel quenched in silicone oil. From Conrad et al [17].

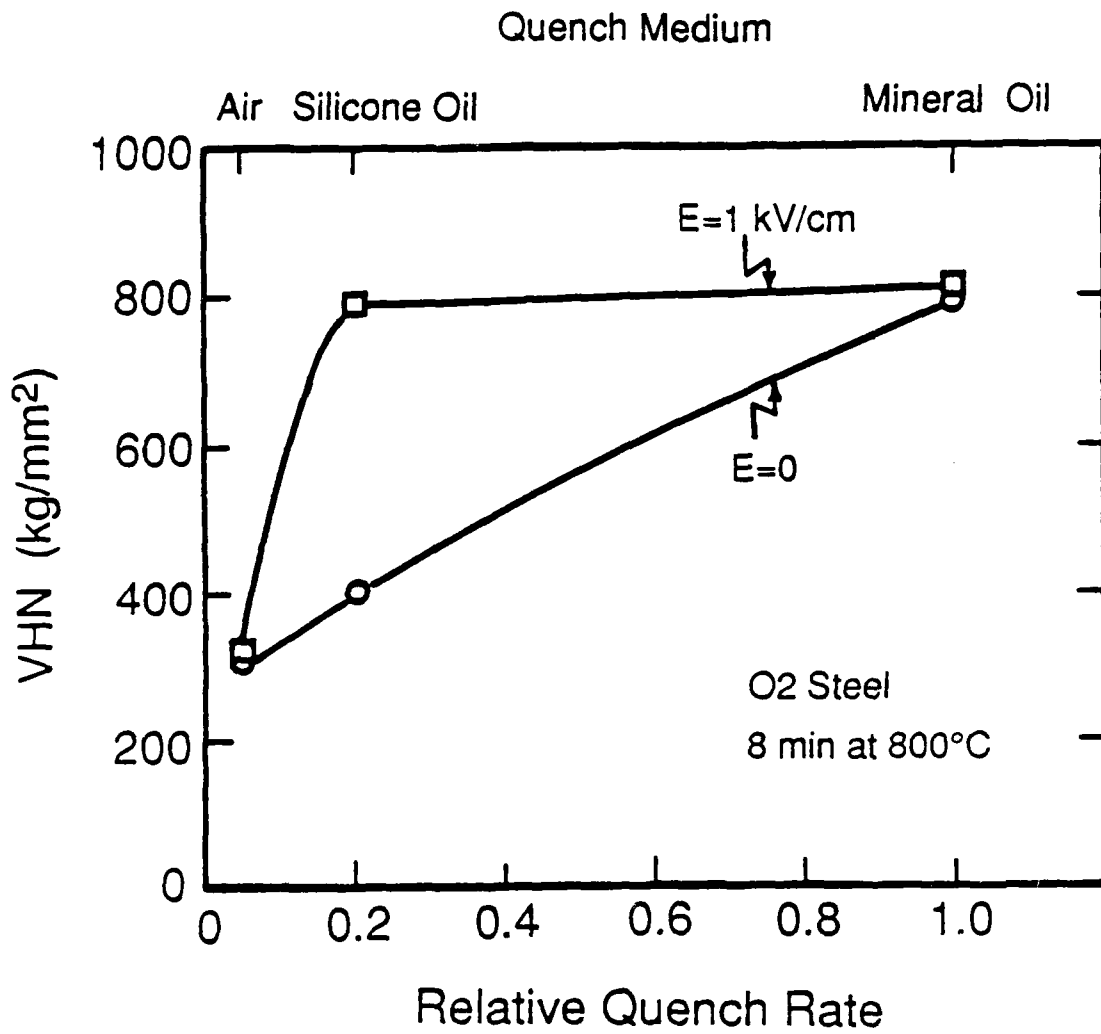


Fig. 12 Effect of electric field on the hardness of O₂ steel as a function of the cooling rate produced by several quench media. From Conrad et al [17].

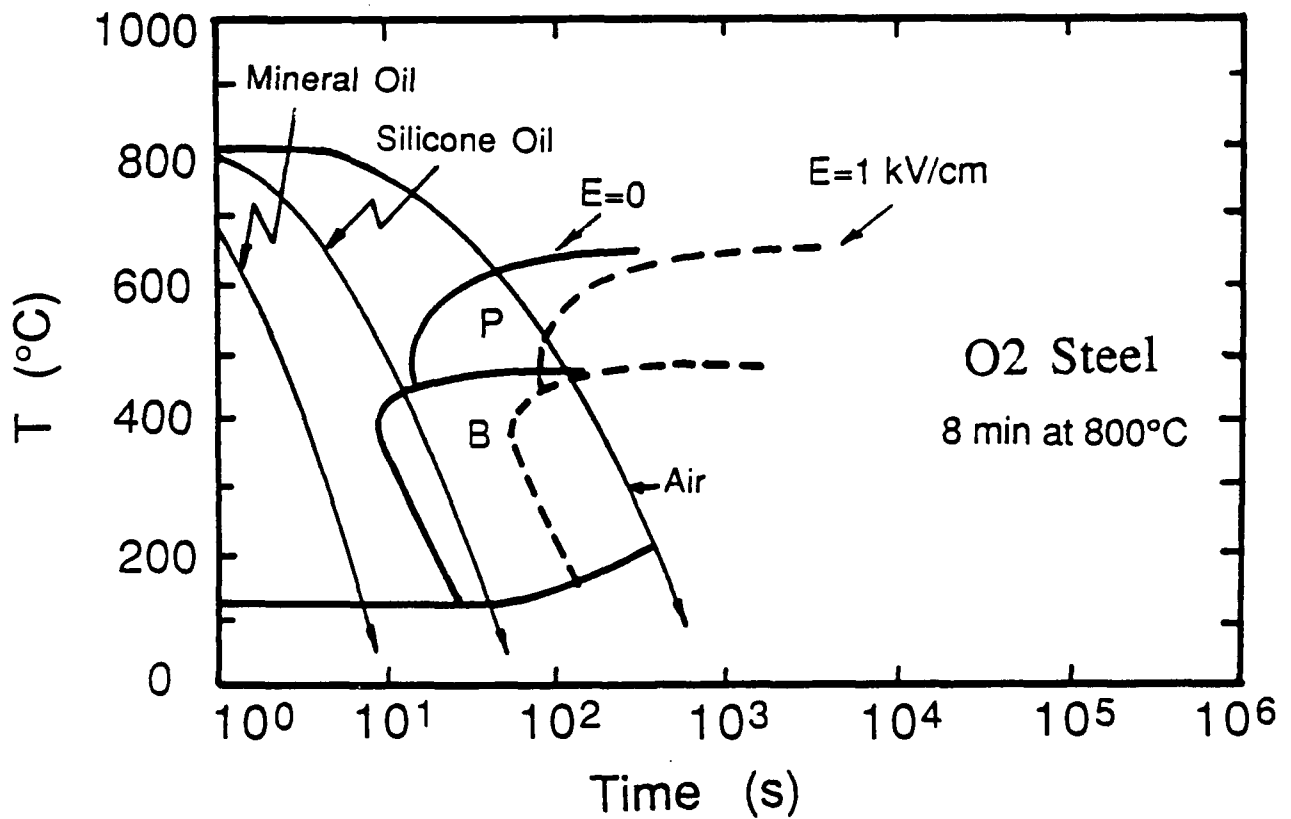


Fig. 13 Estimate of the CT curves for the O₂ steel with, and without an electric field based on measured cooling rates, hardness, microstructure and data in [8,9].

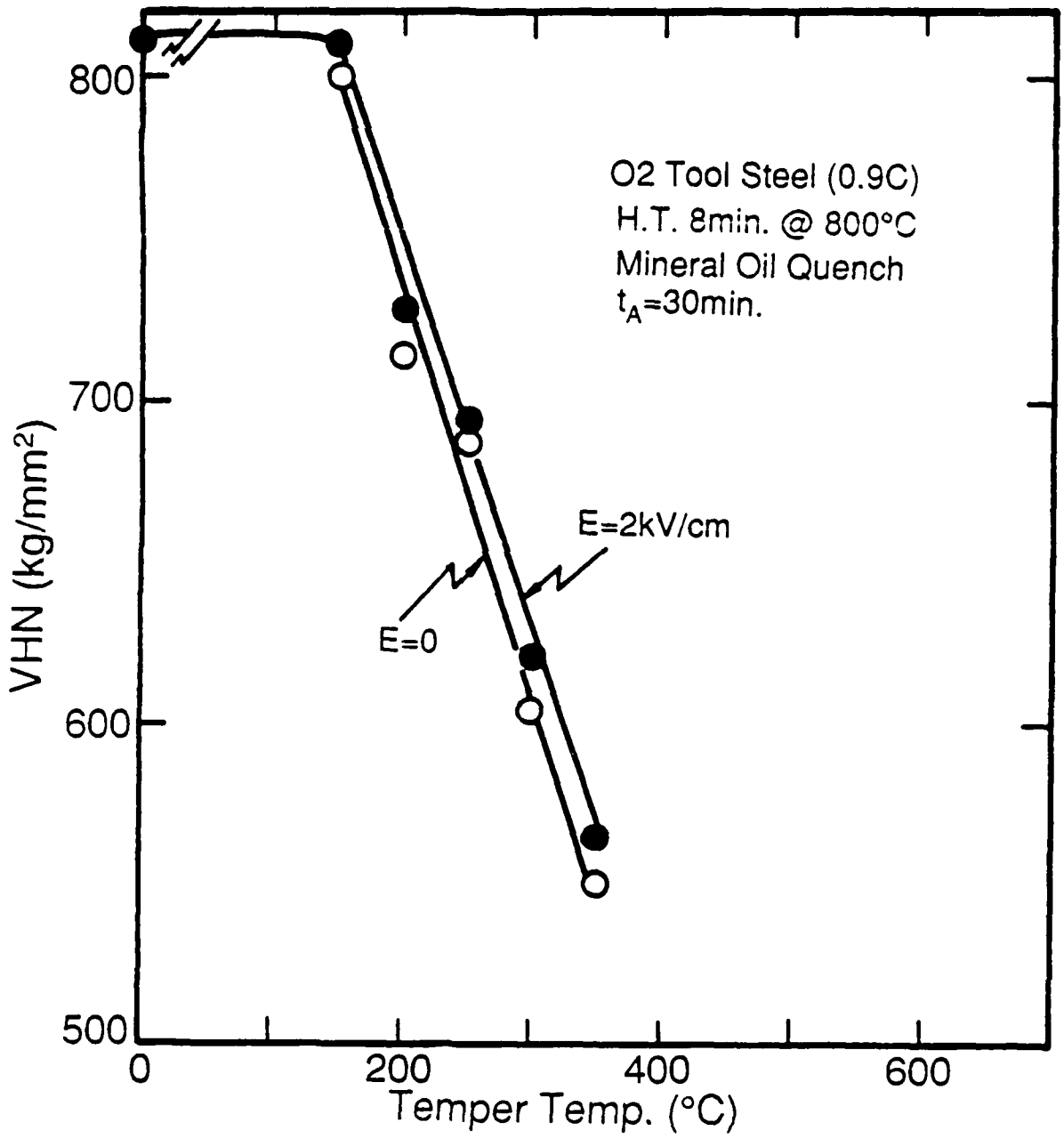
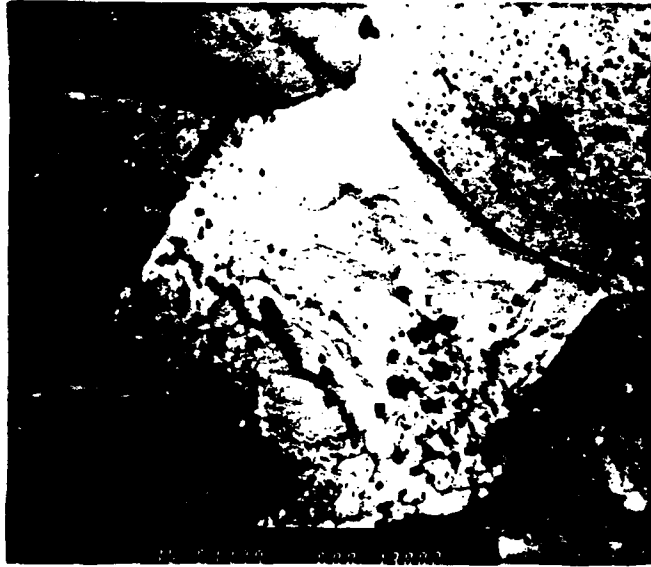
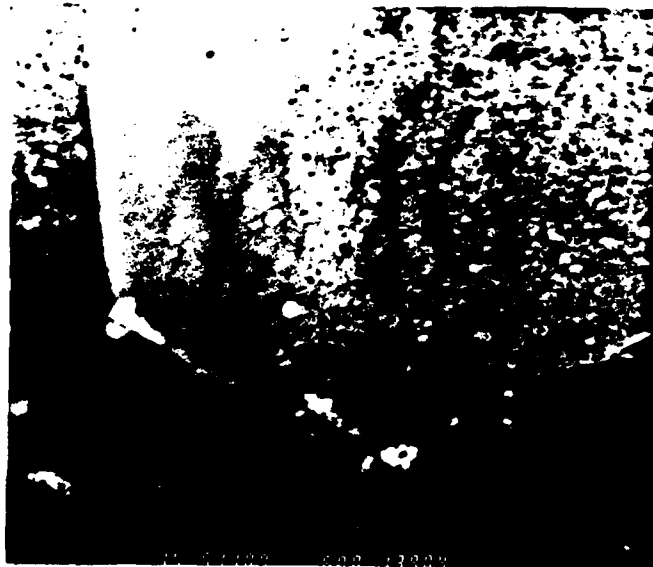


Fig. 14 Effect of a continuous d.c. electric field on the tempering of an O2 tool steel quenched in mineral oil. From Conrad et al [17].



(a)

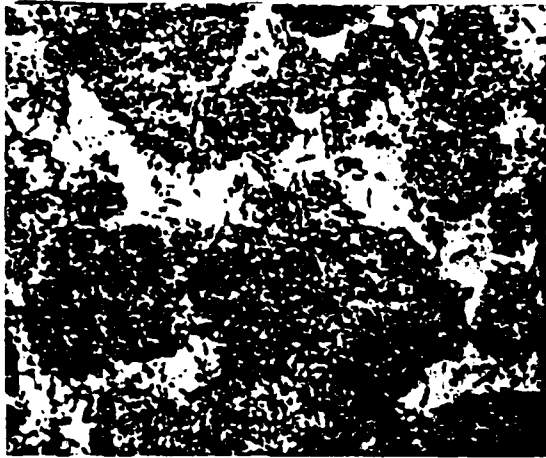
$E=0$



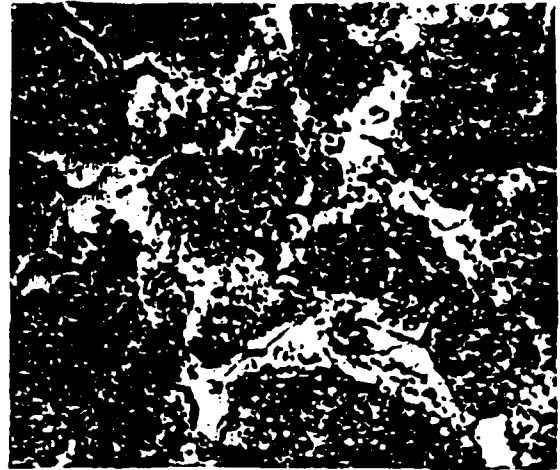
(b)

$E=2 \text{ kV/cm}$

Fig.15 Effect of electric field on the microstructure developed during the superplastic deformation ($T=516^{\circ}\text{C}$, $\dot{\epsilon}_0=1.1 \times 10^{-4} \text{ s}^{-1}$, $\epsilon=0.7$) of 7475 Al (I): (a) $E=0$, (b) $E=2 \text{ kV/cm}$. From Conrad et al [17].



$E=0$



$E=2\text{kV/cm}$

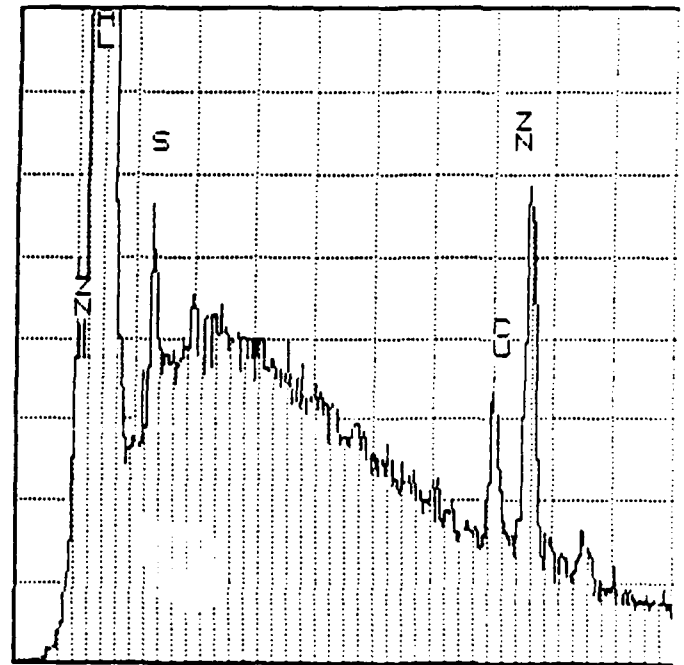
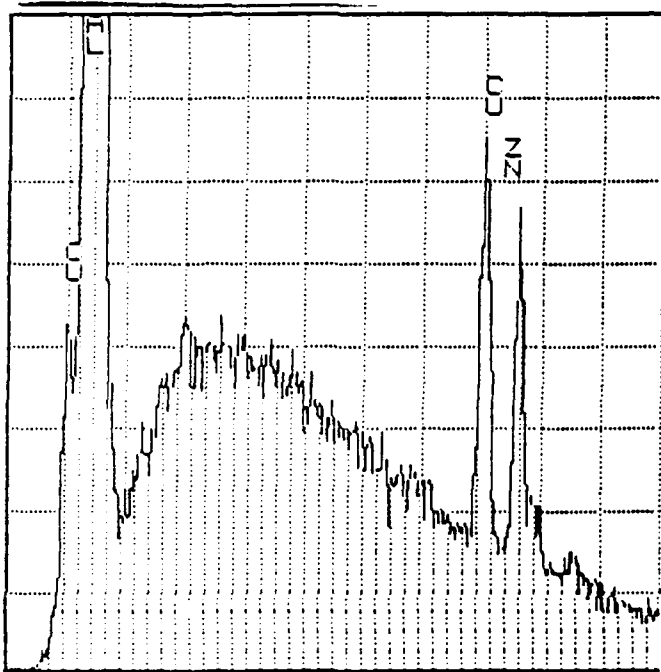


Fig.16 Effect of electric field on the structure and composition of the precipitate-free zone in superplastically deformed ($T=516^{\circ}\text{C}$, $\dot{\epsilon}_0=1.1\times 10^{-3}\text{s}^{-1}$, $\epsilon=0.7$) 7475 Al (I). Air cooled without field from deformation temperature. From Conrad et al [17].

THE EFFECT OF MAGNETIC FIELDS ON
MATERIALS PROPERTIES AND PROCESSING

Robert F. Hochman, PhD
Professor, School of Materials Engineering
Georgia Institute of Technology
Atlanta, GA

Naum Tselesin, PhD
President, Duratech, Inc.
Atlanta, GA

I. SUMMARY

This paper is composed of two major sections. The first is a summary of several decades of research, principally in the USSR, on the effect of magnetic fields on material properties and processing. The second section will deal with our ongoing research in this area. The research is principally an evaluation and modeling of changes in defect structure and residual stress as a function of pulsed magnetic field treatment.

The review section on the USSR work will deal mainly with a number of books and major articles which can be then referred to in more detail regarding specific references. Because of the volume of the Russian work it will be presented in the summary form, listing the broad scope and ideas developed in both their basic and applied research. A short section will also provide the principal studies outside the USSR on the magnetic field effects on material properties.

In the research section, nickel and copper were chosen as the materials for the basic characterization and modeling of changes in residual stress in cold worked, or locally deformed areas (potential fatigue damage). Stress relief in the heat affected

zone of welds was studied in 304 stainless steel and a 1018 plain carbon steel. Positron annihilation to evaluate changes in the characteristics of defect structure plus x-ray strain analysis was used to examine the effects of pulsed magnetization on cold worked and welded materials. A marked effect was found for magnetically induced defect recovery in both cold worked nickel and OFHC copper. The use of PAS and x-ray diffraction techniques indicated a substantial amount of recovery during the first few cycles of a pulsed, 1,000 oersted, magnetic field. It was also found that "R parameter" calculations for positron annihilation showed a change in the dominant defect structure during magnetically induced recovery. Magnetic processing also indicated the potential for changing the surface microhardness in the weld stress relief studies. Because of the complexity of weld zones in general, positron annihilation spectroscopy was the only clear cut method showing a change in the actual defect structure following magnetic stress relief.

II. BACKGROUND

The objective of this part of the paper is to present experimental and theoretical background which has been published in the USSR. This review will cover the basic studies as well as their work in utilization of property changes of materials affected by magnetic fields. A short section at the end of this portion of the paper will be devoted to a review of non-USSR studies in this area.

~~Since~~ The first Soviet work on the subject was published in 1937 by A.V. Alekseev (1) (who reported an increase of hardness on HYS steel by magnetic treatment). Since then, principally in the last 30 years, hundreds of articles and several monographs have been published in the USSR. In a monograph by V.M. Finkel (2), treatment of materials in magnetic and electrical fields is considered as a part of a complex approach to physical-mechanical methods of failure and crack retardation. A series of ideas, methods and equipment related to crack retardation in metals and monocrystals is presented in this monograph. The publisher of the monograph suggested this book for study by scientists whose specialties are strength and failure analysis and who are involved in the metallurgical, machine manufacturing and ship building industries. The monograph contains 449 bibliographical references, 6 tables and 143 figures.

Another more recent monograph by Y.M. Baron (3) is devoted to one of the most practical applications of magnetic field processing; treatment of cutting tools. The monograph (3) contains information about equipment design and the technology of magnetic and abrasive-magnetic treatments. Different theories and working hypothesis of magnetic treatment effects are discussed in this work. The monograph contains 110 bibliographical references.

A third book by B.V. Malygin (4) has been announced for publication in the fourth quarter of 1989. This will be devoted to the strengthening of tools and machine parts by magnetic treatment.

In the monograph by Baron (3) various schemes for magnetic treatment are presented depending upon the application and the magnetic field parameters. For example, for cutting tool production the following procedures can include:

- magnetic treatment of the tool in the process of cutting,
- magnetic treatment after sharpening of the tool,
- magnetic treatment during the thermal treatment of the cutting tool.

According to monographs (2,3) the results of magnetic treatment are determined by combinations of several effects:

- A magnetic field can produce irreversible changes in structure and properties for ferromagnetic materials as well as for those materials which do not have spontaneous magnetization.
- Orientation of the magnetic moment of a simple defect or a defect complex by applying an external magnetic field is equivalent to applying additional outside stress.
- Even if the energy, provided by the magnetic field, is significantly lower than required to develop new substructural defects this energy is enough to initiate some processes which are driven by the inner energy of the distorted crystallographic lattice.

There are numerous works devoted to study of the effect of the combination of thermal and magnetic treatments. Among these works is a monograph by M.L. Bernshtain and V.N. Pustovoit (5), and several major reference articles (6-9).

The effect of magnetic treatment on nonferromagnetic materials was studied in works (10,11). Significant changes in performance of treated materials were reported in these studies. In works (2-11) and in many of the references included in these works, the authors report magnetic field effects on:

- Physical-mechanical properties of treated materials,
- Diffusion and transformation processes,
- Residual stress and stress relief,
- Wear resistance,
- Fatigue life.

Some of these results are presented in summary form in the following sections.

Physical-Mechanical Properties

Most of the results have been reported when specimens were magnetically treated at room temperature, for example:

- During electron transitions in a magnetic field, considerable changes have been found in magnetic, thermal, optical and mechanical properties of the materials treated (2,11).
- Increases in hardness after magnetic treatment have been shown as a change in the hardness as a function of the depth into the specimen (Figure 1) (5).
- As a result of exposure of ferromagnetic materials to a pulsed magnetic field microscopic deformation occurs in the material, causing changes in the structure termed:
"Magnetostriction Substructural Strengthening of

Ferromagnetic Materials (3)."

- Multiple remagnetization was produced in Cr-W-Mo steel specimens (58-62 HRC) in a relatively weak constant field of 0.4-0.6 kA/m (5-7.5 Oe) by rotating the specimens between different poles of an electromagnet of constant current (up to 4,000 cycles of remagnetization). This resulted in up to 30% increase in hardness of the treated specimens (3).
- For paramagnetic Niobium and Molybdenum specimens a constant magnetic field (1,500-2,000⁰_A; 120-160 kA/m) brought about a change of temperature dependence of the yield point (Figure 2), an increase in the plasticity and stress relaxation at constant strain within a given temperature range (Figure 3), a decrease of the Peierls activation energy (Figure 4) and an increased mobility of screw dislocations.

Diffusion and Transformation Processes

Some of the metallurgical changes reported when materials are magnetically treated at room temperature were:

- A decrease in the lattice parameter of martensite as a result of magnetically induced precipitation.
- Precipitation of a fine-dispersion strengthening phase, particularly, carbides in steels (3).
- Changes in ordered defect mechanisms which control the increase of free defects in electroconducting materials. Defects change at the surface of crystals as a result of electron bursts arising from a pulsed magnetic field (3).

- The local absorption of energy at structural inhomogeneities. In steels this leads to the rearrangement of these inhomogeneities. Further rearrangement of the structure takes place after the completion of pulsed magnetic treatment. On the whole, strengthening by pulsed magnetic treatment is postulated following a mixed dislocation - diffusion mechanism (2,3).
- Sections of dislocation loops may move when interacting with moving domain walls resulting in a small increase of the total length of the dislocation loop. After removal of a magnetic field there is incomplete relaxation of the dislocation deformation. This is offered as an explanation for observed increases of microhardness (2,3).
- Relaxation of intra-crystalline stresses can be related to the decay of metastable defect complexes which brings increased mobility of structural defects and increases in the rate of diffusion. On the other hand, after relieving defects, the possibility arises of developing a more stable association of defects of higher energy (3,10).

The following effects have been observed and studied when thermal treatment and magnetic treatment have been combined (5-9):

- Thermodynamic and kinetic properties of phase transformations in steel are markedly changed under selected conditions of applied magnetic fields.
- The effect of a magnetic field on diffusion and recrystallization processes has been shown.

- The effect of a magnetic field on transformations of subcooled austenite.
- The effect of a magnetic field on the physical and mechanical properties of solids and liquids.
- The effect of a magnetic field on the martensitic phase transformation.
- The effect of a magnetic field on the annealing of steel.

Residual Stress Relief

An increase in the compressive residual stresses in surface layers of 0.1% carbon steels has been reported in (3) (see Figure 5). In addition, changes in the stress distribution of heat treated materials in a magnetic field has also been shown (5) (see Figures 6 and 7).

The Effect on Wear Resistance and Cutting Tool Life

The following results relating to cutting tools have been reported and discussed in the Russian literature.

- An increase of wear resistance (up to 2.5 times) of 18%W steel and 6%W-5%Mo steel following magnetic treatment (3).
- The wear interrelationships between the magnetic condition of the steel and carbide cutting drills and tools (3). For example, tool life can be increased or decreased depending on polarity of the magnetic field in the cutting tool and direction of the feed (for lathe bits).
- An increase of HSS tool life of 1.5 to 3x, if multiples of an unidirectional pulsed magnetic field of 500-1000 kA/m (6.3 - 12.6 kOe) amplitude is applied. However, higher field

strengths can result in embrittlement and destruction of the cutting edge.

- Multiple remagnetization of a cutting tool in a relatively weak field (up to 0.4-0.6 kA/m (5-7.5 Oe)), performed by rotating the tool between different poles of an electromagnet at a constant current results in an increase in tool life.
- The heat effect in HHS inserts of the right geometry placed in a magnetic field of 240 kA/m (3.0 kOe), is large enough to change the temperature balance in the cutting area.
- A change in hardness of the chip surface next to the cutter and a decrease of shrinkage of the chip has been suggested as the reasons for the changes in the coefficient of friction between a magnetically treated cutter and the work piece being machined.

Fatigue Life

The effect of magnetic treatment on fatigue life has been mentioned in several works (2,3), but only in the monograph by Malygin and Varulenro (7) (combination of magnetic and thermal treatments) have conclusive results been reported (see Figure 8). It is stated in monographs 2 and 3 that superimposing a sufficiently strong magnetic field makes it possible to alter the principle mechanical and thermodynamic constants of materials in a desired way. This is of tremendous interest from the point of view of controlling the fatigue strength and failure of solids.

It is obvious that Soviet research has provided a large

reservoir of data confirming material property changes produced by the selected application of magnetic fields of varying intensity. These changes are of a fundamental nature and are significant enough to be utilized in industry.

Other Research

Several non-Russian studies have also shown the possibility of modifying the properties of metals by utilizing a magnetic field. These investigations have demonstrated that fatigue properties, stress relief, wear resistance, and surface composition can be altered by the application of a pulsed magnetic field (12-13).

Cullity et al. demonstrated the stress relaxation in a nickel specimen loaded in compression (14). The stress was observed to decrease dramatically with the application of a magnetic field.

The study of magnetically induced recovery of magnetic susceptibility in diamagnetic metals, such as copper, was documented as early as 1946 (15,16), but only recently has mechanical recovery been reported in an article by Hochman et al. (17).

The first theoretical study of the interaction of dislocations with magnetic fields was published by Vicena in 1954 (18). Since that time several additional papers have been published on this topic (19-22).

In addition, it has been shown that very low concentrations of impurities such as Fe, Cr, and Mn in commercial materials can provide localized magnetic moments (23-26) resulting in unique

changes of properties when subjected to a magnetic field. These defect magnetic moments may afford some of the energy necessary to assist in rearrangement and annihilation of vacancies and dislocation structures in diamagnetic materials.

III. CURRENT RESEARCH

Positron Annihilation Spectroscopy (PAS)

Positron annihilation spectroscopy (PAS) is a noncontact and nondestructive technique which can be used to characterize the atomic defect structure of materials. Using currently available instrumentation it is possible to investigate: i) defect types, distributions and densities, ii) the atomic structure of defect such as interstitial/vacancy complexes, iii) the size of vacancy cluster, iv) the electron density in the vicinity of a vacancy, and v) extended defects such as dislocations and grain boundaries.

In a typical experiment, positrons are injected from a radioactive source and quickly reach thermal velocities. When the annihilation event occurs, the nonzero net momentum of the positron/electron pair modifies the characteristics of the annihilation radiation. The two γ -rays will have their energies altered from 511 KeV and will no longer be emitted in exactly opposite directions.

The technique used in present work is Doppler broadening PAS which measures the deviations from 511 KeV. Such measurements can be used to characterize (and under certain conditions identify) the location of positron "traps" within the crystal lattice. Since positrons can be preferentially attracted to, and become localized

within, open volume, and/or negatively charged defect sites, changes in the relative concentrations of such sites will influence the observed annihilation energy lineshapes.

These Doppler PAS energy distributions are usually interpreted using a characteristic lineshape parameter (S) defined as the sum of the counts in a central region of the peak divided by the total number of counts in the annihilation energy spectrum. In general, for open volume defects like vacancies, grain boundaries, etc., the electron momentum distribution in the defect region will be narrower than in the (nondefective) bulk (i.e., S (defects) S (bulk)). Thus, an increase in S (usually) corresponds to an increase in the defect concentration in the specimen.

While the S -parameter gives an indication of total defect density, it can not be used to determine the types of defects present. To overcome this difficulty the R -parameter was introduced which is concentration independent, but characteristic of the type of trapping site from which the positron is annihilated.

X-ray Diffraction Experiments

The x-ray diffraction strain experiments were performed using a Philips model PW1800 computerized diffractometer.

In order to obtain a completed separation of K alpha 1 and K alpha 2 peaks, a high angle radiation was chosen for these experiments. This is based on the differentiation and rearrangement of Bragg's law into the form:

$$\Delta\theta = (-\Delta d/d) \tan \theta$$

where θ is the nominal Bragg angle, $\Delta\theta$ is the peak shift, and Δd is the change in d-spacing as compared with the unstrained specimen. Since $\tan \theta$ increases with an increase in θ , higher values of θ result in an enhanced separation of the alpha 1 and alpha 2 peaks.

Mean strain values were calculated using the Warren-Averbach method with the (200)/(400) or (111)/(222) pair reflections.

Experimental Results

Oxygen free copper (99.99% with 10ppm oxygen) and commercially pure nickel, obtained from Material Research Corporation, were selected as the materials for the basic investigations. Each as-received material was treated using the procedure listed below in order to minimize the influence of previous processing and to obtain a uniform grain size.

Step 1. Cold work to 80% reduction of area (RA)

Step 2. Heat treatment at $2/3 T_m$ (4 hours in argon)

Step 3. Furnace cool

Step 4. Cold work to desired percentage RA by rolling

A sample size of 10 mm x 10 mm x 2 mm was cut and polished from the previous cold-worked samples.

After the initial PAS experiments the samples were treated in a pulsed magnetic field of 80 oersted for various number of cycles. Throughout this paper we will employ Duratech's definition of a fluxatron cycle. A single fluxatron cycle is actually composed of approximately 315 reversals of magnetic field. The period of each complete reversal is 0.133 s giving a total cycle time of 42 s.

For the purpose of limiting the temperature rise during magnetic treatment, however, any single pulsed magnetic field treatment (PMF) was limited to a maximum of 10 cycles. PAS measurements were performed immediately after each selected number of PMF cycles.

Table I lists the values of the four PAS lineshape parameter, S , R , I_v , and I_c , for the experiments on commercially pure nickel as a function of percent reduction in area (%RA). Figure 9 is a plot of the S and R parameters for these same samples. Typical error bars (± 1 sigma) are shown. The S data exhibit the well known behavior of a gradual approach to a saturation value. As expected, the behavior of I_v is similar to that of S while I_c shows the inverse trend. The R -parameter is constant to within experimental error for all levels of % RA.

The pair of nickel specimens cold worked to 50% RA were subjected to PMF treatment. The changes in the PAS S - and R -parameters for these samples, as a function of number of PMF cycles, are shown in Figure 10. In general, the S -parameter decreases with an increase in the number of PMF cycles. The R -parameter shows a gradual change from ≈ 0.5 to ≈ 0.425 .

In order to investigate the dependence of magnetically induced recovery on the amount of prior deformation, the experiments described above were repeated for a sample with 80% RA. The S -parameters for these samples are shown as case 1 in Figure 11.

A similar set of experiments was performed for OFHC copper. The general trends in the changes in PAS parameters with %RA were

similar to those for Ni. That is, S and I_v increase to a constant value while I_c decreases to an asymptotic value. The changes in the S - and R -parameters for the 80% RA samples, as a function of number of PMF cycles, are shown in Figures 12 and 13. The S -parameter initially decreases, reaches a minimum value after approximately 50 cycles and then increases again. The R -parameter changes abruptly at approximately 40 cycles from a value of ≈ 0.45 to a value of $\approx 0.42-0.43$. This step-like change in R indicates a change in the dominant defect structure occurring between 35 and 45 PMF cycles. Note that the minimum in S occurs at the same number of PMF cycles at which the dominant defect type changes. Also shown in Figure 13 is the change in mean strain, as measured by x-ray diffraction, as a function of the number of PMF cycles. The mean strain decrease from 0 to 10 cycles and then remains essentially constant.

In order to understand the influence of PMF on point defects a pair of OFHC copper samples were heated to 900°C and quenched in water. The R -parameter for these samples, as a function of number of PMF cycles, is shown in Figure 14. Note the sharp drop in R after only a single PMF cycle.

The data shown in Figure ¹²14 strongly indicates magnetically induced defect recovery in samples initially deformed to 80% RA. The decrease in the S -parameter reflects a decrease in the density of positron traps as the number of PMF cycles increases. Most of the recovery occurs during the first 40 cycles. It is interesting to note that during the first few cycles of PMF treatment there is

an increase in the S-parameter. In addition to a gradual decrease in the S-parameter, the R-parameter changes significantly after approximately 15 cycles of PMF. This result reflects a change in the dominant positron trapping state and suggests a change in the relative concentration of defect states. In order to identify the types of defect present one must obtain reference R values from carefully prepared samples with a known dominant defect type. Such experiments are underway.

The data in Figure 14 also shows the results of an experiment designed to establish the effect of PMF on quenched in vacancies in OFHC copper. Note that the R-parameter changes significantly after only a single cycle of PMF indicating a strong interaction between the magnetic field and the as-quenched defect structure.

Stress Relief of Welds of 304 Stainless Steel and 1018 Plain Carbon Steel

A series of butt welds of 304 stainless steel and 1018 plain carbon steel were prepared utilizing one pass to fill a modified "V" crevice. Samples were then cut from the larger welded pieces and areas near, and in, the heat affected zones were subjected to metallography and PAS.

Significant changes in defect concentration "S" in the heat affected zone (HAZ) were noted. Pulsed magnetic field treatment in the HAZ significantly changed the "as welded" "S" parameter as a function of treatment time. Figures 15 and 16 show the marked effect of a 1000 oersted, pulsed magnetic field on the HAZ. Preliminary x-ray stain measurements indicate the "S" parameter

changes may be related to a lowering of the local residual stress in the HAZ as a result of magnetic field treatment.

Conclusions

This study has demonstrated both the viability of magnetically induced defect recovery and the utility of PAS for investigating this phenomenon. The PAS S- and R-lineshape parameters have been used to investigate changes in defect structures as a function of amount of prior cold work and number of pulsed magnetic field cycles. These results have been correlated with x-ray measurements of mean strain and texture.

IV. GENERAL CONCLUSIONS

The extensive literature, in excess of 500 citations (principally in the USSR literature), leads one to the conclusion that the use of magnetic fields, particularly pulsed magnetic fields, can provide unique changes in the structure and properties of metals and alloys. The potential of being able to put energy into material and have it interact with vacancies and dislocations provides the possibility of altering both transformation kinetics and mechanical properties of these materials.

A summary of the effects of high magnetic fields is presented in Table II. This summary points out the unique potential for high magnetic fields. With very high fields the bond energy of most solids can be exceeded. However, working with much lower fields will induce significant interaction with the solid defect structure which can produce beneficial changes in fabrication, failure prevention, stress relief, diffusion promotion or control, fatigue

control, etc., of not only metallic materials, but other solids and liquids as well.

The authors feel that the development of the understanding of the basic function of the interaction magnetic fields with the defect structure of solids will provide useful techniques to deal with a broad range of structure-property problems. Once the basic understanding of these phenomena has developed, a whole new high technology utilizing this information will evolve.

V. ACKNOWLEDGEMENT

The authors wish to acknowledge the Army Research Office for partial support of this program through contract #DAAL03-88-K-0178 as well as Innovex, Inc., Hopkins, Mn. for their technical and financial assistance. The authors are also grateful to Dr. James P. Schaffer, Assistant Professor, and Mr. Y.Y. Su, Graduate Student, School of Materials Engineering, Georgia Institute of Technology, for their work performed related to the PAS and x-ray studies.

VI. REFERENCES

1. A.V. Alekseev, 1937, Mentioned in Russian References but no specific cite given.
2. V.M. Finkel, Physical Foundation of Failure Retardation, Moscow, Metallurgia, 1977 (in Russian).
3. Y.M. Baron, Magnetic-Abrasive and Magnetic Treatment of Parts and Cutting Tools, Moscow, Machinostroenie 1987 (in Russian).

4. B.V. Malygin, (announced for publication in fourth Quarter 1989), Magnetic Strengthening Tools and Machine Parts, Moscow, Machinostroenie (in Russian).
5. M.L. Bernshtain and V.N. Pustovoit, Therman Treatment Steel Parts in Magnetic Field, Moscow, Machinostroenie, 1987 (in Russian).
6. V. N. Pustovoit and A.L. Smolyninov, Effect of Thermal Treatment in Magnetic Field on Mechanical Performance of TCH 3 Steel., Isvestia Vyschich Uchebnych Zavedemy, 1983 #11 (in Russian).
7. B.V. Malygin and Yu Ya Varulenro, Improving of Life of Cutting Tool with the Aid of Magnetization, Izvestia Vyschich Uchebnych Zavedemy, 1984, 57 (A) (in Russian).
8. L.N. Romashev, A.A. Leont'EV, V.M. Schastlivtsev and V.D. Sadovski, The Effect of Pulsed Magnetic Field on the Martensitic Transformation in Low-Carbon Chromium-Nickel Steel, Fizika Metallou, 1984, 57(a) (in Russian).
9. V.N. Pustovoit and V.A. Blinovskij, Heat Treatment of R6M5 Steel in Magnetic Field, Metallovedemic i Termicheskaya Obrabotka Metallov, 1983 (52-54) (in Russian).
10. V.A. Pavlov, I.A. Percturina and N. Peckerkina, The Effect of Constant Magnetic Field on Mechanical Properties of Niobium and Molybdenum, Phys. Stat. Sol (a) 57, 449, 1980.
11. S.N. Vonsovsky, Modern Theory of Magnetizm, Moskow, Gos Techteorizdar 1952.
12. M.S.C. Bose, Phys. Stat. Sol. (a) Vol. 86, pp. 649-654, 1984.

13. J.F. Evans, Private Communication, 1986.
14. B.D. Cullity, et al., Acta Metallurgia, Vol. 13, No. 8, pp. 933-935, 1965.
15. J. Reekie, et al., Nature, Vol. 157, pp. 807-808, 1946.
16. T.S. Hutchison, et al., Nature, Vol. 158, pp. 537-538, 1947.
17. R.F. Hochman, et al., Advanced Materials and Processes, Vol. 134, pp. 36-41, 1988.
18. F. Vicena, Czech. J. Phys., Vol. 5, p. 480, 1954.
19. S. Chikazumi, "Physics of Magnetism," John Wiley and Sons, Inc., New York, 1964.
20. A.E. Berkowitz, et al., "Magnetism and Metallurgy," Vol. 2, Academic Press, New York, 1969.
21. D.E. Scherpereel, et al., Metallurgical Transaction, Vol. 1, pp. 517-524, 1970.
22. B.D. Cullity, "Introduction of Magnetic Materials," Addison-Wesley Publishing Co., Reading, Massachusetts, 1972.
23. P.W. Anderson et al., Phys. Rev. 124, 41, 1961.
24. P.A. Wolff, Phys. Rev. 124, 1030, 1961.
25. V. Jaccarino et al., Phys. Rev. Lett. 15, 258, 1965.
26. J.L. Beeby, Phys. Rev. 141, 781, 1966.

Table I. The Influence of Percent Reduction of Area (%RA) on the PAS Parameters (S, R, I_v , and I_c) for Commercially Pure Nickel.

RA(%)	S	R	I_v	I_c
6	0.474816	0.4998	0.1583	0.1940
11	0.481750	0.4785	0.1611	0.1863
25	0.487051	0.4969	0.1633	0.1839
37	0.495713	0.4887	0.1662	0.1776
50	0.497696	0.5032	0.1674	0.1760
70	0.503207	0.4968	0.1690	0.1724
80	0.505907	0.4727	0.1702	0.1681

Table II. The General Effect of Magnetic Field Strength on the Metals.

<u>Magnetic Field Strength</u>	<u>Phenomenon</u>
400 KOe	Exceeds the yield limit of most metals.
800 KOe	Surface begins to melt.
1.2 MOe	Part of metal melting.
1.5 MOe	Evaporation commences at the surface.
5-10 MOe	Density of magnetic field energy exceeds the bonding energy of most solids. (i.e., they cease to exist as solid bodies.)

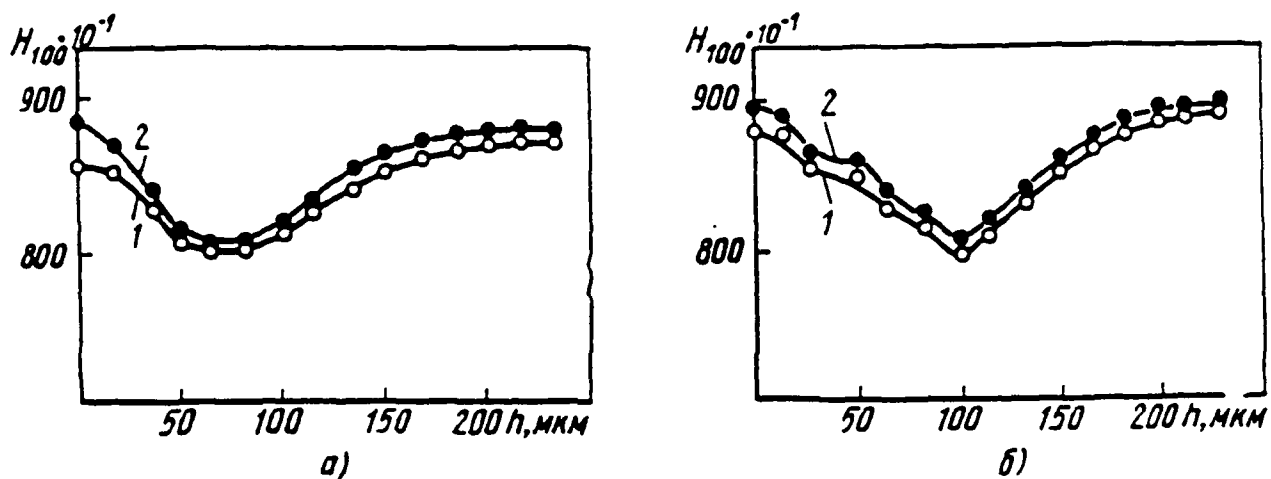


Figure 1. The change of microhardness as a function of depth in steel specimens of R6M5 (a) and R18 (b). 1 - before magnetic treatment and 2 - after magnetic treatment.

From: "Thermal Treatment of Steel Parts in Magnetic Fields," by M.L. Bernshtain and V.N. Pustovoit, Moscow, Machinostroenie, 1987.

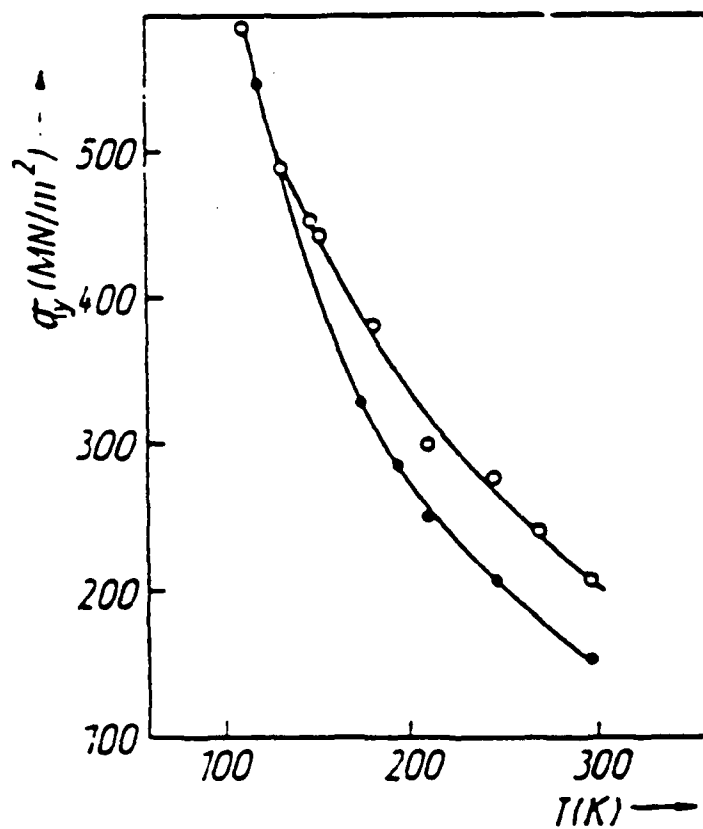


Figure 4.² The temperature dependence of the value σ_y for niobium strained with the 1500 Oe magnetic field on (●) and off (○). Strain rate $7 \times 10^{-3} \text{ S}^{-1}$.

From: Same reference as in Figure 2.

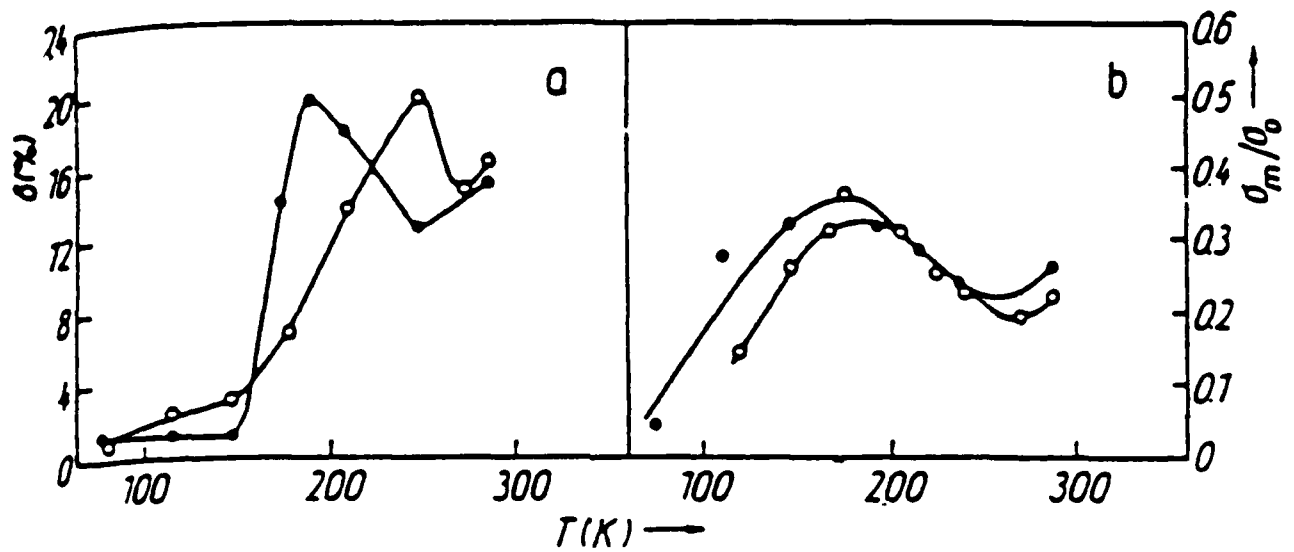


Figure 3. The temperature dependence of: a) the plasticity δ and b) the stress relaxation at a constant strain σ_m/σ_0 for niobium strained with the 1500 Oe magnetic field on (●) and off (○).

From: Same reference as in Figure 2.

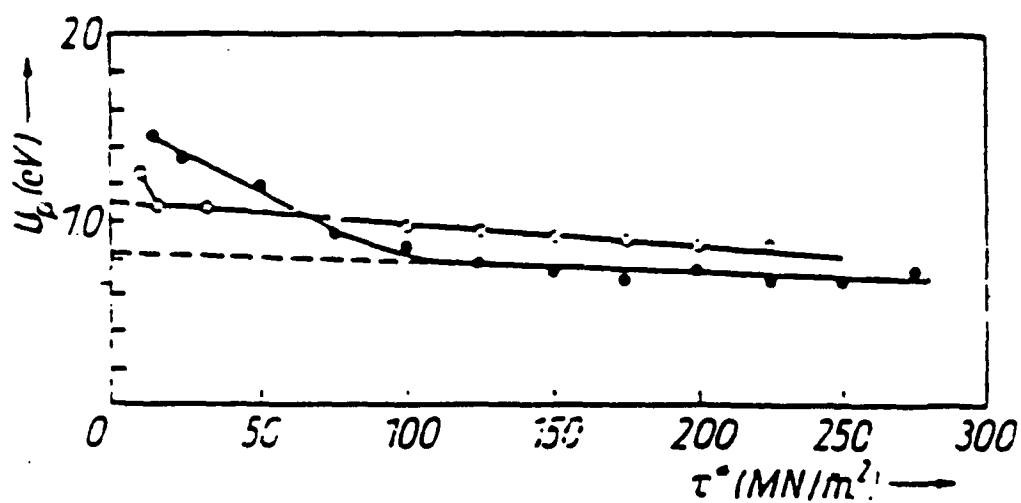


Figure 4. The activation energy vs. stresses in molybdenum under tensile deformation in a 2500 Oe magnetic field on (●) and off (○).

From: "The Effect of Constant Magnetic Field on Mechanical Properties and Dislocation Structure of Niobium and Molybdenum," Phys. Stat. Sol. (a) 57, 449, 1980, by V.A. Pavlov, I.A. Percturina and N.L. Pecherkina.

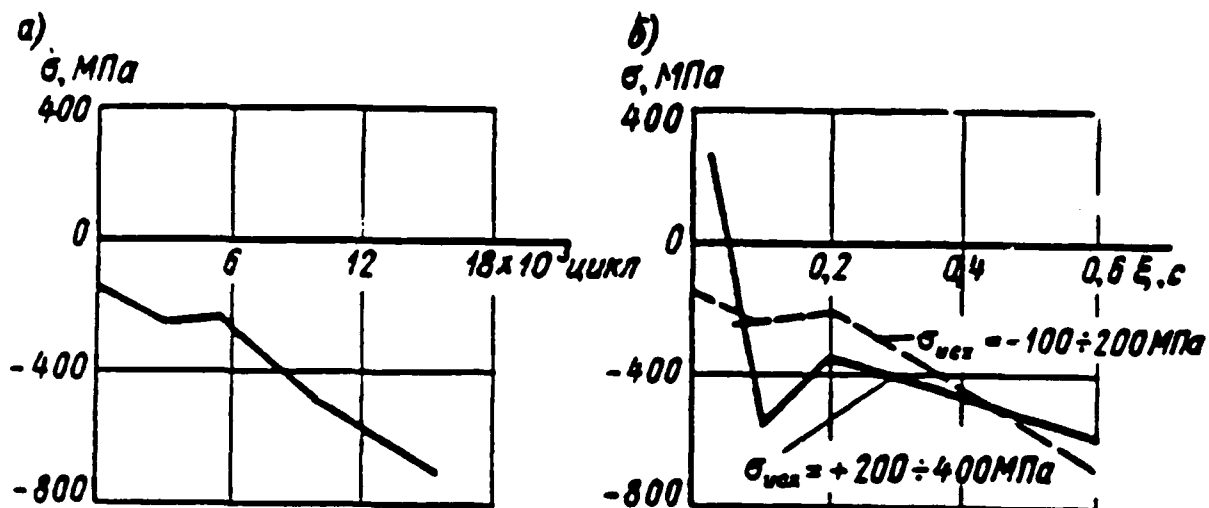


Figure 5. Residual stresses after remagnetization of U10 HRC 65 - 68 steel: a) $B = 1.4\text{T}$, Time = 0.6 seconds, varying number of cycles and b) $B = 1.4\text{T}$, $N = 2500$ cycles, varying time.

From: "Magnetic-Abrasive and Magnetic Treatment of Parts and Cutting Tools," Moscow, Mashinostroenie, 1987, by Y.M. Baron.

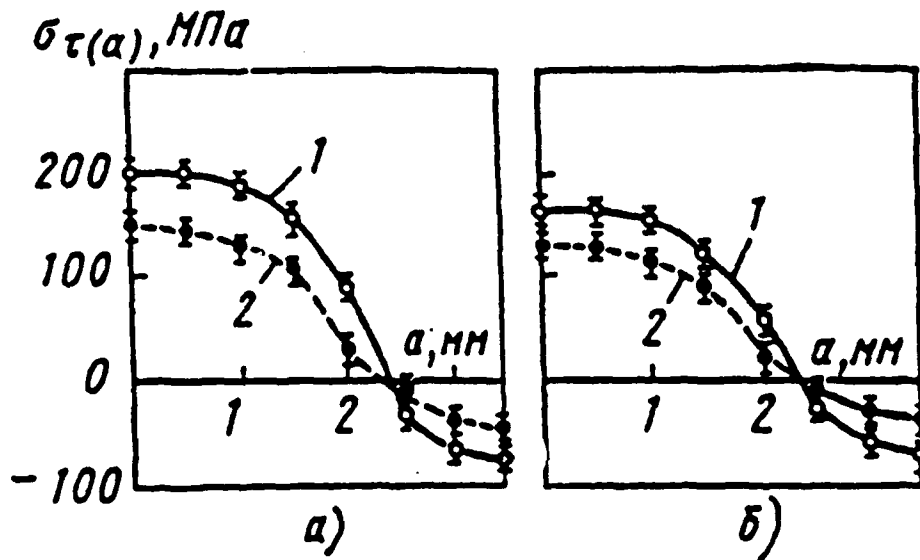


Figure 6. Distribution of stresses across the cross-section after quenching (in nonagitated water) from 1000°C of: a) steel 45 and b) cast ferritic iron. 1 - without field and 2 in magnetic field of 1.4 MA/m.

From: "Thermal Treatment of Steel Parts in Magnetic Fields," Moscow, Mashinostroenie, 1987, by M.L. Bernshtain and V.N. Pustovoit.

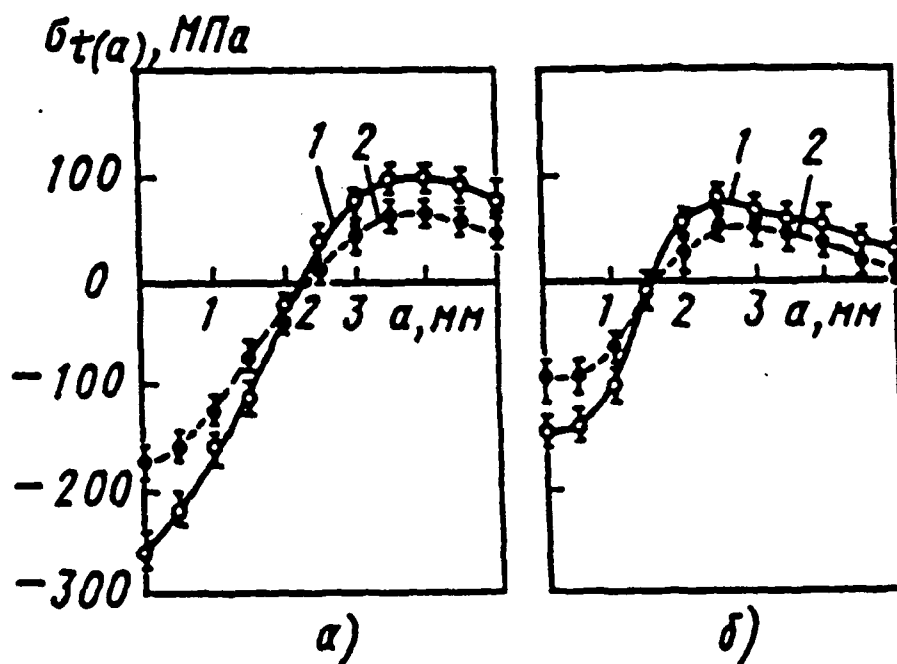


Figure 7. Distribution of stress after quenching from 1000°C (in spray-water cooling, $\delta = 2\text{m/sec}$) of: a) steel 45 and b) cast ferritic iron. 1 - without field and 2 in magnetic field of 768 kA/m.

From: Same reference as in Figure 6.

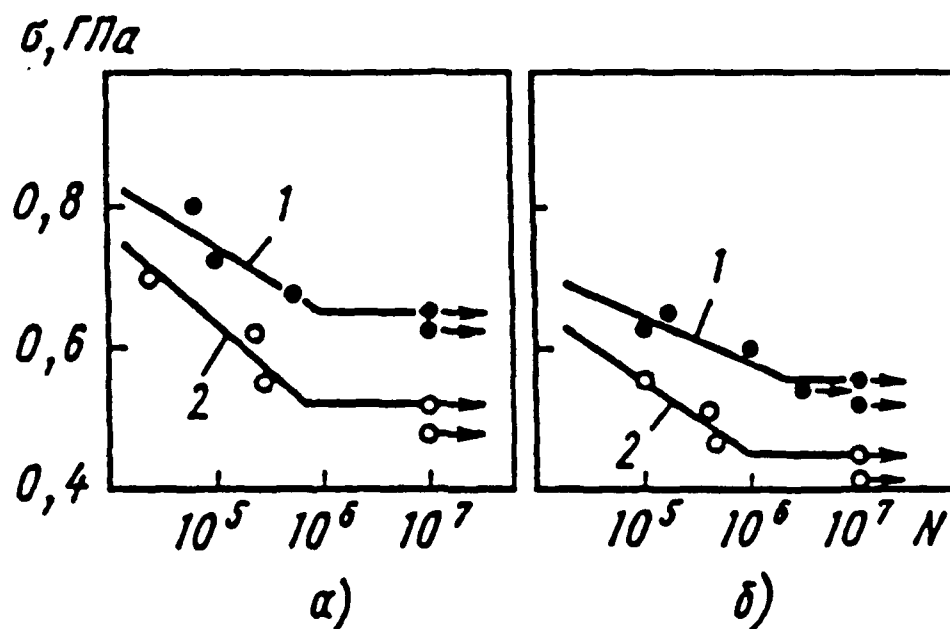


Figure 8. Fatigue curves of steel 45 after quenching from 880°C and annealing at 250°C(a) and steel 14X2GMR after normalization at 940°C and annealing at 660°C. 1 - cooling in a magnetic field of 1.68 MA/m from the temperature of austenization and 2 - cooling without field.

From: Same reference as in Figure 6.

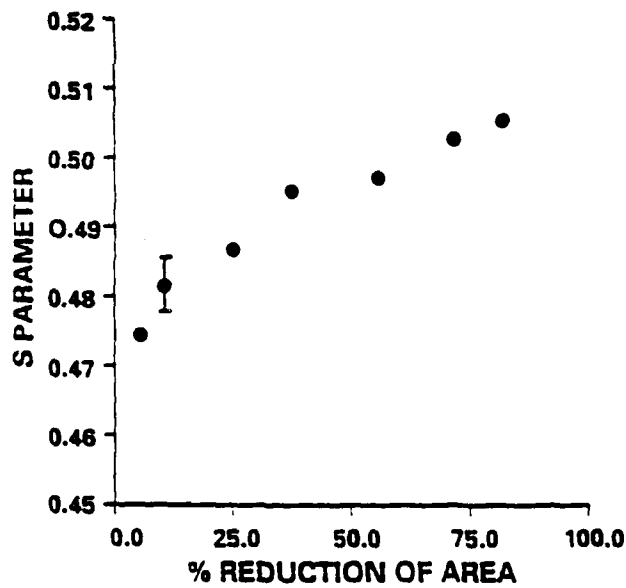
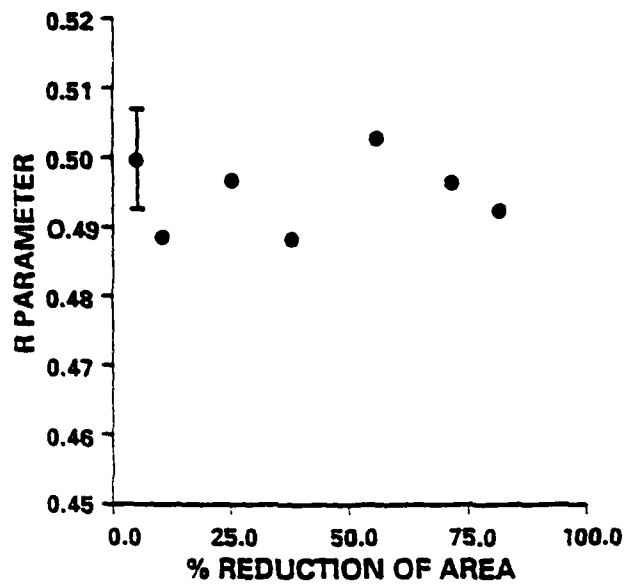


Figure 9. The values of the PAS S- and R-parameters as a function of % RA for a series of cold worked nickel specimens. Typical error bars are shown.

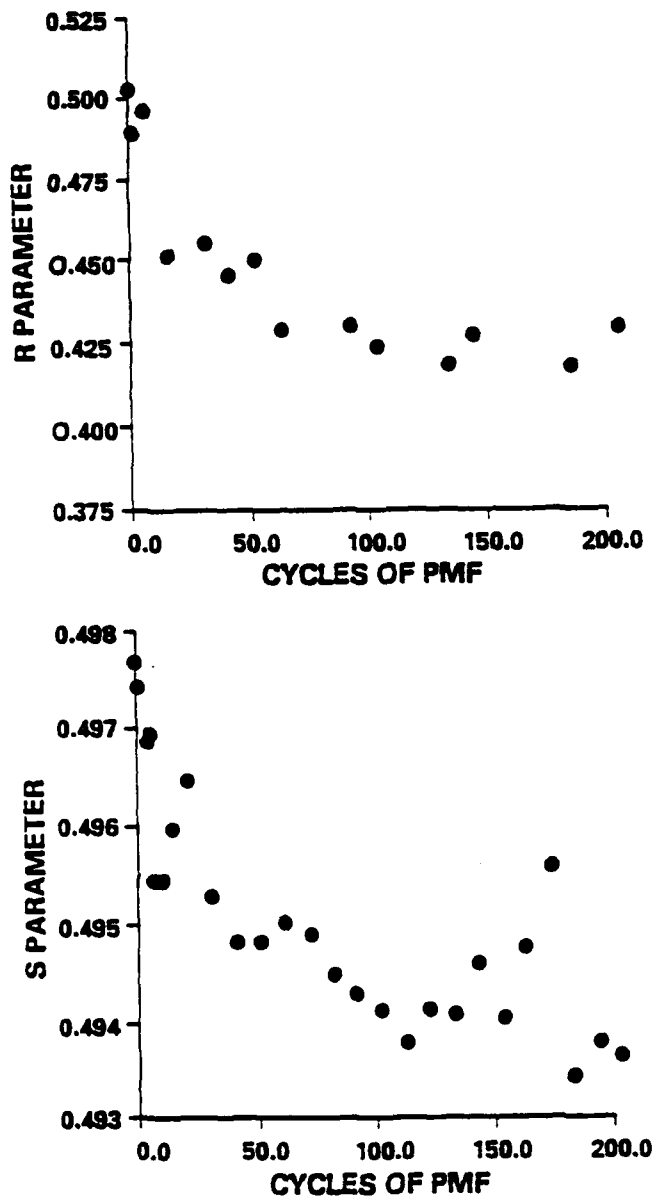


Figure 10. The changes in the PAS S- and R-parameters for the 50% RA nickel samples as a function of number of PMF cycles.

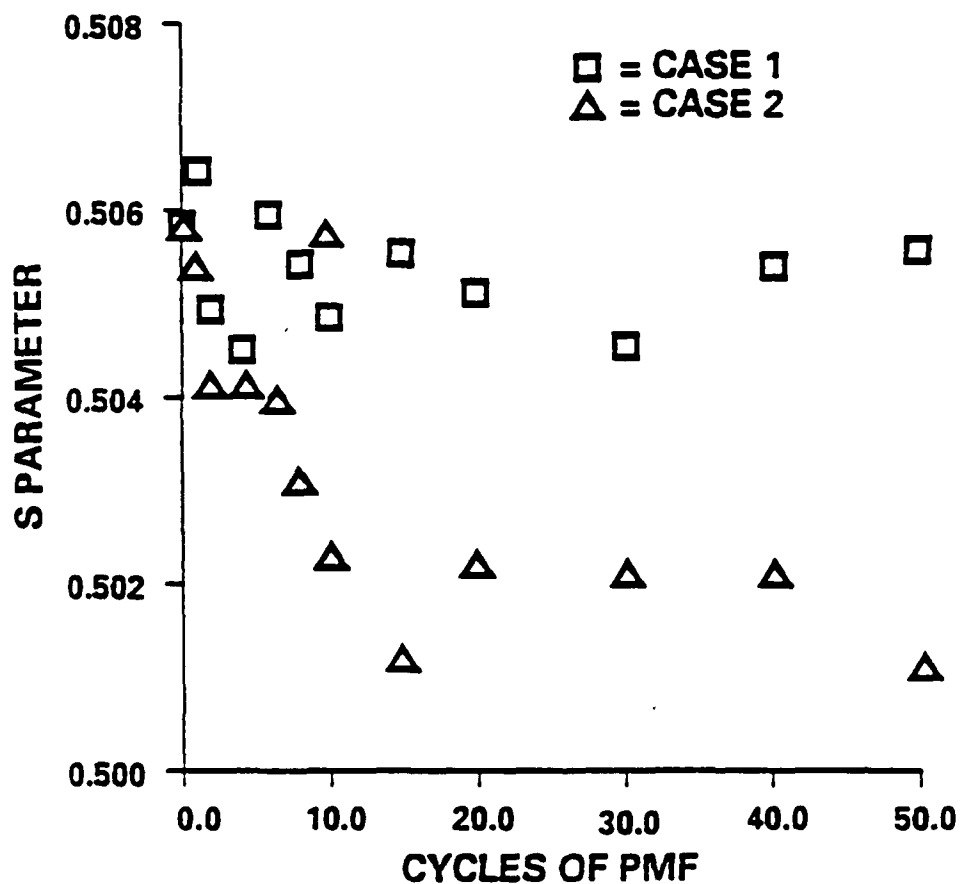


Figure 11. The changes in the PAS S- and R-parameters for two sets of 80% RA nickel samples as a function of number of PMF cycles. The primary difference between the two pairs of samples was found to be their texture.

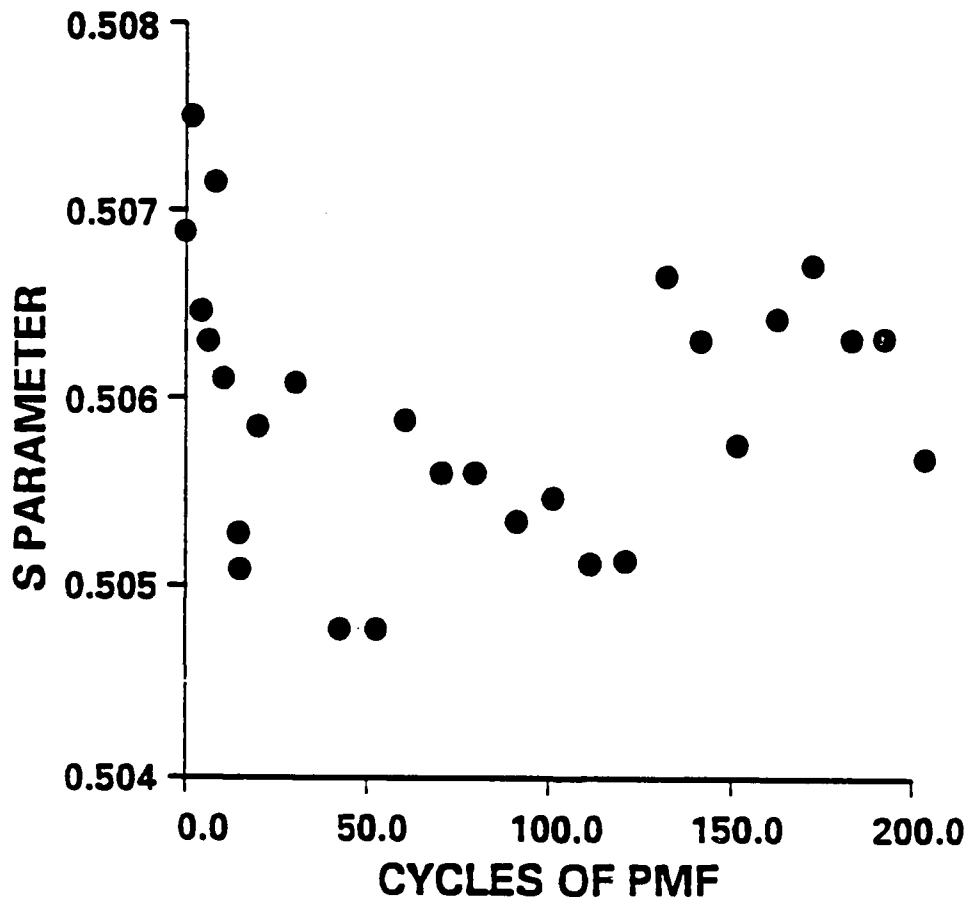


Figure 12. The change in S-parameter for 80% RA OFHC copper samples as a function of PMF cycles.

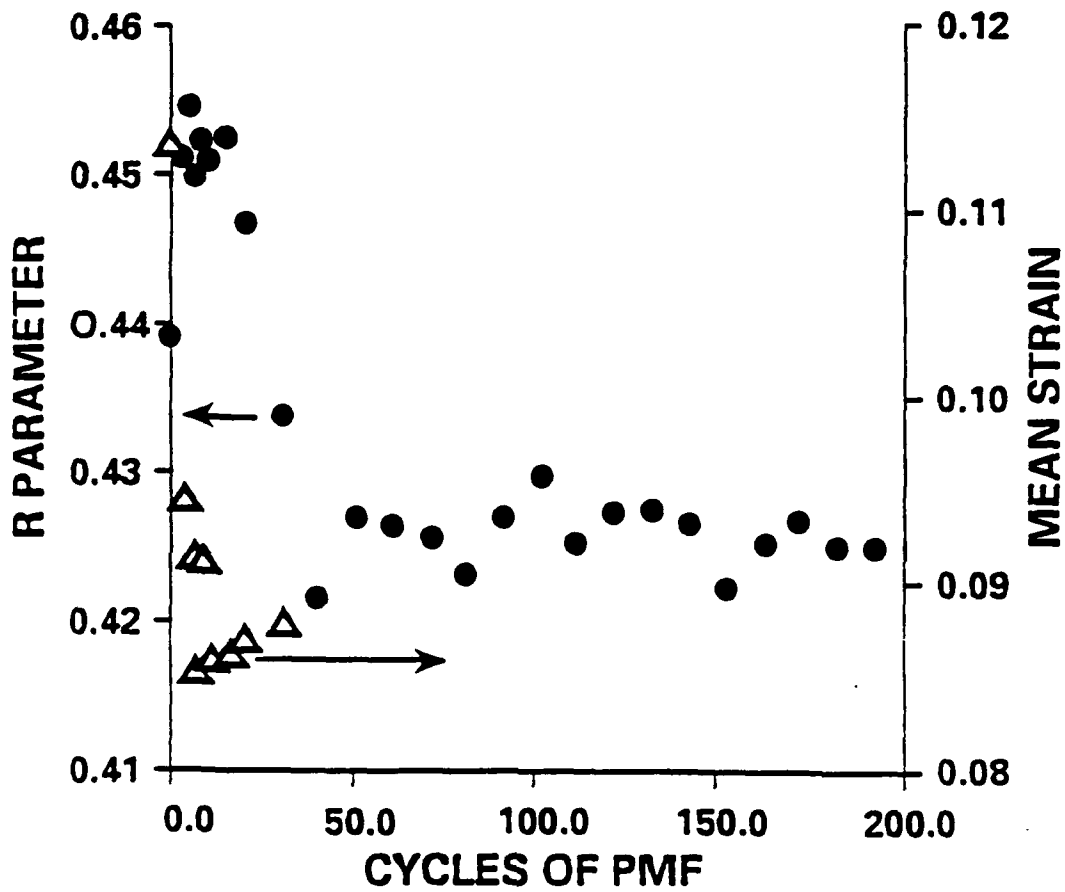


Figure 13. The changes in the mean strain as measured by x-rays and the R-parameter from the 80% RA OFHC copper samples as a function of number of PMF cycles.

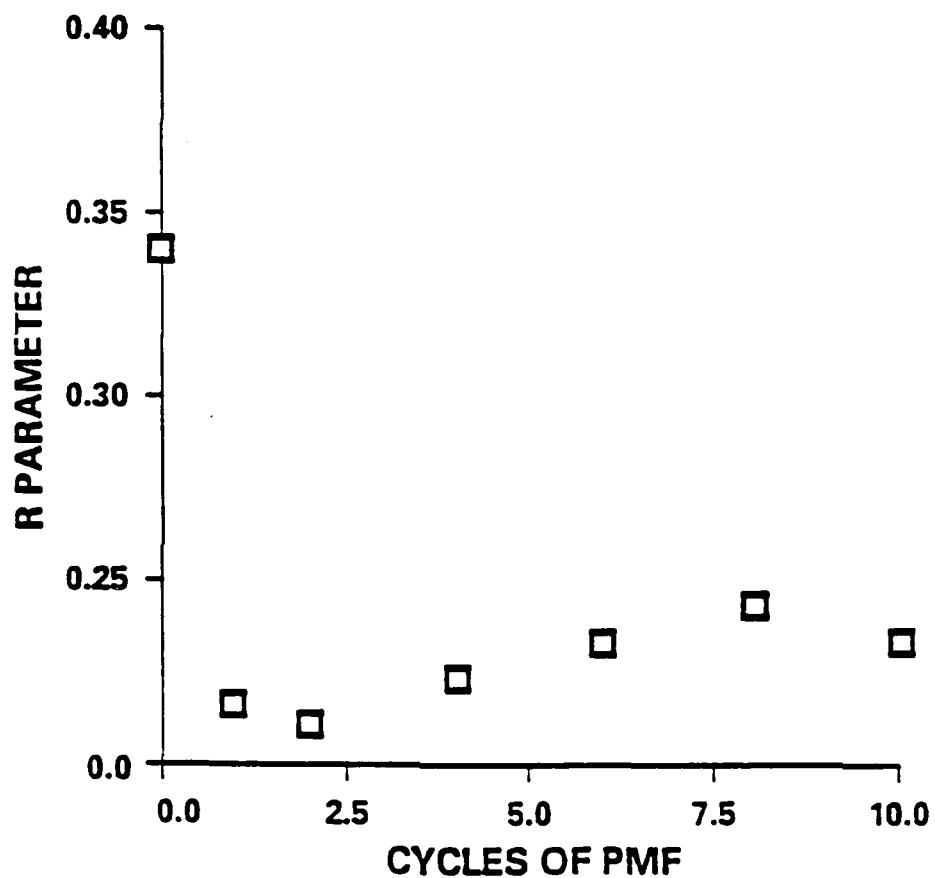


Figure 14. The R-parameter, as a function of number of PMF cycles, from an OFHC copper sample originally water quenched from 900C.

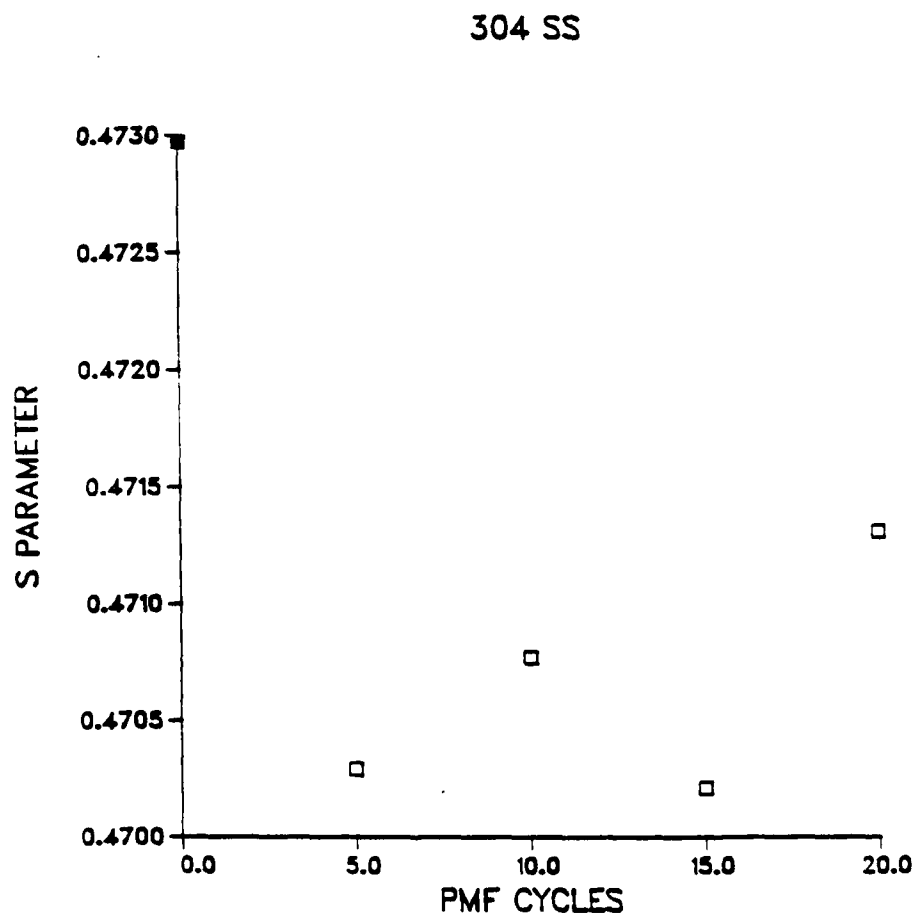


Figure 15. The change in S-parameter (defect concentration) in the heat affected zone (HAZ) of welded 304 stainless steel.

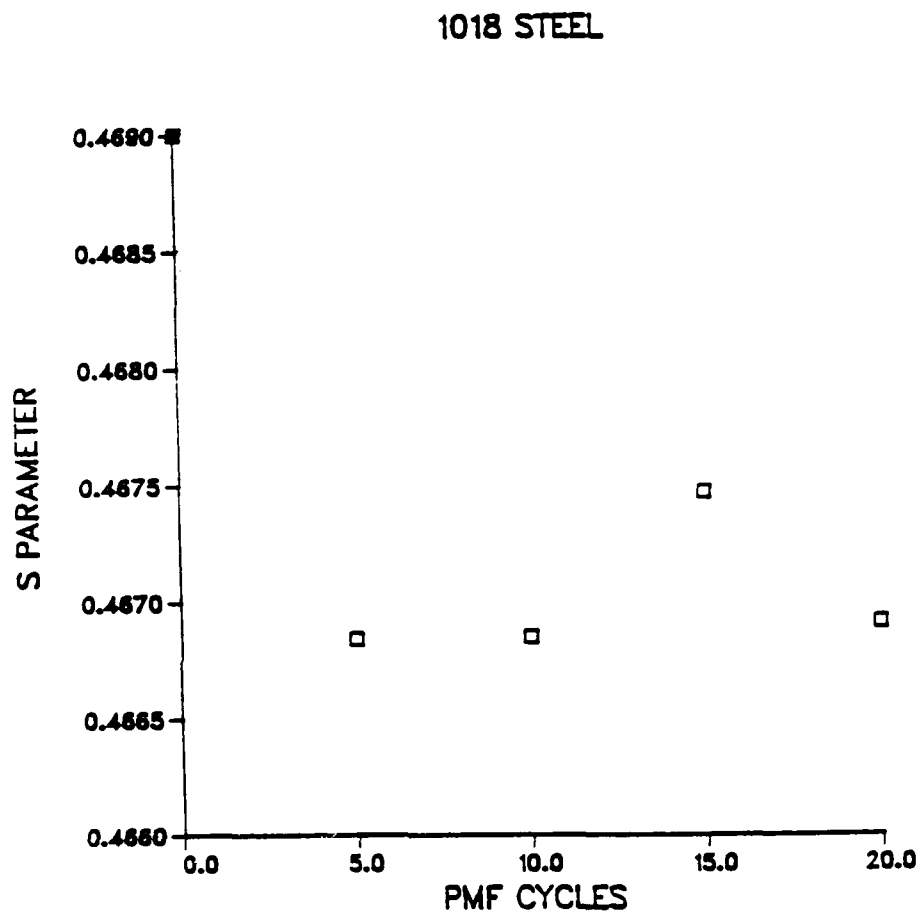


Figure 16. The change in S-parameter (defect concentration) in the heat affected zone (HAZ) of welded 1018 plain carbon steel.

APPLICATION OF ELECTROPLASTICITY IN METAL WORKING-REVIEW OF SOVIET WORK

A. F. Sprecher and H. Conrad
Department of Materials Science and Engineering
North Carolina State University
Raleigh, NC

ABSTRACT

A review of the soviet work employing the electroplastic effect (EPE) to metal working operations is presented. It includes the application of current to wire drawing and to the room temperature rolling of thin sheets of W, Cu, stainless steel, and iron-cobalt alloys. D.C. current densities of $\sim 10^5$ A/cm² were applied continuously or in the form of pulses ~ 10 – 100 μ s in duration with a repetition frequency ranging from 10^2 – 10^4 Hz. Applying high density electric current to the deformation zone of a metal during a working operation generally improved the effectiveness of the process. Reduced forming loads, changes in texture, changes in relative amounts of phases present, and improved subsequent mechanical properties resulted. The vectorial nature of the EP effect was clearly shown in wire drawing experiments. By employing the EPE in rolling operations, a high quality product resulted that was unattainable under conventional conditions.

APPLICATION OF ELECTROPLASTICITY IN METAL WORKING-REVIEW OF SOVIET WORK

A. F. Sprecher and H. Conrad
Materials Science and Engineering Department
North Carolina State University
Raleigh, NC 27695-7907

1. INTRODUCTION

About ten years after the discovery by Troitskii and Likhtman (1) that moving electrons in a metal can enhance its plasticity, work was reported using the electroplastic effect (EPE) in wire drawing and rolling operations (2,3). The EPE was believed to result from an electron push on the dislocations during plastic flow. It was reasoned therefore that it should either improve the metal working process or the quality of the subsequent product. By applying high density electric current (10^4 to 10^6 A/cm²) continuously, or in the form of short pulses (10 to 100 μ s), both of these benefits are realized. This paper presents a review of the Soviet work utilizing the EPE in wire drawing as well as rolling operations.

2. EXPERIMENTAL

2.1 Wire Drawing

The experimental arrangement for applying electric current during the wire drawing experiments is presented in Fig. 1. Copper (Cu), stainless steel (SS), and tungsten (W) wires with original diameters of 50 to 100 μ m were generally used. However, one set of experiments (4) used wire with a somewhat larger diameter of 150 to 300 μ m. Small diameters were employed to more easily provide a uniform, high density current in which heating effects could be minimized. Current was

supplied by sliding or rolling contacts and a triethylamine/oleic acid cooling emulsion was provided to remove some of the Joule heat.

The diamond draw dies ($2\alpha = 16^\circ$) employed provided electrical ground isolation. The effects of drawing speed ranging from 5 to 300 m/min were often studied. In addition, deformation amounts (reduction in area) per pass from 4 to 20% were investigated. The various current conditions employed are summarized as follows:

Current density	$J = 10^4$ to 3×10^5 A/cm ²
Pulse duration	$t_p = 3$ to 100 μ s
Pulse frequency	$\nu_p = 100$ to $30,000$ Hz
On-Off ratio (duty cycle)	$Q = 2$ to 20

Continuous and pulsed DC; also AC (to simulate heating)

The vectorial nature of the EPE could be observed by simply reversing the current polarity relative to the drawing direction, thereby changing the direction of the electron force.

2.2 Rolling

The rolling experiments (12,13) employed DC (rectified 60 cycle AC) continuous current, which was supplied through the rollers of the flattening mill (Figs. 2 and 3). This scheme provided current perpendicular to the rolling direction with densities of 10^4 to 10^6 A/cm². Wires of tungsten (W), W-27% Re, and iron-cobalt ($D_0 \approx 0.1$ to 0.5 mm) were thus flattened into micron thick ribbons. Sample cooling was provided by compressed air.

3. RESULTS AND DISCUSSION

3.1 Wire Drawing

Upon application of current to the drawing process, a drop in the drawing force occurred. This drop is illustrated in Fig. 4 (a,b) for the drawing of Cu wire

and is a consequence of the combined effects of the current, that is, Joule heating, pinch, and EPE. The vectorial nature of the EPE can be seen in Fig. 4, when the current is reversed, i.e. changing from the case of negative downstream of the die and positive upstream to just the opposite connections. In the latter case, Joule heating and pinch effects reduce the drawing force, while the EPE tends to increase it. Also to be noted by comparing Figs. 4a and 4b is that pulsed DC current has a greater effect than the continuous current. One explanation for this observation is that it resulted from the ultrasonic vibrations induced by the pinch effect (5). The load reduction was found to saturate at about 20 kHz, the point where the deformation zone (material in the die) receives at least one current pulse.

The effects of current density, pulse width and Q^{-1} (on-off ratio) on the relative reduction in drawing force is presented in Fig. 5. These parameters are linear with current density and consequently support the interpretation of an electron push mechanism. The linear behavior with pulse width and Q^{-1} reflect the total power input to the deformation zone. It was also observed that the effect was reduced as the drawing speed increased. At about 60 m/min and greater, the load reduction reaches its lowest value. It was suggested (6) that this speed approximately coincides with the electron drift velocity, so that the net push on the dislocation is at a minimum.

In addition to reducing the drawing force during the actual process, changes in the deformation texture have been noted (7,8) and an improvement in subsequent properties (4,9,10). In stainless steel (SS), electrical resistivity was reduced and the percentage of α -phase formed in the operation was lowered, while the aging process (precipitation of finely dispersed phases of carbides and intermetallics) was accelerated. All of these phenomena influenced the magnetic

properties. Fig. 6 shows how the magnetic energy, $H_c \times B_r$, (where H_c is the coercive force and B_r is the remnant induction) is enhanced by the electric current (9). This was attributed to the additional formation of domain structure due to the presence of more γ -phase and by increasing the aging process.

Subsequent mechanical properties were also improved (4-6). The yield strength of Cu increased 5 to 8%, while the ductility increased by 6 to 10% (5). In SS the ultimate tensile strength (UTS) was reduced when current was used, although the ductility was still improved.

3.2 Rolling

Good quality W, W-Re and Fe-Co ribbon material was produced by employing high density electric current (3, 12-16). Application of electric current simplified the rolling process, since these materials normally require high temperature, vacuum rolling conditions. In addition, products with superior mechanical properties resulted. Klimov et al (3) rolled 0.1 mm W and W-Re wire over 90% (reduction in area) using current densities of $\sim 10^5$ to 10^6 A/cm². The product was free of surface or edge cracks and its UTS increased from about 530 to 610 kg/mm². It was estimated that the temperature of the deformation zone was in the range of 200 to 300°C.

Troitskii and co-workers (8,13) had similar results with W. By utilizing current in the rolling operation, 0.4 mm diameter wire was flattened to 0.1 x 0.15 mm ribbon with good tensile strength and ductility. When it was rolled without current, the material laminated and fractured.

Another hard to roll material (Fe-Co alloys) was also found to benefit from the concurrent use of electric current. Klimov (15) produced micron thick ribbons from a 2 mm diameter rod of Fe-Co-2%V alloy without the intermittent annealing or quenching that is normally required. Fig. 7 illustrates the quality of the

product obtained. The upper ribbon was produced without the aid of electric current, while the lower ribbon utilized current in the process. As can be seen, the current eliminates the edge cracking. An estimate of the temperature in the deformation zone was 300 to 350°C. Effects on the dislocation structure were observed. Specimens rolled without current contained high dislocation densities without signs of a pronounced cellular structure. With current, the samples had much lower dislocation densities. This was believed to result from easier transverse slip.

Klimov put forth a model for the electron push associated with the EPE effect (14). He based it on a classical approach of an electron gas in a metal. The vectorial nature of the effect was shown in that the force on the dislocation was proportional to the difference between the dislocation velocity and the drift electron velocity. This vectorial behavior, as well as the linear dependence of the force on current density, has been suggested by others as well (17,18) and seems to be supported in the wire drawing experiments. However, some years later Klimov (16) put forth another theory of the EPE based on an internal temperature and vacancy concentration gradient model. These effects depend on the current density squared and are therefore nonvectorial. Given that some Joule heating is inevitable in these metal working experiments, it is difficult to separate out the J^2 effects that may be associated with the EPE from that due to the heating.

4. CONCLUSIONS

It has been demonstrated by the Soviets that a drawing or rolling operation is in general improved by the simultaneous application of high density electric current to the deformation zone of a material. Drawing forces were reduced, and brittle materials were rolled without high temperature or vacuum systems. In addition to the operational improvements, the materials' subsequent properties

were generally better than those obtained using the normal procedures. The YS UTS and ductility were improved, magnetic properties enhanced, and a redistribution of the drawing texture observed. Also, phase transformations were affected.

5. REFERENCES

1. O. A. Troitskii and V. I. Likhtman, *Dolk. Akad. Nauk SSSR* **148** (2) (1963) 332.
2. V. I. Spitsyn, O. A. Troitskii, V. K. Gusev and V. K. Kurdyukove, *Izv. Akad. Nauk SSSR, Ser. Metally*, No. 2 (1974) 123.
3. K. M. Klimov, G. D. Shnyvev, I. I. Novikov and A. V. Isayev, *Izv. Akad. Nauk SSSR Met.* **4** (1975) 143.
4. O. A. Troitskii, V. I. Spitsyn and V. G. Ryzhkov, *Dolk. Akad. Nauk SSSR* **243** (1976) 330.
5. V. I. Spitsyn, O. A. Troitskii, V. G. Ryzhkov and A. S. Kozyrev, *Dolk. Akad. Nauk SSSR* **2** (1976) 402.
6. O. A. Troitskii, V. I. Spitsyn, N. V. Sokolov and V. G. Ryzhkov, *Phy. Stat. Sol.* **52** (1979) 65.
7. O. A. Troitskii, V. I. Spitsyn, et al *Phys. Met. Metall.* **50** No. 1 (1980) 132.
8. O. A. Troitskii, *Mat. Sci. Eng.* **75** (1985) 37.
9. O. A. Troitskii, V. I. Spitsyn, N. V. Sokolov and V. G. Ryzhov, *Dolk. Akad. Nauk SSSR* **237** (1977) 1082.
10. O. A. Troitskii, V. I. Spitsyn, N. V. Sokolov, V. G. Ryzhov and Yu. S. Dubov, *Russ. Metall.* **2** (1979) 92.
11. V. I. Spitsyn, O. A. Troitskii, et al *Russ Metall.* **4** (1978) 88.
12. K. M. Klimov, G. D. Shnyvev and I. I. Novikov, *Dolk. Akad. Nauk SSSR* **219** (1974) 323.
13. V. I. Spitsyn, A. V. Kop'ev, V. G. Ryzhkov, N. V. Sokolov and O. A. Troitskii, *Dolk. Akad. Nauk SSSR* **236** (1977) 861.
14. V. D. Mutovin, K. M. Klimov, et al *Russ. Metall.* **4** (1978) 91.

15. K. M. Klimov, A. M. Mordukhovich, A. M. Glezer and B. K. Molotilov, Russ. Metall. **6** (1981) 68.
16. K. M. Klimov and I. I. Novikov, Dolk. Akad. Nauk SSSR **253** (1980) 603.
17. V. Ya. Kravchenko, Zh. Eksp. Teor. Fiz. **51** (1966) 1676.
18. H. Conrad, A. F. Sprecher, "The Electroplastic Effect in Metals", Chapt. 43 in **Dislocations in Solids**, F. R. N. Nabarro ed., Elsevier Science Publishers (1989) pp. 497.

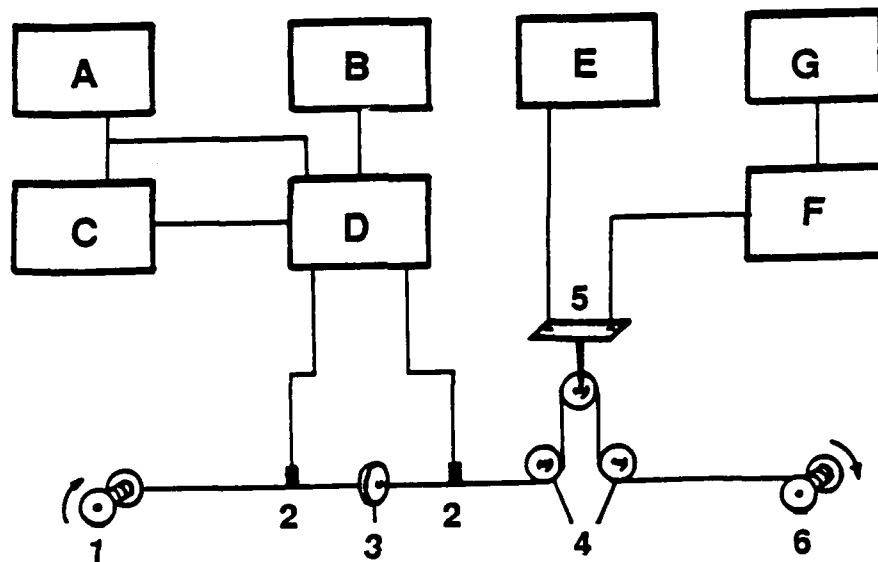


FIG. 1. Block diagram of the set-up for investigating the electroplastic drawing of metal. A-pulse amplifier power supply; B- pulse generator; C- oscillograph; D- pulse amplifier; E- strain gauge bridge power supply; F- direct current amplifier; G- recorder; 1-unwinder; 2-contacts; 3-diamond die; 4-guide rollers; 5-small beam with strain gauge bridge; 6-receiving reel. From [6]

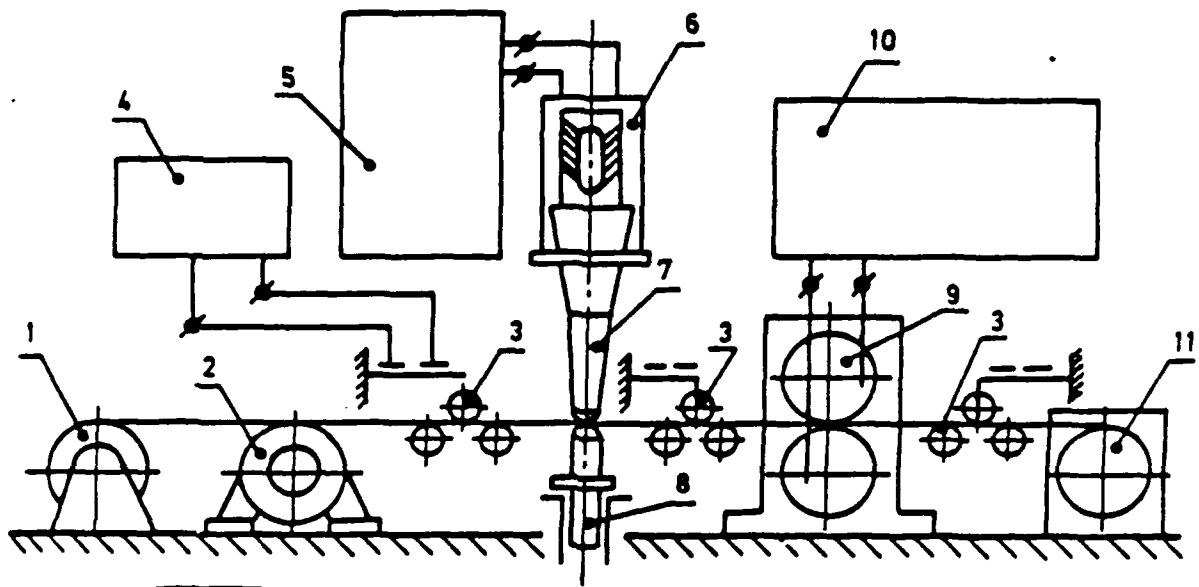


FIG. 2. Experimental strip flattening mill. 1) uncoiler; 2) dc motor; 3) tension transducer; 4) tensometer station; 5) ultrasonic generator; 6) transducer; 7) condenser; 8) reflector; 9) two-high rolling mill; 10) source of electric current; 11) cooling and packing unit. From [13]

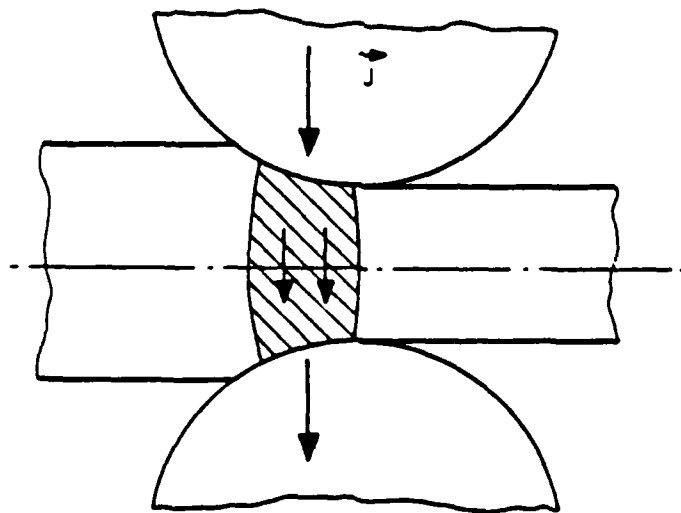


FIG. 3. Schematic diagram of electric current placement through the deformation zone in electroplastic rolling. From [12]

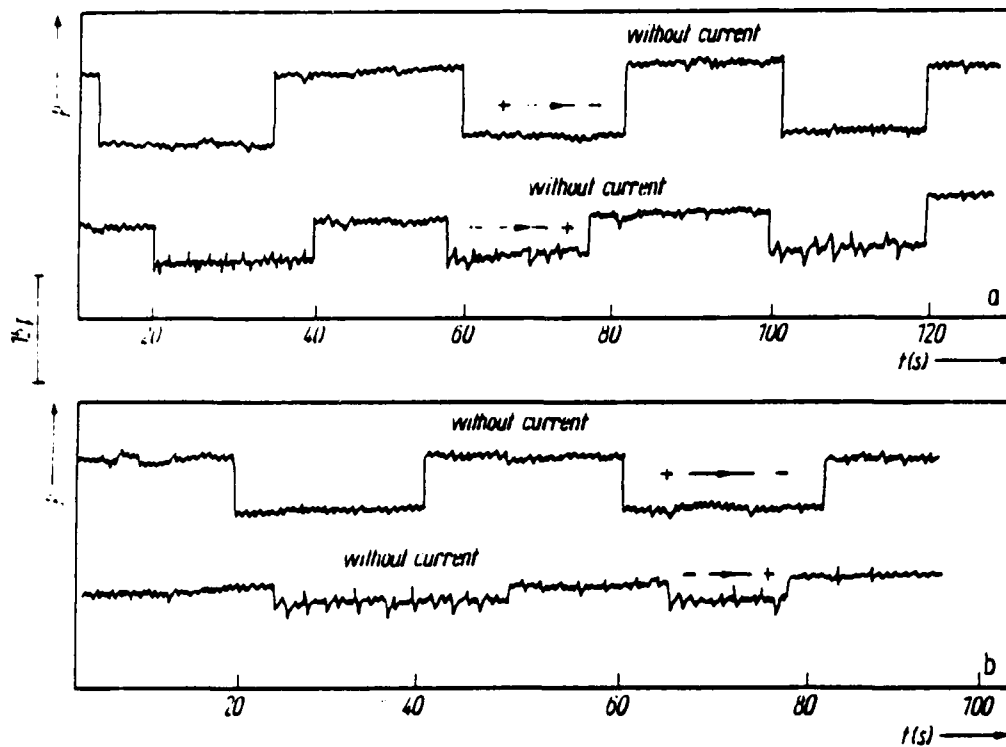


FIG. 4. Typical diagrams of the drawing force reduction of copper wire 60 μm in diameter with and without the application of an electric current to the deformation zone: mean effective current density $J_{\text{mean, eff}} = 3.5 \times 10^5 \text{ A/cm}^2$; wire movement rate = 0.45 m/s; reduction ratio = 16.1%: (a) pulsed current with a frequency of 10kHz and a pulse duration of 60 μs : (b) direct current with fluctuation not exceeding 10%. From [6]

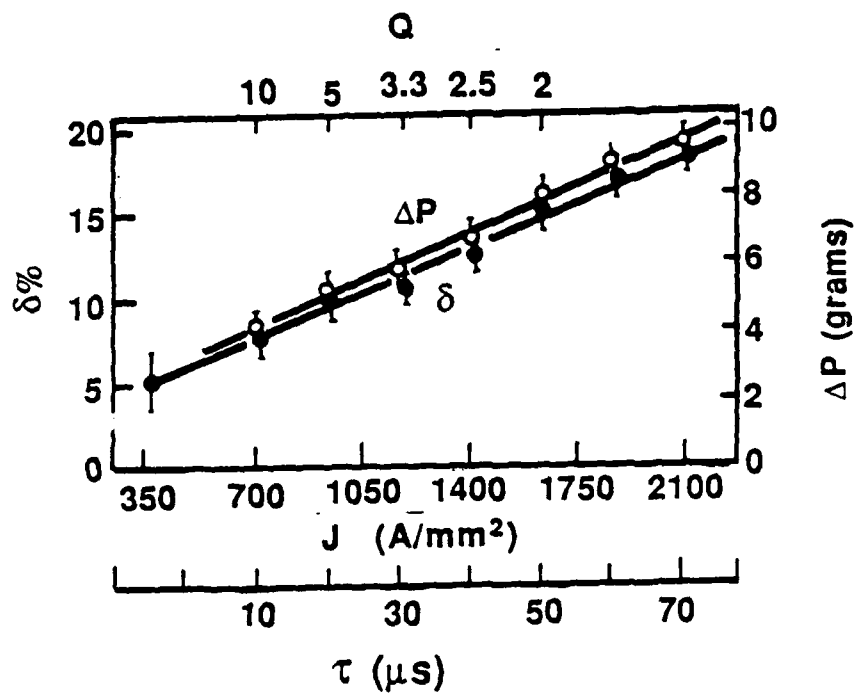


FIG. 5. Dependence of the absolute load drop, ΔP , and the relative load drop, $\delta = (\Delta P/P)100\%$ versus current density (J), pulse duration (τ), and on-off ratio (Q). From [6]

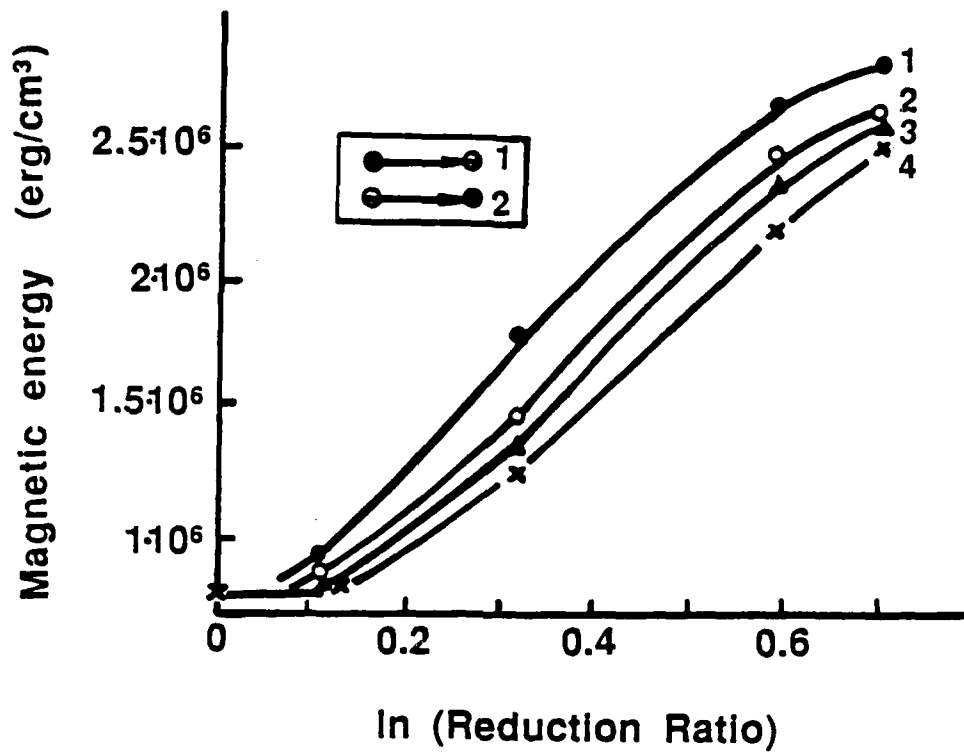


FIG. 6. Magnetic energy as a function of the total deformation of wire after drawing. 1,2) electroplastic drawing with direct current; 3) electroplastic drawing with alternating current; 4) ordinary drawing. From [9]

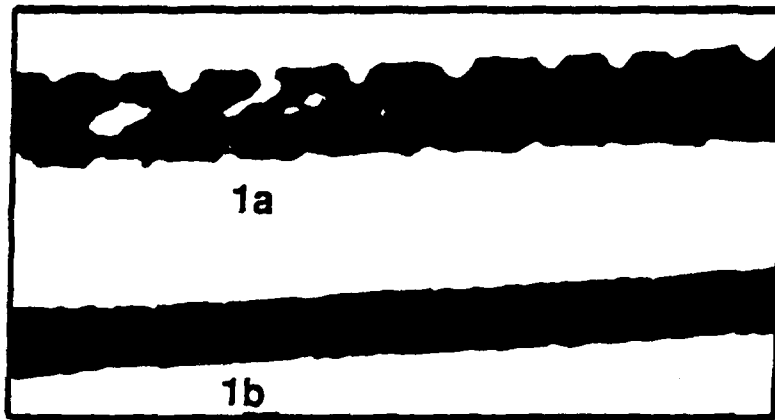


FIG. 7. Flats (ribbons) produced from Alloy 49k (Iron-Cobalt) : a) without passing electric current; b) with passing electric current. From [15]

"Electric Current Effects in the Sintering of Powder Materials- Electro-Discharge Compaction"

Kenji Okazaki

Department of Materials Science and Engineering
University of Kentucky, Lexington, Kentucky 40506-0046

This paper describes an unconventional P/M processing, "electro-discharge compaction" (EDC) for consolidation of rapidly solidified powder materials. EDC applies a high voltage, high density current pulse (for example, up to 30 kV, 10 kA/mm² for 150 - 300 μ s) to powders under pressure.

The conventional P/M processings are to compact powder materials first by vacuum-hot-press or Hipping and then to mechanically densify to 100% by extrusion, forging or rolling at elevated temperatures. All of these processes involve extended heating of powder materials; the larger the mass is, the longer time is required to achieve a homogeneous temperature. In case of rapid solidified or mechanically alloyed powders, this inevitably leads to degradation of unique features associated with RSP or MA. They are undesirable precipitation of solute atoms which are otherwise in solution, excessive ripening of originally fine precipitates and even grain growth, all of these occur due to the extended exposure to heat. Another problem inherently associated with P/M of RSP or MA Al alloy powders is the existence and persistence of oxide films on the prior particle boundaries even after severe hot-working of the preform, the remaining oxide film on the particles' interface becoming the sites for crack initiation upon applying stresses to result in poor mechanical properties.

The advantages of this EDC under the applied pressure in microseconds are the capability of removing oxide films on the powder surface to greatly enhance the bonding of powder particles together, the preservation of the unique microstructure characteristic of RSP, the densification and the ability to compact reactive materials even in an ambient atmosphere.

Background of EDC

A review of EDC may be found elsewhere [1]. Briefly, Taylor [2] made the first attempt to compact cemented carbide by applying an electric current in 1933. Cremer [3] showed in 1944 that nonferrous powders of Cu, brass, bronze and Al could be compacted. Cremer also indicated that the variables were current density of 62 kA/cm², sintering times of 1 to 2 cycles of a 60 cycles current and pressure of 69 to 138 MPa. Lenel [4] in 1955 attempted the compaction of metal powders by passing a low voltage (10 - 40 V), high current (15 - 25 kA) through powders and simultaneous sintering under pressure. The significant differences between this discharge compaction process and the conventional hot-pressing are as follows: The sintering times are very short (of the order of a few seconds). The powder and die are initially cold. Heat is generated within the powder. The pressure for the discharge sintering is high. And the subsequent cooling after the sintering is quite fast and amounts to self-quenching.

On the contrary, Saito et al [5] used a high voltage discharge using a capacitor as the source of energy. They named it "flush electric discharge sintering". Aluminum powders of about 15 μm size were pressed with an isostatic pressure of 59 MPa and electric energy from a 60 μF capacitor charged up to 15 kV was dumped across the powder specimen. They claim that the sintered density by discharge of 3 kJ under a pressure of 59 MPa, followed by sintering at 803 K for 3.6 ks in vacuum, is increased by 12% compared to that without a discharge. A very low resistance of the resultant compact was interpreted that the oxide film had almost completely been disrupted. They were the first to observe that EDC results in the densification and removal of the oxide film.

Al-Hassani and coworkers [6,7] carried out EDC of metal powders by discharging a bank of 15 capacitors of 5.32 μF each, which stored a maximum energy of 16 kJ at a charging voltage of 20 kV. Their primary concern was however to obtain the P/M bar of a density high enough to withstand subsequent mechanical fabrication such as rotary swaging. The highest density obtained for iron powders is about 60%. They [7], from the voltage and current curves versus discharge time, postulated that EDC occurs in three stages, while the present author [1] conducted the EDC experiments for deliberately oxidized nickel powders to conclude that the EDC process is actually composed of the four stages, instead; stage I, electronic breakdown of oxide films and heat accumulation at the metal-oxide interface; stage II, explosive breakdown of oxide film owing to sublimation of the metal layer beneath the oxide film; stage III, neck formation; stage IV, neck growth and dissipation of energy through the conductive mass.

Characterization of EDC compacts

The most important features of EDC are the removal of oxide films on prior particle surface, preservation of RSP microstructure, densification and improved mechanical properties. First, Davis and Al-Hassani [7] speculated the oxide film removal is due to high heat generation at the contact of particles that separates the metal and oxide film due to their different thermal expansion coefficients. Secondly, they considered that the densification occurs due to the electro-magnetic forces produced by a sudden flow of a high voltage, high density current for a very short time that deforms powder particles (so-called pinch effect). If the oxide disruption occurs by the mechanism they proposed, the pieces of disrupted oxide film or oxide particles will remain at the interface between welded particles. In order to verify this oxide disruption, the present author [1] carried out the EDC experiments with deliberately oxidized nickel powders (0.3 μm thick oxide film on 150 μm nickel particles). The detailed examinations by TEM of the particle interface after EDC provided a conclusive evidence that nickel oxide films have been explosively disrupted and dispersed as oxygen atoms into the nickel matrix without leaving any oxide particles of detectable sizes within the interface by a sudden and enormous increase in heat at the contact point of particles which transforms the substrate nickel from solid into gaseous nickel.

The present author [8] specifically focused the aforementioned first two features of EDC, i.e. the removal of oxide films and the preservation of RSP microstructure of an RSP Al alloy (melt-span Al-11Fe-2V, ground to -60 mesh powders of mostly "A" structure [9]). Under the EDC conditions (dis-

charges of a 480 μF capacitor charged at 2 to 5 kV to produce the input energies of 1 to 6 kJ to 2 grams powder), no oxide particles of detectable sizes were observed in the powder particle-particle interface which is produced by welding of two particles. Also TEM micrographs clearly indicated that both the areas across the interface exhibit microstructures almost identical to that seen in the rapidly solidified state. A typical TEM micrograph showing such an interface region is presented in figure 1.

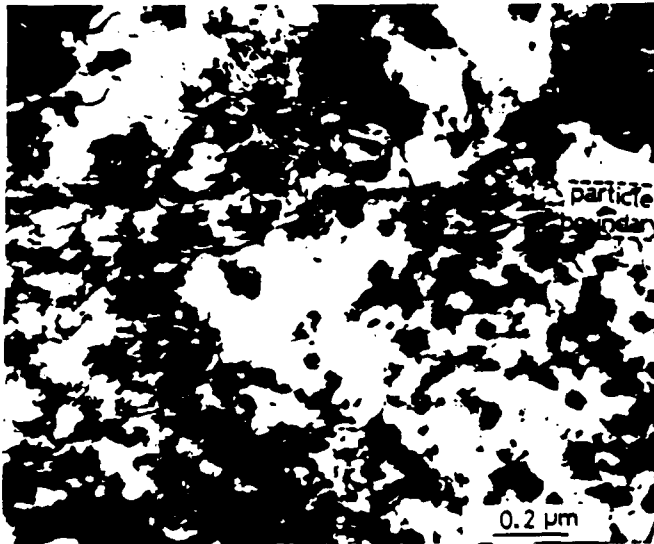


Figure 1 A TEM micrograph of an EDC compact of RSPAl-11Fe-2V powders, showing the interface region which is free from any oxide particle of detectable sizes.

One-pulse discharges were made in the input energy range of up to 12 kJ from a capacitor bank of 720 μF charged up to 5.8 kV to the atomized Al-8Cr-2Ti powder specimens of 20, 30 and 50 m Ω under 45, 70 and 103 MPa pressures. Depicted in figure 2 is the relation of the achieved density, ρ_a , versus the input energy, E_i as a function of the specimen resistance, R_i . It should be noted that the achieved density can reach up to 96% of the theoretical for a 20 m Ω specimen discharged at 12 kJ. As expected, the increase in density is

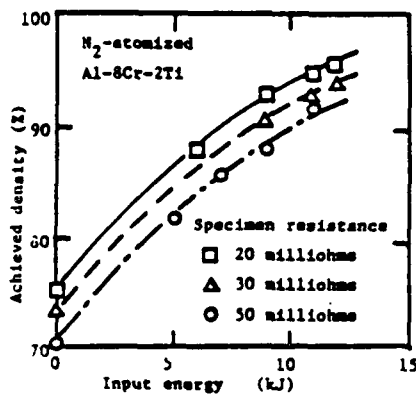


Figure 2 The achieved density vs. input energy as a function of specimen resistance for Al-8Cr-2Ti powders

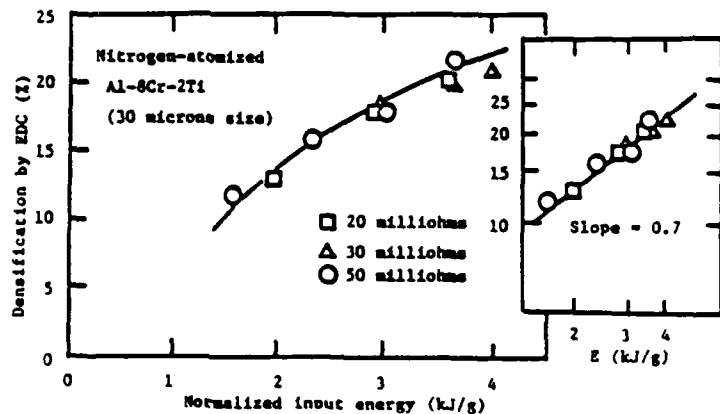


Figure 3 Densification by EDC vs. normalized input energy for Al-8Cr-2Ti atomized powders

of parabolic with increasing the input energy and the curves for three different specimen resistances are parallel. This implies that the densi-

fication during EDC simply depends on the input energy, but not the initial packing density; the applied pressure has a minor effect on sintering. To clearly depict this input energy dependence, the data are replotted in Fig.3 in a relation between the net densification by EDC and the normalized input energy, E_n (kJ/g). It is seen that the maximum densification amounts to 22% at a 4 kJ/g. This 22% is much greater than that (12%) previously reported [5]. It is then concluded that the parameter predominantly affecting the densification by EDC is the normalized input energy.

The EDC conditions were examined to achieve the highest density without altering the microstructure inherent in RSP. The structural change is primarily due to the excessive heat, ΔH that is related to the specimen resistance, R_i , discharge current, I and the discharge time, t by $\Delta H = I^2 R_i t$. Since the input energy, E_i is directly related to $CV^2/2$, the product of E_i and R_i is constant ($A\Delta H t/2C$). Figure 4 depicts the relation of E_i vs. R_i where the boundary curves clearly separate the region I in which the microstructure is not altered at all, the region II in which the interface region has been modified and the region III in which the matrix microstructure has been changed to significantly increase the size of originally fine precipitates. The condition for the region III is undesirable.

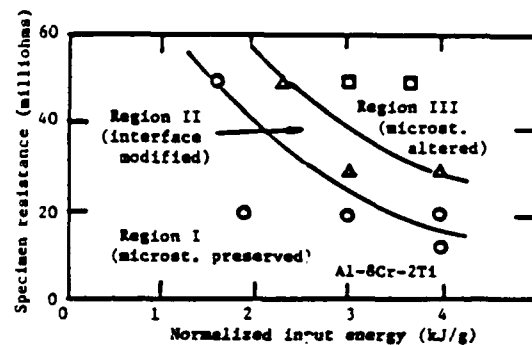


Figure 4 R_i vs. E_n to identify three regions

From the curve to thread the data points of the interface modified in region II, one can obtain a value of 0.094 for A. Once A is given for a given condition of EDC (R_i , C) the input energy E_i can be uniquely chosen to specifically avoid the undesirable microstructural change. A typical example of the microstructure in region I is illustrate for a 20m Ω specimen discharged at 12 kJ. It is in Fig. 5 that first the interface produced by welding two powder particles is very narrow and free from any oxide particle of detectable sizes and secondly the microstructures on the both sides sandwiching the interface exhibit the same structure as that of the as-atomized powder. On the other hand, once the specimen resistance is increased (the applied pressure is reduced), the amount of heat generated by the same input energy is increased according to the Ohmic law. Depicted in figure 6 is an example of the microstructure produced in region II for a 30 m Ω specimen discharged at 12 kJ. The width of the interface is increased but the matrix microstructure is not altered. Further, the interface morphology is quite unique. Namely, the interface has somewhat recrystallized structure that is completely free from precipitate phases. It is then considered that the heat generated under this condition not only disperses the oxide film on the prior powder particle boundary but also melts a fairly significant amount of the particle surface layer which was otherwise accompanied with precipitates. This molten layer, however, is quenched very quickly, leaving the re-solutioned solute atoms in solid solution. Also the recrystallization might have proceeded while the heat is dissipated into the matrix but in a manner not to extend its recrystalli-

zation beyond this interface region. Accordingly it can be said that the microstructure in the interface region has been modified due to a very high quenching rate. Once in while, even an amorphous structure was produced in the interface region [8].

Since this atomized powder has been exposed to air, it is believed that powder particles have oxide films of at least a few hundreds angstroms. When a pulse of high current density is subjected, the oxide film would be explosively dispersed into the matrix [1]. So far TEM observations of as-EDC compacts revealed that neither oxide film nor oxide particle of detectable sizes exist at and in the neighborhood of the interface. The resurgence of oxide particles from the matrix was examined by heating the EDC compact at 873 K for 86.4 ks. The oxide films disrupted by a discharge, then mixed into the matrix in a form of forced solid solution, must come out as oxide precipitates upon heating either in the interface or in the matrix since oxygen atoms have only a very limited solubility in aluminum (less than 50 ppm). TEM observations of heat-treated compacts also revealed no oxide particles of detectable sizes exist both at the interface and in the matrix, while the precipitate phases have been significantly grown.

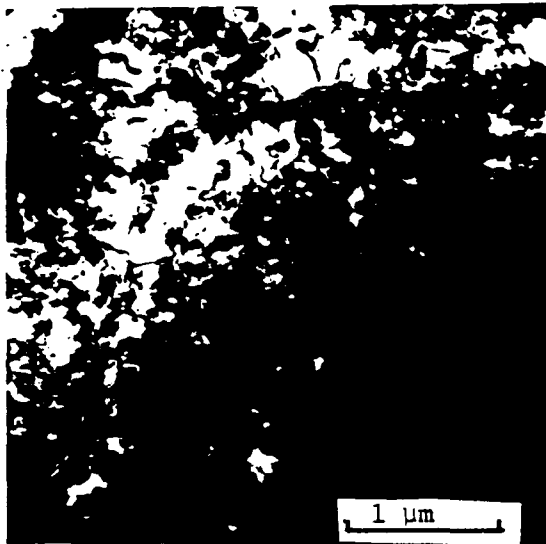


Figure 5 A TEM micrograph of a compact discharged in region I, the microstructure being preserved.

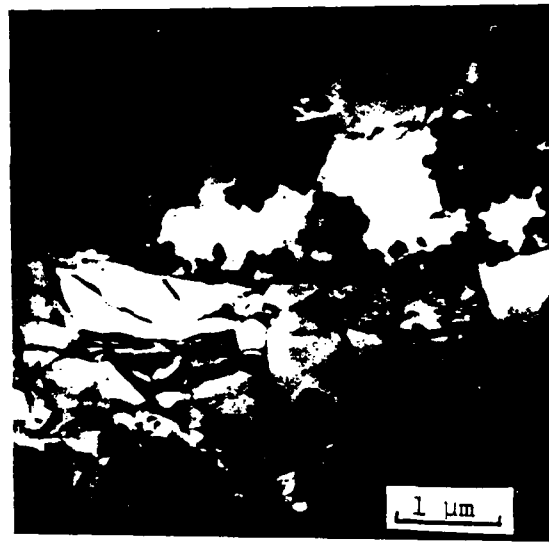


Figure 6 A TEM micrograph of a compact in region II, the interface region being modified.

Since it was not possible to produce a 100% density by a single pulse discharge, microhardness tests, in stead of tensile tests, were carried out to check out the improvement of mechanical properties. The results of hardness measurements are presented in figure 7, where the data points are plotted against the achieved density. The room temperature tensile strength here is converted from the hardness using an equation of $\sigma = H_v/3$. It is seen in this figure that the estimated strength increases with increasing the achieved density and extrapolates to 620 MPa at 100% density. This value is compared with that of the bulk material produced by CIPping and hot-extrusion (412 MPa for 0.2% proof strength, 452 MPa for UTS, 14% elongation, 93 GPa for Young's modulus and 448 MPa for $H_v/3$), clearly indicating that not only the estimated strength values (520 - 600 MPa) at densities of 90 - 95% exceed the bulk strength (452 MPa) but also the extrapolated value of

620 MPa at a 100% density is outstanding. This suggests that improved strength is one of the advantages of EDC for consolidation of rapidly solidified powder materials.

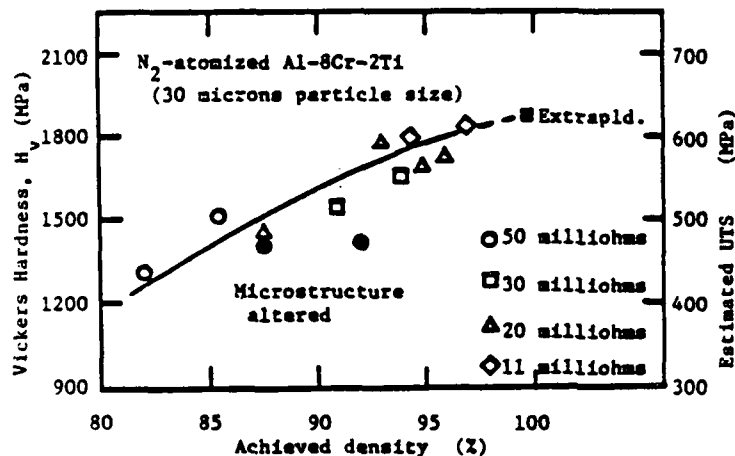


Figure 7 The estimated strength versus achieved density for nitrogen-atomized Al-8Cr-2Ti powders consolidated by EDC.

Conclusion

Electro-discharge compaction of nitrogen atomized Al-8Cr-2Ti powder was carried out in air under the applied pressure of up to 103 MPa. Four characteristics of EDC, namely the preservation of the unique microstructure inherent in rapid solidification, the capability of removing oxide films on powder particle surface, the densification and the improvement of mechanical properties were examined in detail by microstructural observations, density measurements and microhardness measurements of EDC compacts. It is concluded that the above mentioned four characteristics of EDC are fully demonstrated and EDC is a promising compaction technique for rapidly solidified materials.

References

1. D. K. Kim, H. R. Pak and K. Okazaki, *Materials Science and Engineering*, A104 (1988) 191
2. G. F. Taylor, *Apparatus for making hard metal compositions*, U. S. Patent #1, 896, 854 February (1933)
3. C. D. Clemer, U. S. Patent #2, 374, 605 August (1944)
4. F. V. Lene, Jr. *of Metals*, 7 (1), (1955) 158
5. S. Saito and A. Sawaoka, *Powder Metallurgy International*, 7 (1973) 70
6. S. Clyens and S. T. S. Al-Hassani, *Intl. Jr. Mech. Sci.*, 18 (1976) 37
7. T. J. Davis and S. T. S. Al-Hassani, *Adv. Mater. Tech. in America*, 2 (1980) 140
8. K. Okazaki, D. K. Kim and H. R. Pak, *Rapidly Solidified Materials: Properties and Processing*, Proc. of 2nd Intl. Conf. on Rapidly Solidified Materials, ASM Intl., Metals Park, Oh, (1988) 183
9. H. Jones, *Materials Science and Engineering*, 5 (1969/70) 1

POTENTIAL ARMY APPLICATIONS FOR ELECTRIC FIELD AND
CURRENT EFFECTS ON MATERIAL PROPERTIES

Paul J Cote
Benet Laboratories
Watervliet Arsenal, Watervliet, NY. 12189

Several investigators have reported that electromagnetic fields and currents can have a direct effect on mechanical properties and behavior of metals and alloys. Included are results showing field and current effects on martensite transformations, metal forming, and metal consolidation.

As the implications of these observations become better understood, there will be a need to accommodate or exploit any significant new phenomenon. The purpose of this presentation is to review a variety of potential application areas at our installation.

MARTENSITE TRANSFORMATIONS

A major function of the Watervliet Arsenal is the manufacture of large martensitic steel components. Major processing steps include hot rotary forging, austenitizing, quenching, and tempering. Research and development efforts are conducted on a continuing basis to improve manufacturing processing and material properties in order to optimize component strength and toughness. Therefore, there would be substantial interest at our installation if demonstrable property improvements could be effected by a simple application of current or field, either before or during a processing step.

RAIL GUNS

The Army has the major responsibility for the rail gun portion of the SDI program and Benet has several efforts in support of this program. Included are the design and manufacture of 50mm round bore rail gun barrels, the design and test of an internal flux compressor power source, and the development of a superconducting augmentation concept for rail guns. Since currents levels are in the Megamp range and magnetic field strengths are in the 10T range, any appreciable effects of large currents and fields on mechanical behavior must be considered for proper component design.

ELECTROTHERMAL GUNS

The electrothermal concept combines conventional gun technology with electrical power drive in order to enhance muzzle velocity. In this device the projectile is accelerated down the bore of a conventional tube by rapidly expanding gases. Unlike conventional guns, the gas is not generated by the rapid burning of a propellant; instead, the gas is produced by applying a high voltage to vaporize a fluid and form a plasma. Among the advantages of the electrothermal concept over the EM concept is that electrical power is delivered by the use

of high voltage (10-20kV) instead of high currents (Megamps). In this case, the high voltage is applied in the high pressure region (breech) of the gun where an electric field effect, if present, is most likely to be manifest.

ELECTRODEPOSITION

The bore surface of gun tubes is subjected to high temperature and high pressure gases. The standard bore surface protection is electroplated chromium. Benet has recently developed and installed a "low-contractile" chromium plating facility which provides a better quality electrodeposit than the conventional process. D.C. current densities of $.001a/mm^2$ and pulse current densities of $0.02a/mm^2$ are typical. Information on the effects of electric currents on elastic flow and on transformations may be relevant to understanding and improving the deposition process.

Effects Other Than Heating by High-Intensity, High-Frequency Microwaves in Materials Processing*

H. D. Kimrey and M. A. Janney
Oak Ridge National Laboratory
Oak Ridge, TN 37831-8071

Microwave sintering possesses unique attributes and has the potential to be developed as a new technique for controlling microstructure to improve the properties of advanced ceramics. Because microwave radiation penetrates most ceramics, uniform volumetric heating is possible. Thermal gradients, which are produced during conventional sintering by conductive and radiative heat transfer to and within the part, can be minimized. By eliminating temperature gradients, it is possible to reduce internal stresses, which contribute to cracking of parts during heat-up and sintering, and to create a more uniform microstructure, which may lead to improved mechanical properties and reliability. Recent investigations comparing microwave and conventional sintering have identified additional benefits to microwave sintering. Using 28-GHz radiation, it has been demonstrated that alumina can be densified at temperatures 300 to 400°C below those temperatures used in conventional processing and that a uniform, fine-grained microstructure can be obtained. Microstructural analysis has revealed no difference in the variation of surface area with density for the two sets of samples. However, the evolution of pore size with densification differs considerably for conventionally sintered alumina and for microwave-sintered alumina. Furthermore, comparing pore-size distribution curves at similar densities (e.g., microwave at 77.2% and conventional at 78.5%) shows that not only is the median pore size different, in addition to microstructural analysis, but the shape of the pore-size distribution curves is different as well. The sintering data have been refined to calculate an apparent activation energy for sintering. For conventional sintering, the apparent activation energy was ~575 kJ/mol [typical for alumina; Wu et al., Adv. Ceram. 10, 574—582, (1983)], whereas the value for microwave sintering was only ~170 kJ/mol. These data suggest that the microwave firing enhances the diffusion of aluminum and oxygen ions during sintering. Several approaches are being used to identify the primary mechanism(s) responsible for influencing microstructural development during densification. One is to study grain growth in dense, hot-pressed alumina, where the kinetic process is much simpler than in sintering; only movement of the grain boundaries is involved, which is controlled by either grain boundary or volume diffusion. Another approach is to study the sintering process using dilatometry. The latest results will be reported.

*Research sponsored by the Office of Energy Utilization Research, Energy Conversion and Utilization Technologies (ECUT) Program, U.S. Department of Energy, under contract DE-AC05-84OR21400 with Martin Marietta Energy Systems, Inc.

EFFECTS OTHER THAN
HEATING BY
HIGH-INTENSITY, HIGH-FREQUENCY
MICROWAVES
IN MATERIALS PROCESSING

H. D. KIMREY, and M. A. JANNEY
OAK RIDGE NATIONAL LABORATORY
OAK RIDGE, TENNESSEE

ARO WORKSHOP ON
HIGH-INTENSITY ELECTROMAGNETIC AND
ULTRASONIC EFFECTS ON INORGANIC
MATERIALS BEHAVIOR AND PROCESSING
RALEIGH, NORTH CAROLINA
JULY 18, 1989

ACKNOWLEDGEMENT

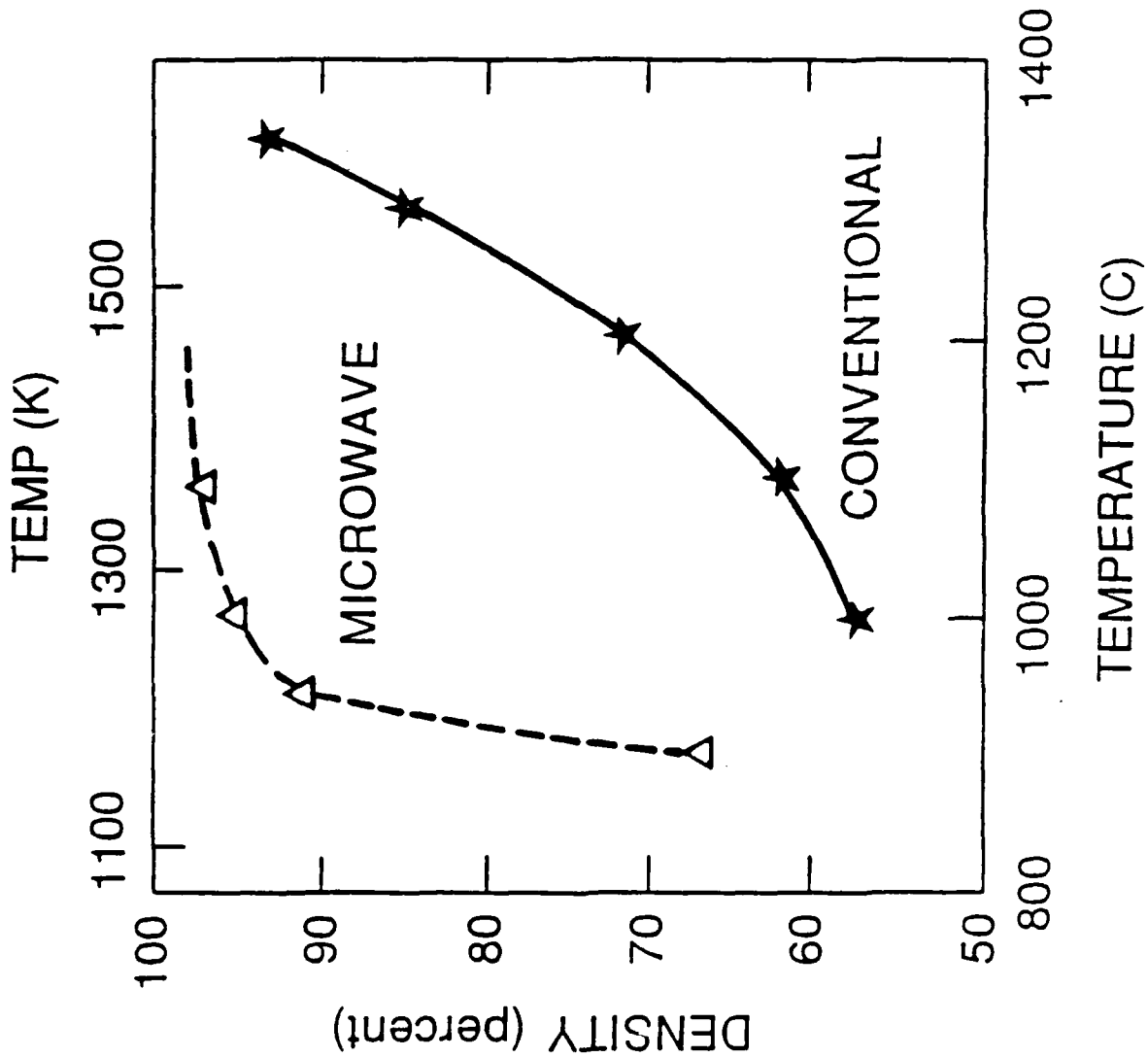
RESEARCH SPONSORED BY

THE ENERGY CONVERSION AND
UTILIZATION TECHNOLOGIES PROGRAM

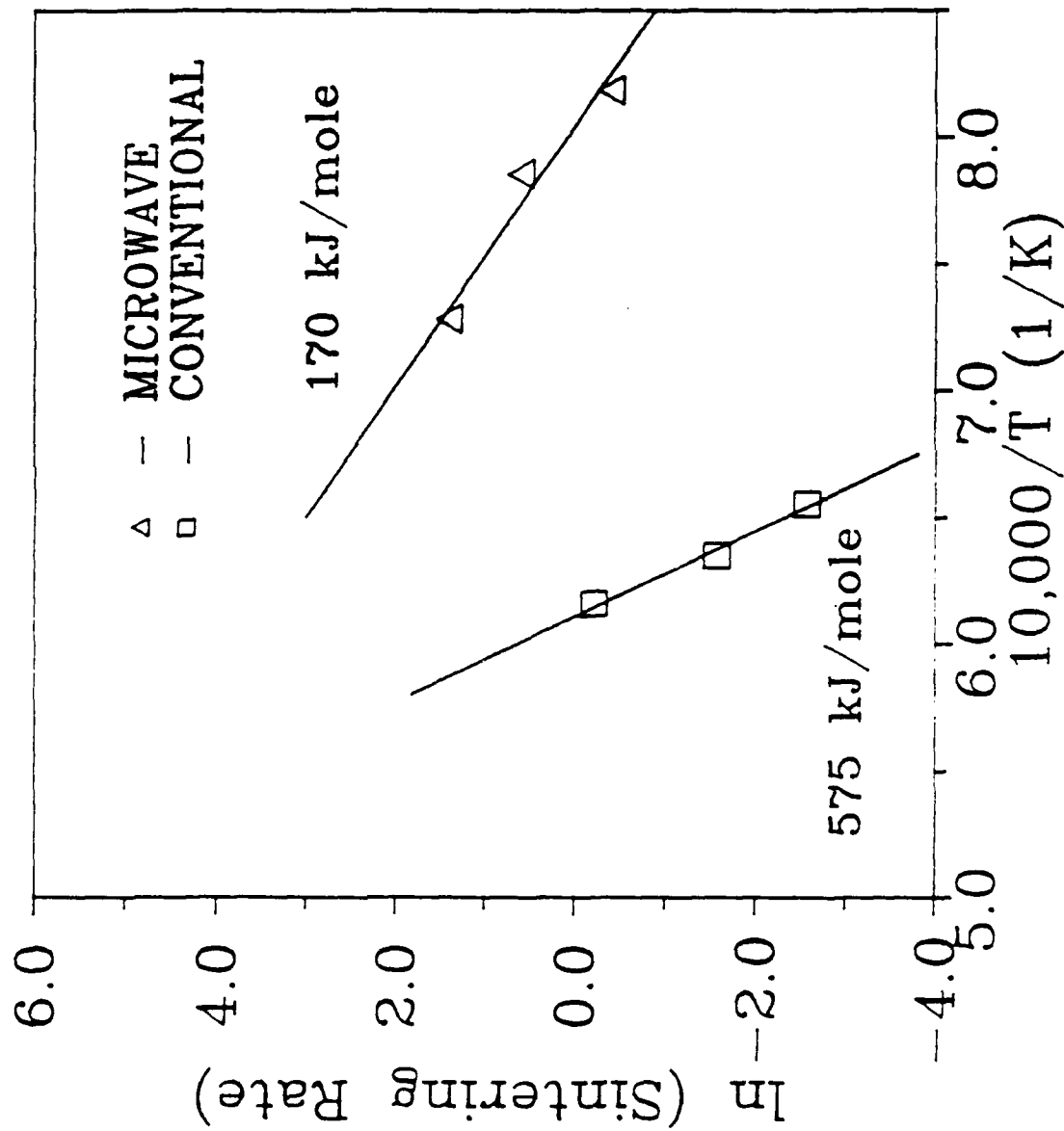
U.S. Department of Energy

INTRODUCTION

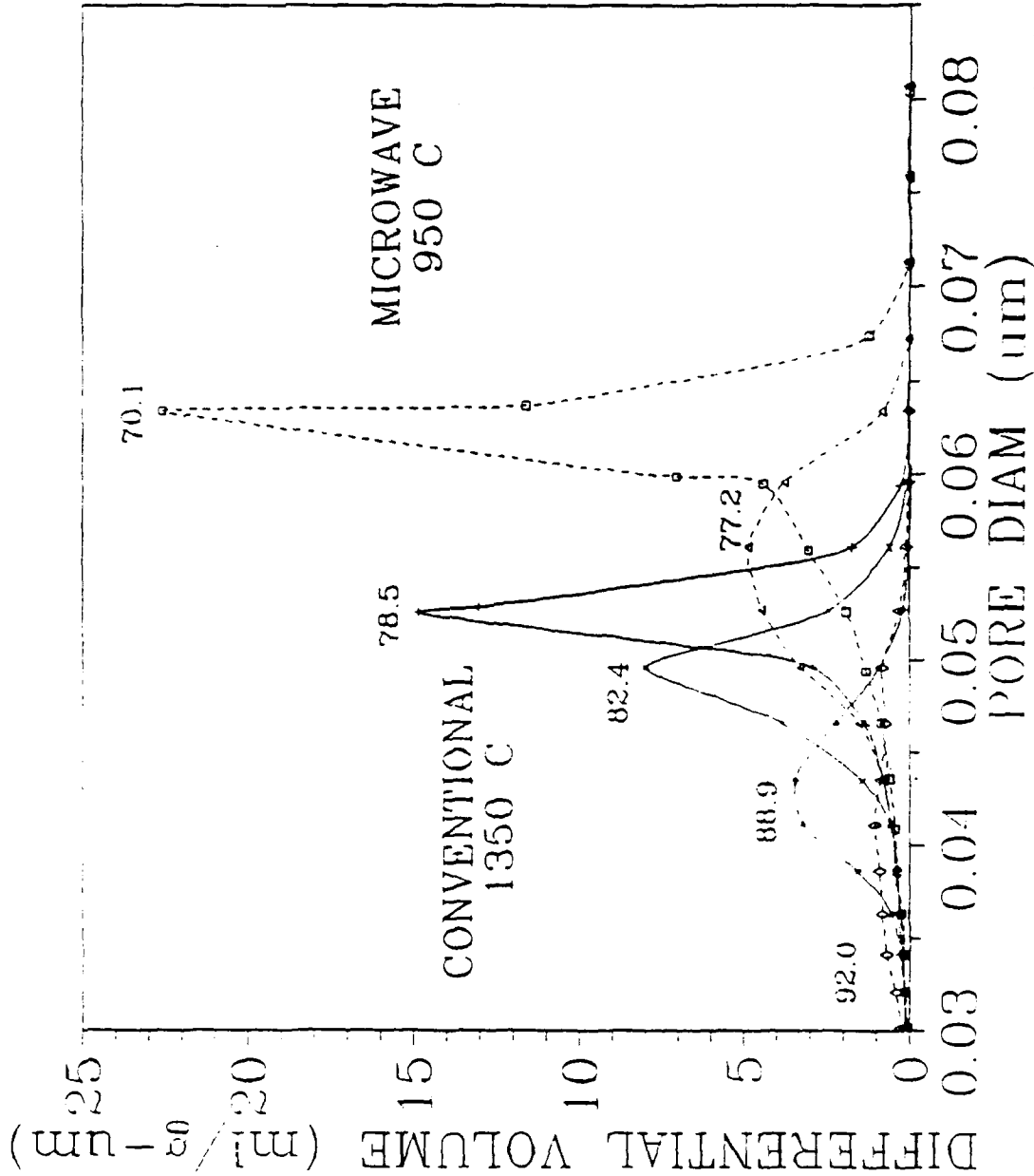
- o MICROWAVE PROCESSING HAS BEEN DEMONSTRATED TO BE DIFFERENT IN-KIND FROM CONVENTIONAL THERMAL PROCESSING.
- o EXAMPLES COME PRIMARILY FROM SINTERING STUDIES
 - o ALUMINA
 - DENSITY vs TEMPERATURE
 - APPARENT ACTIVATION ENERGY
 - PORE EVOLUTION DURING SINTERING



MICROWAVE PROCESSING LOWERS THE APPARENT ACTIVATION ENERGY FOR SINTERING



MICROWAVE SINTERING PRODUCES
A DIFFERENT PORE EVOLUTION PATH
THAN DOES CONVENTIONAL SINTERING



MAJOR FEATURES

DUAL PUSHRODS- (CONCENTRIC CYLINDER DESIGN)

INTERCHANGABLE HOT ZONE RODS

- MOLYBDENUM METAL
- BORON NITRIDE
- ALUMINUM OXIDE

CONCENTRIC REMOVABLE THERMOCOUPLE

QUARTER WAVELENGTH REJECTION FILTERS

0.05 % ACCURACY OVER A ONE INCH RANGE

WATER COOLED STAINLESS BASE PLATE

MICROWAVE COMPATIBLE DILATOMETER

SILICON
NITRIDE
INSULATION

SILICON
NITRIDE
SAMPLE

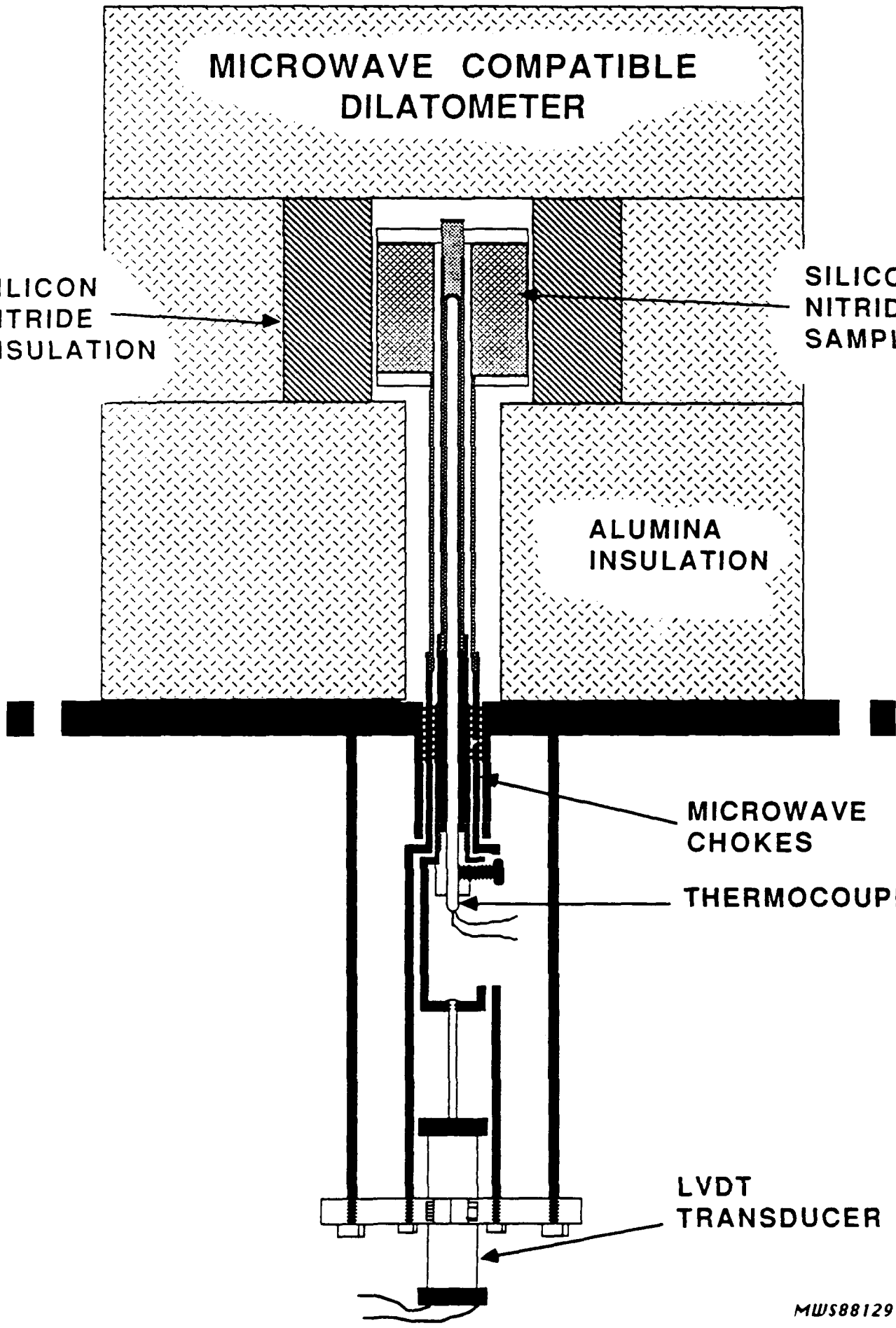
ALUMINA
INSULATION

MICROWAVE
CHOKES

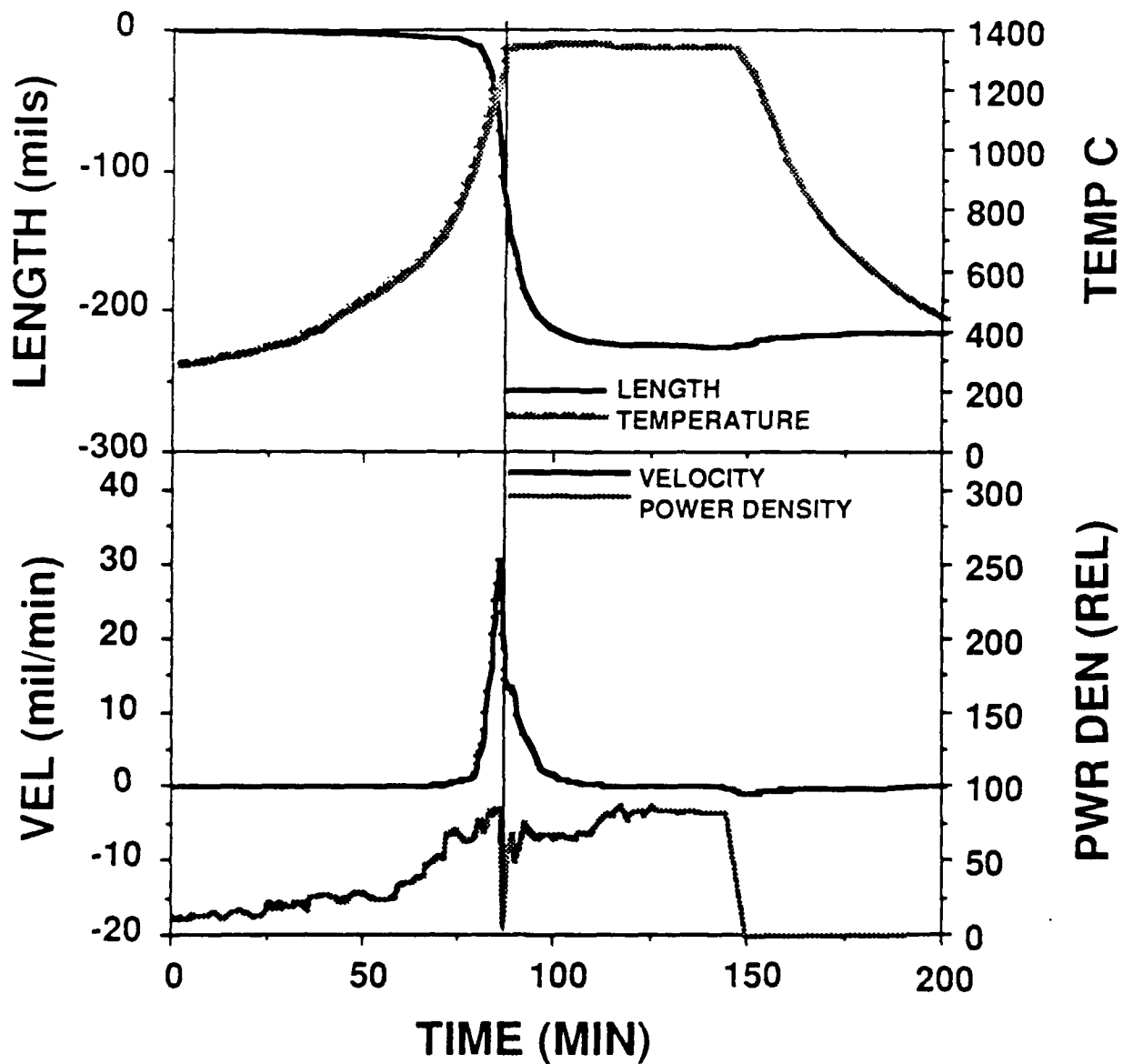
THERMOCOUPLE

LVDT
TRANSDUCER

MWS88129



RAW DATA FROM THE MICROWAVE DILATOMETER FOR AN ALUMINA SINTERING RUN



DILATOMETER CONCLUSIONS

SINTERING DILATOMETRY IS QUITE FEASIBLE
IN A MICROWAVE FIELD

WITH CAREFUL DESIGN CHOICES OPERATIONAL
ERRORS CAN BE REDUCED TO THE LEVELS OF
CONVENTIONAL DILATOMETRY

THIS TECHNOLOGY WILL DRAMATICALLY
DECREASE THE AMOUNT OF CAVITY TIME
REQUIRED TO CHARACTERIZE THE SINTERING
BEHAVIOR OF CERAMIC MATERIALS

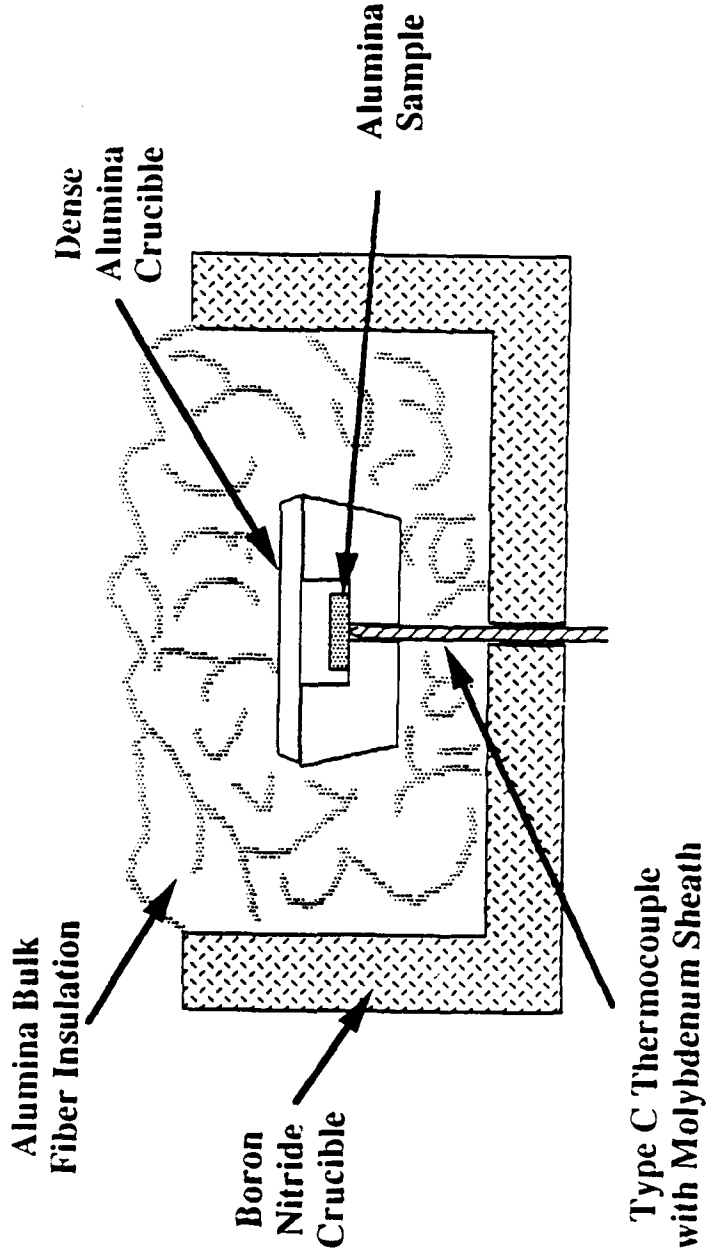
SIGNIFICANCE OF
GRAIN GROWTH STUDY

- o D_b OR D_v MUST BE HIGHER IN THE MICROWAVE CASE
BECAUSE MICROSTRUCTURAL CHANGE AND KINETICS ARE
IDENTICAL FOR BOTH MW AND CONVENTIONAL ANNEALS.
- o ACTIVATION ENERGY IS LOWER - HOWEVER NOT AS LOW AS
FOR SINTERING.

WHY GRAIN GROWTH ?

- o MECHANISM OF SINTERING TOO COMPLICATED FOR CRITICAL ANALYSIS
- o MULTIPLE MECHANISMS DURING SINTERING
 - DENSIFICATION
 - COARSENING OF PARTICLES
 - GRAIN GROWTH
 - PORE GROWTH
- o GRAIN GROWTH
 - GRAIN BOUNDARY MOVEMENT ONLY
 - DRIVEN BY SURFACE TENSION FOR NORMAL GRAIN GROWTH
 - BOUNDARY OR VOLUME DIFFUSION CONTROLLING

SCHEMATIC OF EXPERIMENTAL SET-UP FOR ALUMINA GRAIN GROWTH EXPERIMENTS



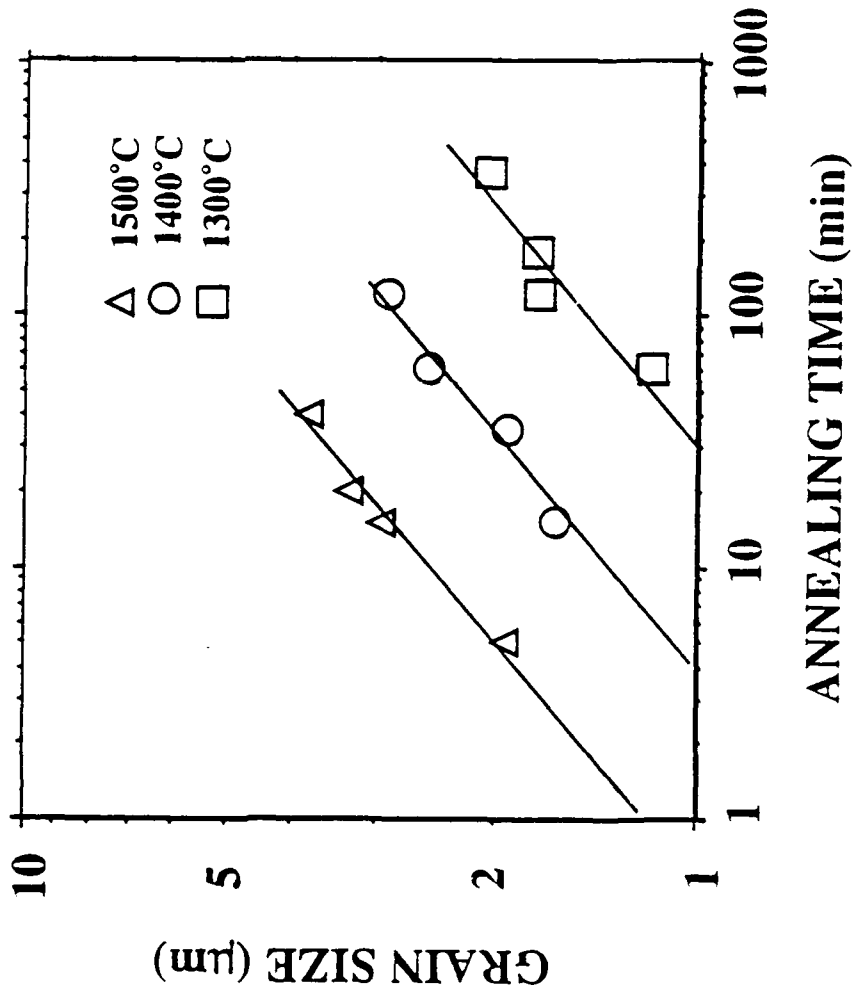
EXPERIMENTAL PROCEDURE

- o DENSE HOT-PRESSED ALUMINA
 - REYNOLDS RCHP-DBM
 - 0.1 wt % MgO SINTERING AID
 - HOT PRESS AT 1450°C, 2 h, 5000 psi
 - $\rho \sim 100\%$, GRAIN SIZE = 1.1 μm

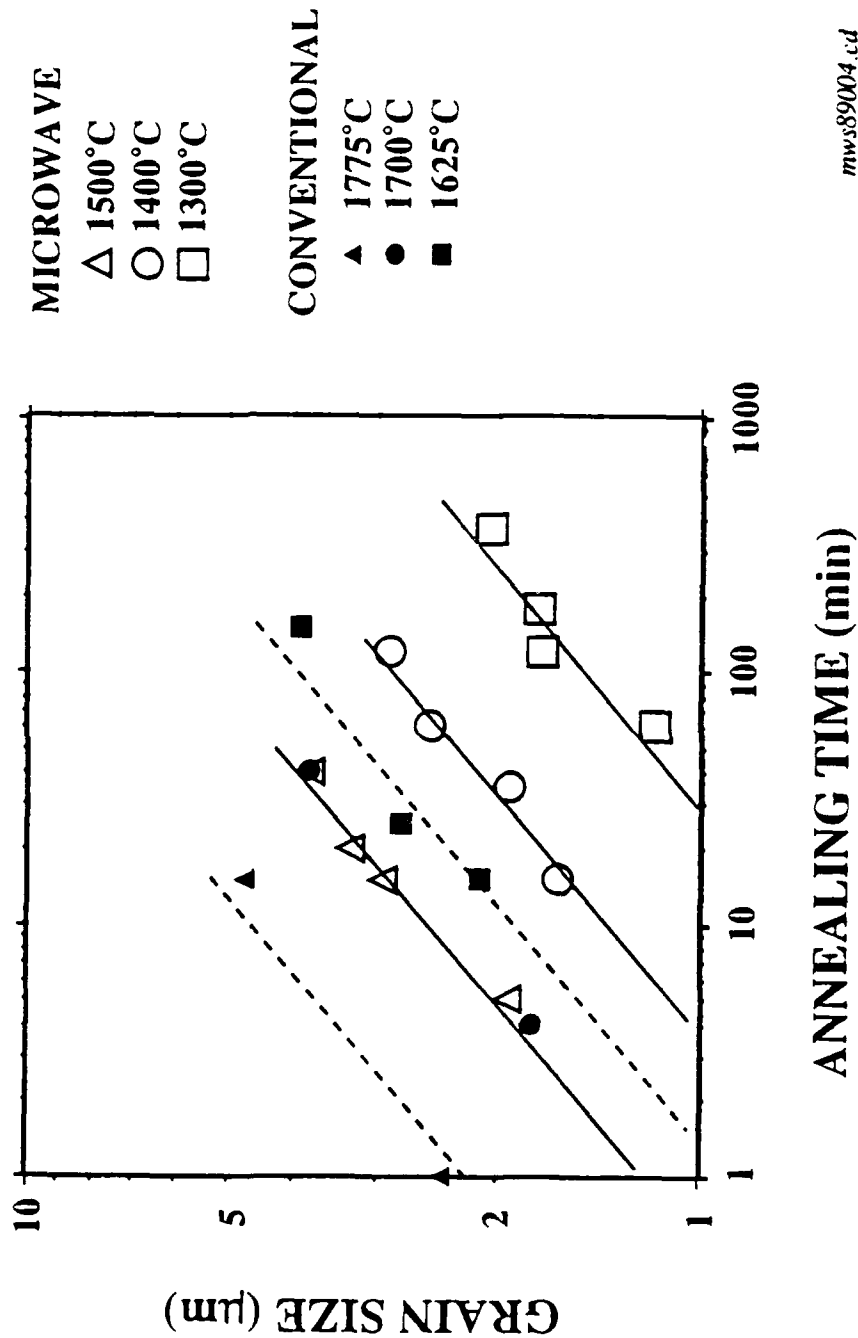
- o ANNEAL IN CONVENTIONAL AND MW FURNACES
 - CONVENTIONAL - 1625, 1700, & 1775 °C
 - MICROWAVE - 1300, 1400, & 1500 °C

- o GRAIN SIZE ANALYSIS
 - TRACOR SYSTEM ON HITACHI S-800 SEM
 - GATHER IMAGE, DIGITIZE, ANALYZE

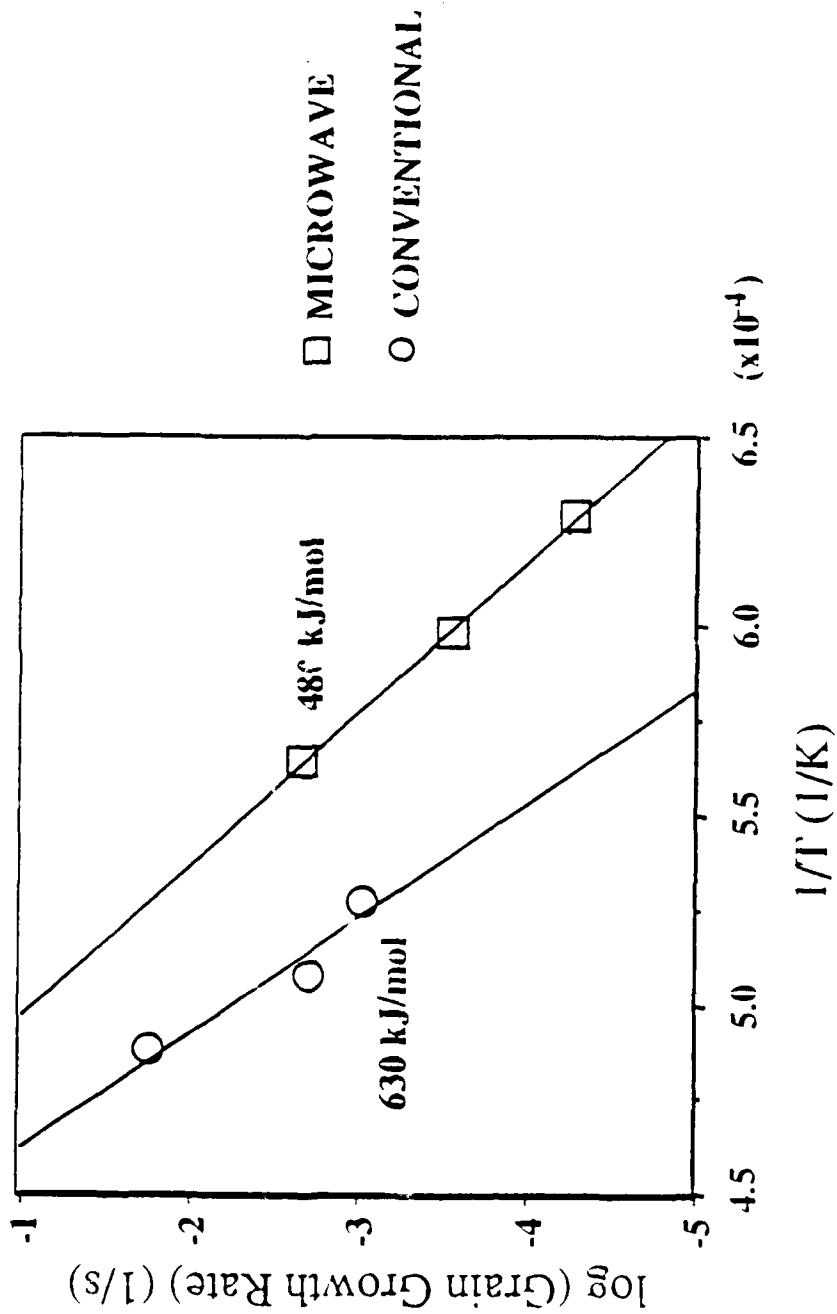
GRAIN GROWTH IN MICROWAVE-ANNEALED ALUMINA FOLLOWED POWER LAW KINETICS



GRAIN GROWTH KINETICS FOR CONVENTIONAL AND MICROWAVE ANNEALING OF ALUMINA



MICROWAVE ANNEALING EXHIBITED A LOWER ACTIVATION ENERGY THAN DID CONVENTIONAL ANNEALING



mvx89003.ccd

SUMMARY

o MICROWAVE AND CONVENTIONAL GRAIN GROWTH ARE STRUCTURALLY AND KINETICLY SIMILAR.

o MW KINETICS SIGNIFICANTLY FASTER

1500°C MW = 1700° C CONVENTIONAL

o ACTIVATION ENERGY WAS LOWER FOR MW ANNEALING

480 vs 630 kJ/mol

o ACTIVATION ENERGIES FOR GRAIN GROWTH DIFFERENT FROM THOSE FOR SINTERING

170 vs 575 kJ/mol

LASER PROCESSING OF MATERIALS*

J. Narayan
Materials Science and Engineering
North Carolina State University
Raleigh, NC 27695-7916

ABSTRACT

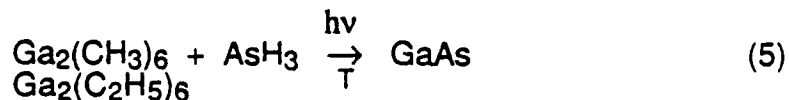
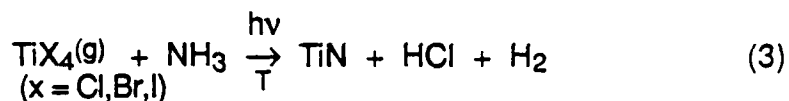
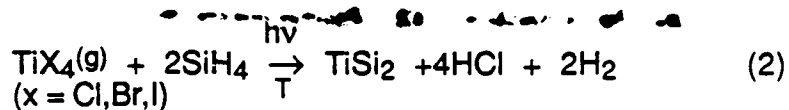
Lasers Provide a controlled source of atomic and electronic excitations which can be used for a variety of materials processing applications.¹⁻⁶ Photons interact with electrons as atoms are too heavy to respond. The laser-solid interactions are related directly to macroscopic properties such as absorption and reflectivity. As a function of laser parameters (wavelength, pulse duration, and energy density), the materials processing methods can be classified broadly into three regimes: (a) high-energy regime-surface cleaning, etching, thin film deposition, shock deformation, etc.; (b) medium energy-melting and solidification, near surface alloying, semiconductor looping, zone refining, etc.; and (c) low energy-electronic and vibrational energy transfer producing nonthermal, photolytic effects.

In the high energy evaporation regime, the laser physical vapor deposition can be used to achieve deposition of high- T_c superconductors, diamond and diamondlike thin films. Using nanosecond (pulse duration 20-40ns, energy density $\sim 2\text{Jcm}^{-2}$) lasers, the stoichiometry of a multicomponent target can be reproduced into the laser evaporated film. As an example, the stoichiometry of the four (YBaCuO) and five (BiSrCaCuO) component high-temperature superconductors have been shown to be preserved in the form of thin films. Using this method, excellent quality films of $\text{YBa}_2\text{Cu}_3\text{O}_7$, $\text{Bi}_2\text{Sr}_2\text{Ca}_1\text{Cu}_2\text{O}_6$, TiN, TiC, WC, BaTiO₃, stainless, MgO, ZrO₂, diamond and

diamondlike ... have been obtained. Selective etching and patterning with a high-degree of spatial selectivity are expected to lead to maskless lithography in the near future. Shock deformation of near surface regions can lead to enhanced hardness as well as toughness for certain materials. Formation of deformed layers in the near surface regions of extra hard materials with low toughness provides sources of dislocations, thus enhancing toughness and ductility.

In the medium energy range, the lasers can be used as a controlled source of heat with a high degree of spatial selectivity. In this regime of laser energy, rapid melting and solidification can lead to formation of novel materials with unique microstructure and with chemical compositions much higher than solubility limits. The microstructure, ranging from amorphous to single crystal of laser modified regions can be controlled by changing laser parameters and substrate properties. In this regime or slightly below, the lasers can be used to atomically clean the surfaces and remove any absorbates.

Finally, lasers can be used to break chemical bonds by exciting the electrons to antibonding states or by coupling the energy to vibrational modes. The electronic antibonding absorption in SiH_4 starts at 167nm ($60,000 \text{ cm}^{-1}$) via single photonic process, whereas, CO_2 laser ($10.6\mu\text{m}$ with very low photon energy $\sim 100 \text{ meV}$) can be used to break bonds via coupling to vibrational modes. Since the energy remains into the electronic system or a small amount into the vibrational modes, thin film deposition of silicon is possible at very low temperatures (as low as 100 to 200°C). This is expected to revolutionize the formation of advanced integrated circuit devices. Similar examples can be drawn for TiN, Al and GaAs thin film formation, as shown below:



In semiconductors, lasers or photon beams can produce a high density of electron-hole (e^- and h^+) pairs. These electrons and holes can influence materials processing in a variety of ways: (a) Charge states of defects (vacancies, interstitials and dislocations) can be changed, enhancing their mobilities. This has been shown to lead to enhanced multiplication of dislocations. A rapid glide and climb behavior has been observed in semiconductor heterostructures such as GaAs/GaAlAs and InP/InGaAsP; (b) The high concentration of electrons and holes can influence surface reactions, by migrating to the surface, and deposition kinetics of thin films. These carriers can also break the bond of any adsorbates on the surface and provide surface cleaning.

REFERENCES:

1. C.W. White, J. Narayan, and R.T. Young, *Science*, 204, 461 (1979).
2. "Laser-Solid Interactions and Transient Thermal Processing of Materials," ed. by J. Narayan, W.L. Brown, and R.A. Lemons (North -Holland, 1983).
3. "Laser and Optically Assisted Processing of Materials," ed. by J. Narayan, SPIE Proceeding, Vol. 161, Wellingham, Washington.
4. J. Narayan, *J. of Metals* 33, 15 (1980).
5. "Defects in Semiconductors," ed. by J. Narayan and T.Y. Tan (North-Holland, 1981).
6. "Lasers in Metallurgy," ed. by K. Mukherjee and J. Mazumdar, AIME Publication, Warrendale, PA (1981).

*Work supported by ARO, NSF, DOE & DARPA



Robert Rosenberg
914/945/1888
Userid: RROS at YKTVMV

IBM Research Division
T. J. Watson Research Center
P.O. Box 218
Yorktown Heights, New York 10598
Fax: 914/945-2141
Telex: 9102400632

July 20, 1989

Professor Hans Conrad
Department of Materials Science and Engineering
North Carolina State University
Raleigh, North Carolina 27695-7907

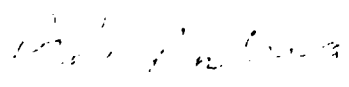
Dear Hans,

I would like to thank you for inviting me to participate in the ARO Workshop. Exposure to the various research efforts involved with the effects of fields on processing of materials was mainly unknown to me and seems quite remarkable, although many questions remain unanswered. Of special interest were the effects of electropulsing, electric field and magnetic field on dislocation flow, recovery, fatigue, grain growth, hardness, etc. Although the phenomena seemed real and reproducible, it is difficult to understand the fundamental mechanisms involved. The same is true for microwave sintering and ultrasonic forming or sintering.

It is clear that the research effort should begin to focus on the more fundamental aspects of field effects, with controlled samples and in situ measurement techniques to help analyze structural changes in real time. If transient effects are important, and they appear to be to me, then after-the-fact analysis will not be helpful to elucidate the mechanistic of the interactions taking place. Perhaps it would be useful to have a meeting specifically for the purpose of identifying appropriate analytical methods that could be utilized. Only by understanding how fields actually cause the observed effects can more generic use of the technique be made; for example, in processes or properties associated with microelectronics. Also, it may be of interest to understand the role of external fields on interface interactions and reactions within layered structures which are of considerable interest to those involved with processing of microelectronic or optoelectronic components. Perhaps IBM people can be of some help in these areas.

As you requested, I edited the write-up I gave you to include a few key references. A copy is enclosed

Sincerely,


Robert Rosenberg

/al

THOUGHTS ON POSSIBLE EXPLANATIONS FOR THE VARIOUS OBSERVATIONS PRESENTED AT THE WORKSHOP

D. Kuhlmann-Wilsdorf[†] and H. Conrad^{††}

[†]University of Virginia

^{††}North Carolina State University

INTRODUCTION

Conveniently, one may separate the basic considerations regarding effects of electromagnetic fields and currents on mechanical properties into three categories, as follows. First, known observations made on electrical contact resistances, especially of electrical "brushes", which place limits on the range of possible explanations. Second, unintended and typically unrecognized side effects of current passage and/or the application of strong electric or magnetic fields. Third, the framework in terms of dislocation theory into which all possible explanations must fit. The relevant considerations will be presented in turn.

OBSERVATIONS ON ELECTRICAL BRUSHES

The performance of sliding electrical contacts, i.e. what conventionally is called electrical "brushes", derives from the mechanical behavior of the surface zones of the contacting materials while subject to very high current densities, and electrical field strengths. Namely, under applied normal force P across the sliding interface of macroscopic area A , real mechanical contact takes place only at a restricted number of contact spots whose total area is, in first approximation,

$$A_c = P/H \quad (1)$$

where H is the impression (Meyer) hardness of the softer of the two sides. The ratio of the macroscopic current density $\bar{j} = I/A$ of a sliding electrical contact to the actual current density at the contact spots j_{act} is therefore

$$j_{\text{act}}/\bar{j} = A/A_c = H/(P/A) = H/p \quad (2)$$

where $p = P/A$ is the macroscopic mechanical pressure between the two sides. With p typically fairly small in order to contain friction and wear, j_{act} therefore tends to be very high in quite ordinary sliding contacts, e.g. $j_{\text{act}} \approx 50,000$ Amp/cm² at $I = 0.4$ Amp passed through some gold-plated copper fiber brushes sliding on a gold-plated copper substrate which are currently under study. And meanwhile the local electrical field is also very large, namely in the present example about 20,000 V/cm across the interfacial film which is only about 5 Å thick. In actual use such brushes could carry at the least 40 Amps of current, and at fixed total contact spot area the local current density and fields would correspondingly become 5 MA/cm² and 2 MV/cm, respectively.

Since, as seen, the local hardness H at the contact spots controls A_c , and since moreover the macroscopic brush resistance, R , is in first approximation inversely proportional to A_c , it is $R \approx C/A_c = \text{const } H/P$. Correspondingly, measurements of R as a function of current I are a potentially extremely powerful method to look for mechanical effects due to electric currents and fields, especially when only "tunneling films" are on the surface whose film resistivity (σ_F) is independent of current density and almost independent of local temperature. Specifically, softening through high current densities and/or electrical fields should cause $R(I)$ to be concave.

In fact, a decrease of R with I is seen quite commonly since many surface films show a strong negative temperature dependence of σ_F . However, for constant σ_F , R appears to decrease with I only under conditions in which contact spot heating becomes strong, and in that case the $R(I)$ dependence can be satisfactorily explained through the decrease of hardness H with rising temperature. Without contact spot heating and while σ_F is constant, all measurements made by or known to these writers yield R independent of I . Such

measurements include metal fiber brushes made of various pure metals and a few alloys, as well as metal-graphite brushes. Most interestingly, in the latter case, specifically silver-graphite brushes, a series of investigations has recently shown no differences in contact spot behavior when contact spot temperatures were changed between room temperature and about 220°C either via heating in an oven without current flow, or via the passage of high current densities through brushes running at ambient temperature.

Not as clear-cut but yet suggestive are recent very careful measurements on the already mentioned fiber brushes made of 50 μm thick gold-plated copper wire and sliding on gold-plated copper. In these, the coefficient of friction was determined as a function of current flow. No difference was discovered anywhere between -0.4 Amp and $+0.4$ Amp, i.e. local electrical current and field changes between zero and plus/minus 5 MA/m² and 2 MV/m, respectively.

The above considerations show that explanations of effects of currents and electrical fields on mechanical behavior should be compatible with established data on the electrical contact resistance between materials as a function of applied normal force and current. Moreover, careful measurements of contact resistances should become part of the arsenal of accepted methods for the study of current and field effects on mechanical behavior.

The electrical interfacial resistance is generally strongly affected by changes of σ_F , the film resistivity of the ubiquitous surface film. Indeed, for the case of fiber brushes, R is proportional to σ_F , meaning that not only current and field effects on the metal itself can be studied, but also those of interfacial film material. The already cited lack of any noticeable effects of current changes in the fiber brush clearly indicates that in this case neither the metal nor the surface film was affected. In this connection it may be remembered that the so-called Rehbinder effects, which aroused much interest about thirty to forty years ago,

have aspects strongly reminiscent of some of the effects due to current and field applications reported in this workshop, and that Rehbinder effects are probably due to very thin surface films. Since there were only monomolecular layers present on the gold-plated brushes and substrate, the above negative result still leaves scope for explanations based on surface films, especially since at least 20 Å surface films are always present on non-noble metals in the atmosphere.

EASILY OVERLOOKED SIDE EFFECTS

The Electro-Mechanical Effect

Side effects which are prone to be overlooked include very importantly the "magneto-mechanical" effect. The latter was repeatedly mentioned during the workshop. It is due to the fact that magnetic fields, and thus also changes of magnetic fields, do not penetrate conductors instantly but "diffuse" into them. Therefore metals which are suddenly exposed to a magnetic field of strength B , are in the first one hundredths second or so subjected to the mechanical pressure

$$P_{\text{mag}} = B^2 / 2\mu_0 \quad (3)$$

with $\mu_0 = 4\pi 10^{-7}$ volt s/Amp m.

In agreement with eq. 3, the sudden application of $B = 1$ Tesla = 1 N/Amp = 10,000 Gauss, as generated by a modest electromagnet and equal to 50,000 times the earth's magnetic field, imposes the transient mechanical pressure of $p_{\text{mag}} = (1/8\pi \times 10^{-7})$ [N/m²] = 0.4 MPA. For a super-conducting magnetic $B \approx 100$ Tesla, and the pressure generated by sudden exposure would thus be 400 MPA, while the sudden discharge of a capacitor through a coil can give rise to still much larger pressures.

The possibility of very powerful compaction which this effect offers is used in a commercially available compactor manufactured by the Maxwell Corporation in

San Diego, for example. The suppression of the bursting of an explosive-filled pipe on ignition reported by N. Tselesin may be an example of the magneto-mechanical effect, and also the experiments reported by Okazaki.

Non-Uniform Heating at Contact Spots, Through the Skin Effect, and at Spots of Locally Increased Resistivity

Local heating, resulting in "flash temperatures" much above the average temperature rise, can cause unexpectedly large local softening. A prime example is machining under current flow. Here the superimposed current dumps Joule heat at the very contact spots which are already being strongly heated through the friction. Since electrical resistivity and thus Joule heating at same current increases with temperature, the contact spots could indeed melt and thus provide for local and very beneficial liquid lubrication.

Another source of uneven Joule heating and thus unanticipated temperature peaks is the skin effect. It derives from the same source as the magneto-mechanical effect, as a current cannot exist without the associated magnetic field and the magnetic field cannot penetrate a metal instantaneously. Thus alternating currents are concentrated at the surfaces, the more so the higher the frequency. In straight wires subject to short current bursts, the Joule heating is correspondingly concentrated at the circumference and local temperature increases can be much higher than anticipated. Since in thin wires the strength at the surface is particularly important (as demonstrated so clearly in Reh binder-type experiments) differential heating of the surfaces must often give rise to differences between current-pulsed thin wires and uniformly heated dummies.

Short current pulses in porous or otherwise multiply connected metals concentrate the current about the circumference of the solid parts for the very same reason. There is therefore yet another component to the effect of pulsed current-assisted sintering studied by Ozakai, i.e. preferential heating where

particles contact mechanically, exactly where heating does the most good. Besides, passing a DC current through a compressed metal powder will lead to local heating at the contact spots also for the independent reason that current constrictions arise there. Indeed evidence of high transient temperature spikes at contacting spots between particles was clearly visible in the micrographs shown by Okazaki.

In solid samples all areas of higher than average resistivity that are not easily bypassed by the current flow, such as inclusions, pores, grain boundaries, cause locally increased Joule heating and the corresponding temperature peaks, since Joule heating is proportional to $j^2\rho$ with ρ the local resistivity and j the current density. The combination of skin effect and locally increased Joule heating at defects, causes temperature peaks at grain boundaries and inclusions at and near the surface of current-pulsed samples. The same occurs as a result of exposure to micro waves. Due to the rapid local equilibration of temperature in metals such effects are entirely negligible in DC heating. However, as already indicated in a discussion remark to the paper by Kimrey and Janney by one of the present writers, this effect can be significant in micro-wave heating, especially in view of the critical role grain boundaries can play in plastic deformation.

Unexpected Stresses

Any and all types of non-uniform heating are associated with the corresponding thermo-elastic stresses. To the extent that in bulk materials local thermal expansions or contractions have to be accommodated by elastic if not plastic strains, there is an equivalence between thermally-induced local tensile or compression stress σ_{th} (assuming essential uniaxial stress) and temperature differences δT , namely

$$\sigma_{th} = \alpha Y \delta T \quad (4a)$$

where α designates the coefficient of linear thermal expansion and Y Young's

modulus. By a well-obeyed empirical formula linking α to the melting temperature T_M in Kelvin, namely $\alpha = 0.02/T_M$, one may also write

$$\sigma_{th} = 0.02 Y \Delta T/T_M \quad (4b)$$

The magnitude of the thermo-elastic stresses will be appreciated if it is realized that in accordance with eq. 4b the 0.02% yield stress corresponds to $\Delta Y_{yield} = T_M/100$, e.g. about 100°C in aluminum.

The application of electric fields is unlikely to cause bulk effects in metals since, according to Gauss's law, the interior of conductors is field-free except for the minor electric fields associated with currents. However, external electric fields cause polarization in both metals and nonmetals, and depending on specimen shape, the forces with which the corresponding dipolar surface charges mutually attract can be sizeable. For flat, smooth specimens subject to a transverse electric field the resulting compressive stress is

$$\sigma_E = \epsilon_0 K(V/D)^2/2 \quad (5)$$

with V the applied voltage, D the distance between the polarized surfaces, K the dielectric constant, and $\epsilon_0 = 8.85 \times 10^{-12}$ Amp sec/Volt m. In J. C. M. Li's experiment, $V/D = 10^7$ V/m and $K = 6$ (as for undoped KC1), more or less, rendering $\sigma_E = 0.026$ MPA. Considering that surface charge density and electric field strength are inversely proportional to local radius of curvature, surface pits and scratches are bound to be associated with stress peaks, and it seems safe to conclude that polarization stresses were responsible for J. C. M. Li's results.

In cases of magnetic field applications to ferro-magnetic materials or materials with ferro-magnetic inclusions, magnetostriction is another source of unsuspected mechanical stresses. Minor internal stresses arise through different orientations among grains, since magnetostriction is crystallographically anisotropic. Higher magnetostrictive stresses are transiently

generated through the already discussed "diffusion" of magnetic fields into metals, whereby the depth of penetration rises proportionally with the root of elapsed time. Thus the depth to which currents, magnetic fields and magnetostriction penetrate in steady state is proportional to $1/\sqrt{\nu}$ with ν the frequency of the current or magnetic field application.

Typically, magnetostriction stresses are smaller than thermo-elastic stresses and they saturate already at relatively low external field strengths. The magnetostrictive saturation strain is $\epsilon_M \approx 8 \times 10^{-6}$ in iron and about five times larger in nickel. The corresponding maximum mechanical stress to compensate for ϵ_M in the same manner as mechanical stresses compensate for temperature gradients is

$$\sigma_M = \epsilon_M Y \approx 1 \times 10^{-5} Y = 0.05 \sigma_{0.02\%} \quad (6)$$

Thus one can hardly expect significant strength changes through magnetostriction. However, Rehbinder-type effects might be triggered by magnetostriction.

Side Effects Through Testing Equipment

Magnetic fields certainly cause magnetostriction also in testing equipment, specifically for example in iron rods and grips of tensile testers. As these saturate already at modest external fields and tend to be larger and more rigid than the samples, the thusly imposed unexpected stresses can be sizeable. To the extent that also current applications typically involve unscreened magnetic fields, one should watch for possible machine-induced magnetostrictive strains also in all cases of AC or pulsed current and/or electric field applications.

Another case of machine-induced stresses presumably is the polarity effect in wire-drawing under current application, as was already pointed out by one of the present writers in the discussion. Namely, the voltage drop across a sliding

contact at a wire is at the least about 0.2 V. The corresponding Joule heat at the "upstream" contact will be largely dumped into the wire and may be sizeable. Certainly it is likely to dwarf the Joule heat evolution along a length of wire of typical metal resistivity $\rho = 5 \times 10^{-8} \Omega\text{m}$. Namely, in such a wire a voltage drop of 0.2 V along a length of 1 m requires the current density

$$j = (V/L) / \rho = 0.2/5 \times 10^{-8} = 400 \text{ A/cm}^2 \quad (7)$$

Thus each of the two sliding contacts required to pass a current through a wire while being drawn will generate Joule heat at a rate which in a typical 10 cm long wire would require a current density of $4000 \text{ A/cm}^2 = 0.4 \text{ MA/m}^2$. Now the voltage drop at a sliding contact has a distinct polarity, i.e. normally it is only about one-half to two-thirds as large when the smaller contact is negative relative to the substrate than when it is positive. Thus, clearly the Joule heat deposited into the wire by the "upstream" brush affects the test section much more than the "downstream" brush. Much the same source of easily overlooked Joule heating subject to polarity exists, of course, in the case of rolling while current is applied.

Much more evident than either of the above, and therefore probably not so easily overlooked, are thermal stresses as samples are heated between rigid grips. Buckling may occur under certain conditions, i.e. with fairly slender samples (and if the elastic strain is smaller than the thermal expansion) and this will simulate a drastic reduction of strength in tensile testing.

LIMITATIONS ON POSSIBLE THEORIES

Dislocation Drag and Surface Films

The most widely accepted hypothesis for explaining effects of currents and fields on mechanical properties are drag forces acting on dislocations, especially due to conduction electrons. We know from the theory of plastic deformation that dislocation drag is a (normally additive) contribution to the so-called "friction

stress". In terms of resolved shear stresses, the magnitude of the friction stress (τ_0) to the flow stress (τ) is typically only $\tau_0/\tau \approx 0.1$. However, τ_0 can be relatively larger. τ_0 can indeed dominate τ at small strains at any temperature, and during creep at all strains.

So far widely overlooked is another source of interesting effects due to currents and fields. This is the already repeatedly mentioned presence of invisible surface films. Thick surface films do, of course, contribute their ordinary mechanical strength to a wire, for example. But more subtly, thin surface films can hinder the egress of dislocations through otherwise free surfaces, thereby converting surface zones from extra weak areas in which dislocations are removed via image forces, into hard layers which present an obstacle against dislocation motion. Rehbinder-type experiments give many examples of such effects, to which in particular samples of relatively high internal perfection and relatively small dimensions are prone.

Highly relevant in connection with effects due to unsuspected surface films is the time-dependent penetration of current and magnetic field into samples during pulsed and AC applications, especially since the mechanical effects of surface films tend to be temperature sensitive. To give a few guideline figures: The penetration depths at $\nu = 10^4$ Hz are $\delta = 0.85$ mm, 0.66 mm and 1 mm for aluminum, silver and brass, respectively, while as already stated $\delta\sqrt{\nu} = \text{constant}$.

Quantitative Limitations on Electron and Phonon Drag

The theoretically derived magnitude of electron drag given by Brailsford is too small as that it could account for any of the reported effects, as follows. The stress contribution to τ_0 due to electron drag at relative velocity v_{rel} between dislocations and conduction electrons is

$$\tau_e = B_e v_{\text{rel}} / b \quad (8a)$$

with $b = 3 \times 10^{-10}$ m the Burgers vector. According to Brailsford, the electron drag coefficient is $B_e = 10^{-5}$ dyn s/cm² = 10^{-6} N s/m², independent of temperature. The phonon drag coefficient is 10 to 100 times larger. Correspondingly, at the extreme upper limit of possible dislocation velocities $v_{\max} = 10^3$ m/s, one obtains $\tau_{\max} \approx 3$ MPA. However, any differences of τ_0 due to changes in τ_e in experiments with and without current application are proportional not to the dislocation velocity but the conduction electron drift velocity, v_e . At the highest reported current density of about $j_{\max} = 10^{10}$ A/m², with $N_e = 10^{29}$ /m³ the numerical conduction electron density and $e = 1.6 \times 10^{-19}$ Amp-sec the electronic charge, this is found as

$$v_{e\max} = j_{\max}/N_e e = 0.6 \text{ m/sec} \quad (9)$$

yielding

$$\tau_{\max} = B_e v_{e\max}/b = B_e j_{\max}/b N_e e = 2000 \text{ N/m}^2 = 10^{-3} \tau_0 \quad (8b)$$

Estimates by Soviet workers (see paper by Conrad et al on Electroplasticity) give as a maximum about an order of magnitude larger value for B_e and in turn for τ_{\max} .

Since phonons travel in the 10^3 m/s speed range and the phonon drag coefficient is one or two orders of magnitude larger than B_e , phonon drag can contribute correspondingly much more to τ_0 , and in fact may well limit actual dislocation velocities to values much below 1000 m/sec.

Dislocation Charge Effects

In insulators, dislocations can be charged in either of two ways: (i) They will flex to approach charged defects to which they may be attracted as closely as compatible with dislocation line tension and mobility. (ii) Charged mobile defects migrate to the dislocations and form Cottrell atmospheres on them. The movement of dislocations charged through the mechanism (i) does not cause charge movement and therefore electric fields do not exert any forces on such dislocations.

If a Cottrell atmosphere has an excess charge of me per length b of dislocation line, wherein m will at the most be unity, the equivalent stress generated by an electric field E is

$$\tau_E = meE/b^2 \approx 2mE \text{ [PA m/V]} \quad (10)$$

At $m = 1$, therefore, an $E = 10^6$ V/m electric field will generate $\tau_E = 2$ MPA equivalent stress on dislocations with charged Cottrell atmospheres. Assuredly, such a value of τ_E can give rise to significant effects, and even more so the proportionately higher stresses due to stronger electric fields. However, the maximum speed of the resultant dislocation motion is that with which the dislocations can drag their atmospheres, and chemical segregation, much as in electrochemistry, will be observed at the electrodes. Once the dislocations break away from their atmosphere, they no longer suffer forces due to the electric field. Clearly these were not the conditions in any experiments reported at the workshop.

SUMMARY AND CONCLUSIONS

Theory shows that electronic drag on dislocations is too small as to generate observable effects due to currents and/or fields. This deduction is in agreement with observations on electrical brushes which suggest that there are no, or at the least only insignificantly small, direct effects of electric currents and fields on the mechanical properties of metals. However, observations on brushes do not rule out such effects in the case of non-metals. Studies on the latter could be favorably carried out by means of electrical contacts including surface films.

An important source of relevant effects are invisible surface films as are ubiquitous on non-noble metals in the atmosphere. Specifically, about thirty to forty years ago Rehbinder of Russia, and following him many Western authors,

have studied subtle effects some of which are similar to those of currents and electric/magnetic fields, which are largely due to unseen surface films. It is proposed that special attention therefore be paid to such a possibility.

Electrical fields can exert equivalent stresses on dislocations in non-metals when they drag charged Cottrell atmospheres. Effects resulting from such forces will be strongly temperature dependent and will be associated with generally small strain rates as well as with chemical depositions at the electrodes. Directly, transverse electric fields can give rise to significant compression stresses in the direction of the field lines. These may be alternatively interpreted as due to the electric attraction of polarization charges or by the volume energy of the electric field.

The application of pulsed or AC currents leads to the skin effect which becomes important for normal laboratory specimens of 1 cm diameter or so when the frequency exceeds 100 Hz. In general, at frequencies of ν Hz, only a skin of $\delta = 10/\sqrt{\nu}$ [cm] of the specimen will be penetrated by the current and similarly by magnetic fields.

The non-uniform Joule heating resulting from the skin effect is bound to give rise to thermo-elastic stresses which are concentrated at the surfaces, just where surface films may have an unsuspected significant influence on mechanical behavior. Similarly, also magnetostrictive stresses will arise at surfaces, albeit at a typically uninterestingly low level.

A potentially very important corollary to the skin effect is the peaking of Joule heat at contact spots in compacted powders as also at crystal defects which are not easily circumvented by a current. In combination with the electro-mechanical effect, due to the sudden application of magnetic fields, pulsed current applications can therefore be very useful in sintering. Beneficial effects of current passage during machining can be understood theoretically through

selective Joule heating at the interface, supplementing friction heat and leading to local softening if not melting.

ISSUES AND OPPORTUNITIES

by
Hans Conrad
North Carolina State University

1. INTRODUCTION

The papers presented at this workshop affirm that externally-applied electric, magnetic, electromagnetic or ultrasonic fields can have a significant influence on the properties of inorganic materials (metals, semiconductors and ceramics). The resulting effects thus need to be taken into account when considering the use of materials (structural or electronic) in environments containing such fields. Further, the effects may be beneficial in the working, forming and processing of materials, offering opportunities regarding: (a) difficult-to-fabricate materials, (b) more efficient processes and (c) improved properties of the product. In this discussion I wish to review some of the issues involved and opportunities for research, and for application, which were brought up during the Panel Discussion session and throughout the workshop. I must point out that my reporting will reflect my background (materials science and engineering) and will be somewhat biased towards the research areas in which I have been active, namely the effects of electric fields and currents on the properties and behavior of metals and alloys. The preceding discussion by Prof. Doris Kuhlmann-Wilsdorf (with input from this writer) offers additional thoughts and views on the subject. The comments in the letter by Dr. Rosenberg are also highly appreciated in view of his extensive background in the subject of the effects of electric fields and currents on the behavior and properties of materials (thin films).

2. ISSUES

Major issues pertaining to the effects of the above-mentioned fields on the properties of inorganic materials include the following:

1. What fraction of a reported effect results from **indirect** (side) effects rather than a **direct** effect of the applied field?
2. What are the operative mechanisms?
3. What are some research opportunities?
4. What potential applications are indicated?

2.1 Side Effects

This issue pervaded discussions throughout the workshop and is considered to be of prime importance. The principal side effects are heating and induced mechanical stresses, including thermal stresses and those resulting from electro-magnetic forces (electromotive or pinch, magnetostriction, electrostriction).

Joule heating is the major side effect when considering the influence of a **continuous** dc current on the mobility of point defects (electromigration) and of line defects (electroplasticity) in metals. It is usually taken into account by considering that the rise in temperature produced by Joule heating has the same effect as that resulting from conduction (convection) or radiant heating, and excludes the existence of local "hot spots" produced by the scattering of electrons at crystal defects. That such hot spots do not play a role in single phase alloys is supported by the good agreement between the measured values of the atomic drift velocity in Al, Cu and Au, and theoretical predictions [1-3].

When **pulsed** dc currents are employed, skin and electro-magnetic side effects need to be considered in addition to Joule heating. The non-uniform current associated with the skin effect can lead to temperature gradients and in turn thermal stresses. Skin effects were avoided in the studies with high-density

electric current pulses by Troitskii of the Soviet Union and Conrad and coworkers (reported here) in that the diameter (~ 1 mm) of the wire specimens they used was less than the calculated skin depth [4]. Regarding electro-magnetic forces, estimates by Conrad and coworkers [4] indicated that they were insignificant compared to the direct effects of the current. Further, the polarity effects reported by Soviet workers [5-7] provide rather strong support that a significant portion of the electroplastic effect results from a direct electron-dislocation interaction, since the side effects of Joule heating and electro-magnetic forces should not depend on current direction. Further evidence that Joule heating could not account entirely for the increase in plastic strain rate which resulted from a current pulse (Conrad) is that the magnitude of the effect in FCC metals increased with increase in prior plastic strain even though an increase in temperature from Joule heating is expected due to the increase in density of crystal defects produced by the deformation [4]. Also, in the work by Conrad and coworkers [4], thermal expansion resulting from Joule heating was always measured and taken into account.

Further support that electro-magnetic forces did not make a significant contribution to the electroplasticity of Zn crystals deformed at 78K is that after correcting for Joule heating a reasonable correlation was obtained between strain rate $\dot{\epsilon}$ and current density j by taking $\dot{\epsilon} = \epsilon/t_p v_p$, where t_p is the pulse duration time and v_p the frequency of pulsing; see Fig. 4 of [8]. This suggests that the effect produced by a given current density depends only on the total time the current is "on" and is independent of the frequency of pulsing, which governs the electro-magnetic forces and possible "shock" effects of the current pulse. Since the rest interval between pulses will vary with v_p (and to a lesser degree with t_p), a constant response for a constant product $t_p v_p$ will however only occur if the defect structure does not change during the rest period. That changes in structure may

sometimes occur is indicated by the results of Stashenko and Troitskii [9], who found that the increase in creep rate of Zn crystals varied with the time interval t_i between the individual pulses of paired pulses, other conditions being held essentially constant. A change in structure during the rest interval between pulses may be the reason that a variation in pulse frequency during the electropulse annealing of Cu affected the rate of grain growth, whereas changes in pulse duration time had no effect; see Fig. 6 in [10]

In studies on the effects of an externally-applied electric field, such as those by Li and by Conrad and coworkers, Joule heating is not a factor. Also, the electrostrictive stresses are not of sufficient magnitude to produce the observed effects. As mentioned in the discussion by Prof. Kuhlmann-Wilsdorf, the equation for such stresses based on a parallel plate condenser is

$$\sigma = \frac{dW}{dx} / A = 1/2 \epsilon_0 K E^2 \quad (1)$$

where ϵ_0 is the permittivity of free space ($= 8.854 \times 10^{-12}$ in mks units), K the relative permittivity of the dielectric medium, x the spacing between the plates, A the area of the plates and E the electric field. Taking $K \approx 6$ and $E = 10^7$ V/m for Li's experiments on KCl, and $K \approx 1$ and $E = 10^5 - 10^6$ V/m for Conrad et al's on Al, Cu and Fe, we obtain $\sigma \approx 10^4$ Pa and $\sigma \approx 10^{-2} - 1$ Pa respectively for the two sets of investigations. These electrostrictive stresses are considerably below the yield stresses of the materials employed (CRSS (KCl) $\approx 10^6$ Pa; Y.S. (Al, Cu, Fe) $\approx 10^6 - 10^8$ Pa).

Heating and induced mechanical stresses are important side effects when pulsed magnetic fields, lasers and ultrasonic waves are applied. The contribution of these side effects to the results produced by the named fields is not clear to this writer. Also not clear is what role the current played other than heating in electrodischarge compaction of metal powders (paper by Okazaki). Further, the

question was raised whether the decrease in activation energies for sintering and grain growth in alumina using microwaves (Kimrey and Janney) was real or merely reflected the occurrence of local hot spots.

From a quantitative standpoint, the **direct effects** of the various fields considered in this workshop can in themselves produce changes in properties or rates ranging from only a few percent to orders of magnitude, depending on the material, the property considered and the intensity of the field. The direct effects combined with the side effects of heating and induced mechanical stresses will in general produce substantial changes in kinetics, microstructure and properties of inorganic solids. **The advantages of the combined direct and indirect effects need to be considered when considering applications. Also, combined fields** (e.g. electric fields or currents plus ultrasonic waves) **should be given consideration.**

2.2 Mechanisms

Our understanding of the mechanisms by which the various externally-applied fields influence the properties and behavior of solids and the kinetics and microstructures associated therewith is still very meager. Only in the case of electromigration do we have a relatively sound fundamental foundation, the concept of an "electron wind" being an important building block. The action of an electron wind also appears to be important in the electroplasticity of metals [8]. However, the magnitude of the experimentally-derived electron wind push coefficient B_{ew} [8] is somewhat higher than the electron drag coefficient B_e predicted by rigorous theoretical calculations (paper by Brailsford). Moreover, the temperature dependence of the experimentally derived value of B_{ew} is not in keeping with theoretical predictions of a temperature-independent B_e . Further, the fact that by far the largest effect of the current was on the pre-exponential of the thermally-activated plastic deformation rate equation is somewhat puzzling and requires further study. The possible role of combined electron-phonon-

dislocation interactions needs to be addressed regarding these departures from predicted behavior based entirely on electron-dislocation interactions.

The explanations of electroplasticity and plastoelectricity in ionic crystals (due to an applied electric field) based on charged jogs on dislocations (Li) seem sound, but additional work is needed to quantify the behavior. Also, the question arises whether charged defects in the lattice (e.g. charged vacancies or solutes) form a Cottrell atmosphere about the dislocations and how does this atmosphere influence the observed behavior (see discussions by Kuhlmann-Wilsdorf).

Charged dislocations also appear to be important in the photoplasticity of semiconductors (papers by Galligan et al and by Hochman). The explanation given by Galligan et al that the increase in stress which occurs upon exposure of a semiconductor to a light pulse results from the injection of electrons and holes and their subsequent migration and interaction with charged dislocations appears to be sound and a good starting point for future theoretical and experimental studies.

How an externally-applied electric field produces changes in the center of 1-3 mm thick specimens in the time periods employed is a challenging question which rises from the work of Conrad and coworkers on the effects of an external electric field on superplasticity, recovery and recrystallization and hardenability of steels. Exceedingly large diffusion coefficients would be required if the field only produced changes at the specimen surface, which then diffused to the center. On the other hand, electron theory of solids does not allow for the occurrence of an electric field in the metal. Some questions which arise include: (a) Do the charges which may exist on vacancies and dislocations in metals play a role? (b) What role do grain boundaries play? and (c) To what degree does the electric field influence the Gibbs free energy of a phase? and (d) Do the small currents which were observed in their experiments play a role?

The mechanism by which high-intensity, high-frequency microwaves reduce the activation energy for sintering and grain growth in alumina is also a challenging question.

In summary, this writer is of the opinion that the mechanisms responsible for the observed changes in properties or behavior resulting from exposure to the various fields considered here are not well understood, first of all in regard to separating the side effects from the direct effects and secondly, in regard to the mechanisms responsible for the direct effects. From a philosophical viewpoint it is clear that to understand the operative mechanisms materials scientists must now include the electron in their hierarchy of microstructures, the dimensions of which over the past fifty years have gradually decreased from 10^{-4} cm (optical microscope) to $\sim 10^{-8}$ cm (field ion microscope, scanning tunneling microscope and high resolution TEM) and must now make a quantum jump to the much smaller dimensions of an electron. Moreover, we will now need to consider in addition to temperature and pressure the possible influence of a given applied field on the various parameters of the Gibbs free energy equation

$$\Delta G = \Delta U - T\Delta S + p\Delta V - f\Delta x \quad (2)$$

where ΔU , T , ΔS , p and ΔV have their usual meaning; f is an externally-applied, or internal force and Δx is the distance through which it acts.

2.3 Research Opportunities

It is evident from the above that the subject matter of this workshop is only little understood and there is need for additional work on the fundamental mechanisms involved. From a fundamental standpoint, studies are needed which define the charges carried by the various crystal defects and their interaction with electro-magnetic fields. Moreover, studies are needed on electronic energies (Fermi surface), phonon energies and electron-phonon, electron-crystal defect and combined electron-phonon-crystal defect interactions.

In this regard, computer calculations similar to those being carried out by Klein (this volume) are very exciting and appear promising. The extent to which they can contribute to answering some of the questions raised in this workshop needs to be investigated. Additional experimental-theoretical studies similar to those by Anderson (this volume) are also very desirable. Important to understanding ultrasonic effects is a knowledge of the interaction between the ultrasonic waves imparted to a solid and the phonon spectrum, and in turn their combined influence on atomic and dislocation mobility.

Planned studies on the interactions between the excitations of the lattice and the crystal defects should be carried out on high purity and well-characterized single crystals to avoid the complicating influence of grain boundaries. Similarly, studies of the phenomena considered here, i.e. electroplasticity, magnetoplasticity, photoplasticity, acoustoplasticity and the other effects of the fields, should be carried out on single crystals. Direct observation of the behavior of point defects (FIM, STM, HTEM) and dislocations (etch pits, TEM, HVTEM) are needed. To establish the influence of grain boundaries, either bicrystals or polycrystals with a wide range in grain size should be employed. To better evaluate the effects of an electron wind, methods whereby ultra-high current densities ($10^3 - 10^7$ A/cm²) can be employed continuously without excessive heating of the specimen need to be developed.

It is clear that the needed research overlaps the domains of solid state physics and materials science and a close interaction between these two disciplines is desirable for most efficient progress. It is however my understanding that only few physicists are being trained in the general subject area of interest here, namely the area previously known as solid state physics. Materials scientists must therefore make up for this and become more knowledgeable in this subject area. Finally, it should be mentioned that much of

the research listed here for the effects of fields on materials also has a bearing on superconductivity.

2.4 Applications

A good amount of the subject matter covered in this workshop is directly relevant to the microelectronics industry (see papers by Huntington and by Rosenberg) and better ties should exist between workers on the interaction of fields with bulk specimens and those involved with thin films, i.e. specimens of micron or nanometer size.

The Soviets claim to have applied high-intensity electric currents, magnetic fields and ultrasonics to manufacturing processes with significant benefits (see papers by Sprecher and Conrad and by Hochman and Tselesin). It is however not clear the extent to which these processes are actually being employed on a production basis in the Soviet Union. Except for electromagnetic forming and related processes, this writer is not aware of any commercial working or processing operation in the Western World which takes advantage of the **non-heating** effects of high-intensity fields. It does however appear that pulsed magnetic fields are being employed by industry to give significant increases in cutting tool life [11-13].

Some of the more promising areas where results obtained to date suggest that significant improvements might be obtained in either processing or in the properties of the product include:

1. Electric Current: Continuous or Pulsed
 - a. Rolling or drawing of refractory metals or intermetallic compounds [8,14].
 - b. Compaction of metal powders [15,16].
 - c. Recrystallization of metals [10].
 - d. Production or retention of non-equilibrium structures [15,16,16a].

2. External Electric Field
 - a. Superplasticity and diffusion bonding of metals and intermetallic compounds [8].
 - b. Hardenability of steels [17].
 - c. Precipitation hardening [17].
 - d. Joining of ceramics [18,19].
3. Magnetic Fields: Continuous or Pulsed
 - a. Hardenability of steels [20,21].
 - b. Rolling or drawing of magnetic alloys [22].
 - c. Aligned composites [23].
 - d. Increased cutting tool life [11-13].
4. Microwaves
 - a. Sintering and annealing of ceramics [24-27].
 - b. Joining of ceramics [28].

The use of lasers is not included in the above list because the principal effects appear to result from local heating, and the potential applications are covered in detail elsewhere [29-31]. The use of ultrasonics in metal working and processing appeared promising about 30 years ago, but interest died out shortly thereafter. The papers by Green, Salama and Hochman at this workshop suggest that this subject needs renewed consideration.

As mentioned above, both direct and indirect effects may be of benefit in application of a given external field to a production process. Also, the combination of two or more fields may be desirable, as indicated by Soviet work [32]. Finally, an important consideration which needs attention and has not been addressed at this workshop is the total energy required and the efficiency of a given process or combination of processes.

REFERENCES

1. F. M. d'Heurle and R. Rosenberg, **Physics of Thin Films**, 7 G. Hass, M. Francombe and R. Hoffman, eds, Academic Press, N. Y. (1973) p. 257.
2. **Electro- and Thermo-Transport in Metals and Alloys**, R. E. Hummel and H. B. Huntington, eds., TMS-AIME (1977) p. 1.
3. F. M. d'Heurle and P. S. Ho, **Thin Films-Interdiffusion and Reactions**, J. M. Poate, K. W. Tu and J. W. Mayer, Wiley-Interscience (1978) p. 243.
4. A. F. Sprecher, S. L. Mannan and H. Conrad, *Acta Met.* **34** 1145 (1986).
5. O. A. Troitskii, *Prob. Prochnosti* No. 7 (July 1975) p. 14.
6. Yu. I. Boiko, Ya. E. Geguzin and Yu. I. Klinchuk, *Zh. Eksp. Teor. Fiz.* **81** 2175 (1981).
7. L. B. Zuev, V. E. Gromov, V. F. Kurlivov and L. I. Gurevich, *Dokl. Akad. Nauk. SSSR* **239** 84 (1978).
8. H. Conrad, A. F. Sprecher, W. D. Cao and X. P. Lu, "Effects of Electric Current and External Electric Field on the Mechanical Properties of Metals-Electroplasticity", this volume.
9. V. I. Stashenko and O. A. Troitskii, *Dokl. Akad. Nauk. SSSR* **267** 638 (1982).
10. A. F. Sprecher and H. Conrad, "Effects of an Electric Current and External Electric Field on the Annealing of Metals", this volume.
11. J. Jablonowski, *Amer. Machinist* (Jan. 1987) p. 80.
12. R. F. Hochmann, N. Tselesin and V. Drita, *Adv. Mat. Processes* **8** 36 (1988).
13. Innovex Brochure, "Fluxation U102" (1989).
14. A. F. Sprecher and H. Conrad, "Application of Electroplasticity in Metalworking - Review of Soviet Work", this volume.
15. K. Okazaki, "Electric Current Effects in the Sintering of Powder Materials - Electro-Discharge Compaction", this volume.
16. H. L. Marcus, D. L. Bourell, Z. Eliezer, C. Persaol and W. Weldon, *J. Met.* (Dec. 1987) p. 6.
- 16a. B. M. Clemens, R. M. Gilgenbach and S. Bidwell, *Appl. Phys. Lett.* **50** 495 (1987).

17. H. Conrad, A. F. Sprecher, W. D. Cao and X. P. Lu, "Effects of Electric Fields and Currents on Phase Transformations in Bulk Alloys", this volume.
18. G. Wallis and D. T. Pomerantz, *J. Appl. Phys.* **40** 3946 (1969).
19. B. Dunn, *J. Amer. Cer. Soc.* **62** 545 (1979).
20. R. F. Hochman and N. Tselesin, "The Effect of Magnetic Fields on Materials Properties and Processing", this volume.
21. T. Kakeshita, K. Shimizu, S. Funada and M. Date, *Acta Metall.* **33** 1381 (1985).
22. S. Hayashi, S. Takahashi and M. Yamamoto, *J. Phys. Soc. Jap.* **30** 381 (1971).
23. G. Sauthoff and W. Pitsch, "Orienting of Fe₁₆N₂ Particles in α -Iron by an External Magnetic Field", *Phil Mag.* (1986).
24. H. D. Kimrey and M. A. Janney, "Effects Other Than Heating by High-Intensity, High Frequency Microwaves in Materials Processing", this volume.
25. M. K. Krage, *Cer. Bulletin* **60** 1230 (1981).
26. D. L. Johnson, W. S. Sanderson, J. K. Knowlton and E. L. Kemer, *Proc. MgO/Al₂O₃ Conf. M.I.T.* (June 12-16, 1983).
27. J. S. Kim and D. L. Johnson, *Amer. Cer. Soc. Bull.* **62** 620 (1983).
28. A. J. Klein, *Adv. Mat. & Processes* **12** 36 (1985).
29. **Laser-Solid Interactions and Transient Thermal Processing of Materials**, J. Narayan, W. Brown and R. Lemon, eds., North Holland (1983).
30. **Plasma, Electron and Laser Beam Technology**, Y. Arata, ed. ASM, Metals Park, OH (1986).
31. **Laser Materials Processing III**, J. Mazumder and K. N. Mukherjee, eds. TMS-AIME (1989).
32. O. A. Troitskii, *Mat. Sci. Engr.* **75** 37 (1985).